

**DESIGN STUDY OF A HEAVY DUTY HYDRAULIC  
MACHINE USING  
FINITE ELEMENT TECHNIQUES**

This thesis is submitted to **DUBLIN CITY UNIVERSITY** as the requirement  
for the degree of

**DOCTOR OF PHILOSOPHY ( Ph.D )**

**BY**

**MOHAMAD M. SALEH, B.Eng., M.Eng.**

Sponsoring Establishment:

**Scientific Studies and Research Center, Damascus, Syria.**

August 1992

## DECLARATION

The material presented in this thesis is my original work, except where specific references are made to the work of others, and no degree has been obtained on this thesis from any other university or institution.

Signed: \_\_\_\_\_

A handwritten signature in black ink, appearing to be 'Mohamad Majed Saleh', written over a horizontal line.

Mohamad Majed Saleh

August 1992

# TABLE OF CONTENTS

<b>CONTENTS</b>	<b>Page</b>
Declaration	I
Table of contents	II
Abstract	IV
Acknowledgements	V
Nomenclature	VI
<b>CHAPTER 1:</b>	
1.1 Introduction	1
1.2 Previous work	2
1.3 Current work	15
<b>CHAPTER 2: THE FINITE ELEMENT METHOD</b>	
2.1 Introduction	20
2.2 The application of the finite element analysis	21
2.3 The element types and geometry	23
2.4 The finite element model	24
2.5 Error in the analysis	25
2.6 Fundamental finite element formulation	27
2.6.1 Linear static analysis	28
2.6.2 Structural dynamics	31
2.6.3 Non-linear static analysis	33
2.6.4 Field analysis	34
2.7 The solution of the finite element equation	35
2.8 Time for solution	37
2.9 The finite element software systems	37
2.9.1 Selection of the finite element software system	38
2.9.2 Training	38
2.9.3 LUSAS finite element system	39
<b>CHAPTER 3: THEORETICAL PREDICTION OF THE DESIGN ANALYSIS OF THE HYDRAULIC PRESS MACHINE</b>	
3.1 Introduction	52
3.2 Original design of the press	55
3.3 Conventional analytical model (C.A.M)	57
3.3.1 Assumptions	58
3.3.2 Model analysis	58
3.3.3 Method of calculation	62
3.4 Numerical model	66
3.4.1 Assumptions	66
3.4.2 Modelling strategy	67

**CHAPTER 4: EXPERIMENTAL MODIFICATION OF THE EQUIPMENT  
AND MATERIAL**

4.1	Introduction	88
4.1.1	Designing the measurement system	89
4.1.2	Designing the platens and the loading tools	110
4.1.3	Designing the hydraulic system	123
4.1.4	Designing the main stand	125
4.1.5	Designing the data acquisition system	133

**CHAPTER 5: RESULTS AND DISCUSSIONS**

5.1	Introduction	148
5.1.1	Performance test	149
5.1.2	Press structure before modification	151
5.1.3	Press structure after modification	176
5.1.4	New design of the press structure	189
5.2	Computing costs	195

**CHAPTER 6: CONCLUSION AND SUGGESTION**

6.1	Conclusion	197
6.2	Suggestion for further work	198

References	200
Bibliography	208

Appendix (A)	A-1
Appendix (B)	B-1
Appendix (C)	C-1
Appendix (D)	D-1

# **DESIGN STUDY OF A HEAVY DUTY HYDRAULIC MACHINE USING FINITE ELEMENT TECHNIQUES**

**By**

**Mohamad M. Saleh, B.Eng., M.Eng.**

## **ABSTRACT**

This thesis describes the systematic procedure for investigating the performance and the design analysis of the welded structure of a 150-tonne hydraulic press machine. This machine was designed by ENERPAC without any measurement or variable hydraulic system. The investigation discusses the theoretical and experimental model of the machine to establish the accurately optimal design analysis and further development of the present machine at minimum time and lower cost. The applicability of the existing PC based FE package, as a computer aided design tool, was also investigated.

The theoretical model takes into account both conventional analytical formula and numerical technique, using Finite Element Analysis. The conventional model is based on the simple bending theory using the total strain energy principle for 2D beams. The LUSAS Finite Element software system is used as a tool to establish the theoretically predicted numerical model. This model has been discussed with different factors. The factors considered are: the boundary condition; the mesh density and the type of the element being used.

The experimental model was based on the electrical method of processing the experimental results using a personal computer through an appropriate data acquisition. The apparatus of the experimental rig and the flow sequence of a computer program, which has been developed to facilitate the measurement of the load deformation of the machine and the load deformation of the workpiece, were discussed.

A comparison has been made between the experimental and theoretically predicted results. A good agreement was found between the finite element and the experimental model. Although the conventional analytical model was in good agreement with the plane frame finite element using beam element, this agreement deteriorated between these models and the experimental models. Also, a comparison was made between the stiffness of the actual present machine and the standard stiffness of a similar machine before and after the theoretical modification and disagreement was found.

A new optimal design of the structure of the press was discussed theoretically using plane stress finite element model. The factors considered in this optimal design are the width and the chamfering of the press structure. The stiffness of this model has been compared with the standard stiffness, as a design goal, and as a result of this a good agreement has been found and a practical conclusion has been drawn.

## ACKNOWLEDGEMENTS

I would like to thank Professor M.S.J.Hashmi and the Staff of the School of Mechanical and Manufacturing Engineering,D.C.U.

I acknowledge the financial support from Scientific Studies and Research Center (S.S.R.C), Damascus, Syria. Thank you to the General Director of S.S.R.C, Dr A.W.Chahid and the Head of Mechanical Institute in S.S.R.C, Dr Akram Nasser,for their assistance

Thanks also to my friends who encouraged me during my study.

My special thanks to Mairead Callan.

I highly appreciate the help of Pat Hudson in Proof-reading this work.

## NOMENCLATURE

The following symbols have been used throughout this thesis:

$[^e], \{^e\}$	Matrix, vector relating to a single element
Suffix <b>ep</b>	Indicates elastic plastic quantities
(sr)	Indicates a surface
(v)	Indicates a volume
$\{t\}$	Vector of surface forces
$\{f\}$	Vector of body forces
$\{F\}$	Vector of concentrated loads
$\{u\}$	Vector of total displacement
$\{\epsilon\}$	Vector of strain
$\{\sigma\}$	Vector of stress
$\{\delta u\}$	Vector of the vertical displacement
$\{a\}$	Vector of the nodal displacement
$[N]$	The shape function matrix
$[B]$	The strain-displacement matrix
$[D]$	The matrix of elastic constants
$\{\sigma_o\}; \{\epsilon_o\}$	The initial stresses and strains respectively
$[K]$	The structural stiffness matrix
$\{R\}$	Vector of the structural forces

$\{u\}$	Vector of the total velocity
$\{\ddot{u}\}$	Vector of the total acceleration
$\{u\}$	Vector of the nodal velocity
$\{\ddot{a}\}$	Vector of the nodal acceleration
$[M]$	The mass matrix
$[C]$	The damping matrix
$[\rho]$	The density matrix
$\{\psi(\{a\})\}$	Vector of residual force dependent on displacement
$[Z]$	The conductivity matrix
$\{\phi\}$	Vector containing temperature at each node of each element
$\{Q\}$	Vector containing the heat flow rate into each node of each element
$U$	The total strain energy
$M$	Bending moment
$L,H$	Total length
$P$	Applied load
$A$	Cross-sectional area
$E$	Young's modulus
$I$	Second moment of area
$ds$	Small length
$\delta$	The deflection
$S_t$	The direct stiffness
$D$	The diameter



# CHAPTER 1

## 1.1 Introduction

Usually, engineering problems can be solved by constructing an appropriate model. This model should be used primarily in engineering design to understand and predict the performance of the problem. Severe constraints of time and cost should be considered when constructing and analyzing engineering models. The solution of the engineering models, by conventional analytical methods, can sometimes prove either difficult or impossible because the geometry or some other characteristics are complex or arbitrary. Therefore, the numerical technique, which usually involves a number of repetitive operations, making them ideal for solution by computer, are well suited to obtaining an approximate solution. Finite element method (FEM) has become the most effective numerical technique used to calculate the most complicated engineering problems compared to other computer aided engineering.

In contrast the conventional analytical methods require the use of high-level mathematics, whereas the finite element method is based on simple algebraic equations. However, an FEM solution may require hundreds of simultaneous equations with hundreds of unknown terms. The advances in the finite element method over the last two decades have contributed greatly to its acceptance, as one of the most effective techniques for practical engineering design analysis. The popularity of this technique is due to its wide applicability to both static or dynamic linear and non-linear structural problems. The structure could be anything that is fabricated, manufactured or erected which must withstand an imposed load. Until recently, cost was a major limitation on

the use of FEM. However, the advances in computing hardware and software have changed this situation. Despite these advances, the high cost of large three-dimensional analysis and the fact that many engineers are not fully aware of the capabilities and economics of the finite element method, remain the main limitations in this method being used.

In the present investigations, the mathematical and experimental modelling strategies of the welded structure of a 150-tonne hydraulic press machine are described. The existing PC based FE package is used to make a comparative study of several models of this press structure. The objective of this was to investigate the applicability of this package as a computer aided design tool for complex engineering structures.

## **1.2 Previous work**

The concept of the finite element has been in use for the last 150 years[1]. Certainly it is not a new feature in structural analysis. Southwell [2] employed a similar method in his work in 1935. That work was carried out by using beam-type elements. The first engineering application of the finite element method was in stress analysis in the aircraft industry in the 1950's [3]. In these applications parts of the structure were modelled using beam elements. The objective was to obtain relationships between the forces and displacements in each element which could be collected together to derive matrix relationship for forces and displacements on the whole structure. Given the forces and constraints on the structure these matrix equations could be solved to give the displacements at the end of the elements, and the stresses could then be estimated. In the late fifties and early sixties, more advanced elements were introduced. Turner et al.

[4] in 1956 first derived an element stiffness matrix for a triangular element using a linear displacement function. Subsequently many investigators, e.g. Argyris [5], Gallagher et al. [6] and Zienkiewicz [7], developed elements for different stress conditions with more refinement, covering bending and with triangular, rectangular, quadrilateral and tetrahedral three-dimensional elements. Argyris et al. [8] extended the method to elastic-plastic stress problems by making use of so-called thermal strain approach similar to that suggested by Mendelson and Manson [9]. Zienkiewicz et al. [10] developed a general formulation for the elastic-plastic matrix for evaluating the stress increments and proposed a new "initial stress" computational process.

The late sixties and early seventies saw the consolidation of the finite element method into a number of large general purpose software systems. To date, there are more than 40 systems [11], examples being NASTRAN from NASA, PAFEC from Nottingham University and LUSAS from London University. Until the mid-seventies finite element analysis was exclusively performed on large mainframe computers with consequent high costs. The emergence of the personal computer and the advances in computer hardware together with a number of sophisticated pre- and post-processor finite element software packages have helped to make the method more economic and popular in engineering design analysis. Stephen and Taylor [12] presented the finite element method as a valuable analysis technique to machine tool structural designers. It was found that the method was best for static analysis. Dimitriou [13] studied the distinctive features of elastic-plastic problems and the role of the notched plate as a classical problem in elastoplasticity. It was suggested that the value of the notched plate as a test of new theoretical and experimental techniques of the solution might be increased by means of specific checks of details. Cowley and Hinduja [14] have developed a finite element computer program for the static deformation of machine tool structures and structural

elements. Their program permitted the structure to be subdivided into rectangular and triangular elements. A sub-structure was also incorporated into the program to save computation time for large structures. It was found that the accuracy of the program was in good agreement with those obtained from the experimentally derived solutions. Zienkiewicz and Phillips [15] presented a computer orientated method which generated meshes of triangular elements in plane and curved surfaces. This was to help to reduce the effort involved in preparing the input data for the FEM models. Some examples were illustrated to show the range of meshes that could be generated. It was indicated that the method could be extended to generate the three-dimensional tetrahedral elements. Hinduja and Cowley [16] have discussed the computing costs and computed results, which correspond to various finite-element representations, of a thin-walled base-type column structure subjected to both torsional and bending loads. The results were compared with experimentally derived values and with calculations based on closed form analytical expressions. It was shown that the accuracy of the computed static deformations depended on the specific nature of the finite-element model adopted. It was also found that the resulting accuracy increased as the finite element model became more refined. Optiz and Noppen [17] have described a finite element computer program system FINEL which permitted the structure to be analyzed with respect to their static characteristics. It was found that for various types of structural elements the finite element method was ideally applicable for the analysis of a wide range of different problems occurring in the design of machine tools. Buell and Bush [18] have different schemes for automating input data to finite element computer programs. Each of those schemes was applicable to a special set of topologies. It was suggested that it would be desirable to have a library of those schemes from which the user could pick the method to best satisfy his modelling problem. Key [19] addressed the computational procedure for large deformation dynamic responses of axisymmetric solids. It was found that the results of the computations were in good agreement with those obtained from the literature. Biffle and Becker [20] used the finite element method to obtain the

solution to wave propagation problems in solids with elastic-plastic material properties. The iterative procedure, which was presented in their work, used the finite element strain-displacement equations and the plasticity relationships to determine the state of stress at the end of the time step. It was concluded that the solution converged satisfactorily for most problems and the convergence could be accelerated without a significant loss in accuracy.

Subsequently there has been many investigations in which finite element method has been used as a tool for practical design analysis. Weck and Zangs [21] discussed the possibilities and limitations of the calculation of thermal behaviour of machine tools using finite element technique as a computer aided design. It was found that this method was limited to give required accuracy and some suggestions were made. Singh et al. [22] applied a beam element to analyze the distortion of a 4-column, 10 tonne press equipped with a 4-guide pillar sub-press. The influence of eccentric load and the change of the main dimensions of the press and the sub-press were computed. It was shown that optimization of the sub-press design can be carried out and the results agreed well, both with the measurements and practical experience. Blum [23] adapted the finite element program system ASKA to study the behaviour of a double-column eccentric press. The relationship between the ram and the slide guide of the press, considering the contact surfaces, was investigated. It was suggested that the method adopted could be applied to a vast field where problems of contact need to be considered. Murthy et al [24] developed a finite element software package to investigate the influence of the thermal effect on the accuracy of a hydraulic surface grinder. The results obtained showed that the method can be applied to estimate the straightness of the machine guideways. Reddy and Rao [25] used the finite element method to study the parameter design of a horizontal knee-type milling machine. The results were discussed theoretically and showed significant usefulness of applying the technique in machine tool

design. Prabhu et al. [26] investigated the experimental and the finite element approaches to determine the natural frequencies and mode shapes of vertical broaching machine. It was shown that the discrepancies between the results obtained in the finite element method and experiments may have been due to the fact that the boundary conditions applied in the finite element method could not be fully met in the experimental method. Haranath et al. [27] used the finite element approach to investigate the dynamic and static behaviour of multicell machine tool columns, using a simple element with two degrees of freedom. It was found that warping affects considerably the bending and torsional behaviour of such columns. This study was found to be highly useful as a design tool. Bahl and Pandey [28] presented the finite element technique as a computer aided analysis and design tool to determine the bending and torsional stiffness of cross and diagonally beams. It was observed that the results were in fairly close agreement with the available analytical and experimental findings. Gupta and Somasundaram [29] studied different methods of stiffening the machine tool columns when subjected to bending and torsional loads. The results indicated the preferential methods of stiffening the machine tool columns. Dube and Talukdar [30] utilized the finite element method for numerical analysis of the dynamic characteristics of milling machine structure employing beams elements with six degrees of freedom per node. The analysis was carried out for a scaled model of perspex. The objective of this study was to obtain knowledge of dynamics characteristics which may have been used in improving the structural design of the milling machine by saving material and increasing the dynamic rigidity of the structure. A conclusion was drawn after a comparison was made among different cases considering the dynamic rigidity as the main comparative factor. Gupta and Somasundaram [31] presented results of the analysis carried out on the joint between a machine tool column and the base employing

the finite element method. It was noted that the presence of joints in machine tool structural components lowered the rigidity of machine tool; proper fastening arrangements could have restored, to a large extent, this rigidity. Okamoto and Nakazawa [32] developed a theoretical method which gave a solution for non-linear contact problems. That method was based on the finite element method and load incremental theory. Some common contact problems in engineering practice were discussed. The calculated results showed a reasonable agreement with experimental data. Murthy et al. [33] discussed the application of the finite element method to functional optimization of machine tools structure. It was stated that the application of this technique helped in reducing the relative deformation between the machine tool column and the base which affects their perpendicularity. Rao et al. [34] investigated two designs of a column of horizontal machine centre using the finite element method. Gupta and Ramanamurti [35] adopted a technique to solve the problem of computing cost and time for stress analysis of a 400 tonne hydraulic press cross-head. That technique was based on the semi-analytical finite element method. Theoretical and experimental results were obtained and it was found that these compared well. Vijayaraghavan et al. [36] dealt with the evaluation of stresses and displacements of broach tools and workpiece using finite element method. Certain criteria for the selection of the right tool geometry for a particular work material was explained. Tayal [37] introduced a solution for the static and dynamic performance characteristics of tilted two-lobe bearings using finite element method. The results were obtained for different values of tilt angle and the stability for the journal bearing system was discussed. Wissmann and Hauck [38] presented higher algorithms for the solution of elastic-plastic problems using the finite element method with the aim of satisfying demands on accuracy and computational costs. It was demonstrated that those algorithms enabled

a very efficient and accurate solution of elastic-plastic problems and were especially useful for general purpose programs. Murthy and Reddy [39] studied the approximate and the exact methods for the finite element representation of the floating hinge, commonly encountered in the modelling of machine tools and allied machinery. It was found that the exact method might have caused an increase in the nodal bandwidth. Voyiadjis et al. [40] investigated the plain-strain problem for a smooth, rigid, circular shaft in contact with a cylindrical, circular cavity in an infinite body subjected to uniaxial stress applied at infinity. The finite element method was used employing constant strain triangular elements. It was found that the method of solution to such problems may have been applied to any other cylindrical shape of the rigid inclusion in the infinite body. Wang et al. [41] described an efficient method for sensitivity analysis in shape optimum design. That method was incorporated into a finite element analysis code and numerical examples were performed and comparisons made with sensitivity analysis based on forward finite differences. The results showed that the method was basically correct, feasible and reasonable. Stafford et al [42] discussed the computational time tests that were used to determine speed of computing on some desk-top computers for finite element analysis. Some comments were made regarding the selection of a desk-top system to do finite element analyses. Shephard and Yerry [43] discussed finite element based modelling procedures which were developed and combined to create an automated procedure capable of producing optimum shapes for three-dimensional components. Kennedy et al. [44] described the development of a finite element program, SAFE/RAS which was used for the purpose of analyzing the performance of nuclear reactor component in the near-failure regime where large deformation and non-linear material response occurred. The performance of that program was also studied in problems which included both geometrical and material non-



linearities and dynamic buckling behaviour. Moyer and Liebowitz [45] formulated the governing finite element system for elastic-plastic analysis of fracture specimens in three dimensions. The full incremental elastic-plastic finite element formulation was presented and specific choices were made in that formulation based on experience with two-dimensional studies. It was stated that the approach presented would be adequate for most engineering metals at room temperature. Chattopadhyay [46] presented an efficient digital computer procedure, along with the complete listing of the associated computer program, which may be conveniently utilized for the solution of certain broad class of elastic-plastic problems. It was concluded that the procedure could have been extended further to economize the computation time for the solution of metal working problems. Dybbro and Holm [47] developed a numerical method for solving three-dimensional shape-optimization problems. That method combined finite element and linear programming in a series of iterations (redesigns). The stress analysis was established by the linear strain tetrahedron element. The approach was applied to two different examples for which the analytical optimum shapes were given. Those examples showed that optimal designs close to analytical optimality were achieved in extremely few iterations. Sinha and Murarka [48] investigated the optimal design of a 918 KN hydraulic press structure using finite element method. It was found that the model adopted was useful for a comparative study. Kumar et al. [49] used the ANSYS FEM package to investigate the role of restricted contact cutting with varying angle and width of the land on the magnitude and distribution of internal stresses in carbide tips during turning. The numerical results were compared with those obtained from the experiment. It was found that tool failure by brittle fracture could have been reduced by incorporating proper land in the cutting edges. Patil [50] utilized the finite element method to develop a numerical model to analyze the stress distribution and torsional

stiffness of irregular machine top cross-sections. It was concluded that the procedure adopted helped the tool designer when conceiving the desired machine top cross-sections without much computation. Chavez et al. [51] developed a software package to automate three-dimensional finite element and boundary element model generation. That software package could interact with the analysis package being used to produce optimal models by automatically improving the discretization via an implemented error estimator and error smoother. Sinha [52] presented a model for a computer aided design course, which included finite element method, for undergraduate/graduate curriculum. He suggested ways and means by which such a course could have been run most economically for the maximum benefit of the students. Tang et al. [53] developed two macros, for the general-purpose finite element code named ANSYS, to monitor errors and automate mesh refinement for a class of stress analysis problems that possessed degenerated cases of known exact solutions. It was found that the approach was significant to the evaluation of reliability of finite element solutions of complex problems. Kuman et al. [54] presented the development of a structural design optimization methodology and a software system DESIGN-OPT by integrating numerical optimization techniques, finite element methods, and pre-and post-processing tools. The commercially available codes COPES/ADS and ADINA were employed for numerical optimization and finite element analysis, respectively; and software packages like MOVIE.BYU, PLOT10 and SUPERTAB were used for pre- and post-processing purposes. A variety of design problems related to both size and shape optimization were presented as illustrative examples. Some remarks were made for further research on the subject.

Grierson and Cameron [55] described the development of a knowledge-based expert system (KBES) involving the coordinated use of finite element analysis, sensitivity analysis and optimization techniques to design minimum weight planar steel frameworks. The essential feature of that work was the separation of the well-structured numeric tasks of analysis and optimization from the non-structured. It was stated that the approach could directly conduct the design in exactly the way specified by the designer without making any judgements on its own. Kramer and Grierson [56] used the finite element to develop a computer-based structural design methodology for the minimum weight design of planar frameworks subjected to dynamic loading. That method could account for combined axial and bending stresses, and was capable of designing minimum weight structures under simultaneous static and dynamic loading. Several examples of framework design were presented to illustrate the features of the design method.

Recent activity in finite element analysis has emphasized refinements in geometry and material properties of articular joints. Galbraith and Bryant [57] used the ABAQUS finite element package to investigate a linearly elastic model of cartilage/bone complex. The resulting solution for stresses, strains and displacements was compared to the published reference model and a good agreement was found. Finnigan et al. [58] discussed the role of the modelling geometry in achieving automation and control of the overall finite element analysis process. The automation of this process from the prospective of single-pass analysis, as well as iterative analysis, where the geometry may change radically as a function of time, was considered. It was suggested that further study should be carried out on three-dimensional finite element modelling. Forde and Stiemer [59] have shown that control logic of the finite element analysis may be

separated from analysis software and that a knowledge-based expert system can use that logic to perform interactive computation. General activities and constraints, practical methods of reasoning and representations, and knowledge-based expert system were discussed with emphasis on applications to interactive finite element analysis. An analysis control expert system was developed for use in numerical analysis of two-dimensional linear problems in solid and structural mechanics. It was concluded that knowledge-based control was more effective and flexible than algorithm-oriented control. Subsequently Baker [60] described a method for generating tetrahedral finite element meshes. Techniques for controlling the distribution of mesh points and tetrahedral quality were also discussed. Kosrowjerdi [61] discussed the integration of the ANSYS finite element software package into mechanical engineering laboratory and design related courses at Western New England College (WNEC). It was shown that the use of ANSYS greatly helped the students to understand good analysis techniques and allowed them to develop improved engineering judgement skills. Singh and Miller [62] developed a three-dimensional finite element model to investigate the design analysis of a twin head horizontal press. Some suggestions were made to improve the stiffness and torsional rigidity of the press.

In parallel with the finite element software developments, advances in computer hardware have largely been responsible for the recent progress in structural optimization. Continued success in this area, together with the increased demand for even more efficient designs, has fostered a growing interest in more difficult problems of shape optimization. In this case a new mesh is generated for each trial design. Consequently, more cost effective finite element mesh generation has become a critical issue in the applications involving relatively complex shapes.

Despite the steady progress in finite element analysis, the three-dimensional mesh regeneration can still be a rather expensive process. The evaluation of discretization errors and the design of suitable meshes via adoptive mesh refinement, for finite element analysis at minimum cost and time, are nowadays the most challenging issues in the practical design analysis of the structure. A viable alternative to the finite element method, the boundary element method has been developed to reduce the cost of the three-dimensional mesh discretization [63]. However, in large problems improved accuracy can be offset by the increased cost in numerical integration.

A major problem of the finite element method is the generation of the initial finite element model. This usually requires well experienced users in order to generate a model with a satisfactory mesh of an appropriate element size. Development of a computational system for finite element modelling has been carried out. Kim and Kobayashi [64] have developed a complete three-dimensional rigid-plastic finite element code for simulating gap-controlled plate rolling. The effect of preform shapes on the geometry of the final plates was investigated. It was revealed that the finite element method was a powerful tool for economical performance and process design for reducing yield loss in plate rolling. Saleh and Hashmi [65] have developed an elastic-plastic finite element computer program for plain strain/stress to investigate the quasi-static deformation mode of a thin ring structure subjected to different loading conditions. A comparison was made between the experimental and theoretically predicted results and reasonable agreement was found. Destuynder [66] has developed a criterion associated with the growth of the crack of a structure under dynamic loading using a finite element model. It was stated that the use of a such a model permitted the development of an active control law to reduce the evolution of the crack.

The generality and versatility of the finite element method enables engineers to tackle complex engineering analysis problems, but its usefulness and efficiency are hampered by the need to generate sufficiently accurate meshes. In the last few years, much research attention has been devoted to the automation of finite element mesh generation which has led to the development of a variety of automatic mesh generators. These mesh generators required the user to specify the mesh density distribution. Young and Grosse [67] have presented a computational system to automatically generate a near optimal initial finite element mesh for a two-dimensional component without user intervention.

Yang [68] has discussed a modular shape optimization system for complex three-dimensional solid component incorporating commercially available modelling and analysis programs. However, the emphasis was placed on the design modelling considerations. Dvorak [69] has described a finite element software system which it was believed to make the design operation, such as shape optimization, easier. El-Sayed and Hsiung [70] have presented a new method for structural optimization by parallel finite element method. Some numerical examples were discussed in relation to their obtained speedups.

### **1.3 Current work**

The current work describes a systematic procedure for investigating the performance and design analysis of the welded structure of a 150-tonne hydraulic press machine. This machine was designed by ENERPAC without any proper measurement facility or variable hydraulic system. Modelling has been carried out mathematically and experimentally. This was to establish accurately, the optimum design and further development of the press machine and to assess the applicability of PC based FE package for such objective.

The theoretical model is based on both the conventional analytical formula and numerical technique, using finite element method. The conventional model is based on the simple bending theory using the total strain energy principle for 2-D beams. This was to predict the characteristics of the stiffness of the structure of the hydraulic press. In order to make comprehensive use of this model, a computer program has been developed to facilitate the calculations of the predicted results at several load increments from a simple input data.

The numerical model was based on the application of the finite element method. The LUSAS finite element software package and a 486 processor personal computer (PC) have been used to perform the analysis. In order to simplify this model and to make use of the present computing software and hardware, the complex hydraulic press structure has been discretised into a number of components and modelling was carried out with different factors. The factors considered were: the boundary conditions; the mesh density; and the type of elements.

The experimental model involved the development of the press machine so as to make a comparative study between the theoretical models and actual press machine. This included the design of the measurement system; the design of the hydraulic system; the design of the electronic interfacing base; the design of the platens and loading tools; and the development of a computer program for facilitating the experimental measurement of the load and deformation of the press machine and the load deformation of the workpiece.

The sequence of the process of the current investigation is shown in Fig.(1). This consists of the following:

(i) The model modifications:

At this stage, several theoretical models were proposed to describe the behaviour of the press structure. The FEM analysis of this structure were performed with different factors. These factors were: the element types, the mesh density and the boundary condition. The theoretically predicted results were compared with the experimental results. This was performed to establish the accuracy of the experimental models and to evaluate the time required for the analysis.

(ii) The theoretical design modifications:

The optimum mathematical model evaluated in the previous stage had undergone a series of theoretical design modifications with different structural parameters. The objective of this was to study the effect of the structural parameters on the stiffness of



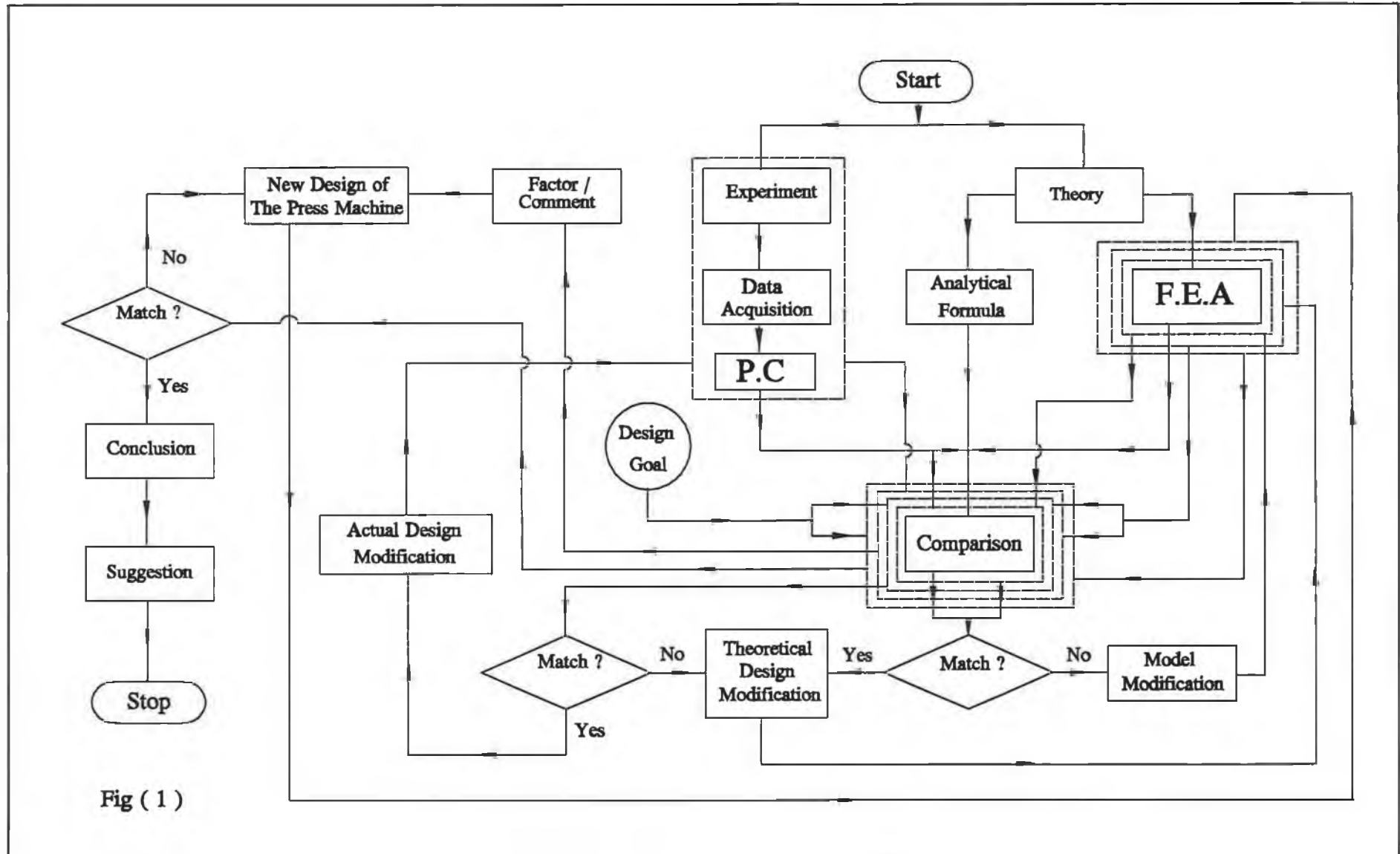


Fig ( 1 )

the actual hydraulic press structure and to assess the possible improvement of this structure. The mathematically predicted stiffness of the structure of the press was compared with the stiffness obtained from the design goal in the literature to evaluate the standardization of this structure. This comparison was carried out using a convergent factor which has been considered to satisfy the requirement of the practicability of the actual design modification. The parameters of the structure considered were: addition of stiffeners to the press bed, the thickness of the stiffeners, and the thickness of the press bed.

(iii) The actual design modification:

The actual press structure was modified according to the optimum theoretical design modification considered in the previous stage. After the modification, a comparison was made between the theoretically predicated results and experimental results. Consequently, the accuracy of the analysis was evaluated.

(iv) The new design of the hydraulic press structure:

As a result of the previous theoretical and experimental analysis, a new theoretical model was proposed to suggest a new performance of the hydraulic press structure. This study was to find the functional conditions of the press structure within the limit of the design goal. Thus, the stiffness characteristic of the press structure was studied with different factors in order to optimize the design of this structure. The factors considered were the width and the chamfering of the press structure.

The detailed description of the basic procedure of the current investigation is given in the following Chapters.

## **CHAPTER 2**

### **THE FINITE ELEMENT METHOD**

There are more than 200 books on the theory of finite element methods [71]. Some of these books have been classified by NAFEMS (National Agency for Finite Element Methods and Standards) in England. Their books "Guidelines to Finite Element Practice" and "A Finite Element Primer" are recommended for a reader as references for finite element. In general, there are many books written on the finite element technique. If required, further specific information on this subject can be obtained from references [72], [73] and [74]. However, it is felt that a general overview will enhance the reader's understanding of the subsequent work.

#### **2.1 Introduction**

The finite element method is a technique for numerically modelling a component to give the value of a desired unknown quantity at any location of that component. This method requires large quantities of data which are manipulated by matrix techniques.

Typically in a such technique the structure or region of interest is subdivided into a mesh of elements which have nodal points at their vertices and possibly at other positions. By assuming certain displacement patterns, which describes the deflection under load for any point within the element as a function of the corresponding nodal displacement, it is possible to derive an approximate solution for the elastic properties of this element. This can be carried out by applying the principle of virtual work. The

elastic behaviour can be expressed by a stiffness matrix, which relates nodal forces and thereby resulting nodal displacements to each other. From this stage it is then possible to derive an approximate solution for the deflection and all the strains and stresses acting within the structure for known elastic properties of the material. This can be done after considering the boundary condition and the load, which are acting externally upon the structure. These general remarks about the prediction of the static behaviour of a structure by means of the finite element method is shown in Fig. (2). In fact, both geometric non-linear (large-deflection) and non-linear stress strain relationships are amenable to this technique, in which the load is applied in small increments over which the structure behaves linearly. In practice, the problem is then solved using a finite element computer program.

From this general overview, it is evident that finite element analysis is a computer aided design technique. This technique is commonly used to predict the failure and help to achieve the optimal design of the structure of a simple, as well as complex geometry. In general, this process requires a large amount of data. This could be a tedious task and time consuming. However, development in computer graphics and CAD are helping to reduce the drudgery involved in the analysis.

## **2.2 The applications of Finite Element Analysis**

The objectives of the finite element method are to establish the potential failure modes and to help achieve the optimal design of the structure being modelled. The applications of the method fall into the following categories:

## The Finite Element procedure

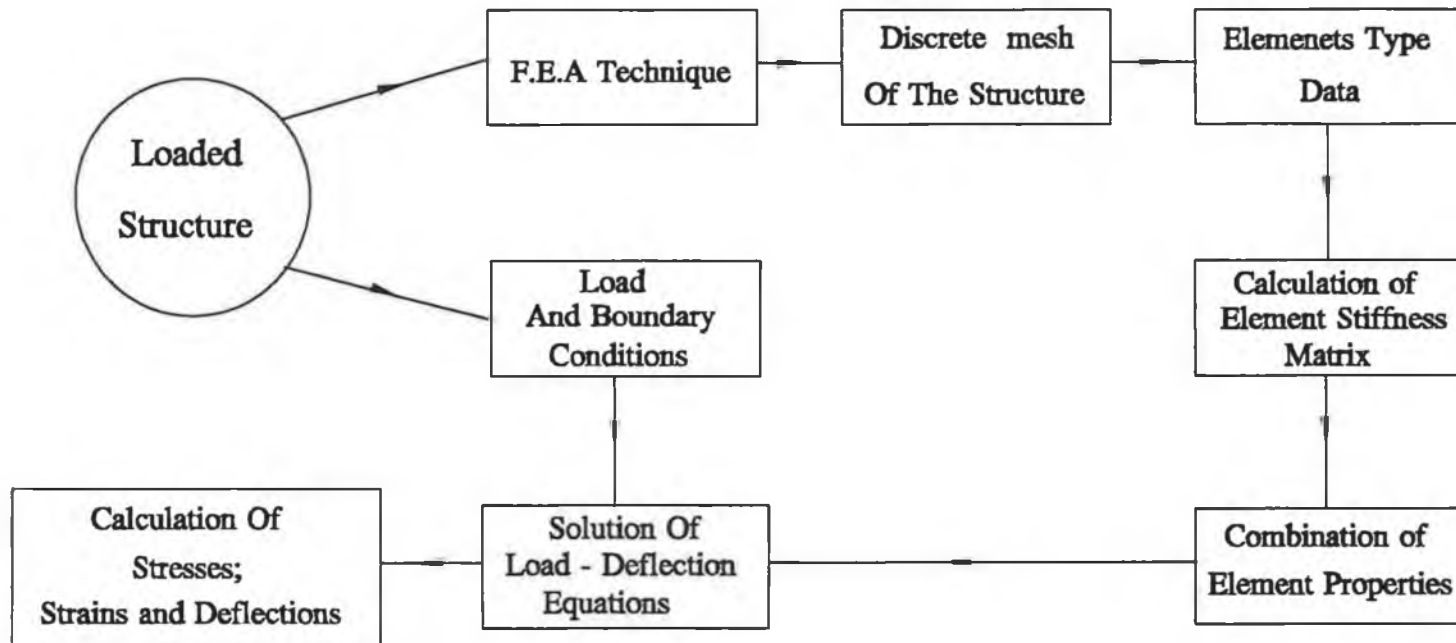


Fig ( 2 )

- (i) Static or equilibrium or steady state or time independent analysis
- (ii) Dynamic analysis
- (iii) Field analysis
- (iv) Linear analysis
- (v) Non-linear analysis.

The most frequent application in the solution of the solid mechanics problem is probably the solution of category (i). In this solution the steady state displacement or stress distribution is required.

### **2.3 Element Types and Geometry**

As previously mentioned, in any application of the finite element method, a complicated structure is subdivided into pieces or elements each of finite size. Hence, there are different groups of elements for different applications. Each element is usually a rectangular or triangular in 2D or 3D, of a reasonably proportioned size. Also, the element has certain material properties, i.e. Young's modulus and Poisson's ratio. Because the elements have a simple shape it is possible to produce equations which relate the forces of the element to the displacements. This is well known as the element stiffness matrix. Accordingly, each category of the application of the finite element method has a particular type of element for which the element stiffness matrix has been established. Elements which use parabolic or cubic functions rather than linear interpolation are commonly used for improved accuracy. These elements often have node points along their sides as well as at their corners and consequently they can be set up to model curved edges. Trusses and frame structures can be modelled using the

one dimensional beam element, whereas solid structures can be represented by brick type of elements.

The three-dimensional structures which are made from thin steel materials can be modelled using shell type elements. Two dimensional elements represent flat plate type structures or cross sections of structural components. The behaviour of components which are bodies of rotation such as cylinders can be presented by modelling cross-sections with axisymmetric elements thus turning a three dimensional problem into an easier to deal with two dimensional problem.

#### **2.4 The Finite Element Model**

The art of the finite element analysis lies in the development of a suitable model idealization. The element discretization, or mesh, must neither be too fine, making the preparation of data, the computer execution time, or interpretation of the results excessively expensive, nor too coarse, rendering the accuracy of the results unacceptable.

In order to develop a suitable idealization, some knowledge of the likely distribution of stress or their field equivalent, is required. Consequently, a knowledge of the interpolation of the chosen element, an estimate of the level of discretization can be made. This could provide results of acceptable accuracy. However, such an estimation is not usually straightforward, especially where a localised response or high gradients are involved. The initial mesh, which is often unsatisfactory, may then be refined or modified in the area of interest, to obtain results which are of an acceptable accuracy. This also requires a specification of appropriate element size.



Nowadays most of the finite element software systems provide a facility to check the area of high gradient. These systems can accommodate either constant or linear variations of stress. The probable stress distribution can be estimated along a line and fit the curve with lines representing the response of the element to be used. Also a good system is a system in which the mesh generator gives a satisfactory mesh of appropriate element size before and after the analysis. However, checking the calculated reaction forces of the structure at the restraints is a useful guide to a reliable mesh.

## **2.5 Errors in the Analysis**

These errors are the numerical inaccuracies which may lead to invalid finite element solutions. The two main causes of such inaccuracies are; either faults in the input data ; or poor modelling, or sometimes both of them. The inaccuracies caused by the faults in the input data appears when the finite element model does not represent the physical model, and it should be appreciated that many errors in the analyses are due to this reason. Poor modelling produces what is commonly known as round-off error and results in the poor condition of the stiffness matrix.

The poor condition of the stiffness matrix results in a loss of accuracy in the evaluation of the large variation in magnitude of the diagonal stiffness terms. This in turn leads to inaccuracies in the predicated displacements and stresses. However, in order to minimize the effects of errors the following steps should be considered when modelling takes place:

- (i) Elements should have well defined shapes, that is, as near to squares and equilateral triangles as possible for quadrilateral and triangular elements respectively.
- (ii) Elements with large aspect ratios, i.e. the ratio of the longest to shortest element side lengths, are not recommended and poorly defined element shapes should not be used in the area of critical interest.
- (iii) The use of poorly graded discretizations should be avoided. Poor grading may be the result of either large relative size or stiffnesses between adjacent elements..
- (iv) In a mesh where different types of elements are joined together it should be ensured that the connections are fully restrained, otherwise unrestraintment may occur due to the mismatch in nodal freedoms.
- (v) Structures must be supported to avoid the singularity which is also caused by rigid body displacement and rotations.

Errors should be detected during the analysis and the computational process should be stopped if these errors are found. Also, in this case, a comprehensive message should be displayed.

## 2.6 Fundamental Finite Element Formulations

It is intended to give a brief introduction to the mathematical formulation of the finite element method. These formulations form the basis for the evaluation of the response of a structure with different applications of the finite element method.

In the procedure of the finite element method, as previously stated, a continuum is hypothetically divided into a number of elements (1D, 2D and 3D) interconnected at nodal points to calculate displacement; strain and stress. The element is constrained to deform according to a prescribed pattern which is expressed in a mathematical formula. There are three types of commonly used elements: The displacement element using assumed displacement patterns; the equilibrium elements based on assumed stress patterns and; the hybrid element based on both assumed displacement and stresses. The overwhelming majority of all the known finite element patterns is the displacement element. It is preferred because it has all the provisions for irregular geometry, isotropic, orthotropic or anisotropic material and arbitrary boundary condition. Also, mathematically, the method can be shown to converge towards the exact solution as the number of elements are increased, provided the criterion for convergence is satisfied by the element.

Of the various approaches to finite element formulation, the variational method has been most widely accepted. This method is an integral expression that yields the governing differential equations and boundary conditions of a problem when given the standard treatment of calculus of variations.

### 2.6.1 Linear static analysis

A solution satisfying the equilibrium, compatibility and constitutive equation is of course the correct solution for a linear static problem. The equilibrium, in this solution, is the relationship between the external load and the stresses, the compatibility represents the relationship between the strain and displacement and the constitutive equation is the relationship between the stress and the strain.

The linear static analysis is one of the applications of the finite element analysis. The analysis is commonly used to calculate the displacement at the nodes for given applied forces at the nodes. Stresses in each element can then be calculate from the deflections. The relationship between the force and the deflection is derived for each element. The contributions from individual elements are combined to give a stiffness matrix. Boundary conditions and load are specified and the resulting set of equations are solved to obtain the displacement.

In order to establish the governing equations of equilibrium a general three dimensional body, subjected to a vector of surface forces  $\{t\}$ , body forces  $\{f\}$  and concentrated load  $\{F\}$ , is considered.

The body will be displaced from its original configuration by the amount  $\{u\}$  which gives rise in strains  $\{\epsilon\}$  and corresponding stresses  $\{\sigma\}$ . The governing equations of equilibrium may be formed by utilizing the principle of virtual work. This states that during any virtual displacement  $\{\delta u\}$  imposed on the body, the total internal work is

equal to the total external work, i.e.

$$\left. \begin{aligned} \int_v \{\delta \epsilon\}^T \{\sigma\} d(v) &= \int_v \{\delta u\}^T \{f\} d(v) + \\ \int_{sr} \{\delta u\}^T \{t\} d(sr) &+ \sum \{\delta u\} \{F\} \end{aligned} \right\} \quad 2.1$$

where  $\{\delta \epsilon\}$  are the virtual strains corresponding to virtual displacements  $\{\delta u\}$ ;  $(v)$  and  $(sr)$  refer correspondingly to the volume and surface area of the body.

In finite element analysis, the body is approximated as an assembly of discrete elements interconnected at the nodal points. The displacements within any element are then interpolated from the displacements at the nodal points corresponding to that element, i.e. for an element

$$\{u^e\} = [N^e] \{a^e\} \quad 2.2$$

where  $[N^e]$  is the vector of displacement interpolating or shape function matrix and  $\{a^e\}$  is the vector of nodal displacements.

The strains  $\{\epsilon^e\}$  within an element may be related to displacements  $\{a^e\}$  by:

$$\{\epsilon^e\} = [B^e] \{a^e\} \quad 2.3$$

where  $[B^e]$  is the strain-displacement matrix. For linear elasticity, the stresses  $\{\sigma\}$  within the finite element are related to the strains using a constitutive relationship of the form.

$$\{\sigma^e\} = [D^e] \cdot (\{\epsilon^e\} - \{\epsilon_0^e\}) + \{\sigma_0^e\} \quad 2.4$$

where,  $[D^e]$  is the matrix of elastic constants,  $\{\sigma_o^e\}$  and  $\{\epsilon_o^e\}$  are the initial stresses and strains respectively e.g. due to thermal effects.

Therefore using equations (2.2); (2.3) and (2.4) the virtual work equation (2.1) may be discretized to give

$$\begin{aligned}
 & \sum_1^n \{\delta a\}^T \cdot \int_v [B^e]^T \cdot [D^e] \cdot [B^e] \cdot \{a^e\} \cdot d(v) \\
 & = \{a^e\}^T \cdot \left[ \sum_1^n \int_v [N^e]^T \cdot \{f^e\} \cdot d(v) \right. \\
 & \quad \left. + \sum_1^n \int_{sr} [N_{sr}^e]^T \cdot \{t^e\} \cdot d(sr) \right. \\
 & \quad \left. - \sum_1^n \int_v [B^e]^T \cdot (\{\sigma_o^e\} - [D^e] \cdot \{\epsilon_o^e\}) \cdot d(v) + \{F\} \right]
 \end{aligned} \tag{2.5}$$

Where  $[N_{sr}^e]$  are the interpolating functions for the surfaces of the elements and  $n$  is the number of elements in the assembly.

By using the virtual displacement theorem, the equilibrium equations of the element assemblage becomes:

$$[K] \cdot \{a\} = \{R\} \tag{2.6}$$

where  $[K]$  is the structure matrix, defined as

$$[K] = \sum_1^n \int_v [B^e]^T \cdot [D^e] \cdot [B^e] \cdot d(v) \tag{2.7}$$

and  $\{R\}$  is the vector of the structure forces defined as

$$\{R\} = \{R_b\} + \{R_{sr}\} + \{R_o\} + \{R_c\} \tag{2.8}$$

$\{R_b\}$  is the force vector due to the element body loads given by

$$\{R_b\} = \sum_1^n \int_v [N^e]^T \cdot \{f^e\} \cdot d(v) \quad 2.9$$

$\{R_s\}$  is the force vector due to the element surface tractions given by

$$\{R_{sr}\} = \sum_1^n \int_{sr} [N_{sr}^e]^T \cdot \{t^e\} \cdot d(s) \quad 2.10$$

$\{R_o\}$  is the force vector due to the initial stresses and strains given by

$$\{R_o\} = \sum_1^n \int_v [B^e]^T \cdot (\{\sigma_o^e\} - [D^e] \cdot \{\epsilon_o^e\}) \cdot d(v) \quad 2.11$$

$\{R_c\}$  is the force vector due to concentrated loads expressed as

$$\{R_c\} = \{F\} \quad 2.12$$

Equation (2.6) maybe utilized for situations where the applied loading is independent of time or when the load level changes very slowly. If rapid changes in the load level occur, inertia and damping forces must be included in the equilibrium equation.

### 2.6.2 Structural dynamics

The reduction of vibration in engineering components is a common design exercise to eliminate fatigue failure, to reduce noise, or to ensure the accurate operation of mechanisms. The finite element method is capable of modelling dynamic effects by taking into account the inertia and the damping forces as part of the body load vector. The resonant frequencies of vibration and the corresponding mode shapes can be calculated and used to predict the response to steady state harmonic forces. Assuming the acceleration and velocities are approximated using the same interpolation function

as displacement i.e. the velocity

$$\{\dot{U}^e\} = [N^e] \cdot \{\dot{a}^e\} \quad 2.13$$

and the acceleration

$$\{\ddot{U}^e\} = [N^e] \cdot \{\ddot{a}^e\} \quad 2.14$$

The body force vector in equation (2.9) then becomes:

$$\left. \begin{aligned} \{R_b\} = \sum_1^n \int_v [N^e]^T \{f^e\} - \rho^e \cdot [N^e] \cdot \{\ddot{a}^e\} \\ - C^e \cdot [N^e] \cdot \{\dot{a}^e\} \cdot d(v) \end{aligned} \right\} \quad 2.15$$

where  $\rho$  is the density and  $C$  is the damping constant for the material.

Substitution of equation (2.15) with equation (2.6) leads to the dynamic equilibrium equations

$$[M] \cdot \{\ddot{a}\} + [C] \cdot \{\dot{a}\} + [K] \cdot \{a\} = R(t) \quad 2.16$$

where  $[M]$  is the mass matrix defined as

$$[M] = \sum_1^n \int_v [N^e]^T \cdot [\rho^e] \cdot [N^e] \cdot d(v) \quad 2.17$$

and  $[C]$  is the damping matrix defined as

$$[C] = \sum_1^n \int_v [N^e]^T \cdot [C^e] \cdot [N^e] \cdot d(v) \quad 2.18$$

It can be seen from equation (2.16) that it is no longer necessary to assume that applied loadings and their effects are instantaneous, and the transient effects of the inertia and damping are considered.



### 2.6.3 Non-linear static analysis

While the assumption of linear static analysis is valid for many applications there are a host of analytical problems which arise from more complex material properties. Plastic and metals above the yield point have non-linear stress strain curves which must be simulated in many types of analysis. The simulation can be done by using the finite element method. This method considers several forms of non-linearities including material non-linearity, geometric non-linearity and non-linear boundary conditions. The materially non-linear analysis should be utilized if the material stress-strain relationship is significantly non-linear (e.g. elastic-plastic; cracking material response). Geometrically non-linear analysis takes into account the changing effect of deformation on the structural stiffness and on the position of applied loads. In the analysis of non-linear boundary conditions the boundary conditions are modified during the course of the analysis depending upon the deformation shape of the structure. Non-linear boundary conditions are imposed by using joint element or sliding boundary condition techniques. Many non-linear solutions work by applying loads in small increments and modifying the properties of the structure at each step.

It has been established that in the non-linear compatible equations the strain-displacement matrix  $[B]$  is of the form

$$[B]=[B_0]+[B_1(\{a\})] \quad 2.19$$

where,

$[B_0]$  is the infinitesimal strain-displacement matrix, and

$[B_1(\{a\})]$  is the non-linear strain-displacement matrix (displacement dependent).

The non-linear constitutive relationship has been given in incremental form i.e

$$d\{\sigma\}=[D]_{ep}.d\{\varepsilon\} \quad 2.20$$

where  $[D]_{ep}$  represents the elastic-plastic matrix.

Considering the principle of virtual displacement, the equilibrium conditions can be written as

$$\{\psi(\{a\})\}=\left[\int_v [B]^T.\{\sigma\}.d(v)\right]-\{R\} \quad 2.21$$

in which  $\{\sigma\}$  are the actual stresses dependent on the strain level reached and  $\{\psi(\{a\})\}$  represents the residual force vector dependent on the displacement. Therefore, a correction procedure is required to restore the equilibrium and hence to make the equation (2.21) equal to zero within the limit of a given convergence.

#### 2.6.4 Field analysis

The temperature distribution in the many components is a continuous function which could be accurately described by the solution of the differential equations describing heat conduction. However, in some cases the mathematical solution of such equations is not possible. The principle of the finite element method is to approximate this continuous distribution by calculating the values at certain points in the component and making an assumption as to the way the function varies between these sampling points. In order to do this a set of points should be selected known as nodes at which the temperature is going to be calculated. These nodes lie on elements which represent the way the temperature varies between the nodes. In such elements it is assumed that the temperature varies linearly with distance between the nodes. Therefore, if the

component was divided into a number of elements then the temperature distribution would be represented by a set of spot values at the nodes. It can easily be understood that the more elements that are used the more accurate such an approximation is likely to be and that the element density should be greatest in regions where the temperature changes rapidly.

In order to obtain a solution it is necessary to find a relationship between the heat flow into the component and the temperature. To do this a further assumption has to be made that the flow into the component occurs at the nodes. Then the equation required, relating the temperatures and heat flow, can be expressed in linear steady analysis in matrix form as follows:

$$[Z].\{\phi\}=\{Q\} \quad 2.22$$

where;

[Z] is a conductivity matrix,  $\{\phi\}$  is a vector containing temperature at each node and  $\{Q\}$  is a vector containing the heat flow rate into each node. The relationships between the nodal temperatures and heat flow into and out of the nodes of each field element in a component can be calculated. These relationships can then be assembled together to obtain the matrix [Z] in equation (2.22) which can be solved using a number of well-established numerical techniques for matrix equations. The non-linear steady state and transient field problems can be mathematically presented and solved using the finite element method.

## 2.7 The Solution of Finite Element Equation

The solution of the finite element equation is obtained by using large amounts of data

which are manipulated by the matrix technique on the computer. The most frequently adapted method of solving the equations in the finite element method is Gaussian elimination. This method consists of eliminating the equations one at a time so that there is a corresponding reduction in the size of the modified matrix until finally the matrix is reduced to one equation containing one variable.

The set of eliminating equations form a triangular matrix and is used for back substitution purpose. By starting at the last equation and working backwards to the first equation, one variable will be determined at each step by using the variables which are already known. This technique requires the structure stiffness matrix to be non-singular. For structural applications, this is equivalent to stating that for any displacement field the strain energy stored by the finite element system must be greater than zero. Therefore, the structure must be supported so that no rigid body displacements or rotations are possible.

When the procedure of Gaussian elimination is applied to the whole structure the matrix becomes too large both in terms of the computer memory requirement and the number of arithmetic operations in achieving a solution. Therefore, the frontal solution and frontwidth optimization technique are specific forms of Gaussian reduction used to minimize the number of operations performed and the core storage required during the solution of the equation. The frontal solution and frontwidth techniques are well suited for solving equations in non-linear, dynamic, eigenvalue and field analysis procedure.

## **2.8 Time for Solution**

The solution process of finite element equations are incredibly tedious, so most people opt to let the computer handle it as a background or batch task. This part of the finite element analysis process may be hardware intensive but the lead up to it, the preparation of the finite element model, is entirely live or people-bound. In general, the more elements that are used and the larger the quantity of unknowns, the longer the computer time needed to arrive at a solution. The computer time used to achieve the solution depends on the technique of ordering the elements or the nodes in the model.

In practice, a two-dimensional problem with a given number of elements is cheaper than a similar given number of elements of a three-dimensional problem. Also, the non-linear analysis can be many times more expensive than a similar linear problem. Typically, the dynamic analysis is about three times as expensive in computer time as an equivalent static problem [3], depending on the number of modes vibration that are to be predicted and on the level of structural damping. Most engineering components are lightly damped but components with heavy damping require more advanced solution approaches that can be very expensive. The response to shock loadings and transient forces can be calculated by time stepping methods; this can be expensive if many time steps are to be used. Therefore, familiarity with the finite element method will make the best use of it and provide a common sense assessment of the analysis.

## **2.9 The Finite Element Software Systems**

The finite element software systems have been classified, according to the applications

by NAFEMS (National Agency for Finite Element Methods & Standards) in England [71]. When a system is defined as general purpose it is applicable in many areas of engineering activity, and for many different types of structures and boundary conditions. Such a system is often especially efficient in certain classes of problems or for different industrial branches. A special purpose program is mainly aimed at solving problems restricted to certain class of problems or class of structures.

### **2.9.1 Selection of the finite element software system**

The choice of the proper system depends on the user's day-to-day needs. Some factors should be considered before the selection of the system. The main factor is the capability of the system i.e. is the system able to handle the user's most common problems? Also, the developer reputation, reliability and responsiveness should be considered. Moreover, the system should run on the computing facilities the user has. The performance of the system must be in standard test. Furthermore, the element library, the maximum problem size and the speed of the system are important factors. In addition, the quality of the documentation and the educational services (training courses, assistance by the consulting centres) are useful factors to be considered. Finally, a short period of time should be given to the user to try the system in-house before signing the final lease.

### **2.9.2 Training**

The basics of the finite element method can be learned relatively easily. However, this is just another engineering analysis tool and as such, skilful use takes practice and

experience. Hence, this can be difficult to acquire easily. Also, there are many analyses where the finite element system functioned perfectly well but the answers were at best unexpected or at worst completely wrong. Lack of experience in transferring the problem to a finite element model effectively can often be found to be the root of the problem.

Therefore, training courses are very important to enhance the practical knowledge of the users of the finite element system. The amount of training depends on the complexity of the analysis and on the size of the system being used. Some of the finite element systems have user manuals that are literally thousands of pages long and years of effort would be required to make a user fully conversant with their features. Therefore, training can make the bulky manuals more useful and understanding.

### **2.9.3 LUSAS finite element system**

LUSAS is a general purpose finite element system designed to solve a range of linear, non-linear dynamic and heat transfer of one, two and three dimensional engineering problems. The system incorporates free-format data generation procedures.

LUSAS-10.1 was selected, purchased and installed onto a 486 processor personal computer to be used for the current investigation. Also, the effort of selecting, purchasing and installing the system was considered as a part of the current investigation. The features described here are not clearly described in the documentation manuals. To understand the system more, these features are explained according to the current practical use of the system.

## **I . General procedure**

Although the general procedure of getting the pre- and post-processing results is summarized in LUSAS manuals for the mainframe and workstation version. There is no description available of the procedure for the LUSAS PC version. In order to clarify this matter, the following is a description of this procedure.

Fig. (3) shows the procedure of the overall LUSAS-10.1 for the PC version. This procedure is started by running MYSTRO system for creating the datafile. This file is expected to be submitted to the standard finite element analysis system LUSAS. Usually the datafile obtained during the pre-processing session does not suit the desired analysis carried by LUSAS i.e.contact, control or optional analysis. After exit from the MYSTRO, a decision has to be made by the user, according to the nature of the analysis, on whether the datafile needs to be modified or not. In the positive case, an editing program should be supplied by the users separately and used to modify the datafile according to the desired analysis. Then the data file is submitted to LUSAS system for typical standard finite element analysis procedure. When the analysis is finished, MYSTRO system is run again for the post-processing session. This session produces the hard copies of the results and the end of this session is the end of the general procedure.

## **II . File types**

During the sessions of the general procedure, different files with different extensions are created. The following are these files according to their extensions.



### **.DAT LUSAS datafile**

This file contains the tabulated finite element model definition in readable ASCII form, generated automatically from MYSTRO during the pre-processing session using the TABULATE command. This file is expected to carry the analysis by LUSAS.

### **.MDL MYSTRO Model file**

This is the MYSTRO-pre-analysis model file containing the graphical finite element model definition in binary form, generated automatically from MYSTRO during the pre-processing session using the MODEL SAVE command.

### **.CMD MYSTRO command file**

Contains a list of MYSTRO Commands which may be opened and replayed during an interactive MYSTRO session, generated automatically from the edited MYSTRO session file.

### **.OUT LUSAS output file**

This file contains the tabulated LUSAS analysis results in readable ASCII form. This is generated automatically by LUSAS. Also, this file has the same name as the LUSAS datafile.

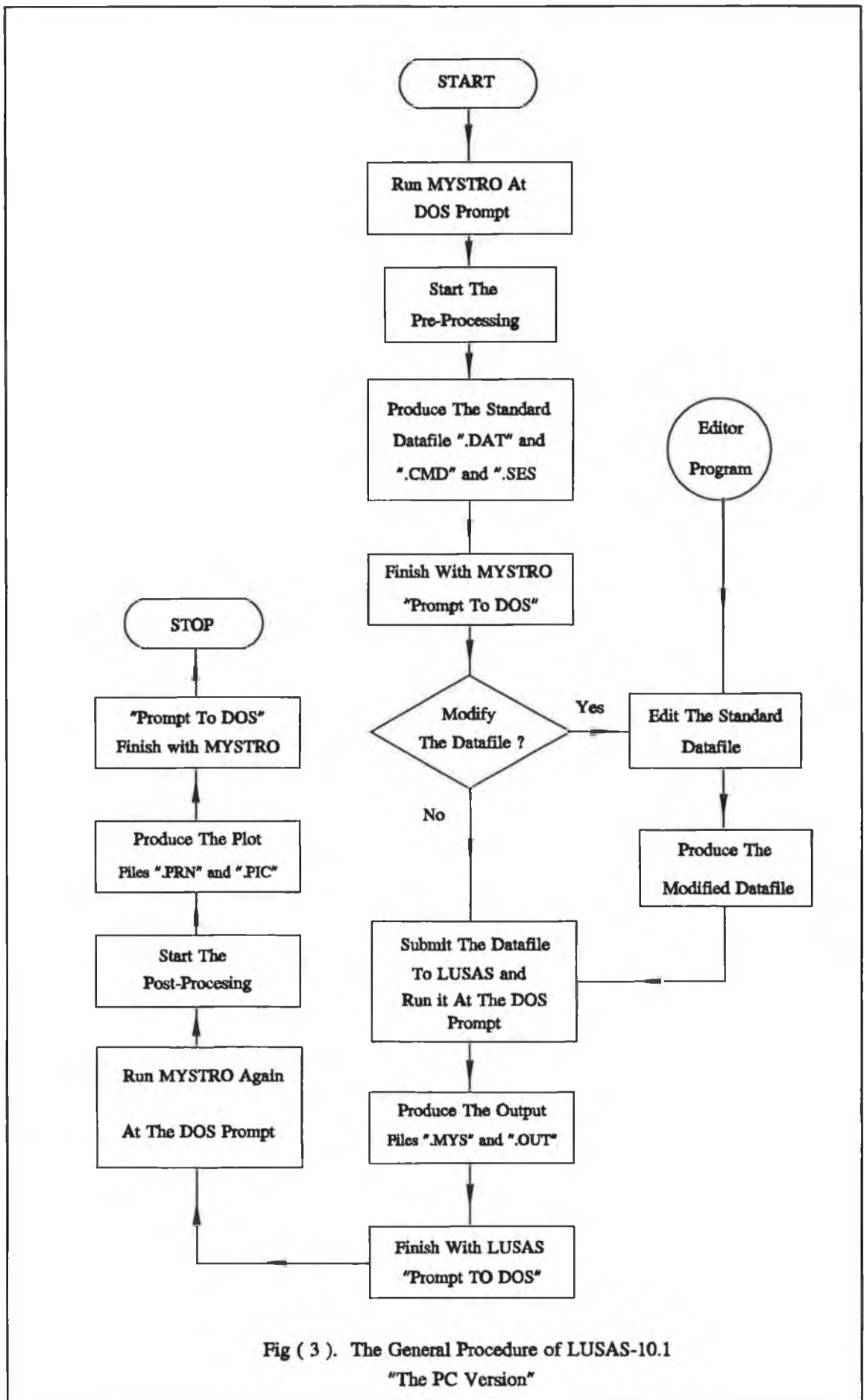


Fig ( 3 ). The General Procedure of LUSAS-10.1  
"The PC Version"

**.ERR system error file**

Contains the error messages during the execution of the general procedure of the system generated automatically and has the same name as the LUSAS datafile.

**.MYS MYSTRO Graphics file**

Contains the LUSAS results in binary form for graphical post-processing using MYSTRO. This file is generated automatically by LUSAS and has the same name as the LUSAS datafile.

**.PRN MYSTRO printfile**

Generated by MYSTRO during the post-processing session using the MYSTRO commands PRINT OPEN and PRINT RESULT. This file contains selected printed results or results summary in readable ASCII form.

**.PIC MYSTRO picture file**

The MYSTRO picture information in unreadable ASCII form is saved in this file, generated using the MYSTRO commands PICTURE OPEN and PICTURE SAVE.

### .SES.MYSTRO Session file

Contain all commands specified during the interactive MYSTRO session. This file could be edited to form a MYSTRO command file or replay in full. The file is called MYSTRO.SES unless MYSTRO was initiated by typing MYSTRO 'file' when it will be 'file' .SES.

### III . The Program Suit

#### MYSTRO

MYSTRO is an interactive finite element graphic system designed as a companion to LUSAS analysis system. MYSTRO is started at DOS prompt with PAP-UP command screen and this can be chosen optionally. MYSTRO incorporates pre and post-processing facilities for an interactive geometry definition, automatic mesh generation, automatic datafile generation, contour value plots and some other graphic interactive aspects. However, at present, the drag mode does not exist in this system, editing facilities for post-processing session cannot be used either for graphics or text in this session; information about the geometry of specific point of structure before and after loading is not available; the reaction forces in the restraint point can not be presented in the post-processing session. All these together make some operations of this system slow and even sometimes inconvenient. Also, in the pre-processing session, the system can not be used to define the non-linear boundary conditions or any "control" analysis.

## LUSAS

LUSAS is the system of the finite element analysis in the overall LUSAS-10.1. This system has been designed to solve the standard and advanced applications of the engineering problems. Although the system contains a good library of element type and material properties and can be applied successfully to a wide range of engineering problems the following features are still not available on the system:

- (i) The stress and the strain distribution for all the beam element types.
- (ii) The remeshing facility during the process of the analysis.
- (iii) The sub-structural facility and thick shell element in 3-D.
- (iv) The slideline facility for the thin shell element in 3-D.
- (v) The source of information about the interfacing facility which allows the users linking their own software with the LUSAS system.

## EXPOSE

To enable hard copy plots to be produced MYSTRO creates neutral files known as picture files. EXPOSE, which is started at DOS prompt, is used to convert the picture file to the appropriate plotting driver. To print out a copy of a picture file, practically speaking, conversion should be done on that file, using EXPOSE, to the compatible graphical format of the other programs i.e. Wordperfect. Then these programs are used to print out the converted copy of that picture file.

#### IV . Datafile Input

Datafile input is required for each data processing stage for LUSAS analysis. This may be summarized as follows:

SYSTEM  
PROBLEM  
OPTIONS  
RESTART READ  
ELEMENT TOPOLOGY  
SOLUTION ORDER  
NODE COORDINATES  
GEOMETRIC PROPERTIES  
GEOMETRIC ASSIGNMENTS  
MATERIAL PROPERTIES  
JOINT PROPERTIES  
COMPOSITE PROPERTIES  
MATERIAL ASSIGNMENTS  
COMPOSITE ASSIGNMENTS  
SLIDELINE PROPERTIES  
SLIDELINE SURFACE DEFINITION  
SLIDELINE ASSIGNMENTS  
CARTESIAN SETS  
TRANSFORM FREEDOMS  
SUPPORT NODES  
LOAD CASES  
ELEMENT OUTPUT CONTROL  
NONLINEAR CONTROL  
PLOT FILE  
RESTART WRITE  
END

Generally the typical LUSAS datafile contains the same hierarchical order of the above underlined data sections. During each of the data processing stages error diagnoses and cross-referencing is carried out. The error message output by LUSAS point to error where the data is wrong or improbable. If fatal data error is detected, LUSAS will automatically locate a restart point further along the data stream, and continue processing data to check for further errors. The full detailed description of the above

data sections can be obtained from the relevant data chapters in the LUSAS User Manual [75].

### **SYSTEM**

The data section SYSTEM may be used to modify certain values which define particular default parameters used by LUSAS. This could be useful for the large problems which need large numbers of database locations. This data section is positioned at the top of the datafile and followed by the PROBLEM name.

### **OPTIONS**

This data section, which follows the "PROBLEM" data section, may be used to specify user definable analysis or control options. Multiple options can be used either by repeating the line or adding more numbers. A full list of user options is given in Appendix B in [75].

### **SOLUTION ORDER**

The main solution processor, used by LUSAS, is the frontal method for the solution of the load deflection equations. The SOLUTION ORDER data section controls the efficient solution of the finite element equations and this can be done optionally. Solution order specification has the following options:

- (i) **ASCENDING:** Equation will be solved in ascending element number.
- (ii) **PRESENTED:** Equations will be solved in the subsequently specified order.
- (iii) **AUTOMATIC:** Automatic frontwidth optimization will be performed.

Solution order **ASCENDING** is the **LUSAS** default, and this is the only option which works with the contact analysis. Therefore, the **SOLUTION ORDER** data section may not be specified in the datafile when the problem involves a contact analysis.

### **GEOMETRIC PROPERTIES/ASSIGNMENTS**

This data section is imposed on the elements in the mesh generation of the model. The geometric properties depend on the element type. Some elements do not need any geometric specifications, so that this data section can be omitted from the input data e.g. the solid continuum elements in 3-D. The full detailed description about the **GEOMETRIC PROPERTIES** data section can be found in reference [75] Chapter 5.

### **MATERIAL PROPERTIES/ASSIGNMENTS**

The **LUSAS** element library contains about 110 element types. These elements accommodate both material and geometric nonlinearities. The types of material which can be selected are linear, nonlinear, joint field and composite material type. The **MATERIAL PROPERTIES** data section contains information about the selected material type for analysis. The **MATERIAL ASSIGNMENT** relates the defined material properties to a specific element number in the mesh. When using the 'ASSIGNMENT'



in the datafile option 118 must be used in the input datafile.

### **SLIDELINE/PROPERTIES/SURFACE DEFINITION/ASSIGNMENT**

These data sections contain information about the slideline which can be used to define the contact region of the structure being modeled. The defined information of the slideline can be related to the specific region of interest in the structure by using the data section SLIDELINE ASSIGNMENTS.

### **CARTESIAN SETS/TRANSFORMED FREEDOM**

A local cartesian axis system may be establish using the data section CARTESIAN SETS. The cartesian set is specified in terms of nodes defining the set origin, local x-direction and local xy-plane. The nodes used may form part of the structure or may be dummy nodes. Defined cartesian sets may be used in order to apply transformed freedoms or concentrated load. By default all concentrated loads and support conditions are applied in global X - Y and Z direction. Concentrated loads or support conditions may be specified relative to local cartesian axis systems using the data sections:

#### **CARTESIAN SETS TRANSFORMED FREEDOMS**

All concentrated loads or support conditions which have been applied to a transformed nodal freedom will act in the transformed direction. This facility may be useful in order to model a small section of symmetrical structure. These data sections are usually followed by the SUPPORT NODES data section which can be used to apply the

restraint condition to the nodal freedom in the global direction.

### **LOAD CASES**

LUSAS incorporates a variety of loading types. The LOAD CASES data section is used to define a selected load and apply this load to the region of interest of the modeled structure. The other data sections which follow the LOAD CASES data section are to control the advanced analysis and control the output data. Also, the support condition may be redefined after the LOAD CASES data section using SUPPORT NODES data section again.

### **RESTART/WRITE/READ**

Data can be written to disk to enable a nonlinear problem to be restarted from a particular step or load combination to be carried out using the RESTART WRITE data section. The dumped data is restored in a restart file. This file may be read again using the data section.

RESTART READ filename

### **V . The pre- and post-processor**

As it was stated earlier, the MYSTRO is used for pre and post-analysis. These two analyses are separate activities which means MYSTRO is used to prepare the datafile in the pre-processing session and then stopped. Following a LUSAS analysis, MYSTRO is started again and a post-processing session begins.

The datafile which is built during the pre-processing session describing the finite element model generally involves three stages:

- (i) Feature and attribute definition
- (ii) Attribute assignment
- (iii) LUSAS data table generation

Following a LUSAS analysis, the unprocessed results are stored in unformatted post-analysis graphics file "filename.MYS. The filename will be same as the datafile name specified during the pre-processing session. The post-analysis graphics results are brought into MYSTRO. The new data base will overwrite the current MYSTRO database thus the results are ready to be prepared. The usual preparation of the results therefore follows the form:

- (a) set the load case
- (b) set the results record
- (c) assemble the results
- (d) display the required results column

As a result of this session, the picture file "PIC" and the tabular results file "PRN" can be obtained. A full detailed description of the pre-and post-processing session can be seen in the MYSTRO User Manual [76].

## CHAPTER 3

# THEORETICAL PREDICATION OF THE DESIGN ANALYSIS OF THE HYDRAULIC PRESS MACHINE

### 3.1 Introduction

A machine is a combination of mechanisms and other components which transforms, transmits, or utilizes energy, forces or motion for a useful purpose. The hydraulic press is the most widespread among all the machines for forming metals and even some non-metals. The behaviour of the hydraulic press depends largely upon the behaviour of its structure during operations. This can be expressed as a closed loop [77] shown in Fig. (4). The structural aspects are considerations in mechanical design which is an iterative and cooperative process.

Designing starts with a need, be it real or imaginary. Existing apparatus may need improvements in durability, efficiency, weight, speed or cost. New apparatus may be needed to perform a function previously done, such as computation, assembly, or servicing. The next step in design either wholly or partially defined, is the conception of mechanisms and their arrangements that will perform the needed functions. For this, freehand sketching is of great value, not only as a record of one's thoughts as an aid in discussion with others, but particularly for communication with one's own mind, as a stimulant for ideas. Also, a broad knowledge of components is desirable, because a new machine usually consists of a new arrangement or substitution of well-known types of components, perhaps with changes in size and material. Either during or following this conceptual process, one will make a calculation or analyses to determine the general size

and feasibility. When some idea as to the amount of space that is needed or available has been obtained, the scaled drawings may be started.

When the general shape and a few dimensions of the several components become apparent, analysis can begin in earnest. The analysis should give a satisfactory performance, plus safety and durability with minimum weight and a competitive cost. Optimum proportion and dimensions will then be sought for each critically loaded section, together with a balance between the strength of several components. Materials and their treatment will be chosen. These important objectives can be obtained only by analysis based upon the principle of mechanics of elasticity and strength of materials of stress and deformation or numerical technique. Finally, a design based upon function and reliability will be completed, and a prototype may be built. If the tests on the prototype are satisfactory the initial design might undergo certain modifications that would enable it to be manufactured in quantity at a lower cost.

Studies on some features of hydraulic and mechanical presses have been reported elsewhere [22 & 23]; [35 & 48] and [78-84]. In a bid to find a simplified theoretical model of the structure of the press, under the current investigation, two theoretical models have been proposed. One of these models is based on the conventional analytical method and the other model is based on the numerical method using finite element analysis.

**Schematic Diagram Of The Applied Load And The Structure Of  
The Machine Tools**

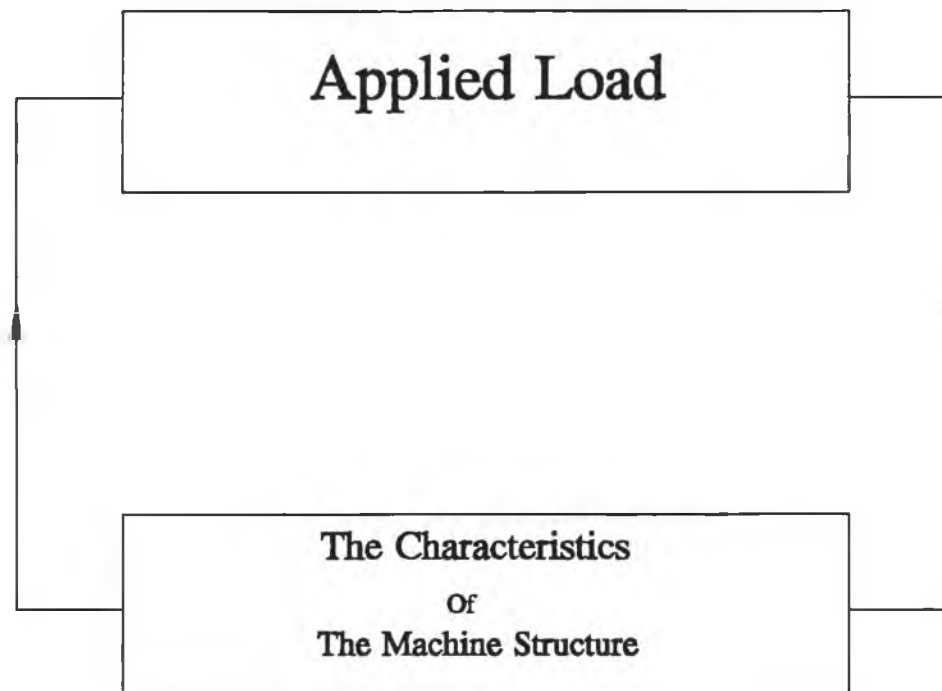


**Fig ( 4 )**

### 3.2 Original Design of the Press

The structural details of the original design of the hydraulic press is shown in Fig. (5) in which the dimensions have been taken from the physical state of the press. The press is a 150-tonne hydraulic press design by ENERPAC and assumed to exhibit a geometrical symmetry about the centre line. The press has a frame made of profiled beams and plates of structural steel welded together and the frame is freely supported on the ground and this consists of:

- (i) Side beams (8)
- (ii) Top beams (9)
- (iii) Bed of the machine (6)
- (iv) Hydraulic system (7)
- (v) Double-acting ram (1)
- (vi) Manual hydraulic pump (2)

Beam (9) was welded with beam (8) at the front of the machine forming the front side of it. Also, there is another assembly of beams (8) and (9) welded together in the same manner forming the backside of the machine. The front and the backside of the machine were welded together, through the stiffeners (13) forming the main assembly of the structure of the machine. The bed of the machine consists of front and back beam welded together through the stiffeners (14). The bed of the machine is linked with the main assembly through two pins (4) on each side of the press. The manual hydraulic pump (2) is used to move the bed up and down by linking the chain (3) with a groove in the bed and with the manual hydraulic pump. The manual hydraulic pump

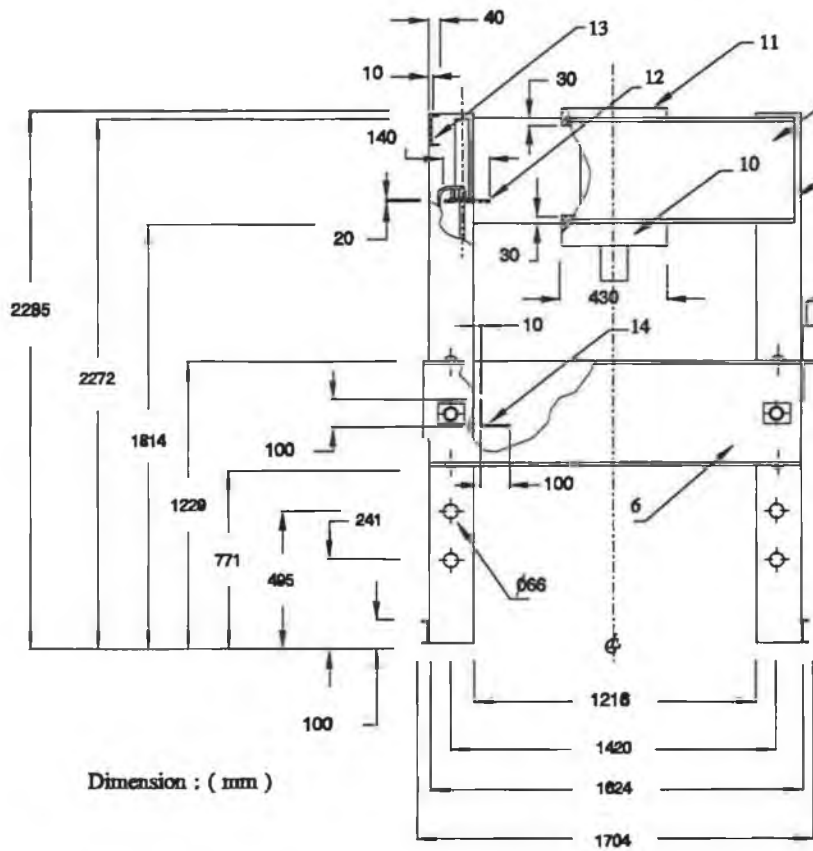
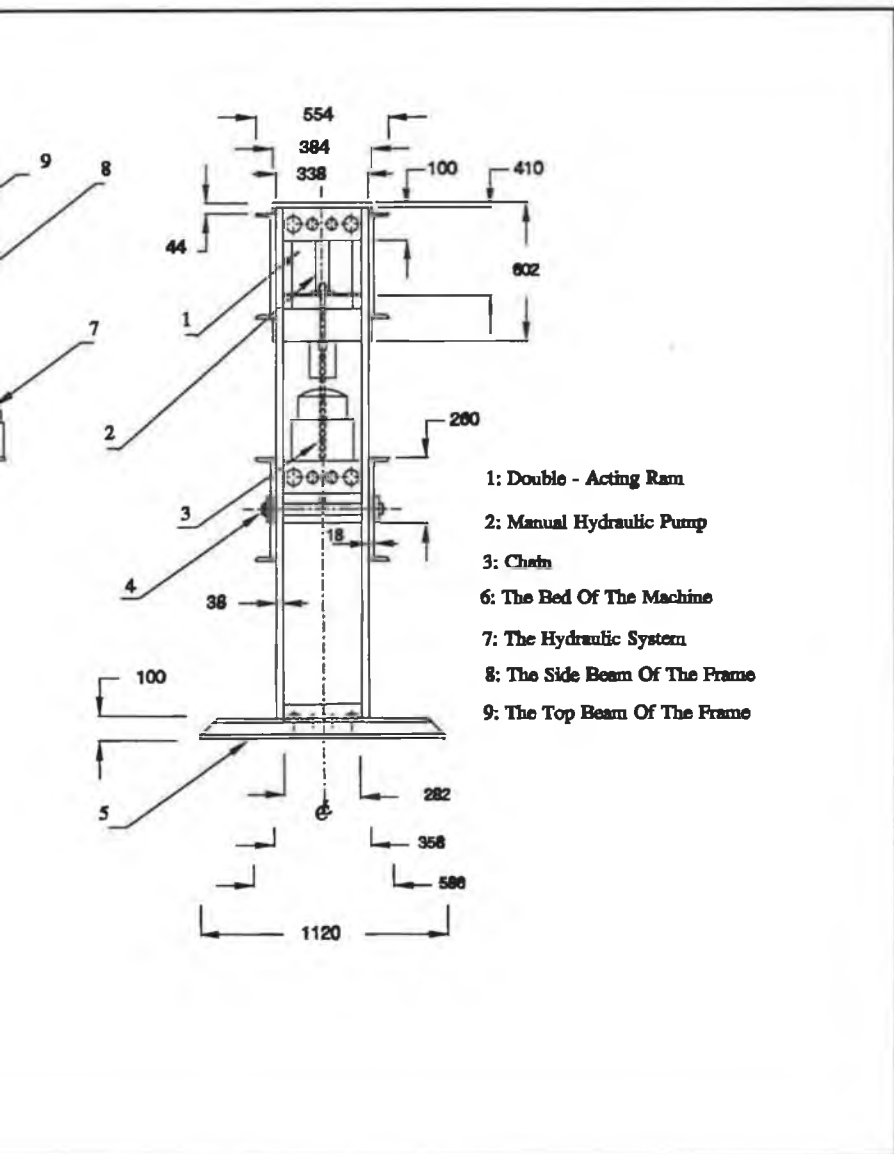


Fig ( 5 )





was bolted at the top of the plate (12) which was welded to the press structure (beam 8).

The double-acting hydraulic ram (1) was clamped to the top beam through the plates (10) and (11) which were fixed to the ram by bolts. In Fig. (5), the two beams (5) were bolted with the frame and used to support the base of the machine.

The hydraulic system (7) consists of a hydraulic pump; two hydraulic lines to the doubled acting hydraulic ram (1) and a 3-position manual centre valve. This system was designed by OTC.

### **3.3 Conventional analytical model (C.A.M)**

The present hydraulic press machine represents a 3-D complex welded structure for which an exact analytical method for stress and deformation analysis [85] is cumbersome and time-consuming. Therefore, the objective of modelling the structure of this press is to establish an empirical method of calculation in which the stiffness and the strength of the press structure can be obtained.

In order to simplify the calculation of the complex structure of the press this structure has been resolved into elements and represented as two dimensional beams subjected to transverse bending and direct load. Thus, the stiffness, which is the reciprocal of the flexibility [86], or performance of the press structure as a whole is determined by the behaviour of these beams. The mathematical model of the press structure was studied in this manner by using the simple bending theory based on the total strain energy

principle. Therefore, the conventional analytical model is an idealization of the framework of the press to predict the stiffness and the strength of this frame. The hydraulic ram and the platens which hold the ram to the structure of the press have been excluded from this model.

### 3.3.1 Assumptions

In order for the conventional model to be applicable it is necessary to make the following assumptions :

- (i) The beams are in 2D and are initially straight and unstressed.
- (ii) The material of the beams are perfectly homogeneous and isotropic.
- (iii) The elastic limit is nowhere exceeded.
- (iv) Neutral axis passes through the centroid of the cross-sections.
- (v) The weight of the press machine - shear and friction forces are negligible.
- (vi) Applied load is symmetrically static and shared equally by the front and the back beams of the press structure.
- (vii) No relative movement between the welded beams.

### 3.3.2 Model Analysis

Due to the symmetry of the press frame only half of it needs to be considered as shown in Fig. (6.a). In order to determine the unknown quantities ( $F$ ,  $M_1$  and  $M_3$ ), beam (3) has been considered separately as shown in Fig. (6.b). Taking that the bending moment

around C equals zero, the unknown force F is given by

$$F = \frac{M_1}{L_2} - \frac{P.L_1}{4.L_2} \quad 3.1$$

where:

- $M_1$  - unknown redundancy bending moment at A
- $L_1$  - the total width of the press machine taken from the neutral axis of the side beams.
- $L_2$  - the total length of beam (2).
- $P$  - the total applied load.

To find the unknown redundancy bending moment  $M_1$  at A the Castigliano's second theorem is used for the full half of the press (i.e. beam 1, 2 and 3).

$$\left. \begin{aligned} \frac{\partial U}{\partial M_1} = 0 = & \int_A^B \frac{M_{xx}}{E.I_1} \cdot \frac{\partial M_{xx}}{\partial M_1} \cdot ds_1 + \int_A^B \frac{F}{E.A_1} \cdot \frac{\partial F}{\partial M_1} \cdot ds_1 + \\ & \int_B^C \frac{M_{yy}}{E.I_2} \cdot \frac{\partial M_{yy}}{\partial M_1} \cdot ds_2 + \int_C^D \frac{F}{E.A_3} \cdot \frac{\partial F}{\partial M_1} \cdot ds_3 \end{aligned} \right\} \quad 3.2$$

where:

- $U$  - the total strain energy for the whole structure.
- $M_{xx}$  - the bending moment at section x-x of beam 1
- $M_{yy}$  - the bending moment at section y-y of beam 2.
- $A_1, A_2$  - the cross-sectional area of the beams 1 and 3
- $ds_1, ds_2, ds_3$  - the small length of the beams 1, 2 and 3 at distances
- $S_1, S_2, S_3$  - The length from the points A, B and D in Fig (6.b), respectively.

### The Forces Analysis Diagram

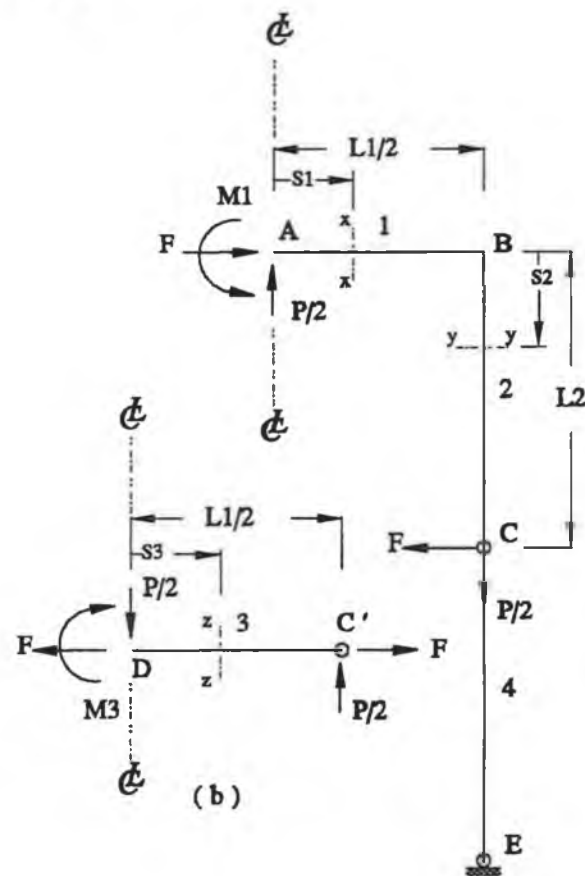
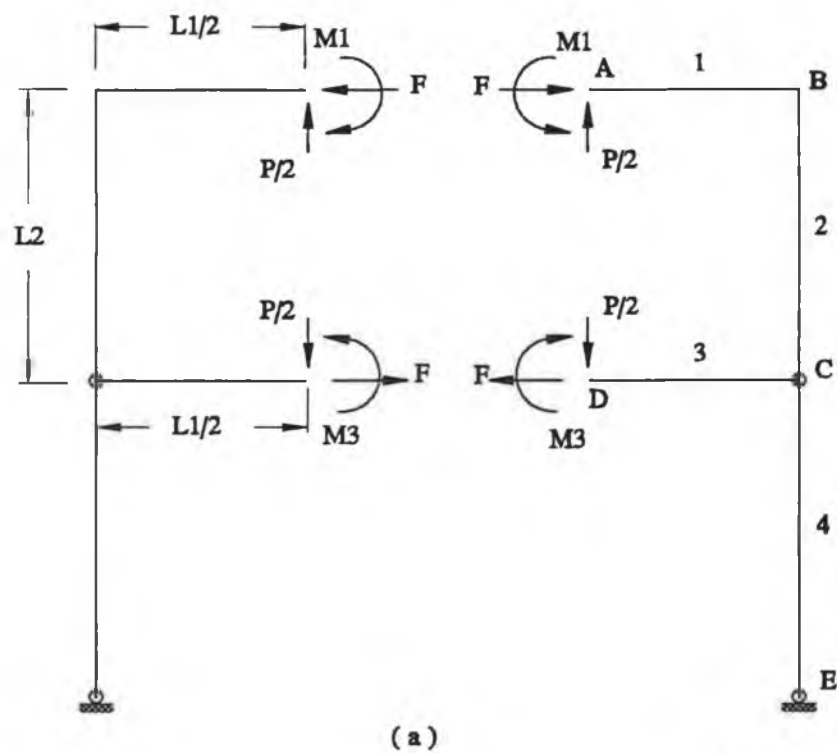


Fig ( 6 )

- $I_1, I_2$             the second moment of area about the neutral axis of the cross-sections of beams 1 and 2
- $E$                  -        Young's modulus.

The solution of equation (3.2) gives:

$$M_1 = \frac{P}{2} \cdot \left[ \frac{\left(\frac{L_1 \cdot L_2}{6 \cdot I_2}\right) + \left(\frac{L_1^2}{8 \cdot I_1}\right) + \left(\frac{L_1^2}{2 \cdot L_2^2 \cdot A_1}\right)}{\left(\frac{L_1}{2 \cdot I_1}\right) + \left(\frac{L_2}{3 \cdot I_2}\right) + \left(\frac{L_1}{L_2^2 \cdot A_1}\right)} \right] \quad 3.3$$

Considering Fig. (6.b) the following can be obtained:

- (i)                 Beam (3) can be taken as a cantilever fixed at the point D and with a concentrated load at C', therefore:

$$M_3 = -\frac{P \cdot L_1}{4} \quad 3.4$$

and the maximum vertical deflection at the point C' represents relatively the maximum deflection of the press at the point D, i.e.

$$\delta_D = -\frac{P \cdot L_1^3}{48 \cdot E \cdot I_3} \quad 3.5$$

- (ii)                 The maximum bending moment at the point B can be obtained as follows:

$$M_2 = F.L_2 \quad 3.6$$

- (iii) The maximum vertical deflection of the point A can be calculated by using Castigliano's first theorem i.e.

$$\left. \begin{aligned} \frac{\partial U}{\partial \left(\frac{P}{2}\right)} = \delta_A &= \frac{1}{2.E} \left\{ \left[ \frac{L_1^2}{4.I_1} \cdot \left( \frac{P.L_1}{6} - M_2 \right) \right] \right. \\ &+ \left. \left[ \frac{L_1^2}{2.A_1.L_2^2} \cdot \left( M_1 - \frac{P.L_1}{4} \right) \right] + \frac{P.L_2}{A_2} \right\} \end{aligned} \right\} \quad 3.7$$

- (iv) The stress acting within the material of each beam has been counted as a combination of direct and bending stresses i.e.

$$\sigma_i = \frac{P}{A_i} \pm \frac{M_i}{W_i} \quad 3.8$$

where the subscript *i* refers to the beam number (i.e. 1,2 and 3) and **W** is the sectional modulus.

- (v) The total direct stiffness of the press machine can be given as follows:

$$S_f = \frac{P}{|\delta_A + \delta_D|} \quad 3.9$$

### 3.3.3 Method of calculations

The manual calculations of the equations 3.1 to 3.8, describing the conventional mathematical model of the frame of the hydraulic press, are tedious and time-consuming.

The slowness of such calculations is due to the iterative nature of the design process in which the design parameters may be calculated at several load levels or cross-sectional geometries. Therefore, a computer program has been developed to facilitate these calculations and make use of the conventional model in the design analysis of the type of the present hydraulic press frame.

The program has been divided into a number of modules. These modules appear as sub-routines and the main line program is a simple routine whose function is to automate selection and the calling of these sub-routines. The execution of this program follows the flow chart shown in Fig (7). The input data consists of information concerned about the number of beams, option of displaying the results, the geometries of the cross-section of each beam, the length of the beam, the first applied load and the material properties of each beam (i.e. Young's modulus and the yield stress). The second moment of area can be calculated for any geometrical shape of the cross-section of the beams about the centroidal axis of cross-section as follows:

- (i) divide the whole cross-section into a number of rectangles
- (ii) calculate for each an individual rectangle, the area ( $a$ ); the distance ( $y$ ) from an axis ( $X-X$ ) passes the base of the whole section; the second moment of area ( $i$ ) about its local centroid parallel to ( $X-X$ ), the product ( $a.y$ ) and the product ( $a.y^2$ ).
- (iii) calculate the distance of the whole section from ( $X-X$ ):



$$\bar{y} = \frac{\sum_1^k a \cdot y}{\sum_1^k a} \quad 3.10$$

where k is the total number of the individual rectangles.

- (iv) calculate the second moment of area of the whole section about (X-X):

$$I_{XX} = \sum_1^k a \cdot y^2 + \sum_1^k i \quad 3.11$$

- (v) calculate the second moment of area of the whole section about its centroid:

$$I = I_{XX} - (\bar{y})^2 \cdot \sum_1^k a \quad 3.12$$

Equations (3.10) to (3.12) can be calculated by the program. This requires the height and the width of each individual rectangle, in the whole section, to be given as a geometry of the cross-sections in the input data of the computer program. Thus the program calculates and tabulates the geometric properties of each cross-section of the beams of the press frame, bending moments, stresses, safety factor, maximum allowable applied load, deflection of individual beams and the total direct stiffness of the whole hydraulic press frame. The computer program with its variable names and input data instructions is listed in Appendix (A).

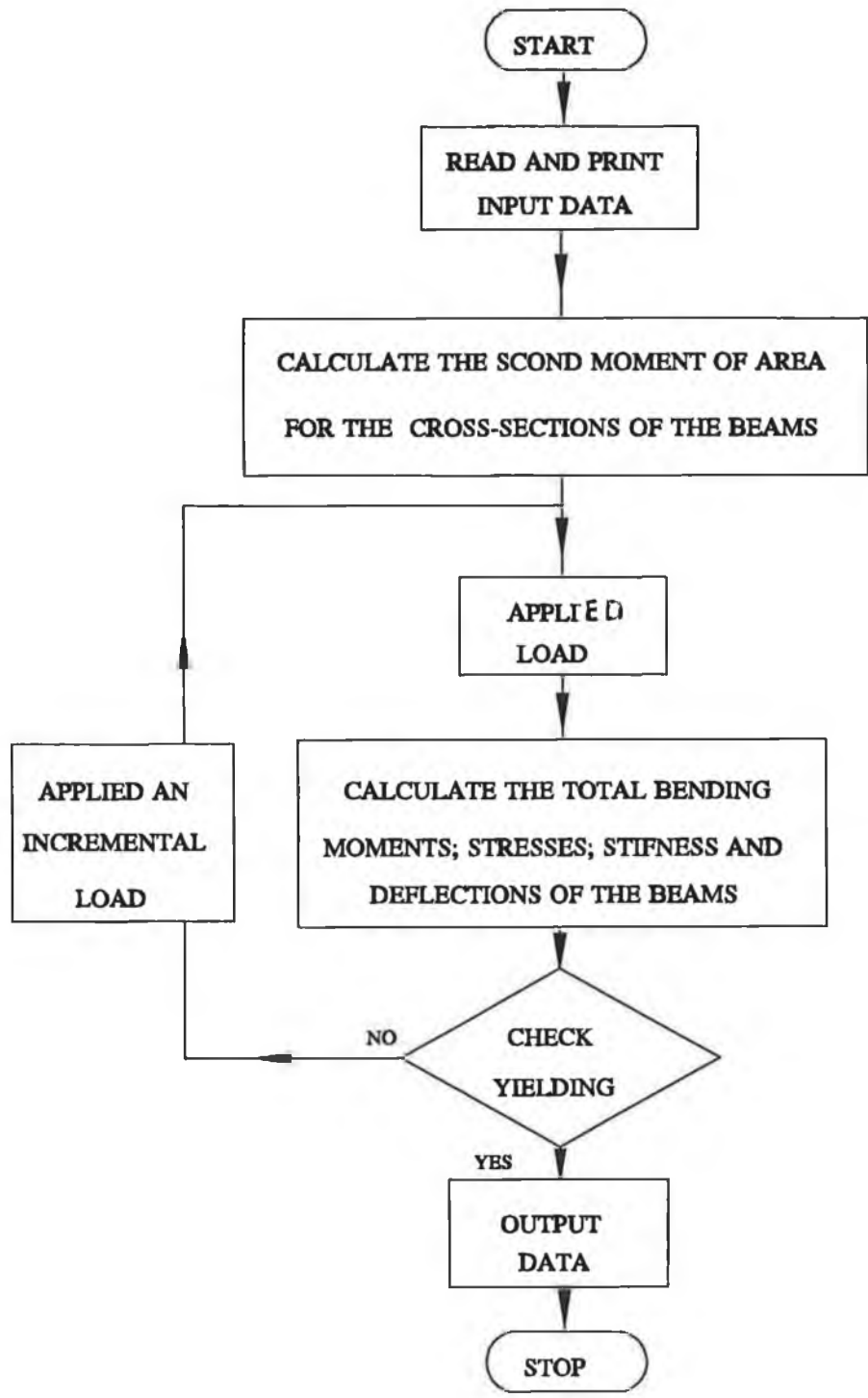


Fig ( 7 )

### **3.4 Numerical Model**

A numerical model has been developed by the application of the finite element method. This model has been proposed because the finite element method permits a much closer topological resemblance between the theoretical model and the actual machine. The objective of this model is to make use of and to evaluate the existing computing hardware and software and also to optimize the design time and material cost of the structure of the hydraulic press under consideration.

The personal computer version of LUSAS 10.1 finite element system, supplied by FEA Ltd., London, has been used as a computer-aided design analysis tool for the structure of the hydraulic press. A 486-processor IBM compatible personal computer, with 7 Mbytes extended memory and 50 Mbytes free disk space, has been utilized to perform the analysis of the numerical model.

#### **3.4.1 Assumptions**

In order to determine the practicability of the model for achieving the numerical solution, without affecting the accuracy, the following assumptions have been made:

- (i) The applied load is a static concentrated load and perfectly vertical.
- (ii) The deformation of the plunger of the hydraulic ram is negligible.
- (iii) The material of the press structure is homogeneous and isotropic.
- (iv) The base of the press is freely supported on the ground and the friction between the base and the ground is negligible.
- (v) No relative movement between the welded members of the press

structure.

(vi) Material properties and relevant data:

Young's modulus	=	$0.1 \times 10^6 \text{ N/mm}^2$
Yield Stress	=	$250 \text{ N/mm}^2$
Poisson's ratio	=	0.3
Density	=	$7.86 \times 10^{-5} \text{ N/mm}^3$
Permissible deformation	=	0.5 mm/m

The material properties have been obtained from reference [87] for structure steel, whereas the permissible deformation has been taken from reference [81] and considered as a design goal.

### 3.4.2 Modelling strategy

The numerical modelling strategy of the hydraulic press structure takes into consideration the following:

- (i) Modelling before any modification.
- (ii) Modelling after the design modification.
- (iii) Modelling the new design.

The factors considered are: the boundary condition; the mesh density; the type of element and the width and the chamfering of the press structure.

## **I . Modelling before any modification**

The modelling activities, at this stage, have been proposed by employing different element types; mesh densities and boundary conditions. The purpose behind this is to experimentally and theoretically evaluate different numerical models of the press structure with different modelling criterion. This means that only the numerical model has been modified to simulate the same experimental setup taken from the actual press.

### **Full 3-D model**

Physically speaking, the back and front beams of the bed of the press and the centres of the housings of the pins in the front of the bed are not exactly at the same level. Also the centres of the housings of the pins in the front of the bed are not at the same centres of the housings at the back of the bed. Therefore, the applied load is not purely vertical and thus slight eccentricity is encountered during the operation of the machine. All these aspects have been considered in the full 3-D model of the press as shown in Fig. (8). The elements used in this model are: 3-dimensional continuum elements with 3 d.f/node and 3-dimensional flat face thin shell elements with 6 d.f/node. The nonlinear joint elements for frictional contact has been used to join the mating parts, which have some relative movement with each other, in the press structure.

The boundary conditions imposed on this model are as follows:

- (i) Nodes at the centre line are restrained in X and Z direction.
- (ii) Nodes on the X-Y plane passes I-I are restrained in Z direction.

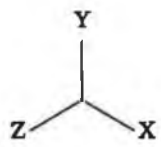
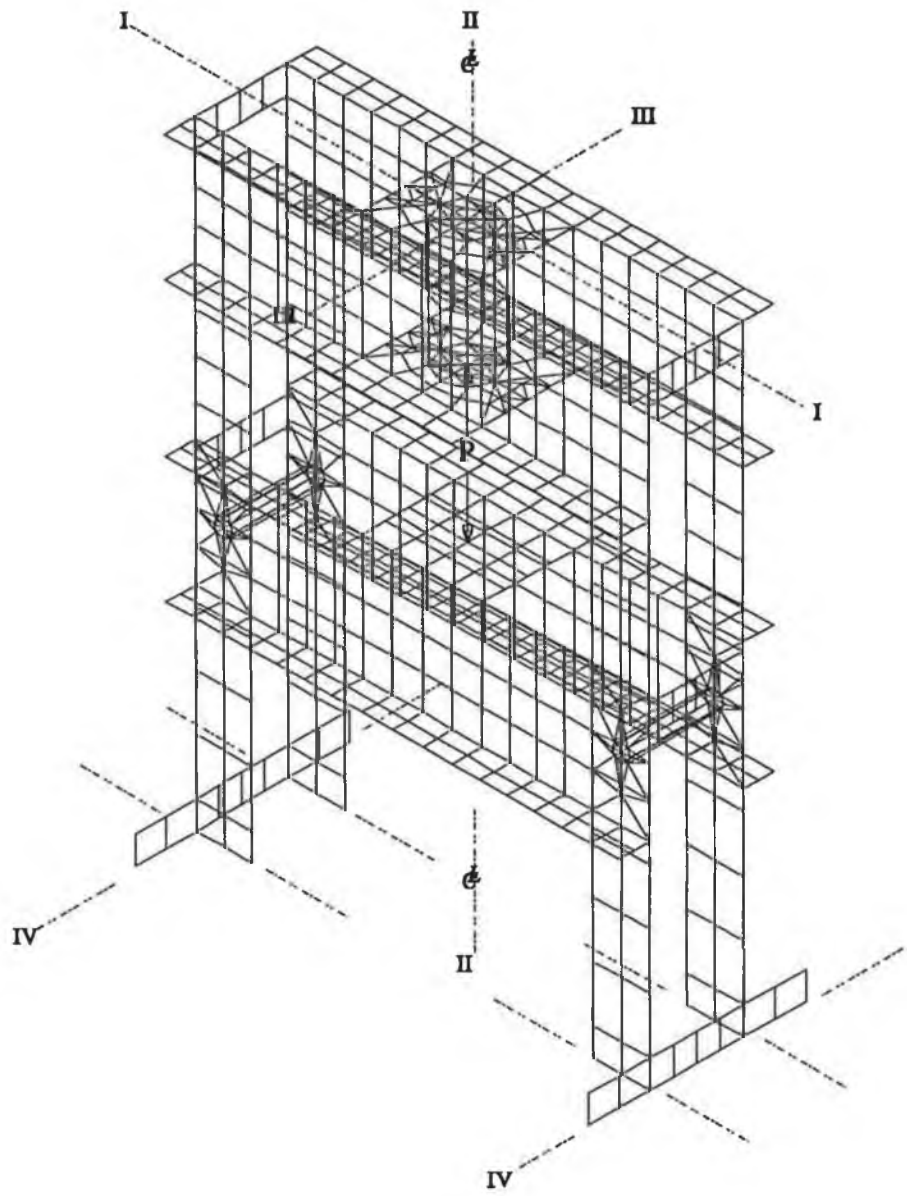


Fig ( 8 )

- (iii) Nodes on the Y-Z plane passes III-III are restrained in X direction.
- (iv) Nodes on the Z-X plane passes IV-IV are restrained in Y direction.

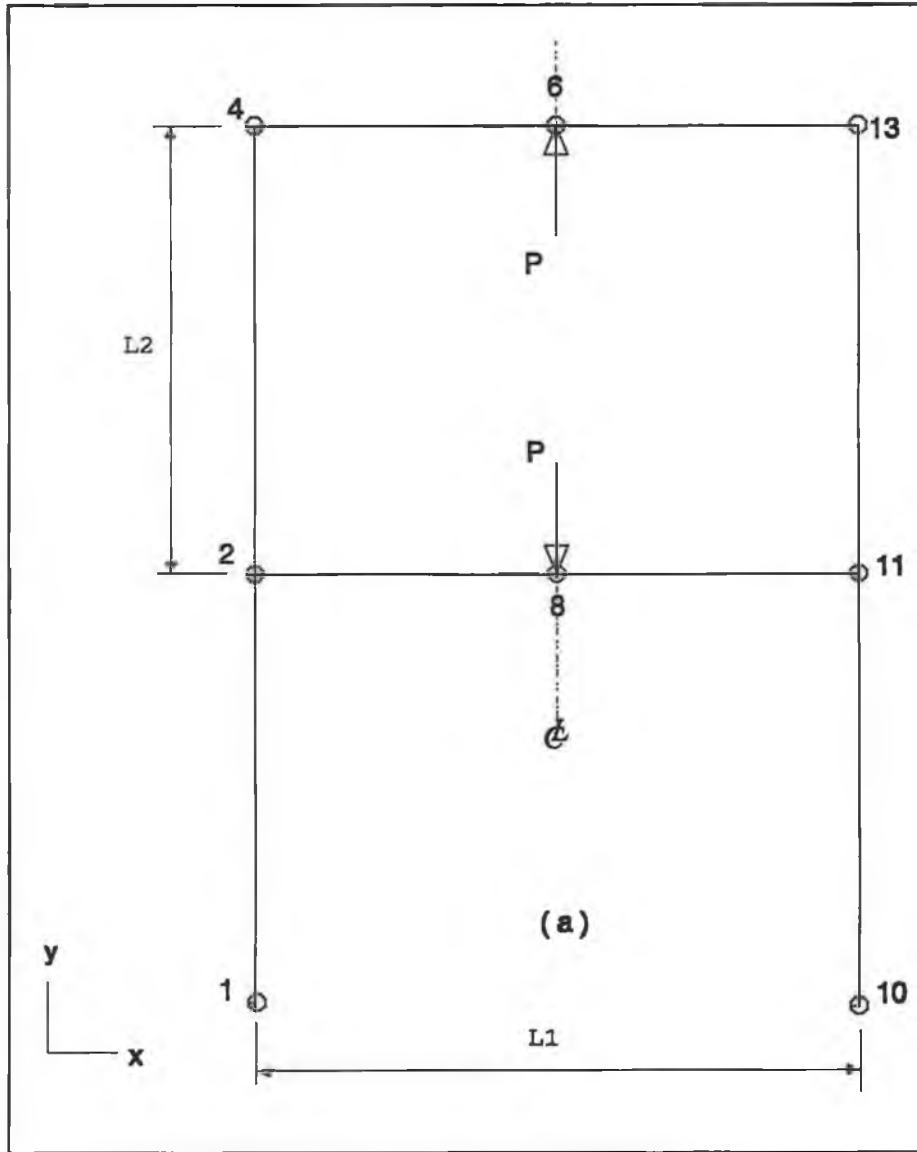
One load increment of the full P and a nonlinear control were used. However, the results could not be obtained using this model because of the short-comings of the computing hardware used.

### **Plane frame model (P.F)**

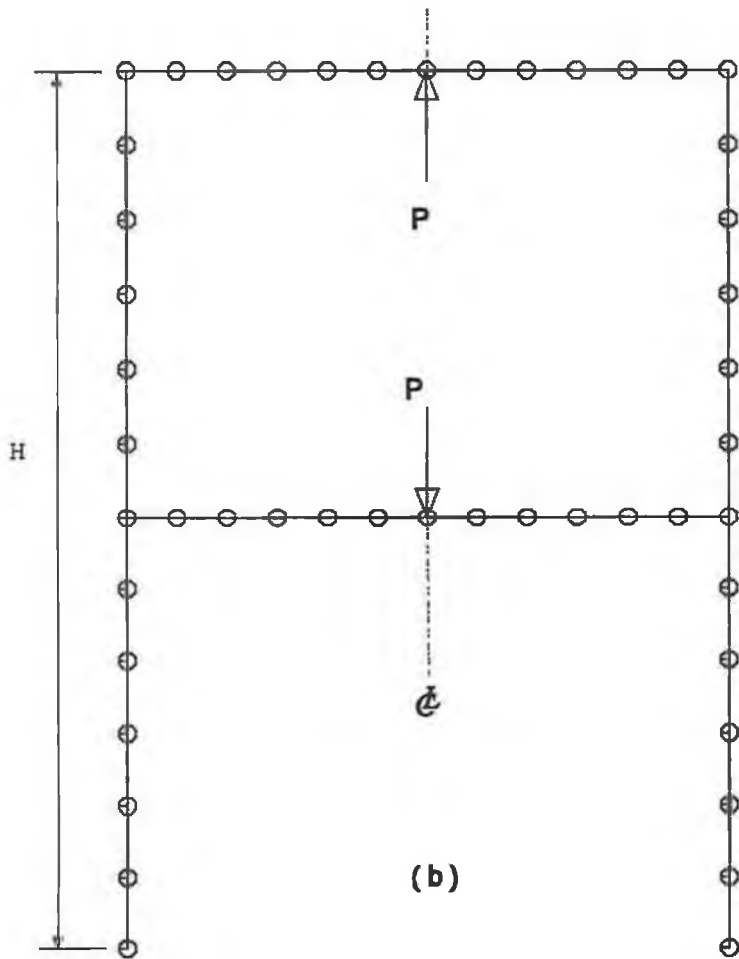
This model is the simplest numerical model of the press structure used in this study. The model has been used to make a comparative study between the conventional analytical and experimental model. A beam element with 3 d.f/node was used in order to model in-plane bending of the press structure. The full load P was applied at the centre line of this model as in Fig.(9). Minimum number of elements as in Fig. (9.a) and maximum number of elements as in Fig. (9.b) have been evaluated. The non-rigid connection of the pin with the press frame at node 2 and 11 in Fig. (9.a) has been modelled in two ways as follows:

- (i) By freeing the moment at nodes 2 and 11 of beams 2-8 and 8-11.
- (ii) By using 2D nonlinear joint elements model for general contact at nodes 2 and 11.

The boundary conditions have been applied as the nodes on the centre line to be restrained in X direction and nodes 1 and 10 to be restrained in Y direction. A full detailed description on the model using the nonlinear joint element can be seen in Appendix (B).







(b)

Fig (9)

### Plane stress model (P.S)

This model has been used to simulate the behaviour of the structure of the press and assess the response of this structure in 2-dimensional plane stress. The plane stress model has been utilized by assuming that the variation of out-of-plane direct and shear stresses are negligible. It was felt that if half of the press structure was assumed to be made up of an L-shaped beam and one half of the bed separately, in x-y plane, a plane stress model could be used for analyzing the structure of the press. This could help in reducing the analysis time of the press structure.

The plane stress model is shown in Fig. (10) in which Fig. (10.a) represents the L-shaped beam model and Fig. (10.b) represents half of the press bed model. Half of the load has been imposed on both models, as shown in Fig. (10). The 2-dimensional plane stress element with 2 d.f/node has been used and the boundary conditions have been applied to the nodes in the models as follows:

- (i) Nodes at the centre line are restrained in X direction.
- (ii) Nodes B1 and B2 are restrained in X and Y directions.

The boundary conditions at nodes B1 and B2 have been deduced after considering the boundary condition against the nonlinear boundary condition of the joint between the pin and half of the press bed in plane stress. The mesh shown in Fig. (10) has been chosen after testing different types of mesh densities.

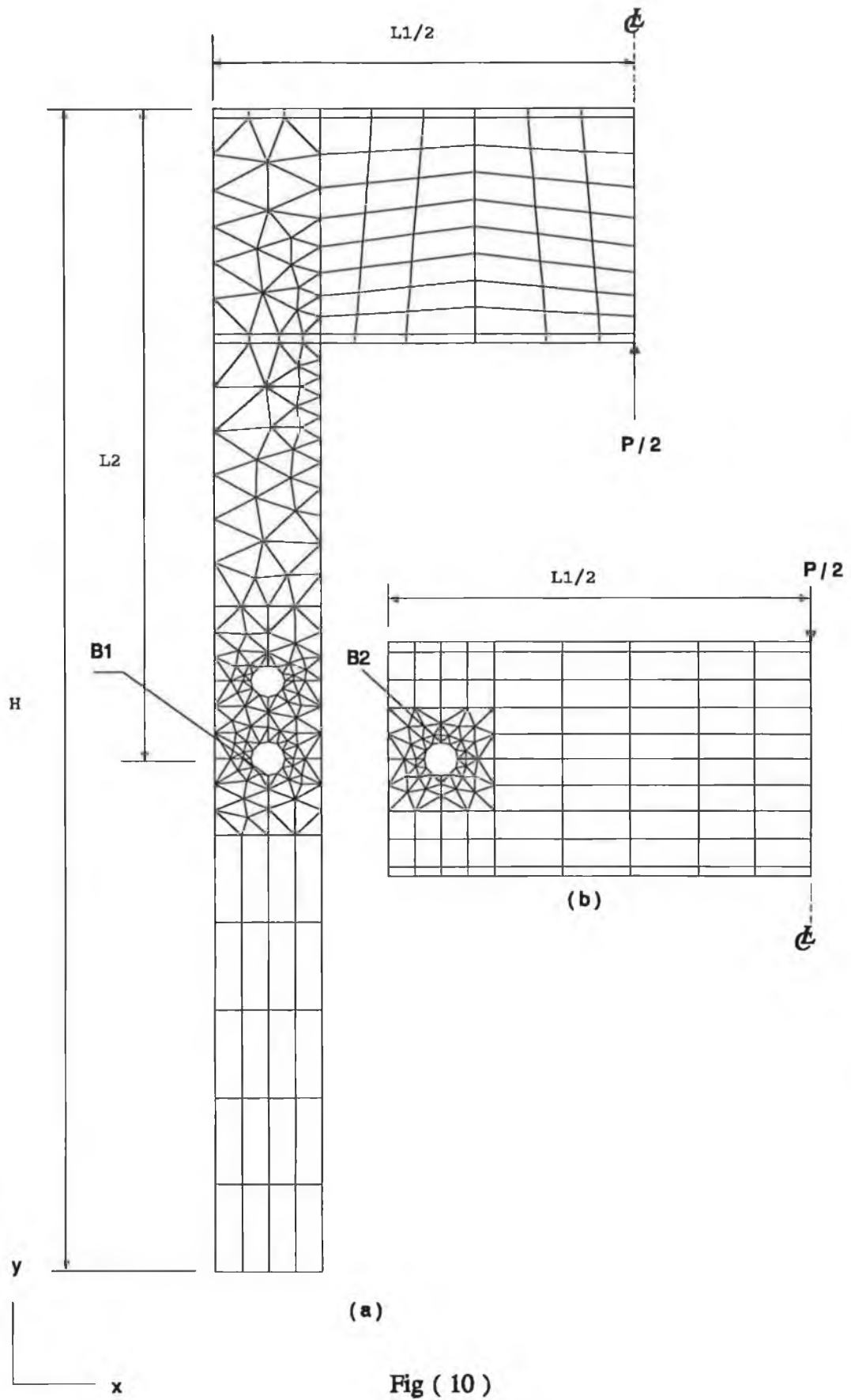


Fig ( 10 )

### **Test of the boundary conditions**

This test has been performed to evaluate the boundary conditions at the housing of the pin in the press bed. Fig. (11) shows two models of half of the press bed in plane stress. Fig.(11.a) represents the plane stress model of half of the bed with simple boundary conditions. In this model node B2 is restrained in X and Y direction and the nodes at the centre line are restrained in X direction. Fig. (11.b) shows half of the bed with the pin modelled also in plane stress with non-linear boundary conditions between the bed and the pin. The nodes at the centre line in this model are restrained in X direction whereas the nodes around the centre of the pin are fixed in X and Y directions to prevent the pin from rotating about its centre.

The number of elements in both models in Fig. (11) has been chosen in a manner that when the elements were exceeded, this did not produce a significant improvement on the accuracy. This was to avoid the errors caused by insufficient number of elements. A detailed description of the instruction of preparing the non-linear boundary condition using a slideline is given in Appendix (B).

### **Test of the mesh density**

This test has been carried out to estimate the number of elements in a model which can give an acceptable accuracy of the results at minimum analysis time. For this reason the plane stress model of half of the bed has been analyzed with a minimum and maximum number of elements of meshes shown in Fig. (12).

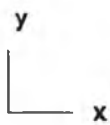
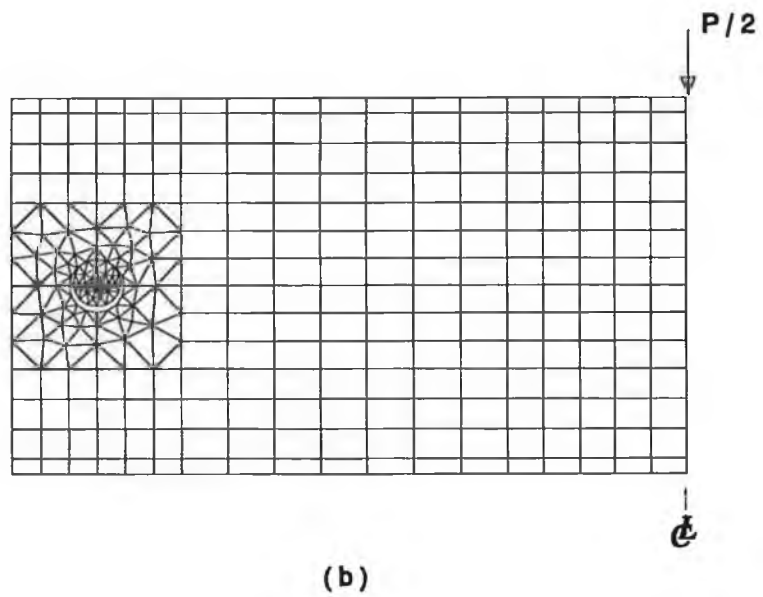
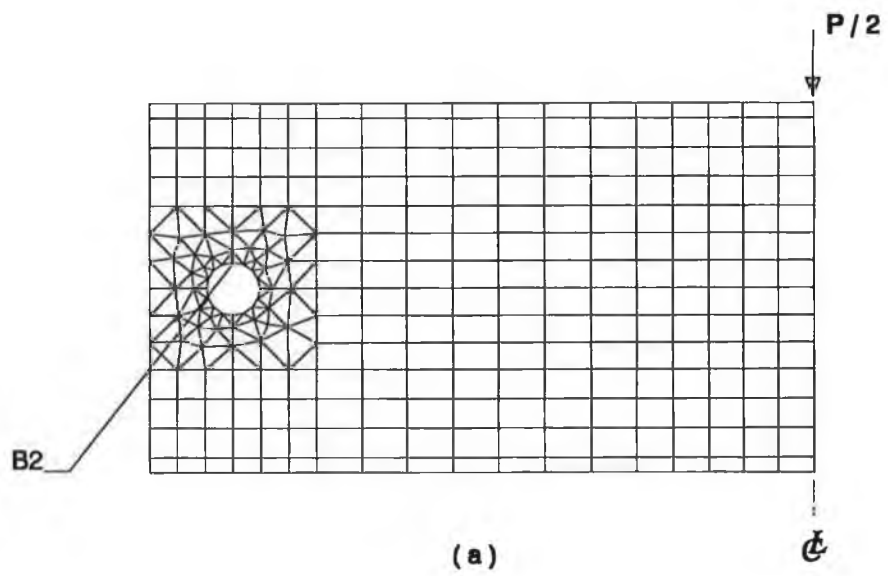
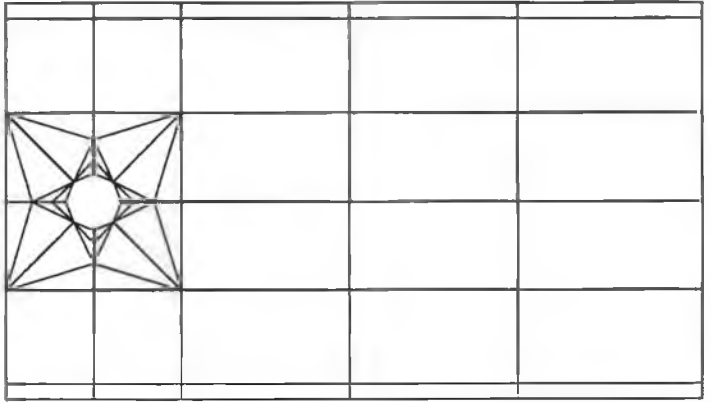
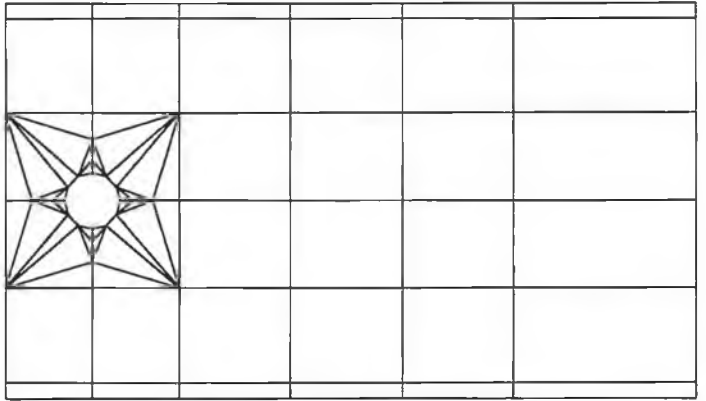


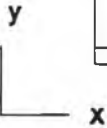
Fig ( 11 )

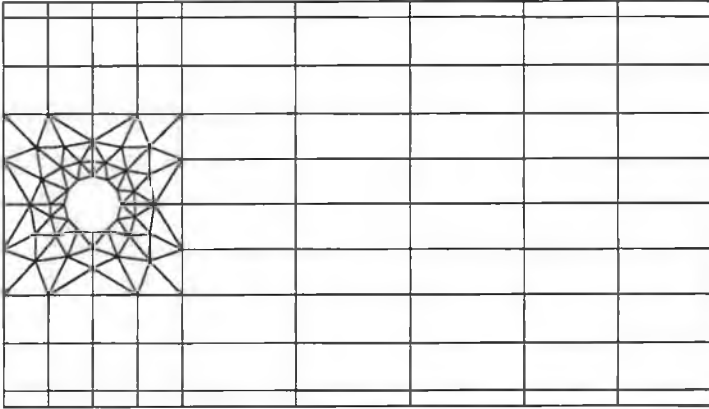


Mesh1 ( 58 )

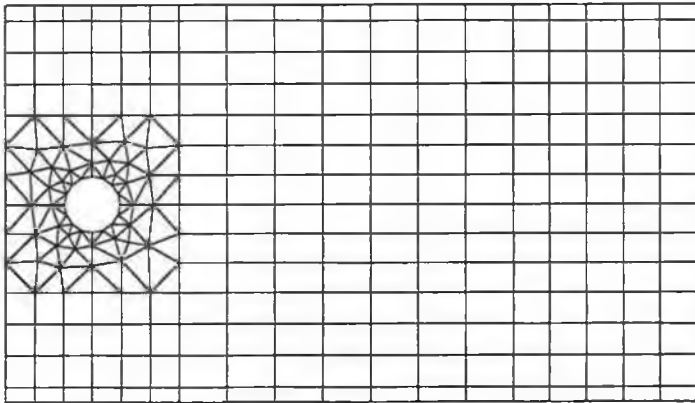


Mesh2 ( 68 )





Mesh3 ( 160 )



Mesh4 ( 324 )



Fig ( 12 )

It is well known that by increasing the number of elements generally the accuracy of the predicted results is increased. However, there is an optimum number of elements which when exceeded does not improve the accuracy of the results but only increases the required computer core store. Therefore, this test provides a factor of accuracy between a chosen mesh, which gives the acceptable accuracy of the results at minimum time, and the mesh of maximum number of elements in Fig. (12). Thus the optimum number of elements should be arrived at after several trial runs of the analysis, in order to satisfy the factor of accuracy found in this test.

### **3-D Thin shell model (3-D T.S)**

This model has been put into practice in order to study the out-of-plane behaviour of the press structure. It has been assumed that the actual hydraulic press exhibited a geometrical symmetry about its centre line. Therefore, in order to simplify the finite element model, the press structure without the hydraulic ram or any loading plates, was assumed to be made of a quarter of the bed and a quarter of the rest of this structure. Fig. (13.b) represents the FEM model of the quarter of the bed whereas Fig. (13.a) shows the FEM of a quarter of the press structure without the bed. Shell elements with 6 d.f/node have been utilised in both models. The boundary conditions, for both models, are as follows:

- (i) Nodes on the Z-Y plane passes the centre line, are restrained in X direction.
- (ii) Nodes on the Y-X plane passes the centre line, are restrained in Z direction.



- (iii) Nodes  $B_1$  and  $B_2$  are restrained in X, Y and Z directions.

## **II . Modelling after the design modification**

The intention, at this stage of modelling, is to study, theoretically and experimentally, the effects of the structural parameters on the stiffness characteristics. This study has been divided into two phases:

- (i) Modelling the optimum design of the press bed.
- (ii) Modelling the platens and the loading tools.

Each phase of this was an iterative process in which the structural parameters have been changed repeatedly until the theoretically predicated results matched the design goal of the press structure. Then, the actual modification, according to the theoretical model, was imposed on the actual hydraulic press. After this, the factor of convergence between the theoretical model being modified and the actual modified hydraulic press was found.

### **Modelling the optimum design of the press bed**

It was observed from the analysis carried out in Chapter 3 (3.4.2) that the press bed had the largest deflection, in Z and Y directions, among all the members in the hydraulic press structure. Therefore, in order to stiffen this bed more stiffeners were added to the

press bed. The effect of the thickness of these stiffeners on the deflection and the stiffness was studied. The effect of the thickness of the press bed after adding the stiffeners was theoretically investigated. Fig. (14.a) shows the FEM model of the bed before adding the stiffeners. Fig. (14.b) introduces the FEM model of the bed after adding the stiffeners  $S_1$  and  $S_2$ . The model in Fig. (14.b) has the same boundary conditions; element types and applied load as the model in Fig. (13.b).

### **Modelling the platens and loading tools**

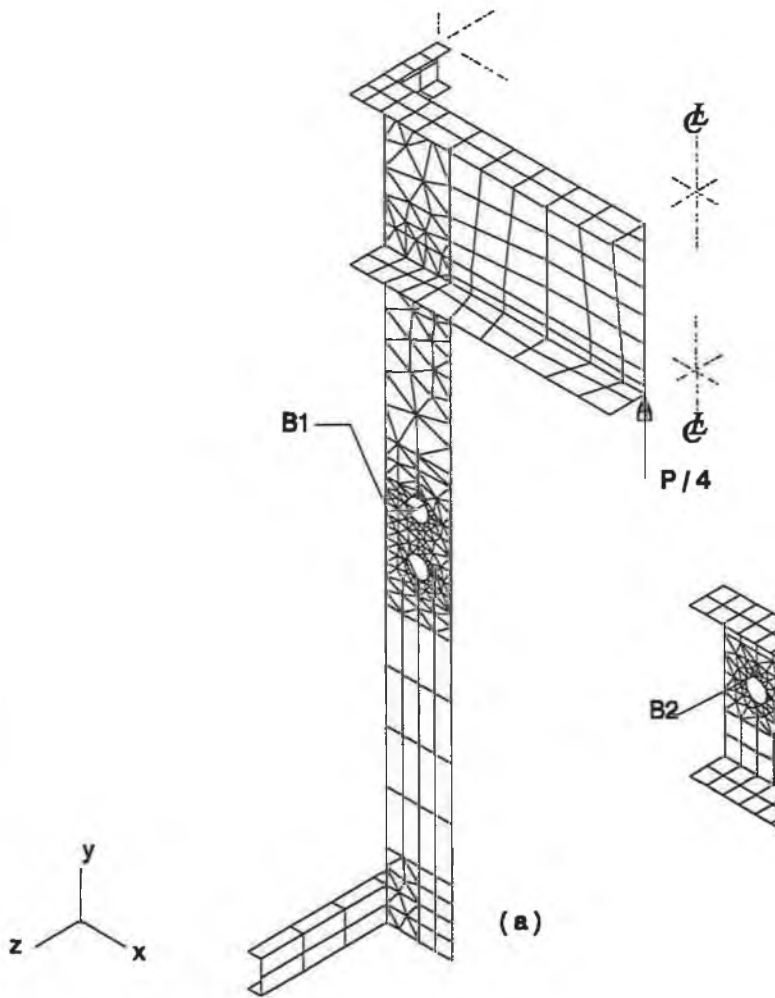
These components have been designed exclusively for the experimental model and consist of:

- (i) A set of the load cells.
- (ii) The cap of the ram.
- (iii) A lower loading plate.

Advantage has been taken of the symmetrical nature of these components and therefore only one quarter of each of them has been analyzed. The objective of the modelling was to optimize the design of these components and to evaluate, experimentally and theoretically, the total stiffness of the hydraulic press as these components are installed on the press. The FEM model of these tool steel components is shown in Fig. (15).

### **The axisymmetric model of the load cell**

This model is shown in Fig. (15.a) which consists of the main element of the load cell



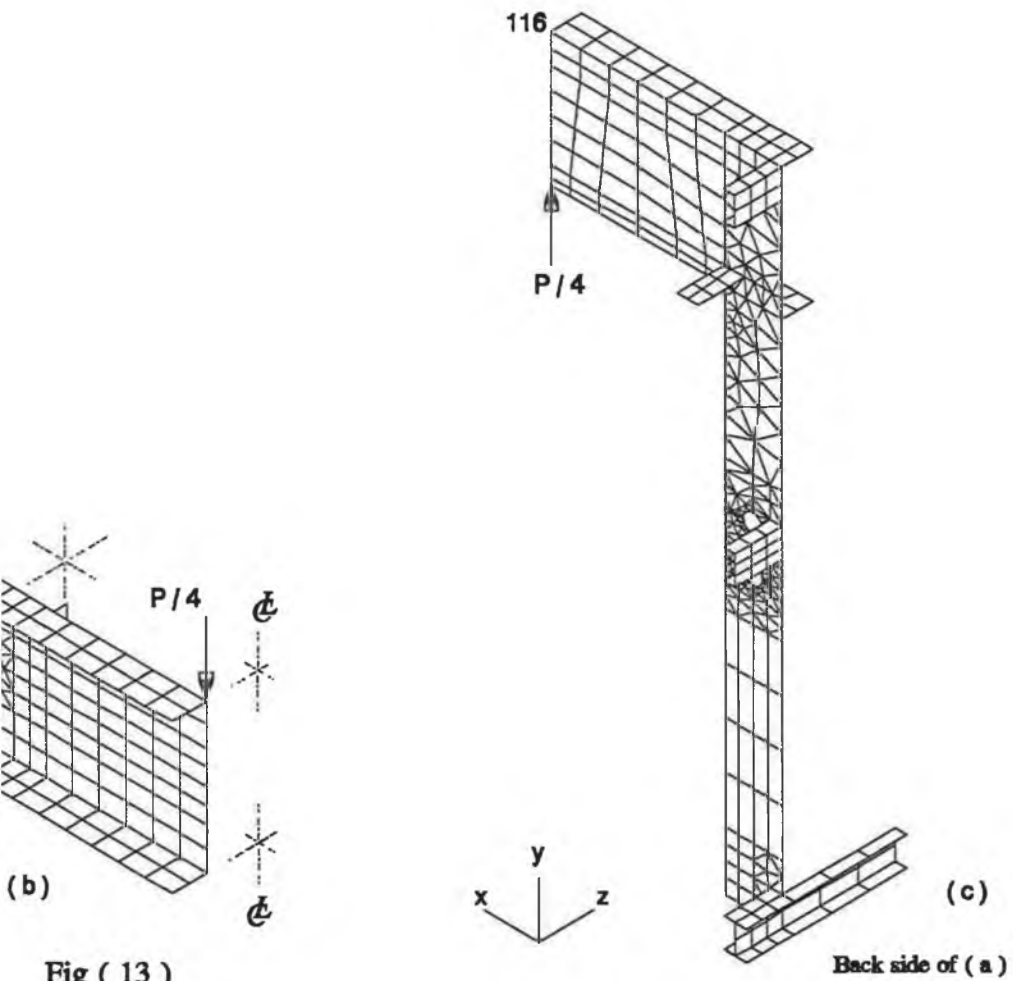
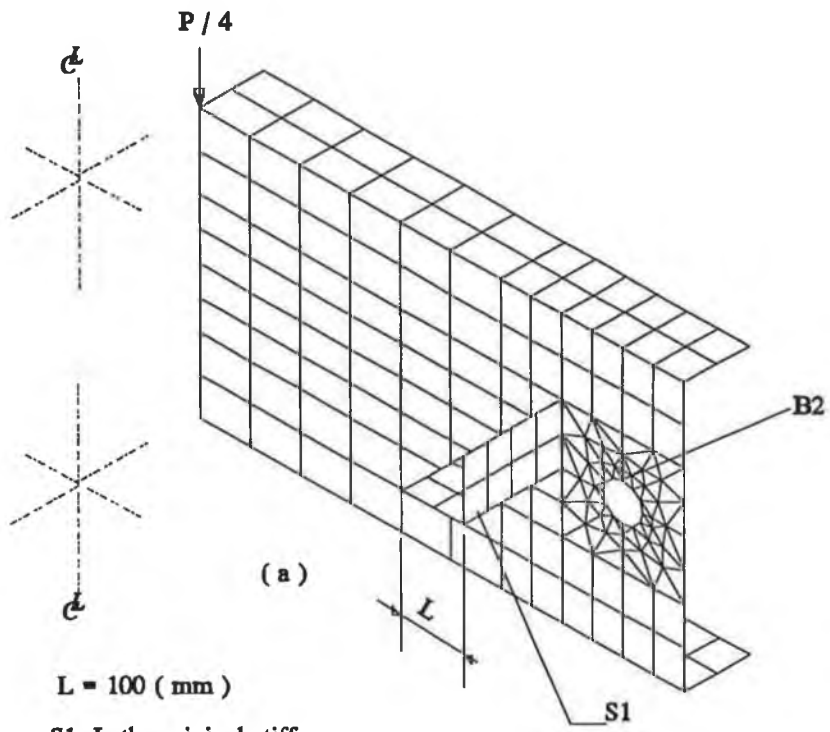


Fig ( 13 )



S1: Is the original stiffener.

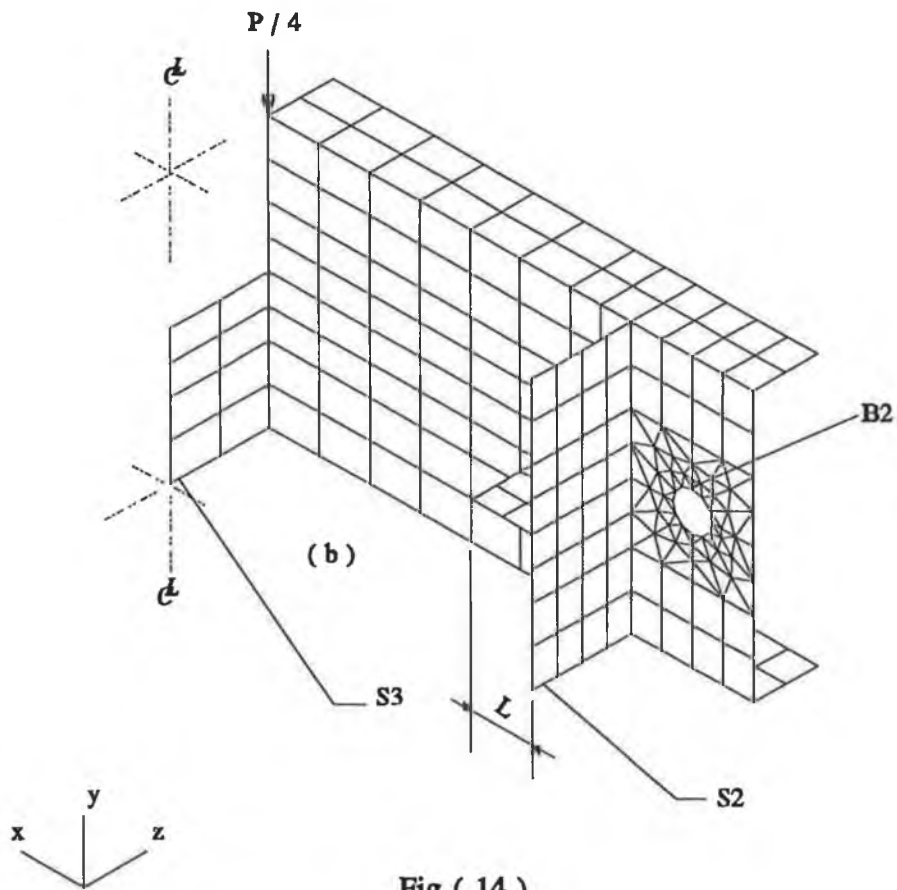


Fig ( 14 )

(1), the top clamp (2); the lower clamp (3); and the base (4). These have been modelled together using the nonlinear boundary condition based on the slideline. Axisymmetric elements with 2 d.f/node and a static faced applied load have been used. The boundary conditions for the nodes in the model are as follows:

- (i) Nodes on the centre line are restrained in X direction.
- (ii) Nodes in  $B_1 - B_2$  are restrained in Y direction.

The dimensions of this model have been optimized in order to (a) give safety of the hydraulic press under the full load operation; (b) maintain the total deflection within the permissible deflection; (c) give as constant a stress as possible across the thickness (t) at half of the height L of the load cell (1); (d) minimize the concentrated stresses at the radius r and  $r_3$ .

### The axisymmetric cap model

This model is shown in Fig. (15.b) in which axisymmetric elements with 2 d.f/node and a static faced applied were utilized. The boundary conditions imposed on the nodes are as follows:

- (i) Nodes on the centre line are restrained in X and Y directions.
- (ii) Nodes on  $B_2$  until the start of the radius  $r_2$  are restrained in Y direction.
- (iii) Nodes on  $B_3$  until the start of the radius  $r_2$  are restrained in X direction.

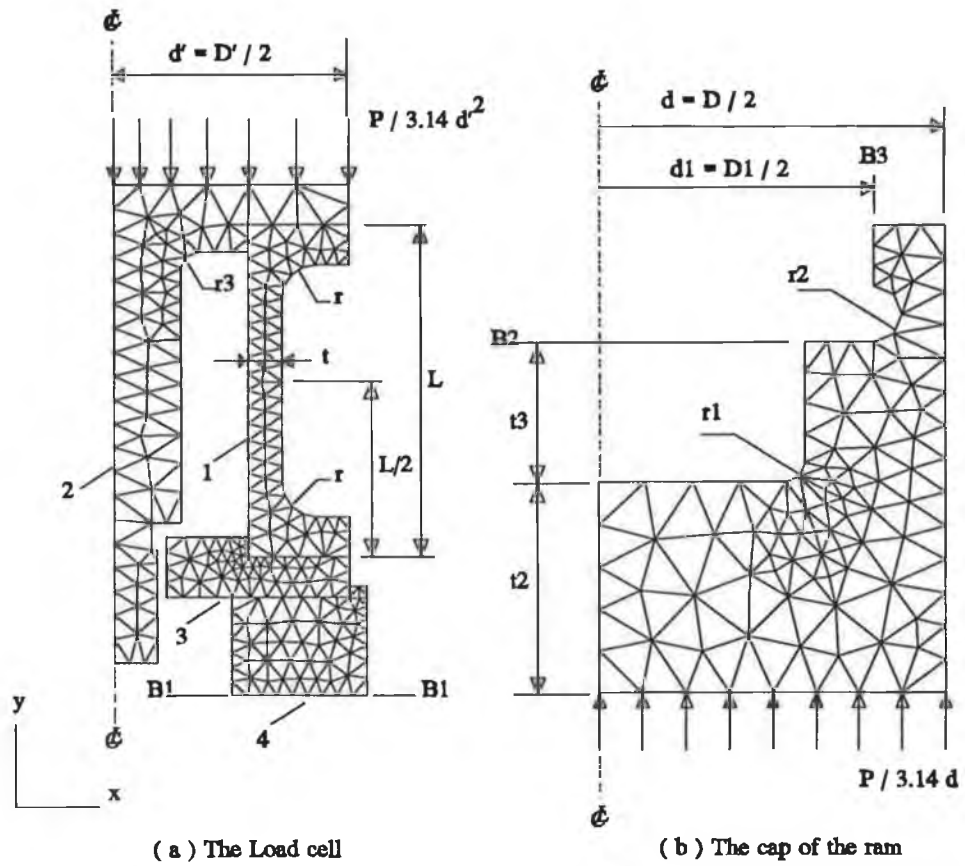
The dimension  $t_2$ ,  $t_3$  and  $d$  were optimized to give maximum strength within the permissible deflection. Whilst  $r_1$  and  $r_2$  were optimised to give the minimum concentrated stress. This optimization was done under the full range of the operational load of the press.

### **The 3-D solid continuum model of the lower loading plate**

This model is represented in Fig. (15.c) in which a quarter of the plate with a quarter of the full operational load of the press were modelled. Solid continuum elements with 3 d.f/node were used in this model. This model has the same geometrical design of the lower plate (10), which holds the hydraulic ram (1) to the top beams (9) in Fig. (5). The objective of this model was to evaluate the strength of this plate within the permissible deflection. The boundary conditions in this model are as follows:

- (i) Nodes on the X-Y plane which passes the centre line are restrained Z direction.
- (ii) Nodes on the Y-Z plane which passes the centre line are restrained in X direction.
- (iii) Nodes on the centre line are restrained in X and Z directions.
- (iv) Nodes along the line  $B_4$  are restrained in Y direction.

The theoretical analysis of this model showed a satisfactorily design of the plate.



$D'$  : The outer diameter of the load cell  
 $D$  : The outer diameter of the cap  
 $D1$  : The inner diameter of the cap " The outer diameter of the ram."

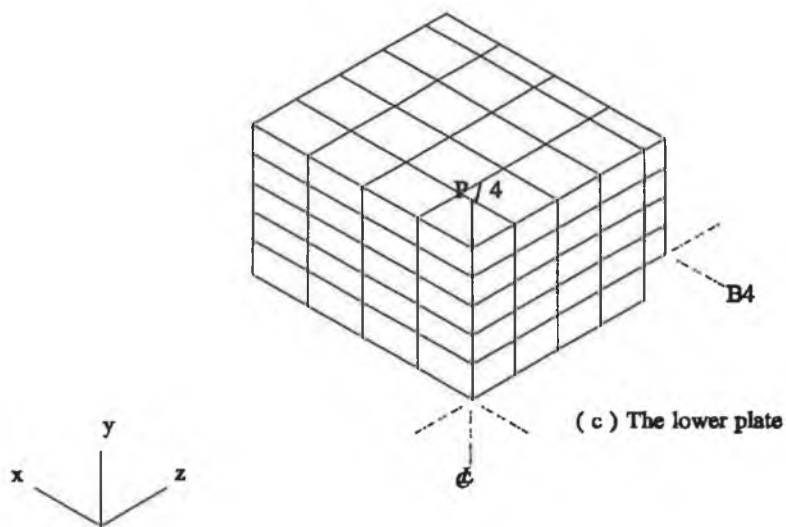


Fig ( 15 )



### **III . Plane stress model of the new design of the hydraulic press structure**

It was observed, experimentally and theoretically after adding the stiffeners to the press bed, that the press structure exhibited insignificant out-of-plane behaviour in terms of deflection. Therefore, plane stress can be used for studying the behaviour of the new design of the press structure in order to reduce core memory requirement and the time for the analysis. The same features of the model in Fig.(10) have been considered in this analysis. However, in the plane stress model of the new design of the press structure, the press bed was linked with the rest of the press through two pins situated on a distance ( $H_2$ ) as shown in Fig. (16). The analysis was carried out when the press bed was at the lower position at  $B_2$  in Fig. (16.a). The nodes  $B_2$  were restrained in X and Y directions whereas the nodes on the centre line were restrained in X direction. The L-shaped beam was divided into 504 linear isoparametric elements with 3 and 4 nodes, having 382 nodal points, Fig.(16.a). Half of the press bed was divided into 232 linear isoparametric elements with 3 and 4 nodes, having 181 nodal points, Fig.(16.c). The mesh gradation principle has been utilized to achieve finer elements in the zones of the stress concentration. Each node has 2 d.f. The total number of degrees-of-freedom for the L-shaped beam was 1008 and for the half of the press bed beam, 362. These optimum figures have been arrived at after several trials of analyzing different meshes with different numbers of elements. Thus, this showed that when the number of elements in the mesh in Fig. (16.a) and Fig. (16.c) exceeded there was no improvement in the accuracy of the analysis but the required computer core store was increased. The factors considered, in order to study the effects of structural parameters on the stiffness characteristics and thus to optimize the material cost, were the width of the hydraulic press ( $L$ ) as shown in Table (II), Fig. (16.a); and chamfering the edge as

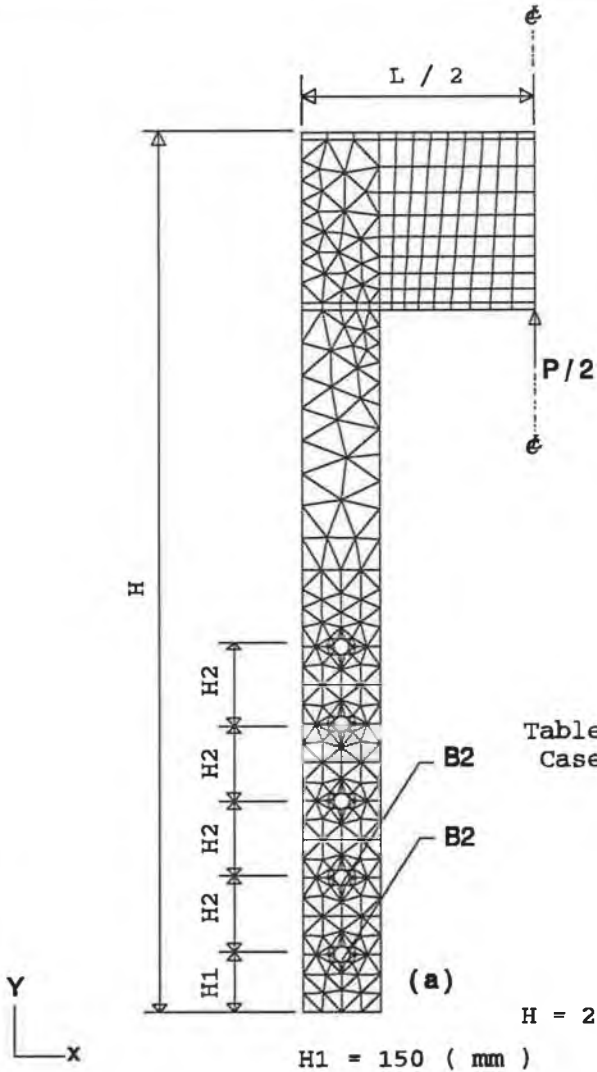
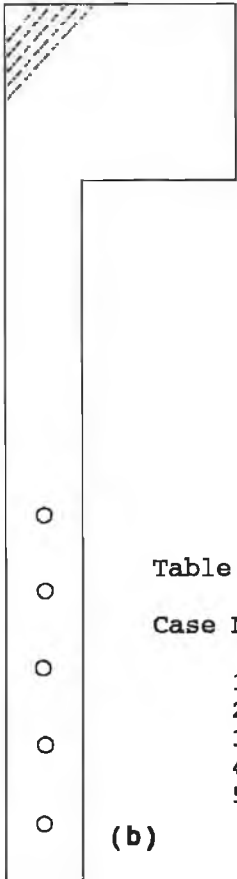
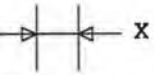


Table ( II )

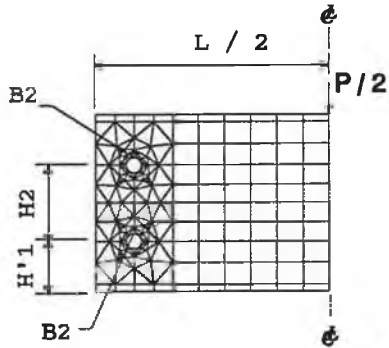
Case No.	L/H
1	0.7107
2	0.675
3	0.640
4	0.605
5	0.570
6	0.535
7	0.5

$H = 2285$  ( mm )

$H_1 = 150$  ( mm )



H2 = 198 ( mm )



(c)

H'1 = 130 ( mm )

Table ( III )

Case No.	X (mm)	Y (mm)
1	50	50
2	100	100
3	150	150
4	250	250
5	300	300

(b)

Fig ( 16 )

shown in Table (III), Fig. (16.b). The height (H) of the press Fig. (16) kept constant during the analysis.

# CHAPTER 4

## EXPERIMENTAL MODIFICATION OF EQUIPMENT AND MATERIAL

### 4.1 Introduction

From the review of the technical development of the hydraulic press, it can be seen that this development goes back to 18th Century [78]. The studies on some technical features of the hydraulic press can be obtained from the sources mentioned in references [88-93]. The modifications of the experimental hydraulic press, is based on the theoretical model. The objective of this modification is to make a comparative study between the mathematical model and actual press machine. Therefore, in order to obtain the measurement of the load deflection and thus the stiffness of the present press structure, the present press machine has been modified in-house to perform these measurements. These developments are shown in Fig. (17) and are as follows:

- (i) Designing the measurement system (i.e. the load cells mobile and fixed L.V.D.T.).
- (ii) Designing the platens and loading tools (i.e. platen system and the cap of the ram).
- (iii) Designing the hydraulic system.
- (iv) Designing the main stand.
- (v) Designing the data acquisition system.

In fact, these developments formed the apparatus used to perform the experimental work.

Fig. (18) shows a photograph of this apparatus.

#### **4.1.1 Designing the measurement system**

The measurement system developed for this current work consists of:

- (i) The Load Cell
- (ii) The Mobile L.V.D.T.
- (iii) The Fixed L.V.D.T.

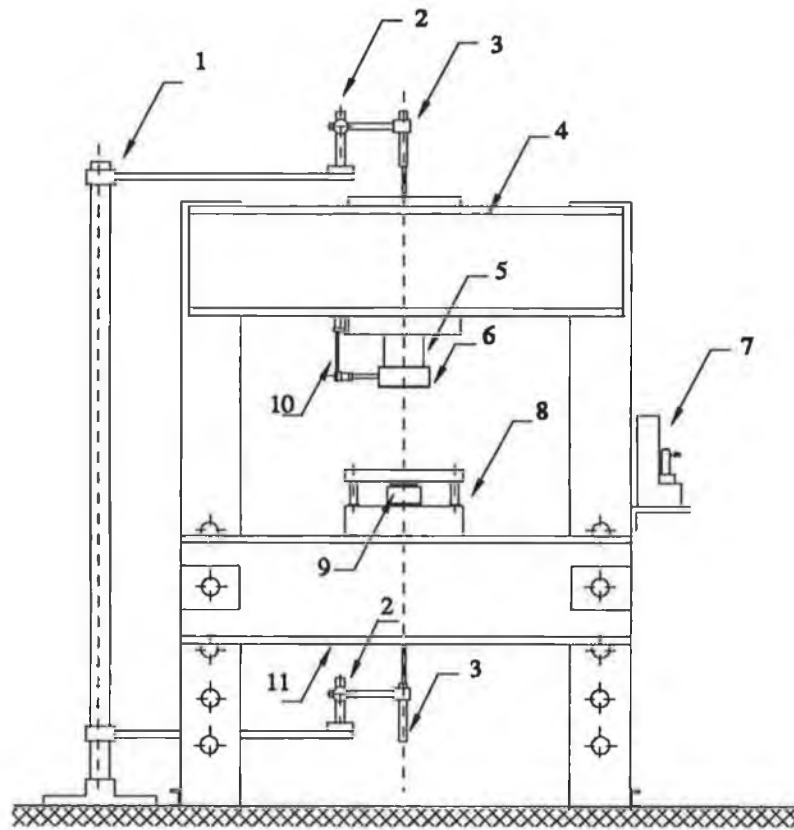
#### **The Load Cell**

This device has been designed to measure up to a 150-tonne static load. The assembly design of this device is shown in Fig. (19.a). This consists of the following components:

- (i) Top clamp (2)
- (ii) Lower clamp (5)
- (iii) The main element of the load cell (3)
- (iv) The case (4)
- (v) The base of the load cell (6).

The main element of the load, where a full bridge strain gauge circuit has been

## Schematic Diagram Of The Apparatus Rig



- |                         |                            |
|-------------------------|----------------------------|
| 1: Main Stand           | 6: Cap Of The Ram          |
| 2: Magnetic Stand       | 7: Hydraulic System        |
| 3: Mobile L.V.D.T       | 8: Platen System           |
| 4: Frame of The Machine | 9: Load Cell               |
| 5: Double-Acting Ram    | 10: Fixed L.V.D.T          |
|                         | 11: The Bed Of The Machine |

Fig ( 17 )

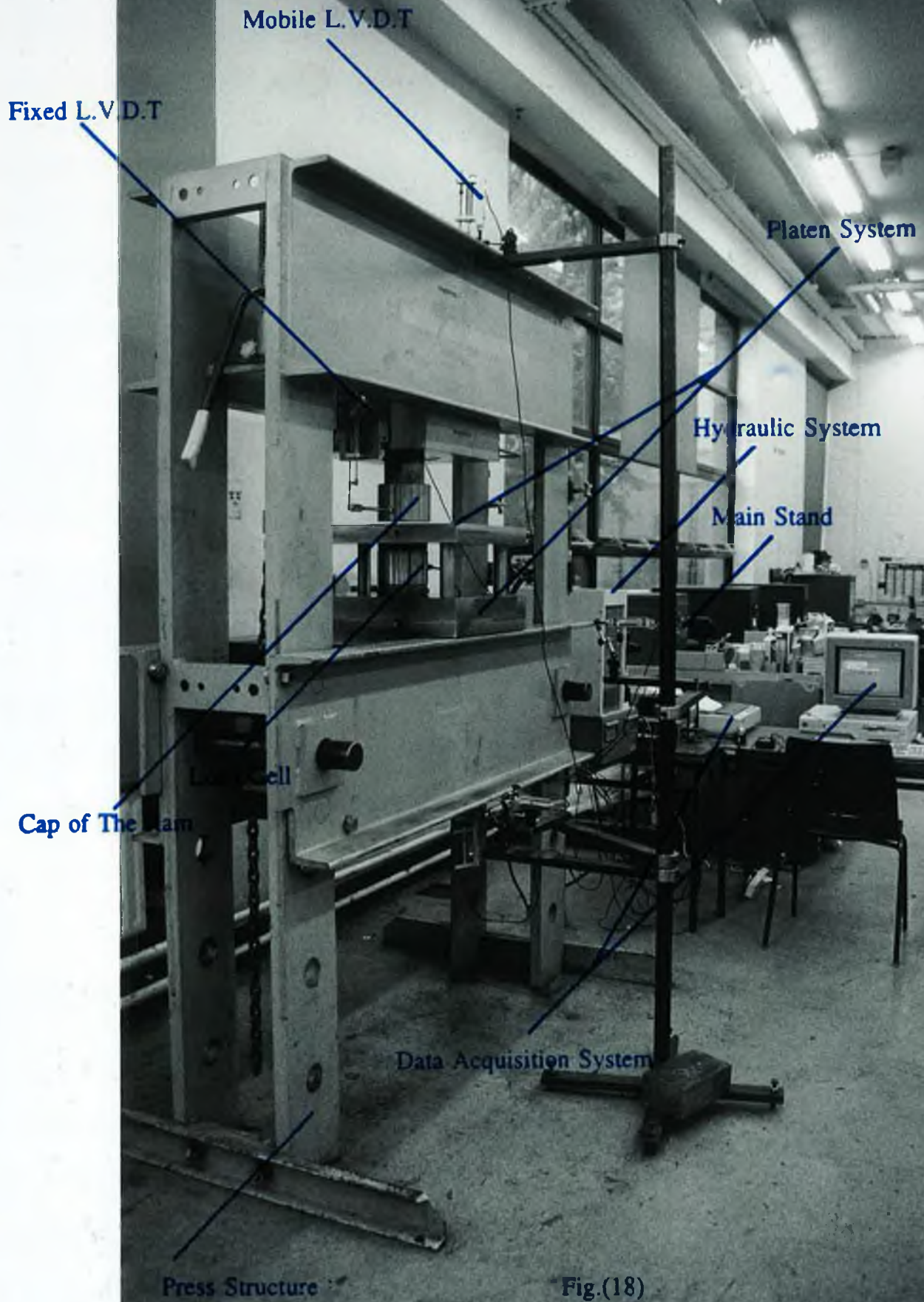


Fig.(18)



connected, has been used as the main sensor of the load cell. The strain gauge circuit is shown in Fig. (19.b) where the  $V_i$  is the excitation voltage of the bridge (VDC) and  $V_o$  is the output voltage of the bridge. The output voltage represents the elastic strain in the main element (3) caused by the applied external load. The measured elastic strain should be converted to an equivalent form of applied load and this has been done in the calibration process of the load cell. The top and lower clamp have been used to pre-load the load cell to overcome the nonlinearities of this load cell. The knurled nut (7) has been used to lock the clamps (2) and (5). The case (4) has been used to protect the strain gauge circuit from any physical environmental damage. The base (6) has been designed to allow the load cell to deform elastically without any restrictions. The indentational hole (1) has been made to denote the centre line of the load cell. The detailed design of the load cell are shown in Fig. (20) to (22) in which the geometrical dimensions have been obtained from the numerical model described in Chapter 3 for Fig.(15.a).

### **The calibration procedure of the Load Cell**

This procedure has been done to find the relationship between the external applied load and the output of the load cell, and thus the sensitivity of the load cell. The calibration procedure has been done on a 250 KN Instron machine. The schematic diagram of this procedure is shown in Fig. (23). A 100 KN has been considered as a pre-load to overcome the non-linearity encountered during the process of calibration. Thus the sensitivity of the load cell has been found as follows:

# The Load Cell

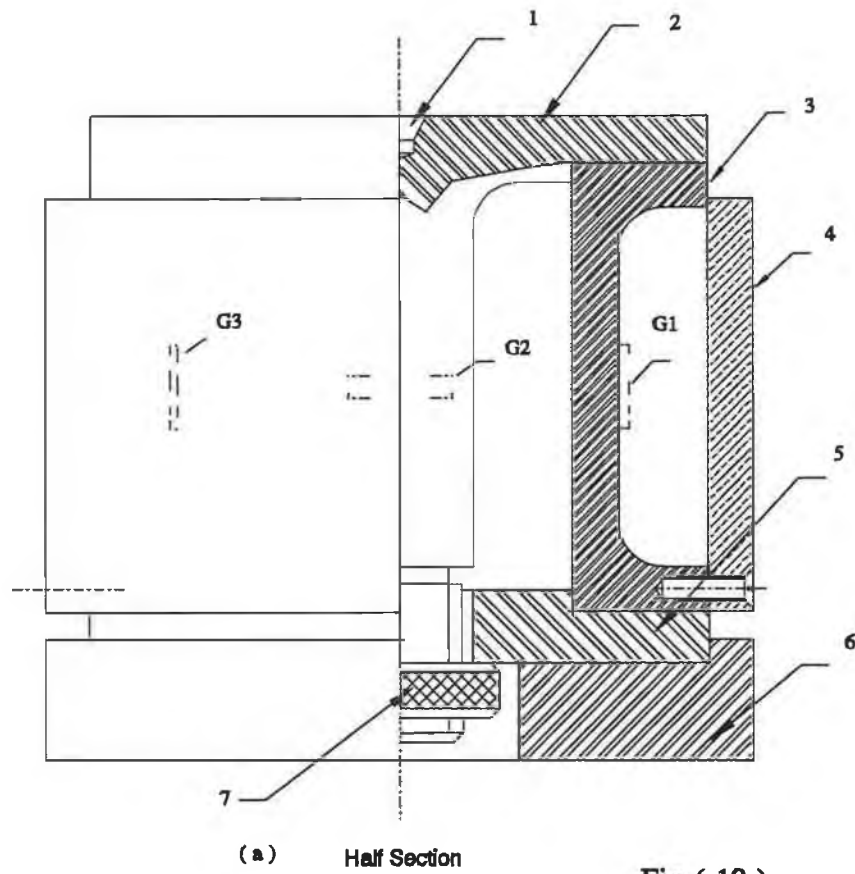
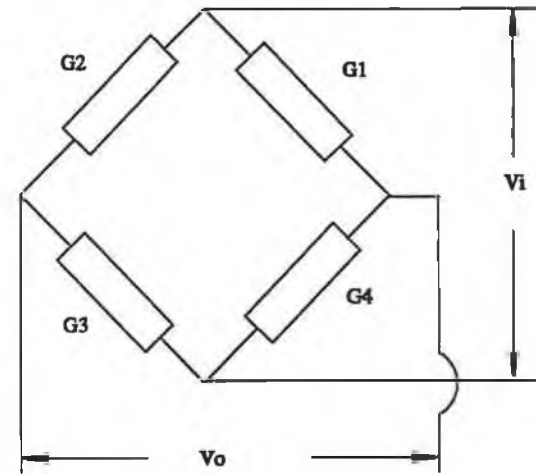


Fig ( 19 )

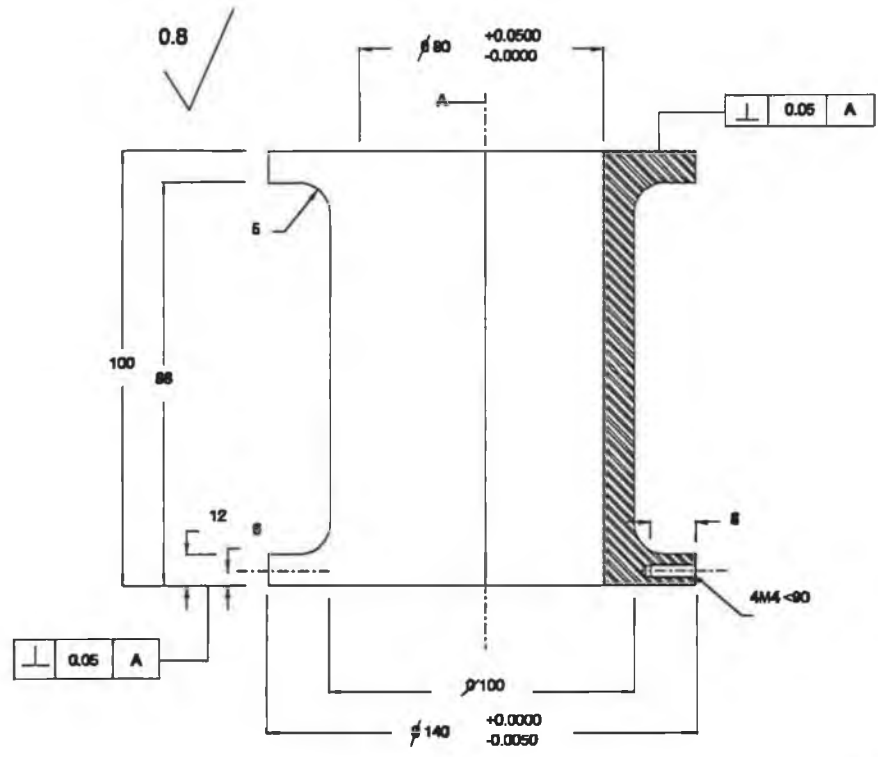
G1,G2,G3 and G4 are strain gauges  
of 120 Ohm each



- G4 is in front of G2 in the  
assembly drawing on the left

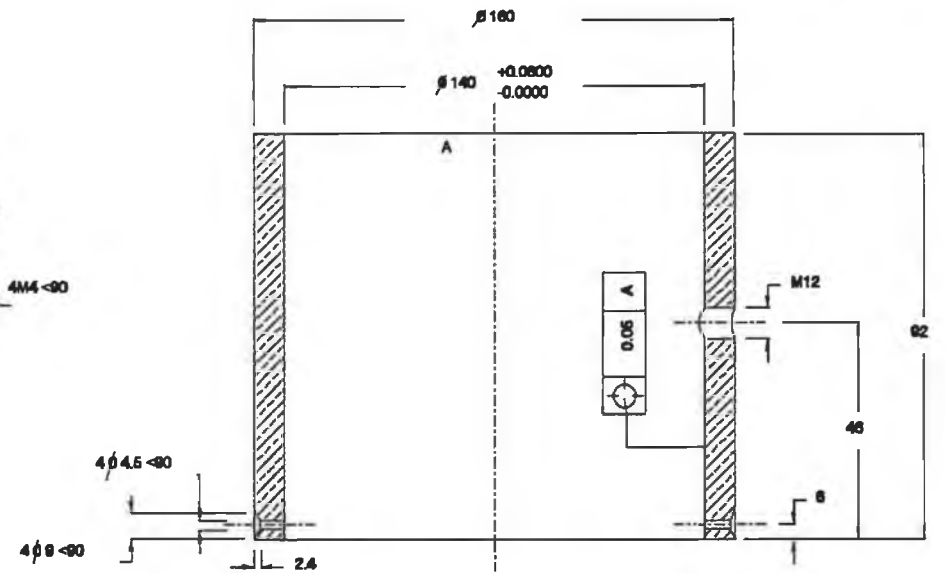
(b)

Assembly : 9



Part : 3  
Material : Tool Steel ( AISI D2 )

Assembly : 9  
QTY : 1 ( Each )  
Dimension : ( mm )



Part : 4  
Material : Copper

- Remarks :
- 1 : All Tolerances Are To Be + 0.01 mm Unless Otherwise Stated .
  - 2 : Break All Sharp Edges To 1/45 Unless Otherwise Stated .

Fig ( 20 )

1.6

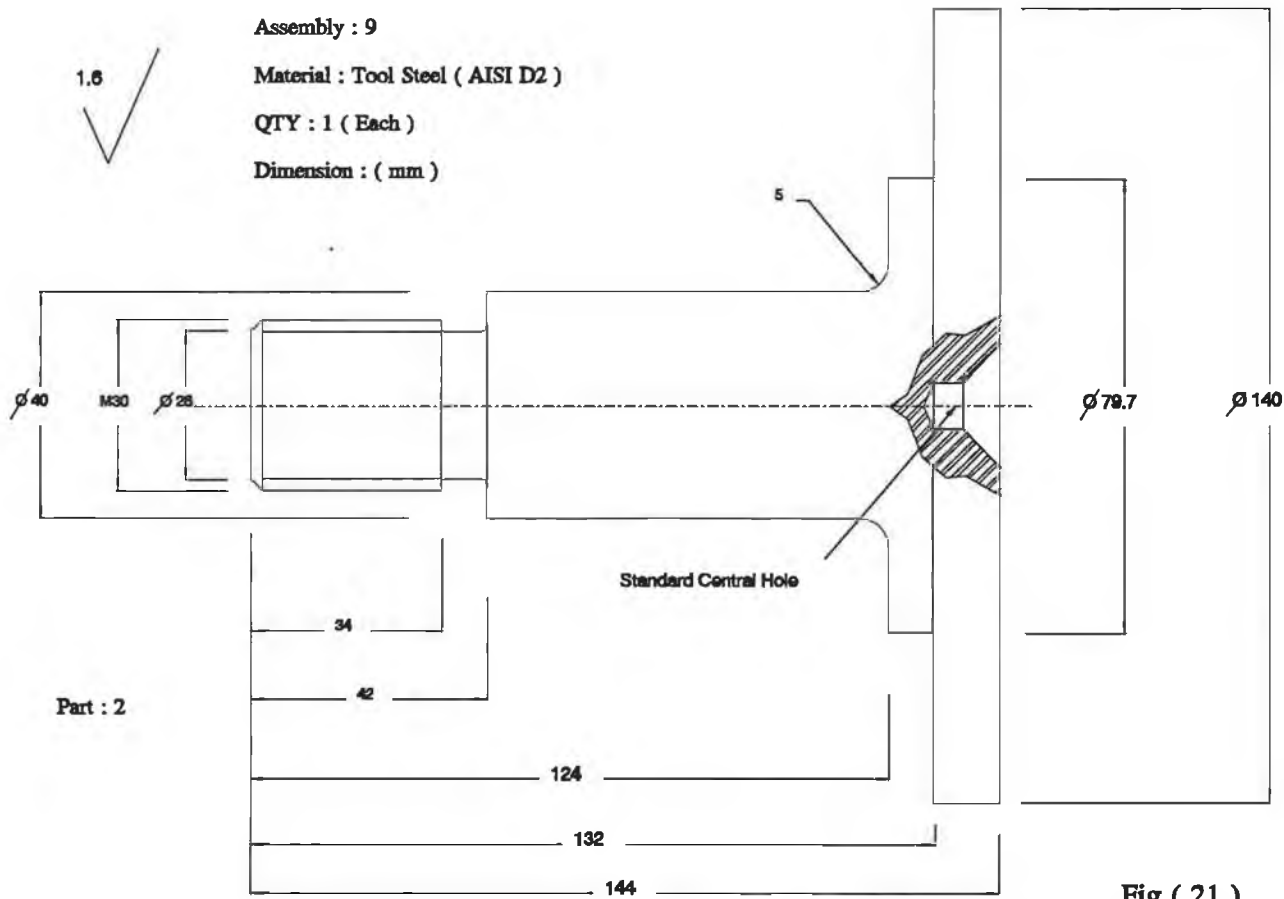


Assembly : 9

Material : Tool Steel ( AISI D2 )

QTY : 1 ( Each )

Dimension : ( mm )



Remarks :

- 1 : All Tolerances Are To Be  
+ 0.01 mm Unless Otherwise  
Stated .
- 2 : Break All Sharp Edges To  
1 /45 Unless Otherwise  
Stated .

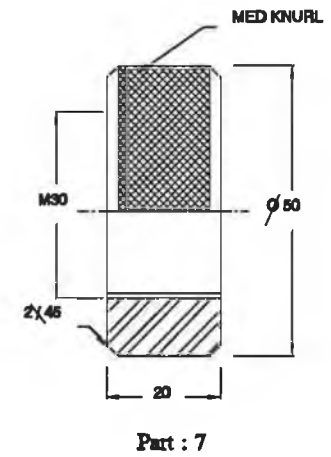
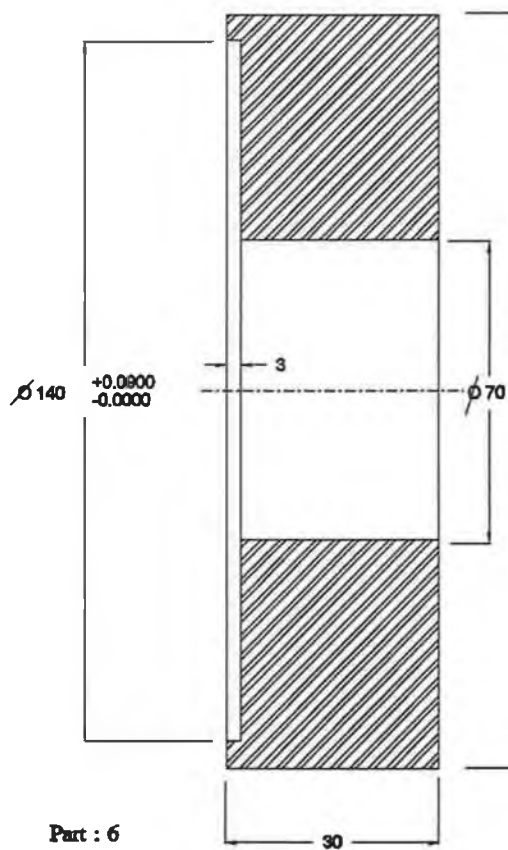
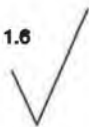


Fig ( 21 )



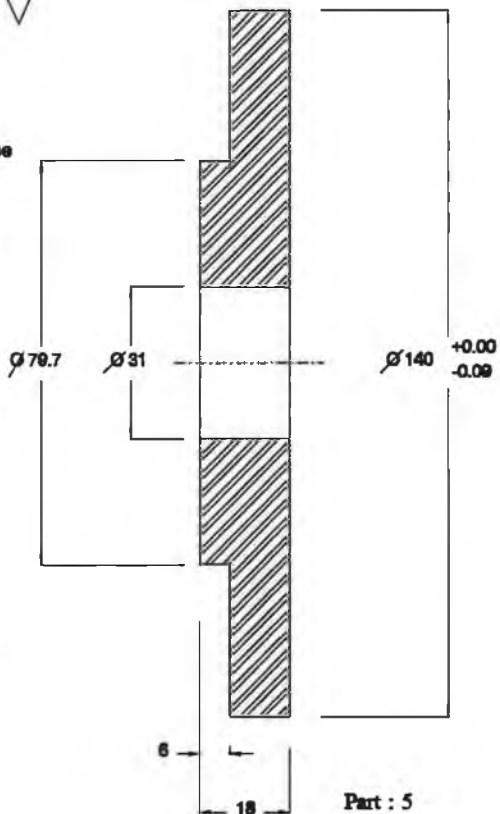
1.6



Remarks :

1 : All Tolerances Are To Be  
+ 0.01 mm Unless Otherwise  
Stated .

2 : Break All Sharp Edges To  
1 / 45 Unless Otherwise  
Stated .



Assembly : 9

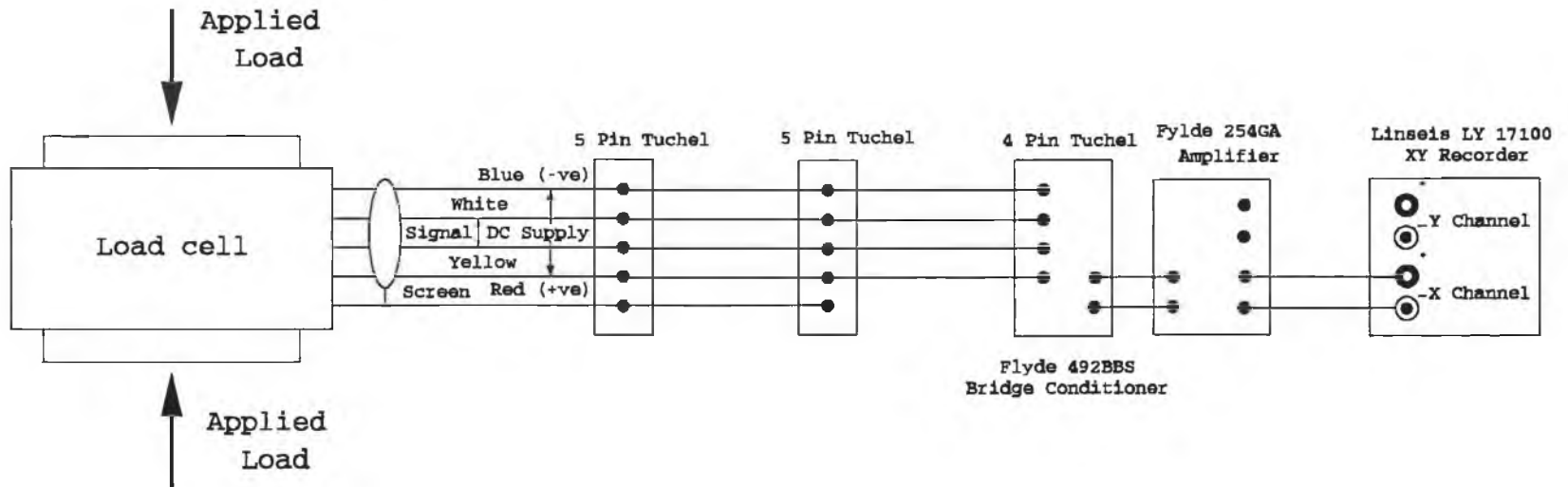
Material : Tool Steel ( AISI D2 )

QTY : 1 ( Each )

Dimension : ( mm )

Fig ( 22 )

### Configuration Of The Calibration Instrumentation



- The Applied Load Is Taken From an Instron Testing Machine Of 250 KN

Fig ( 23 )

$$\text{Sensitivity} = 1.95 \mu V / KN / V_i$$

4.1

This means that the sensitivity of the load cell is 1.95  $\mu$ V for each KN per the excitation voltages. Assuming a 6 VDC excitation voltage ( $V_i$ ) with an amplification of 200 and a 100 KN external applied load, then output voltage of the load cell is:

$$\left. \begin{aligned} V_o &= 1.95 \mu V \times 100 \times 6 \times 200 \\ V_o &= 0.234 \text{ (volts)} \end{aligned} \right\} 4.2$$

Therefore, from 4.2, the applied load in (KN) is:

$$\text{Load (KN)} = \frac{V_o \text{ (volts)}}{1.95 \times 10^{-6} \times 200 \times 6} \quad 4.3$$

The calibration curve of the load cell after the pre-loading according to equation (4.3) is shown in Fig. (24) and a full detailed description of the calibration procedure can be found in Appendix (C).

### The mobile L.V.D.T.

This sensor has been used to measure the displacement of different points of the press structure. During the measurement process this L.V.D.T. was attached with a magnetic stand which in turn was attached to the main stand (1) as shown in Fig. (17). Usually the L.V.D.T.'s are purchased as an electronic element without any mechanical attachments or fasteners. Therefore, in order to make versatile use of this sensor in the



## Load Cell Calibration Curve

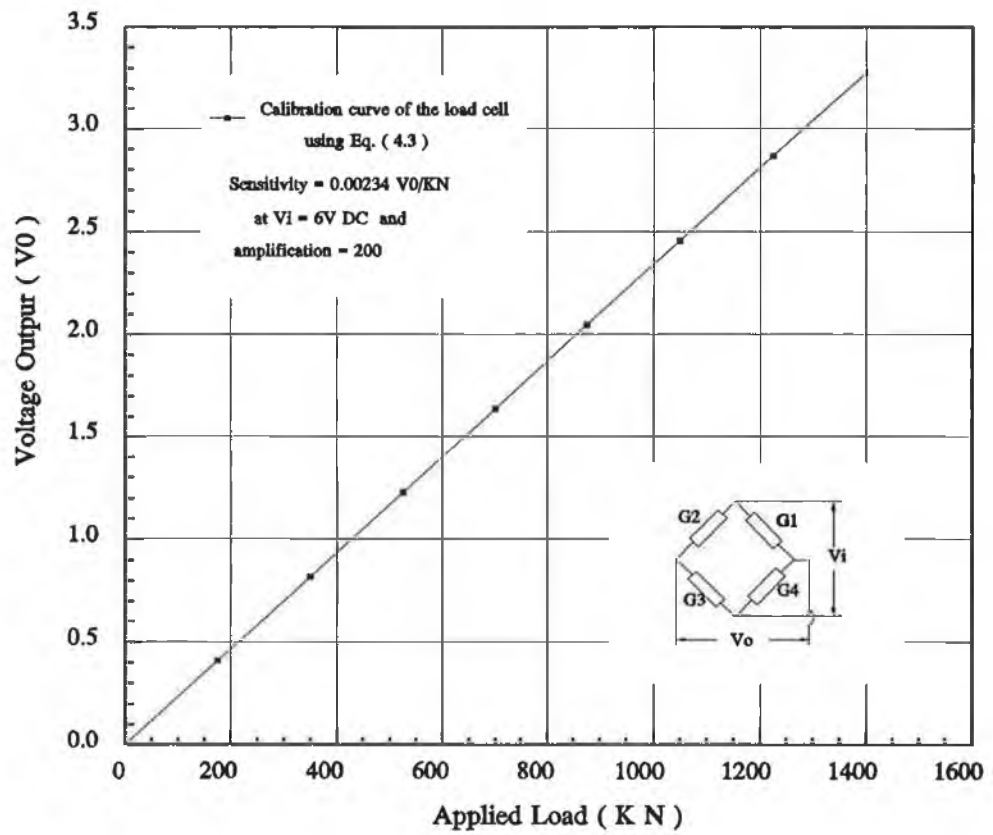


Fig ( 24 )

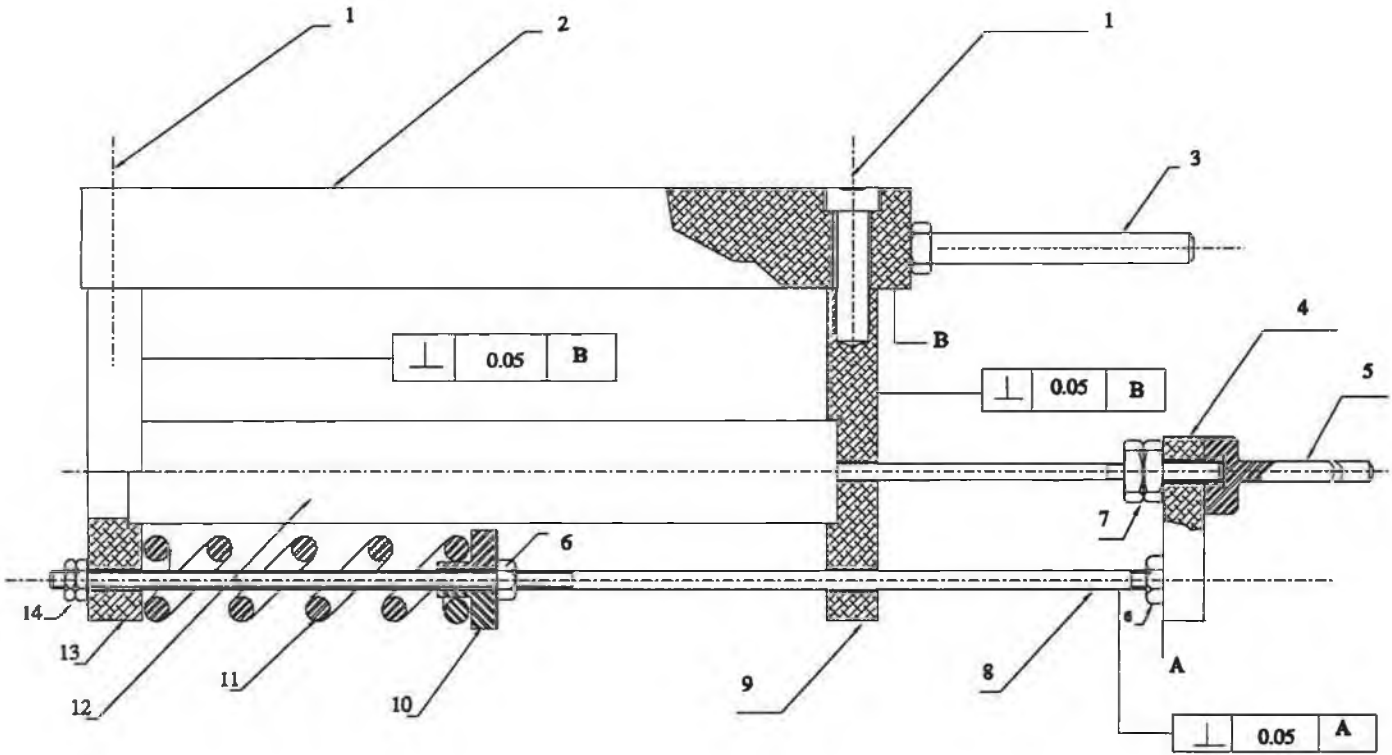
mechanical measurement, a mechanical attachment has been designed as shown in Fig. (25). The L.V.D.T. (12) has been attached to the plates (9) and (13) which are connected to plate (2) through four socket-head bolts (1). The shaft of the L.V.D.T. was connected to the shaft (8) through the plate (4). The shaft (8), the spring (11) and the nuts (10) and (14) were used in the design to keep the stylus (5) in contact with the measuring point and to calibrate the L.V.D.T. to zero reference. The rod (3) has been used to connect the L.V.D.T. to a magnetic stand. Fig. (26) shows a photograph of the assembly design of the mobile L.V.D.T. after the manufacturing. The detailed design of the individual components of the mechanical attachment of the mobile L.V.D.T. are shown in Fig. (27) to (29).

### **The Fixed L.V.D.T.**

#### **I . Description**

The design of the mechanical attachment of the fixed L.V.D.T. is shown in Fig. (30). The plate (14) has been linked to the plate (12) through two screws. Plate (18) can slide through the guideway of plate (12) when screw (5), which holds plate (18) on plate (12), is released. The L.V.D.T. (2) has been linked to plates (1) and (6) which have been linked to plate (18) through four counter sunk screws (11). Two one-way self-resetting microswitches have been attached to the plate (17) which is fixed to the plate (18) through two counter sunk screws (13). The shaft (3), which is connected to the shaft of the L.V.D.T. (2) through the plate (8), can move freely through the hole in plates (1) and (6). The sliding guide (4) can be fixed to any position between the two microswitches (15) by the pin (16). The distance between the two microswitches has

### Mobile L.V.D.T



Assembly : 3

Fig ( 25 )

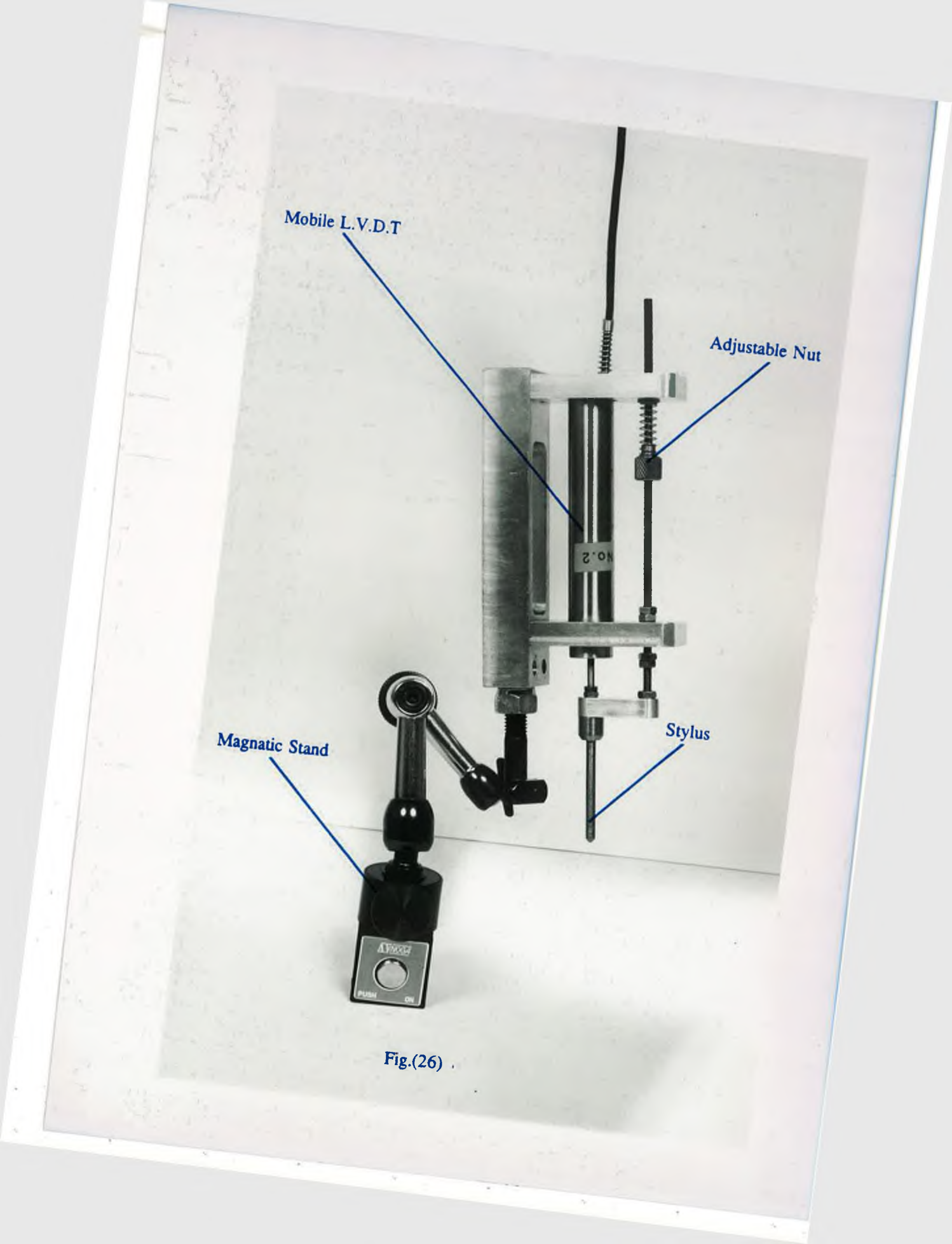
Mobile L.V.D.T

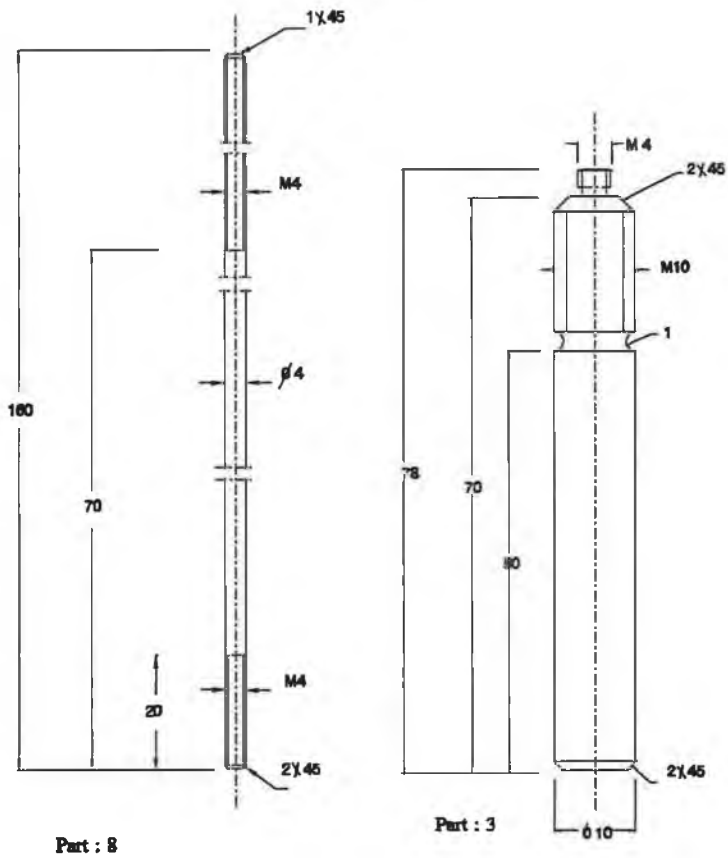
Adjustable Nut

Magnetic Stand

Stylus

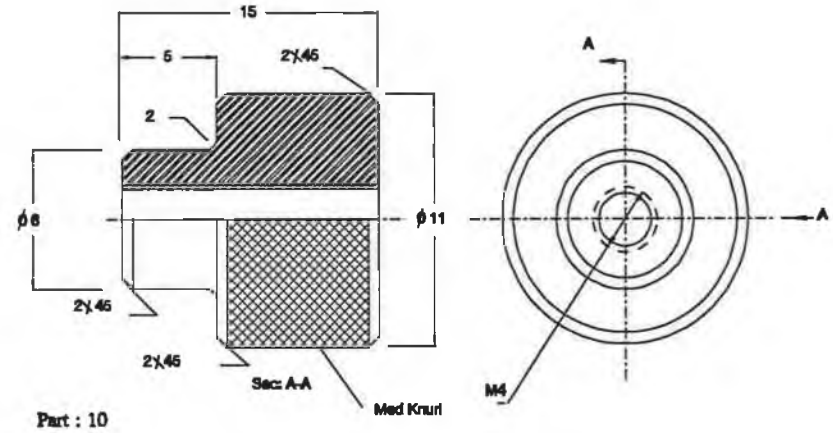
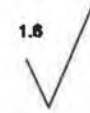
Fig.(26)





Remarks :

- 1 : All Tolerances Are To Be  
+ 0.01 mm Unless Otherwise  
Stated .
- 2 : Break All Sharp Edges To  
1 / 45 Unless Otherwise  
Stated .



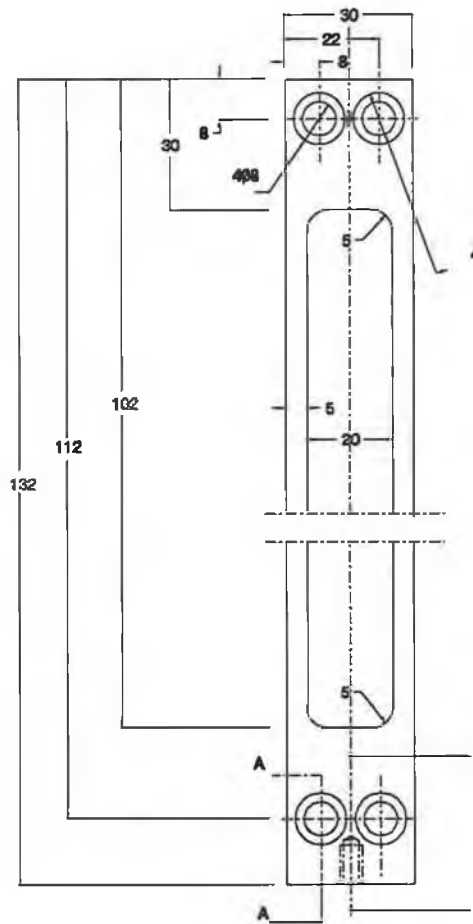
Assembly : 3

Material : Mild Steel

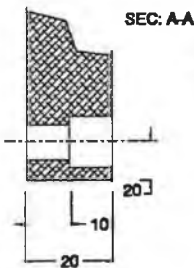
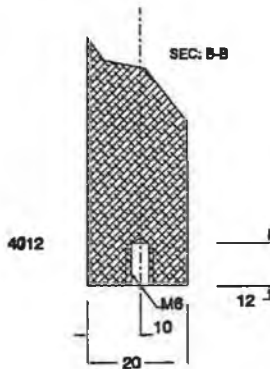
QTY : 5

Dimension : ( mm )

Fig ( 27 )

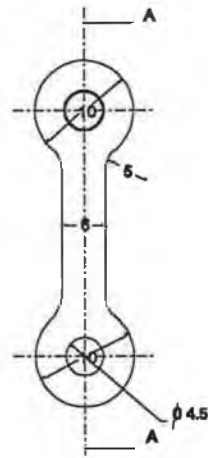


Material : Aluminium  
QNT : 5



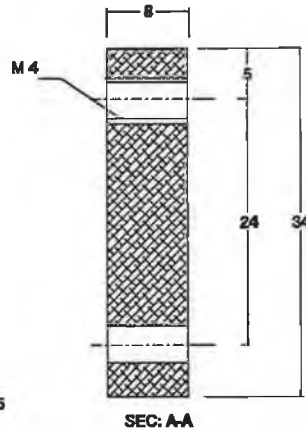
Part : 2

B



Part : 4

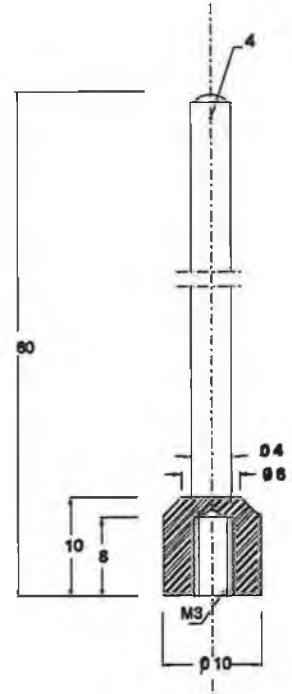
Material : Aluminium  
QNT : 5



Remarks :

- 1 : All Tolerances Are To Be  $\pm 0.01$  mm Unless Otherwise Stated .
- 2 : Break All Sharp Edges To  $1/45$  Unless Otherwise Stated .

1.8/

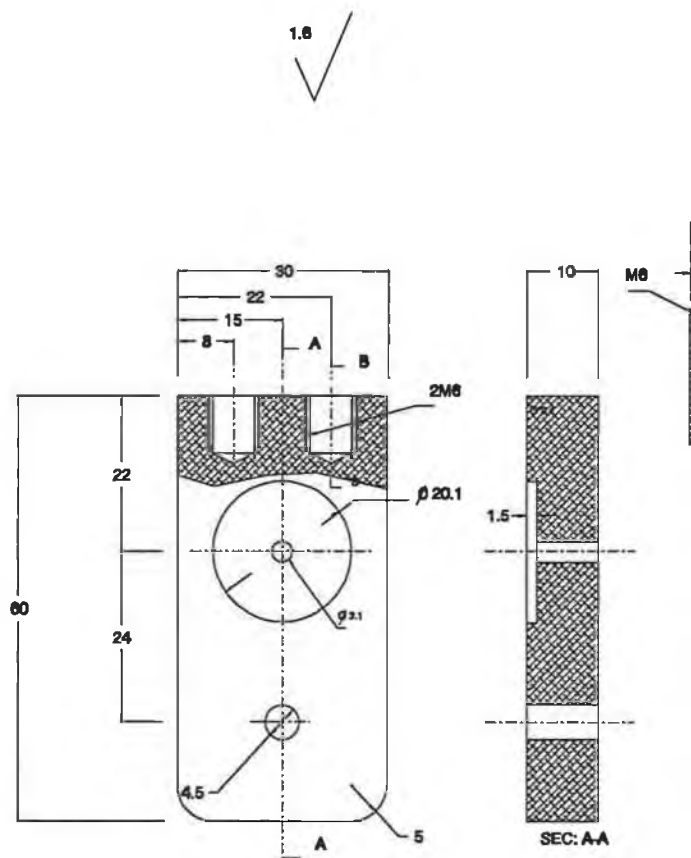


Part : 5  
Material : Mild Steel  
QTY : 5

Assembly : 3  
Dimension : ( mm )

Fig ( 28 )

105



Assembly : 3

Part : 9

Material : Aluminium

QTY : 5 ( Each )

Dimension : ( mm )

Remarks :

1 : All Tolerances Are To Be

$\pm 0.01$  mm Unless Otherwise

Stated .

2 : Break All Sharp Edges To

$1/45$  Unless Otherwise

Stated .

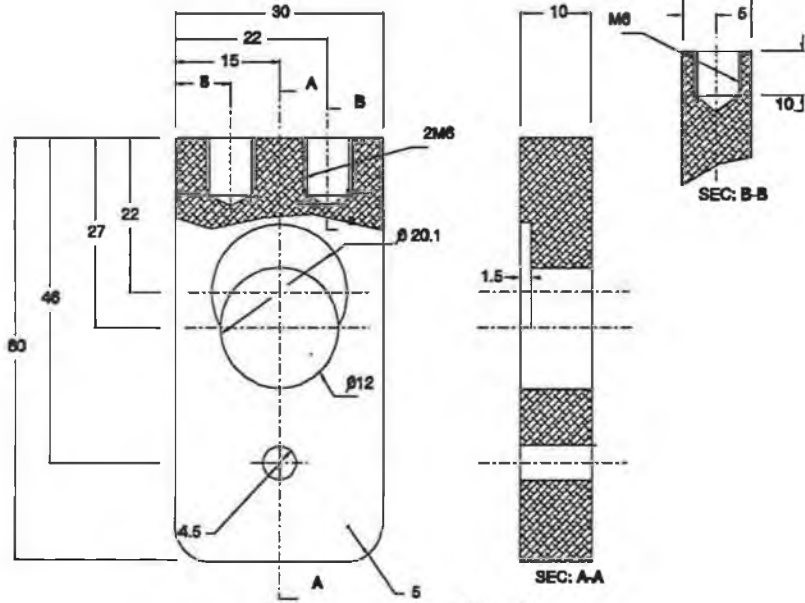
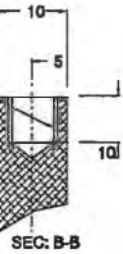


Fig ( 29 )

Part : 13



been designed to be less than the maximum absolute range of the L.V.D.T. (2). The pin (16) can travel through the guideway of the plate (17) in order to switch on and off the operation of the press by the switches (15). The schematic diagram of the electrical circuit of the microswitches is shown in Fig. (31). In this circuit the electrical motor (M) is switched on by switching on (S), (K<sub>1</sub>) and (K<sub>2</sub>). The electrical motor (M) is switched off when either one of (K) or (K<sub>1</sub>) is opened. Fig. (32) shows a photograph of the assembly of the mechanical attachment of the fixed L.V.D.T. installed on the press machine. The fixing plate has been designed to allow the adjustment to be made during the installation of the fixed L.V.D.T. The function of the universal coupling is to overcome the misalignment between the centre line of the fixed L.V.D.T. and the centre line of the hydraulic ram during the operation of the press.

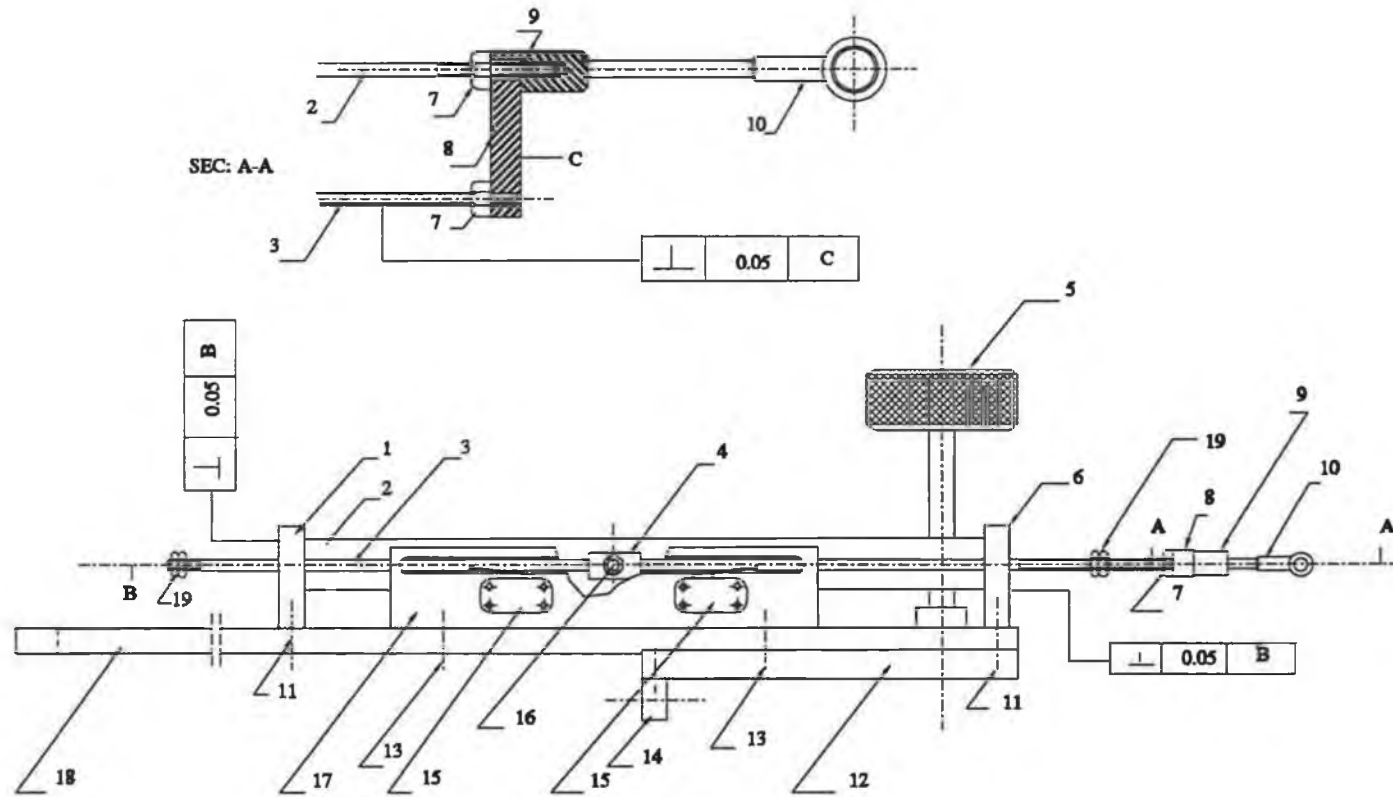
## **II . Objective and functioning**

The objective of the design described in Fig. (30) was to:

- (i) measure the total deformation of the hydraulic press structure in the direction of the operational load after the overall modification.
- (ii) measure the total deformation of the compressed workpiece in the direction of the operational load.

The maximum positive range of the L.V.D.T. (2) is 50 mm whereas the maximum travel of the ram is 333(mm). Therefore, the machine is switched off automatically before exceeding the maximum travel of the ram. This happens when the pin (16) touches one of the microswitches (15). In this case, the range of the L.V.D.T. (2) can be extended

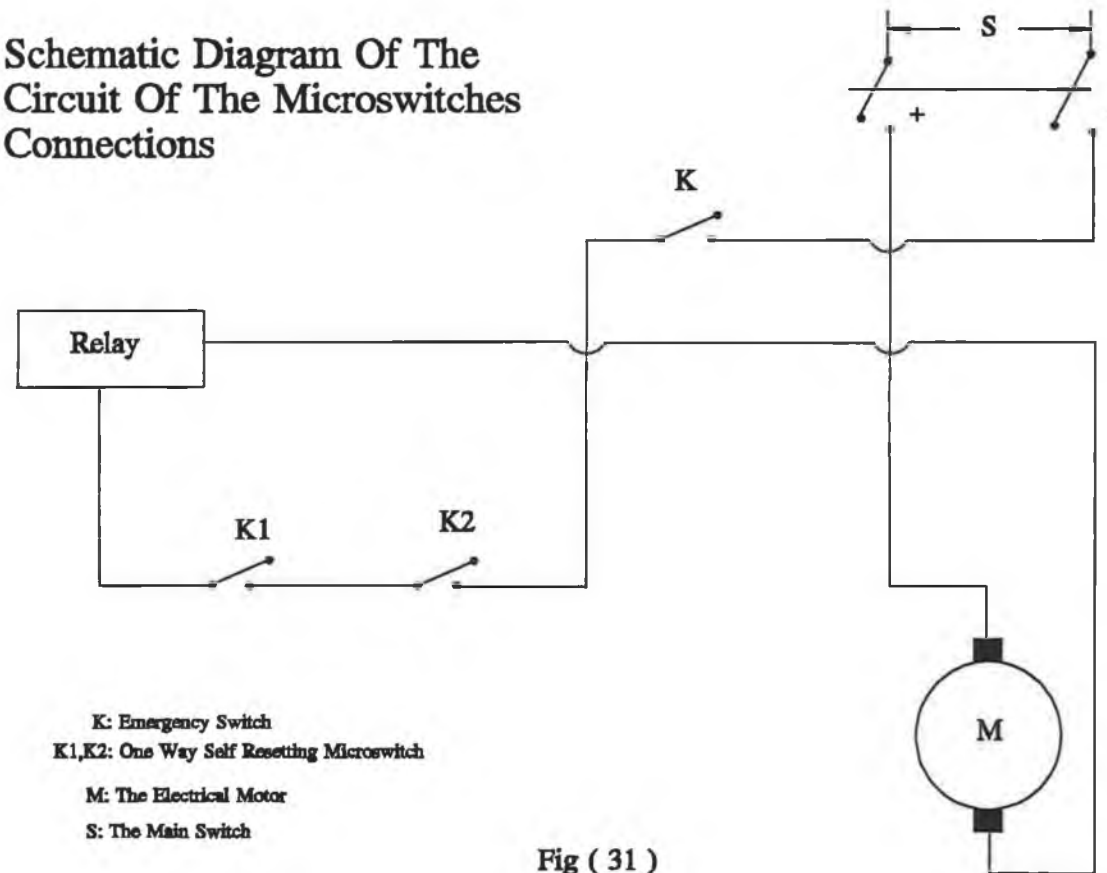
### Fixed L.V.D.T



Assembly : 10

Fig ( 30 )

### Schematic Diagram Of The Circuit Of The Microswitches Connections



**K:** Emergency Switch  
**K1,K2:** One Way Self Resetting Microswitch  
**M:** The Electrical Motor  
**S:** The Main Switch

Fig ( 31 )

Fixing Plate

Microswitches

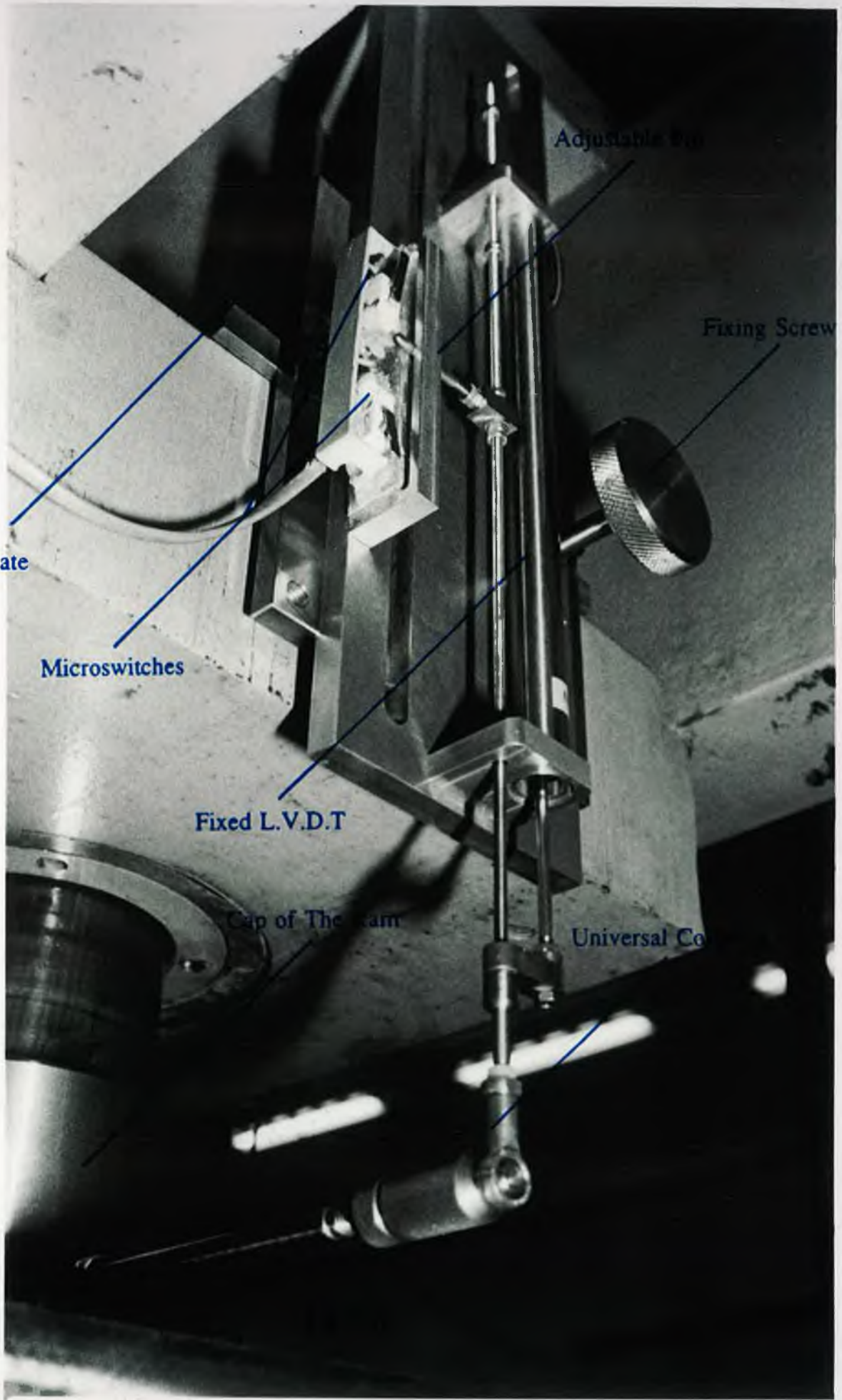
Fixed L.V.D.T

Cap of The Ram

Adjustable Pin

Fixing Screw

Universal Co



by releasing the screw (5) and sliding the plate (18) to move the pin (16) away from the microswitches and locking the screw (5) again. This should happen in the hold position of the ram. After this the displacement of the ram can be started from a new position. This position can be accumulated with the previous one to obtain the total displacement of the ram within its range. The design of the fixed L.V.D.T. can be used to fix a range of displacements where the press machine stops before exceeding the limit of the fixed L.V.D.T. This can be done by calibrating the travel of the L.V.D.T. (2) using the sliding guide (4) and the nuts (19). The individual design of the components of the design in Fig. (30) is shown in Fig. (33) to (37).

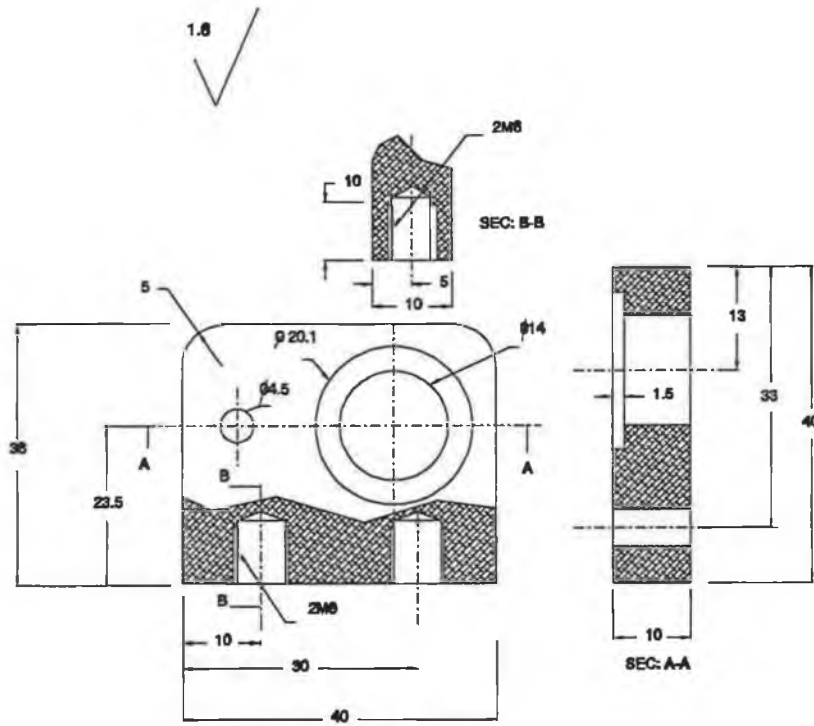
#### **4.1.2 Designing the platens and loading tools**

This contains the design of the following:

- (i) The platen system
- (ii) The cap of the ram.

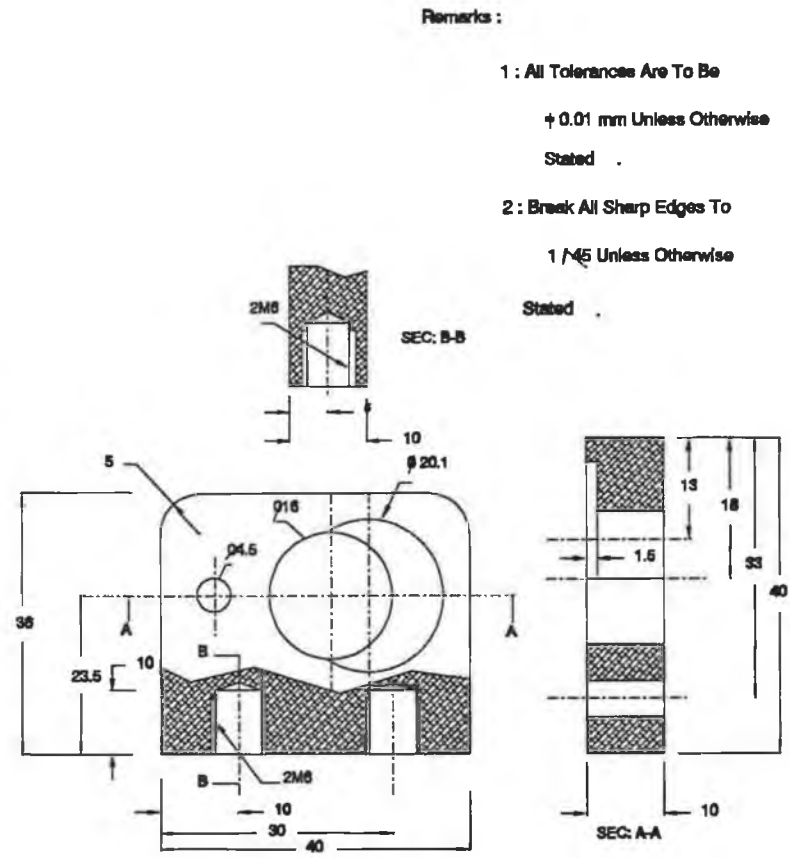
##### **The platen system**

This has been used as a work table of the hydraulic press. The assembly design of the platen system is shown in Fig. (38). The lower loading plate (5) has been positioned on the press bed. This plate was designed with four threaded holes (4) in which four eye bolts have been used for lifting. The four guides (3) have been situated on the lower loading plate (5). These guides have been used to guide the movement of the



Assembly : 10  
 Material : Aluminium  
 QTY : 1 ( Each )  
 Dimension : ( mm )

Part : 6

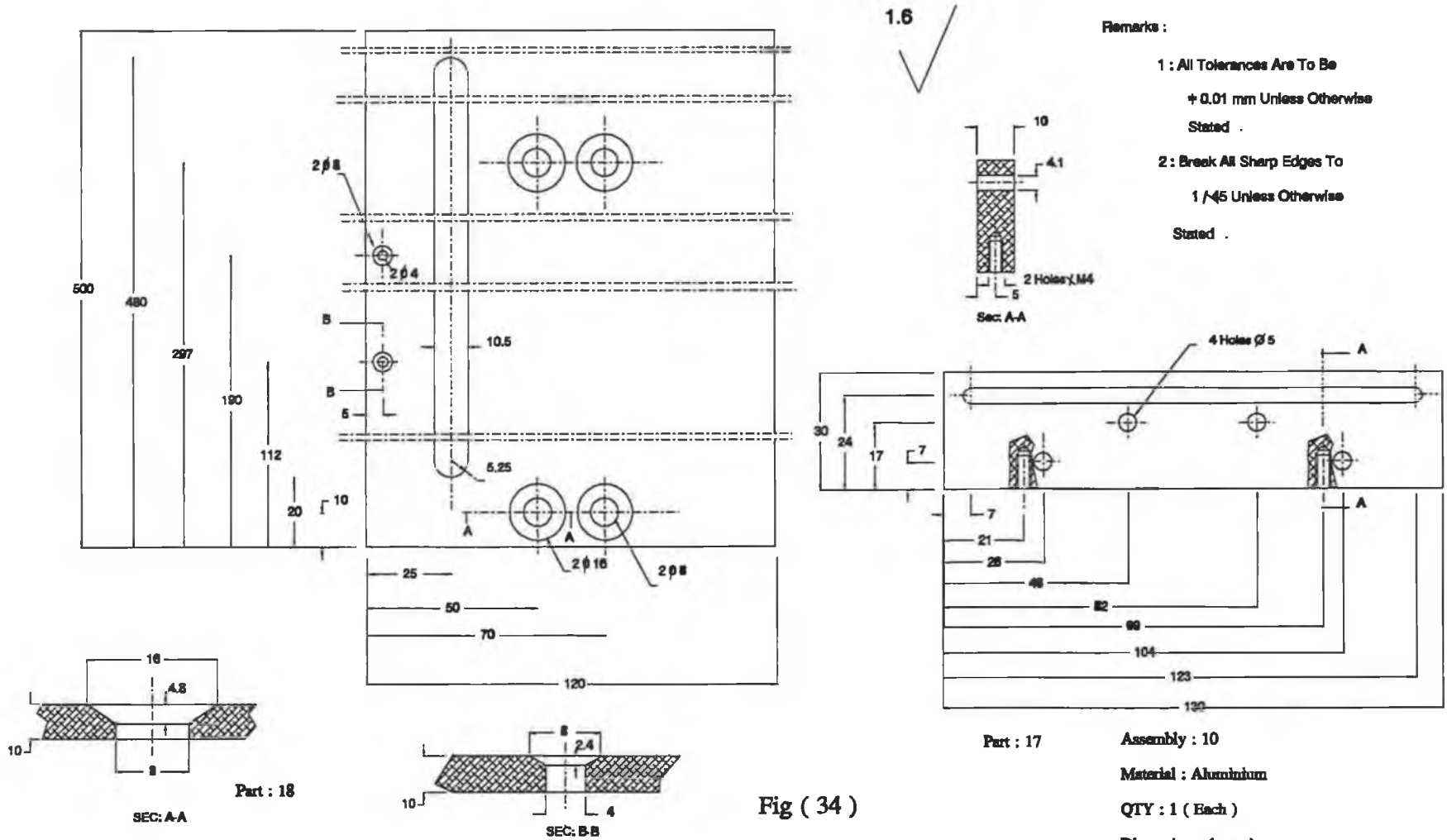


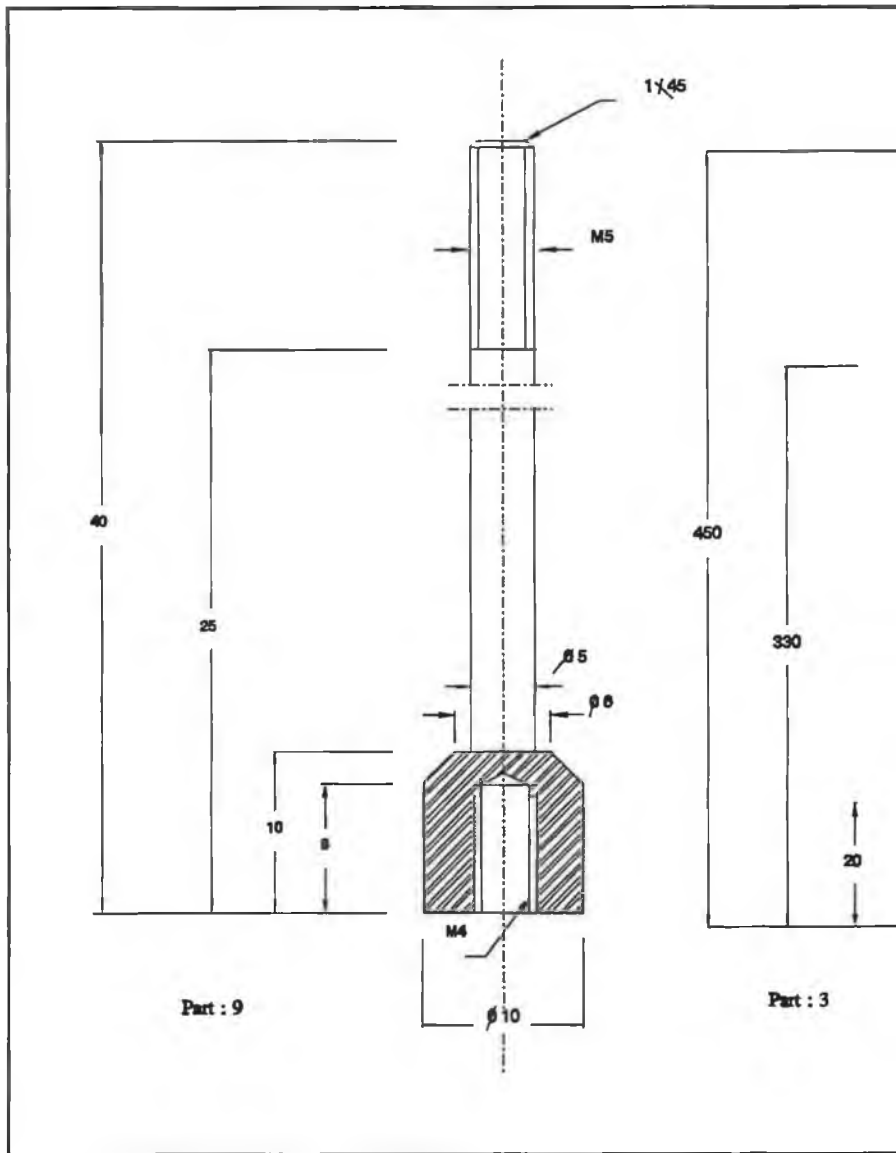
Part : 1

Remarks :

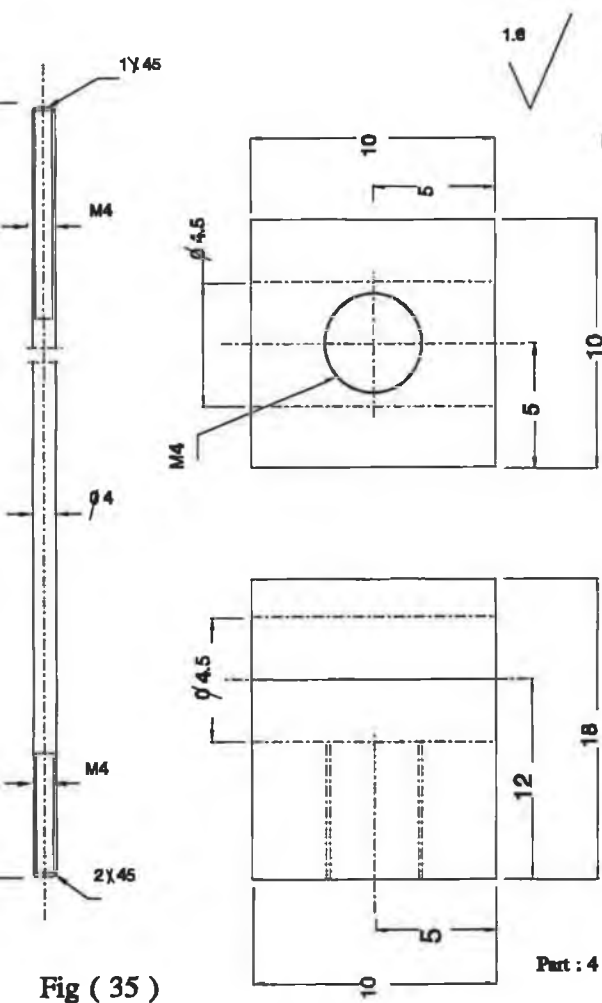
- 1 : All Tolerances Are To Be  $\pm 0.01$  mm Unless Otherwise Stated .
- 2 : Break All Sharp Edges To  $1 \sqrt{R5}$  Unless Otherwise Stated .

Fig ( 33 )









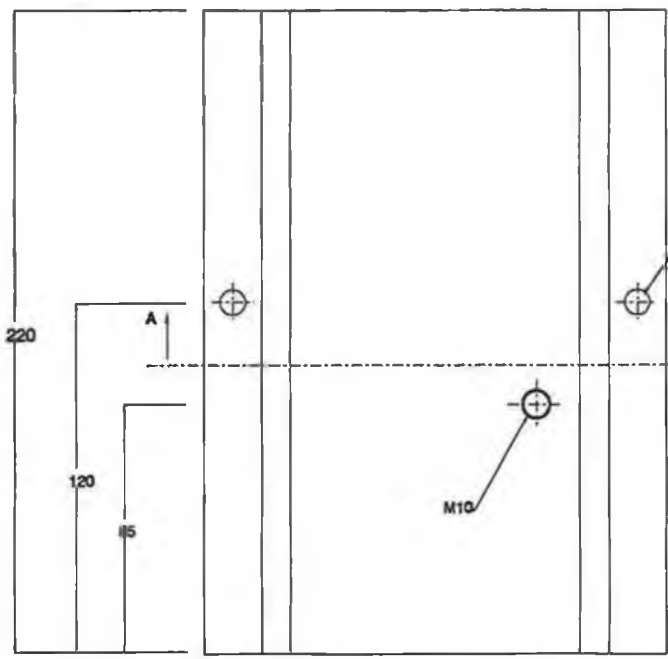
**Remarks :**

- 1 : All Tolerances Are To Be + 0.01 mm Unless Otherwise Stated .
- 2 : Break All Sharp Edges To  $1/\sqrt{45}$  Unless Otherwise Stated .

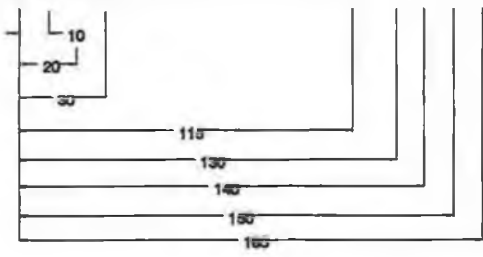
**Assembly : 10**  
**Material : Mild Steel**  
**QTY : 1 ( Each )**  
**Dimension : ( mm )**

**Fig ( 35 )**

**Part : 4**



Part : 12





1.6

Remarks :

- 1 : All Tolerances Are To Be  $\pm 0.01$  mm Unless Otherwise Stated .
- 2 : Break All Sharp Edges To  $1\sqrt{45}$  Unless Otherwise Stated .

2 Holes  $\varnothing 9$

A

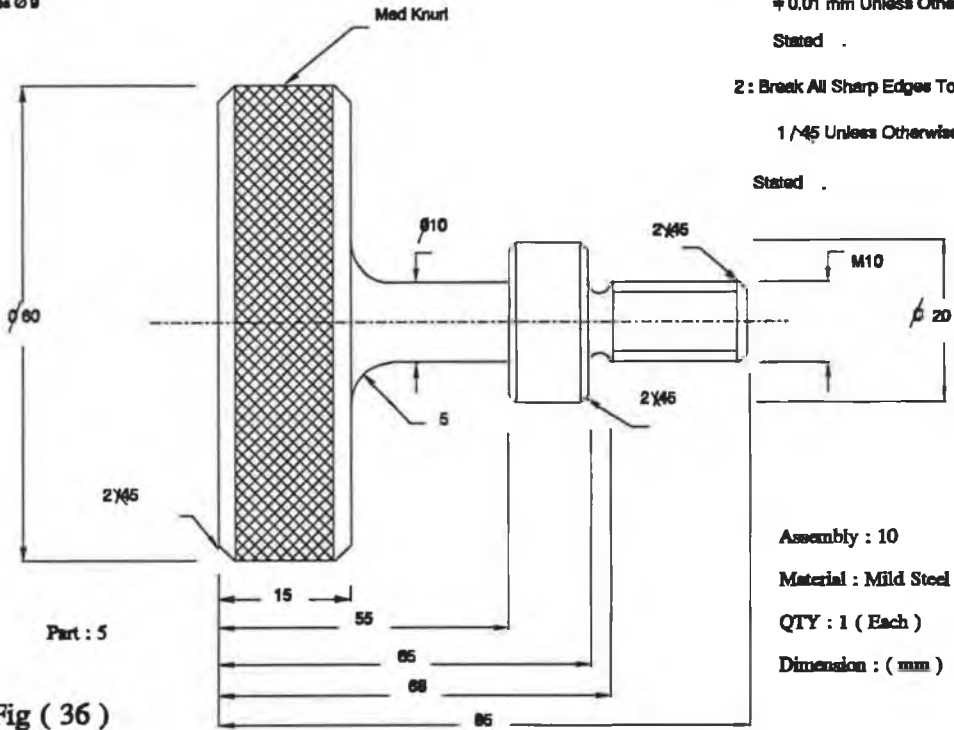
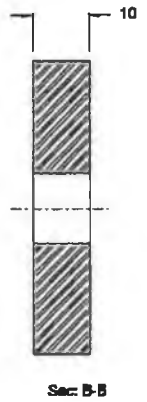


Fig ( 36 )



1.8

**Remarks :**

- 1 : All Tolerances Are To Be  
+ 0.01 mm Unless Otherwise  
Stated .
- 2 : Break All Sharp Edges To  
1 / 45 Unless Otherwise  
Stated .

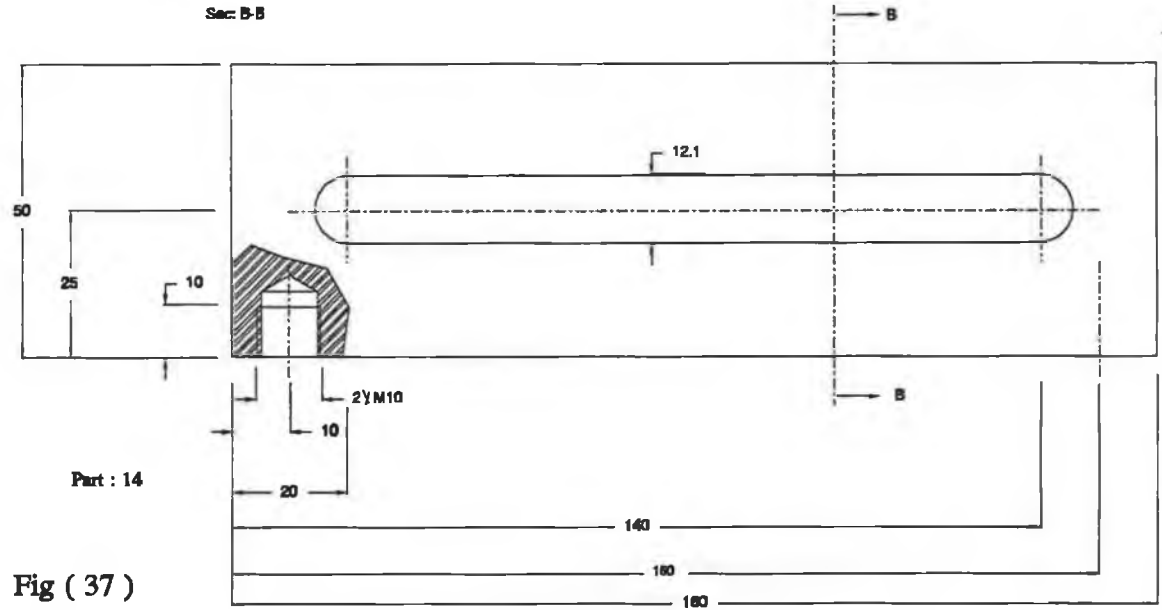
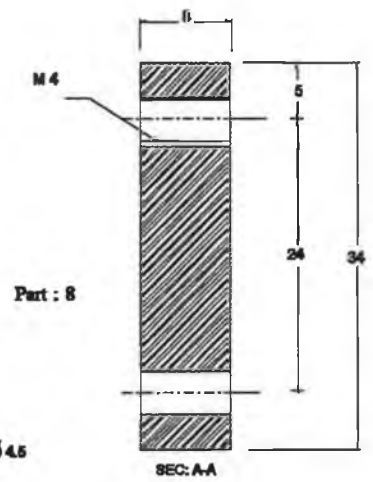
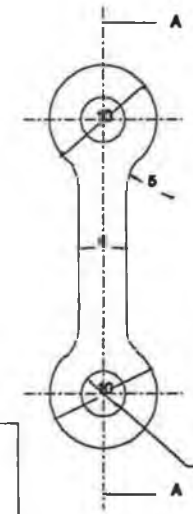
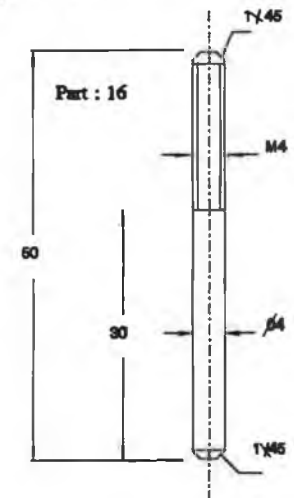


Fig ( 37 )



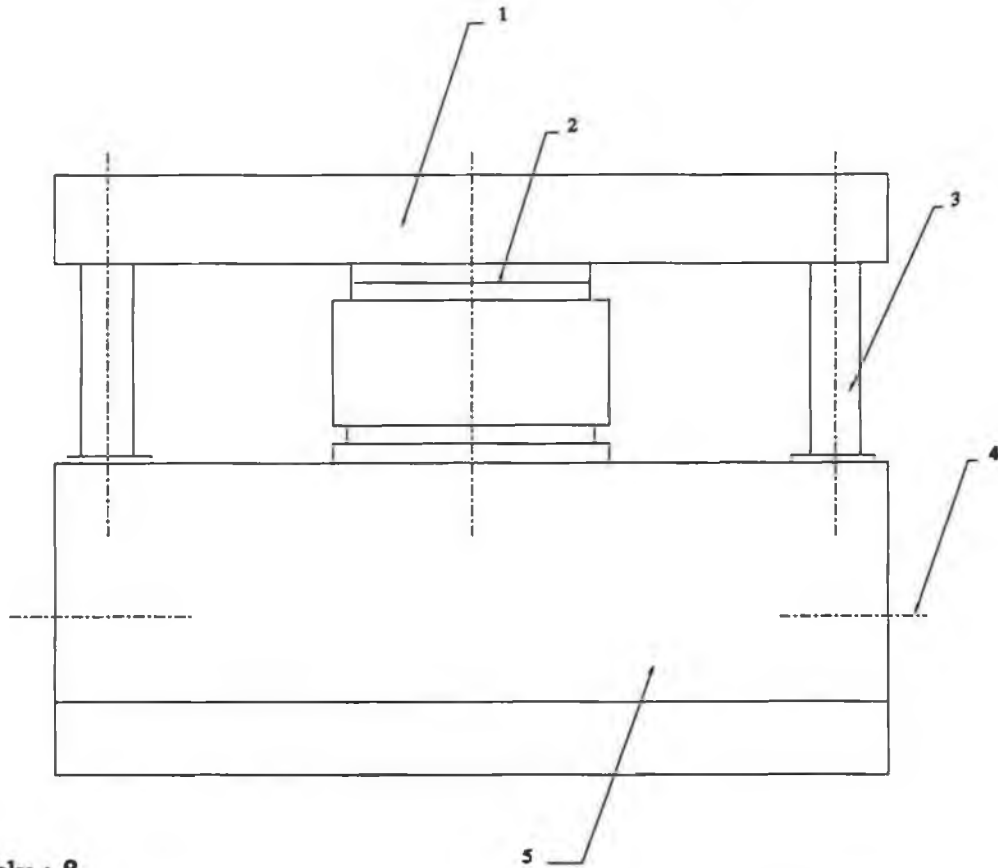
Assembly : 10  
Material : Mild Steel  
QTY : 1 ( Each )  
Dimension : ( mm )

top loading plate (1) which transfers the applied load to the load cell (2). The load cell (2) has been positioned in a circular groove at the centre line of lower loading plate (5). The individual design of this system is shown in Fig. (39) to (40). The dimension of the lower loading plate in Fig. (39) was obtained from the numerical model in Chapter 3 for Fig.(15.c).

### **The cap of the ram**

This has been designed as a support to the hydraulic ram to protect it from being damaged during the operation and to link the ram with the fixed L.V.D.T. Fig. (41) shows the assembly design of the cap of the ram. The cap (1) has been linked to the ram by using a compression interference tolerance between the inner diameter of the cap and the outer diameter of the ram. The rod (3) has been fixed to the cap (1) by a thread and the nut (2) has been used to lock the rod (3) to the cap (1). The rod (3) can be connected to the fixed L.V.D.T. by twisting manually the knurled nut (5) towards the whole of the universal coupling of the fixed L.V.D.T. The knurled nut (4) has been utilized to lock the position of the nut (5) on the rod (3). The individual design for the assembly of the cap of the ram is given in Fig. (41) to (43) in which the geometrical dimensions have been obtained from the numerical model described in Chapter 3 for Fig.(15.b).

### Platen System

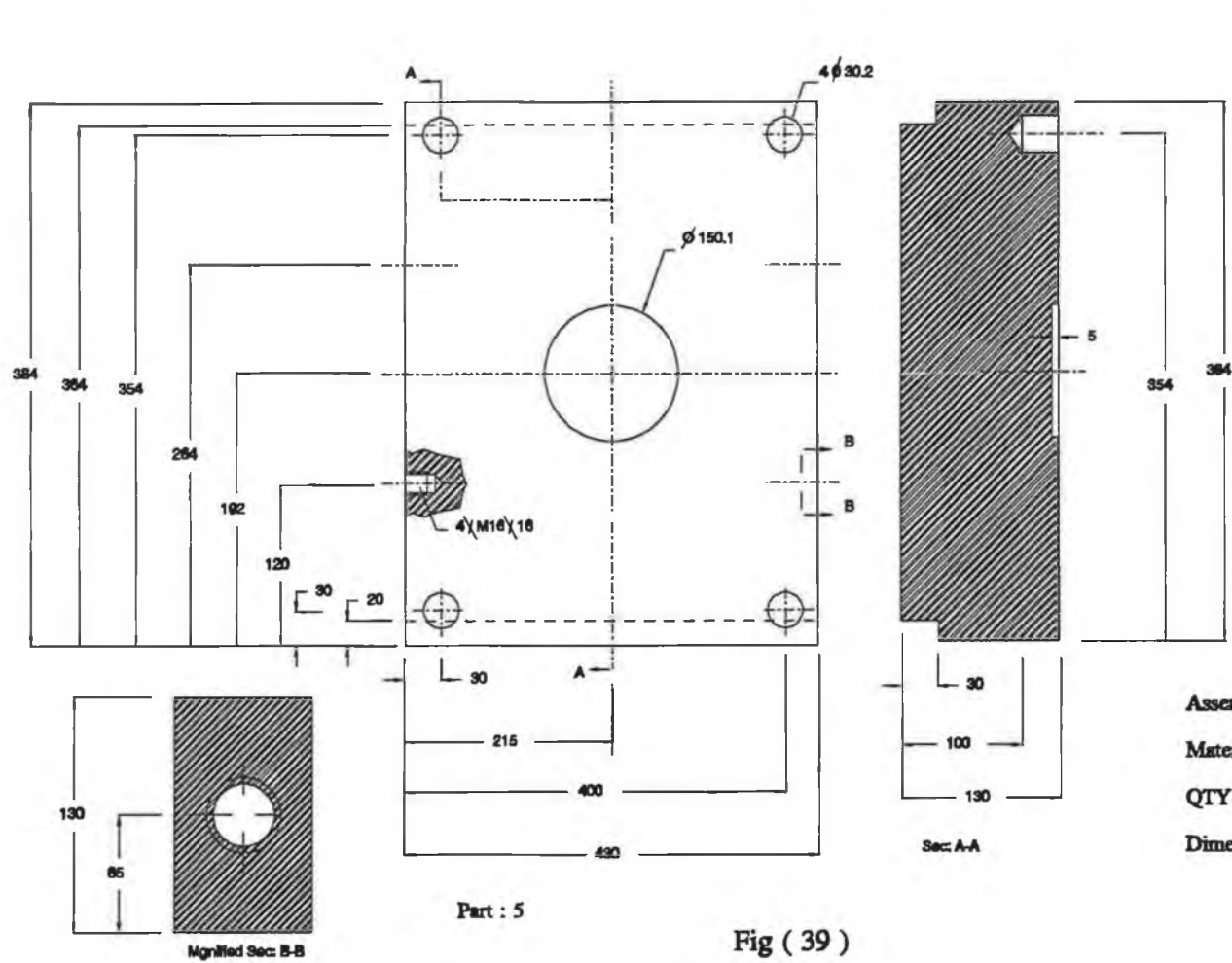


- 1: Top loading plate Plate
- 2: The load cell
- 3: The guide
- 4: Position of the eye Bolts
- 5: Lower loading Plate

- Four Eye Bolts and Four Guides

Assembly : 8

Fig ( 38 )



1.6 ✓

Remarks :

- 1 : All Tolerances Are To Be  $\pm 0.01$  mm Unless Otherwise Stated .
- 2 : Break All Sharp Edges To  $\sqrt{R45}$  Unless Otherwise Stated .

Assembly : 8

Material : Tool Steel ( AISI D2 )

QTY : 1

Dimension : ( mm )

Part : 5

Fig ( 39 )

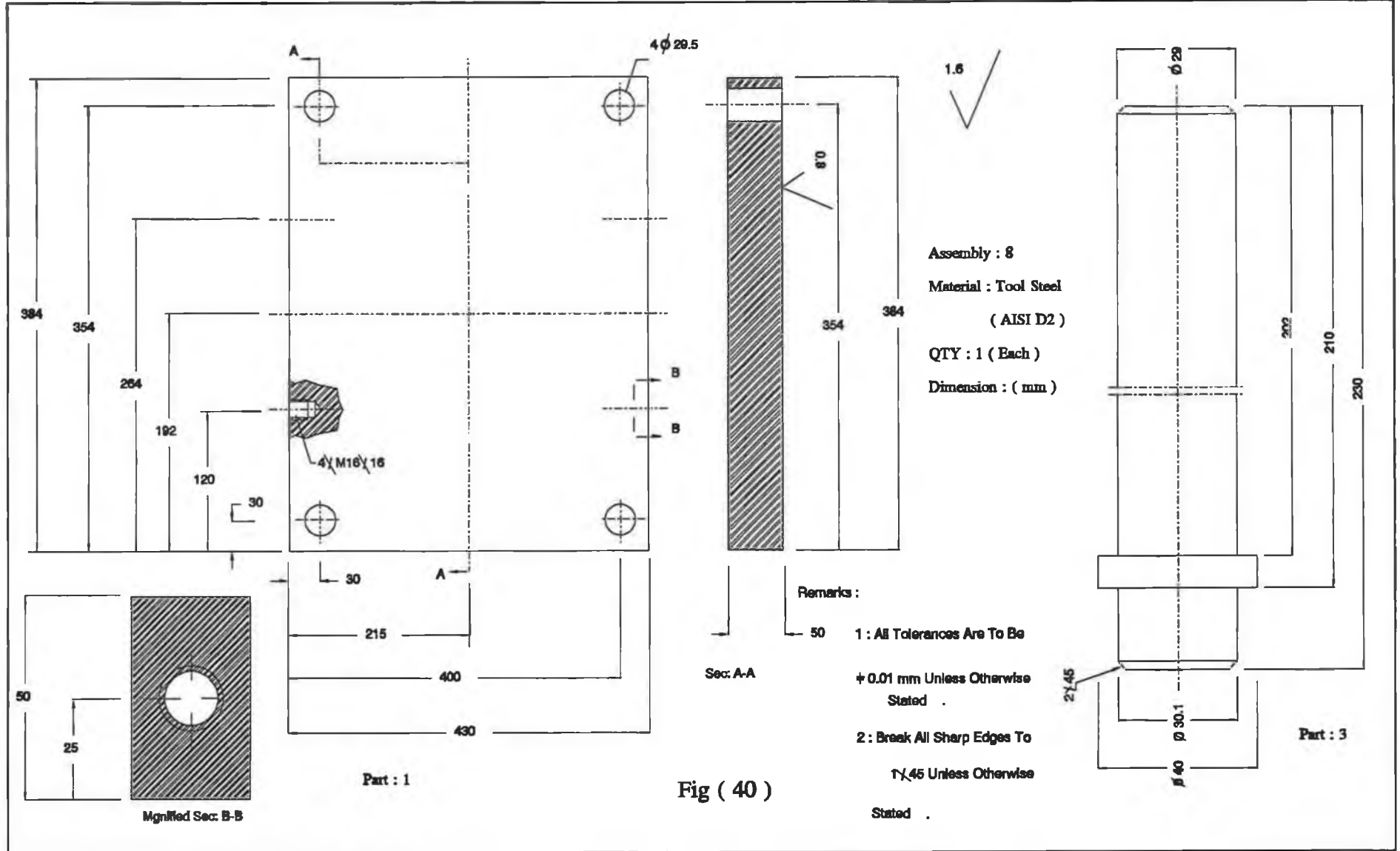
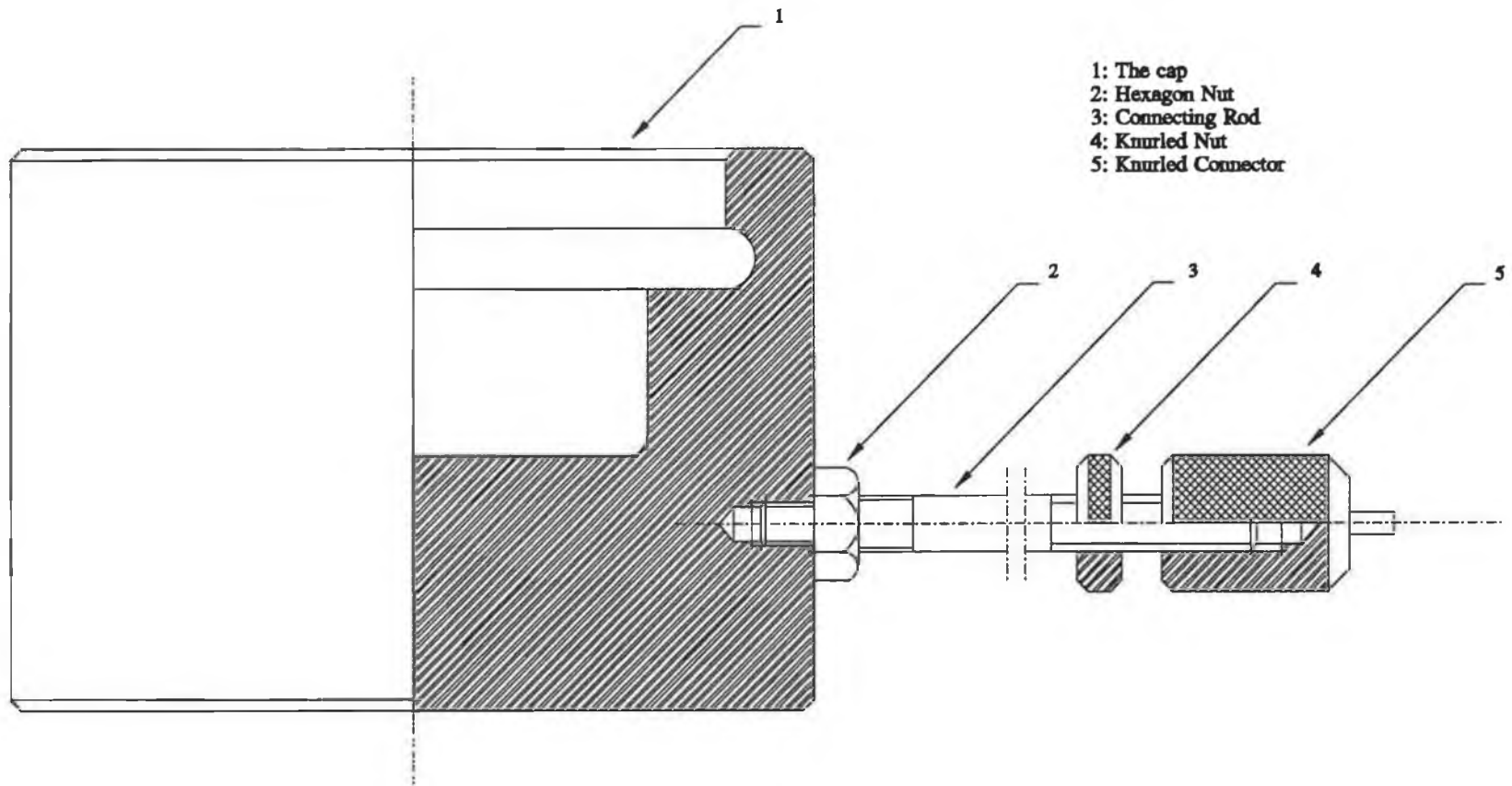


Fig ( 40 )



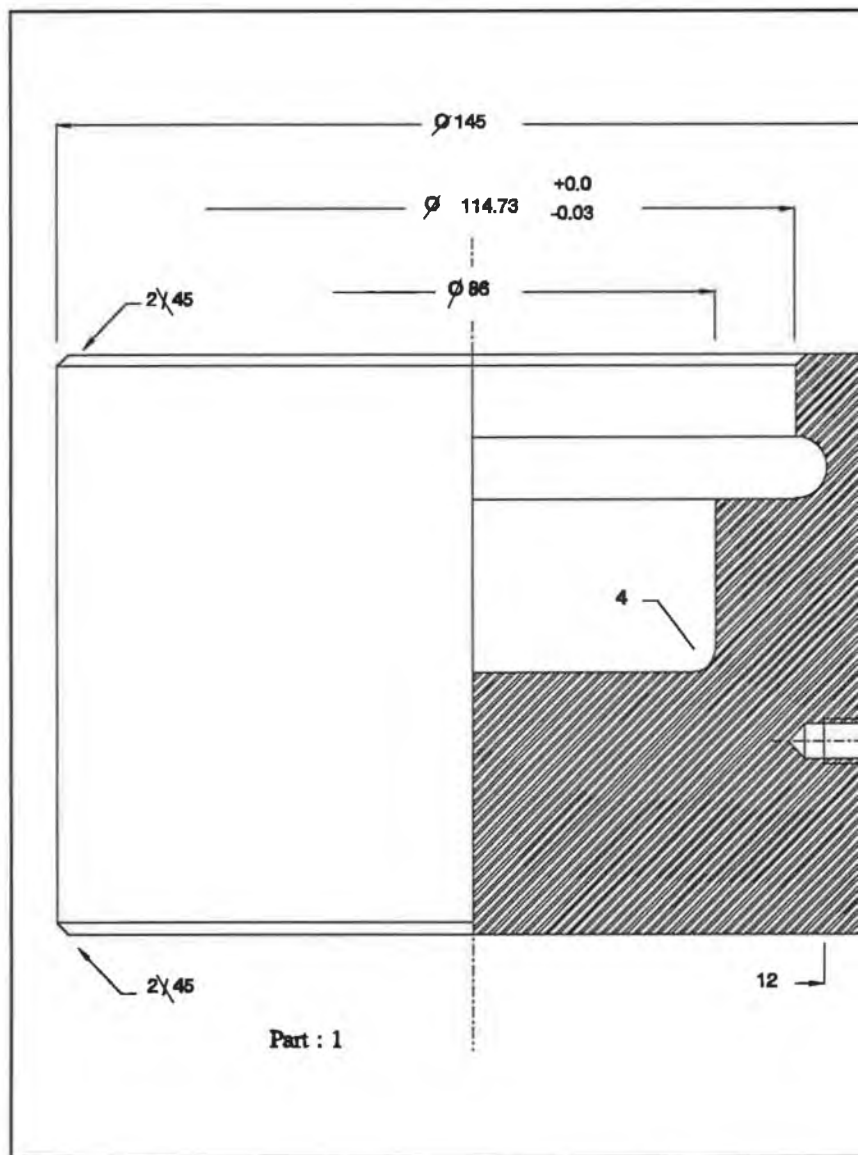
## The Cap Of The Ram



120

Assembly : 6

Fig ( 41 )



1.6



Remarks :

1 : All Tolerances Are To Be

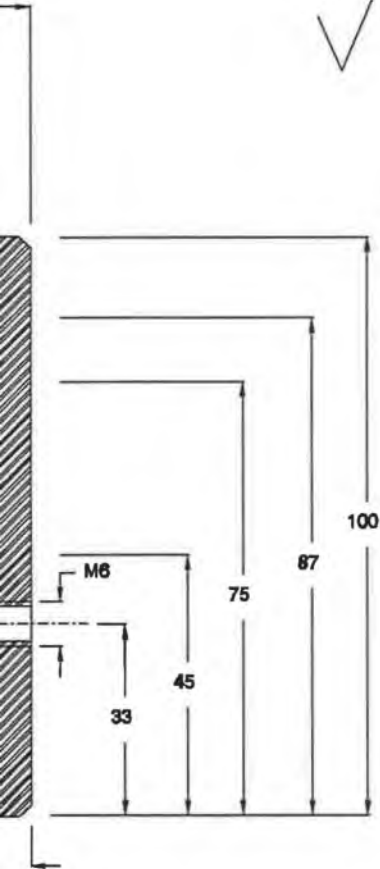
$\pm 0.01$  mm Unless Otherwise

Stated .

2 : Break All Sharp Edges To

$1/45$  Unless Otherwise

Stated .



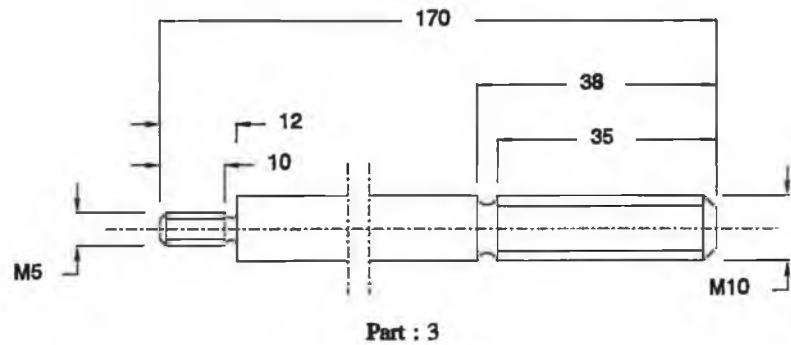
Assembly : 6

Material : Tool Steel ( AISI D2 )

QTY : 1

Dimension : ( mm )

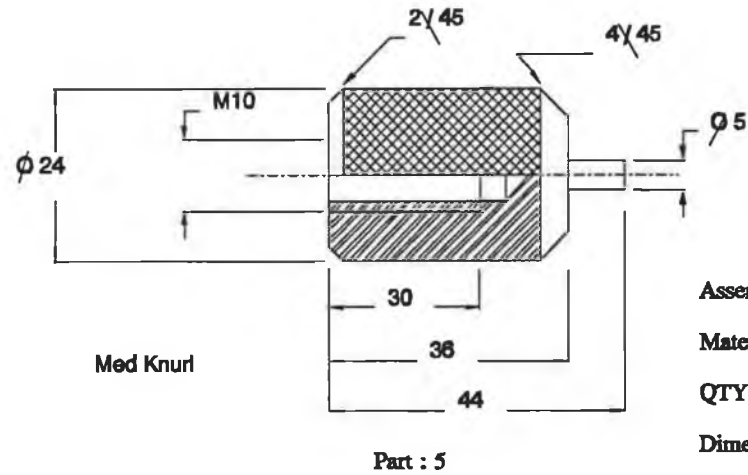
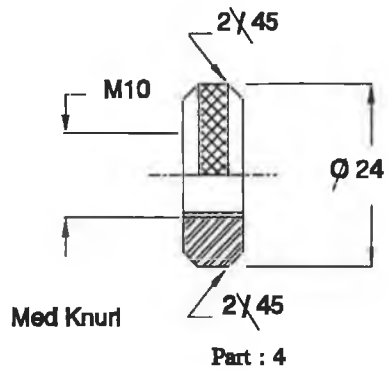
Fig ( 42 )



1.6

Remarks :

- 1 : All Tolerances Are To Be  $\pm 0.01$  mm Unless Otherwise Stated .
- 2 : Break All Sharp Edges To  $1/45$  Unless Otherwise Stated .



Assembly : 6  
 Material : Mild Steel  
 QTY : 1 ( Each )  
 Dimension : ( mm )

Fig ( 43 )

### 4.1.3 Designing the hydraulic system

The original design of the hydraulic system consisted of a hydraulic pump; two hydraulic lines to the ram and a 3-position centre manual valve. The designation of the original hydraulic pump used was an OTC hydraulic pump of 10000 p.s.i. maximum pressure output and 95 dBA level of noise at the maximum pressure output. It was not possible to get a variable speed of the ram or to hold the pressure of the ram at certain operational levels of the ram. Therefore, that design of the hydraulic press has been replaced by the new design shown in Fig. (44). The original hydraulic pump has been replaced by a quieter OTC pump of 10000 p.s.i. maximum output pressure and 70 dBA level of noise at the maximum output pressure. This hydraulic pump is driven by a single phase electric motor with specification as follows:

(i)	Maximum power	=	2 HP
(ii)	Maximum revolution per minute	=	1425 r.p.m.
(iii)	the current	=	27.6/13.8 amps
(iv)	The main supply requirements	=	110/220 V & 50 HZ standard

In Fig. (44) the 4-way, 3-position remote solenoid valve (6) of 150 volt and 50 Hz has been linked to the pump (3) and the tank (1) at the inlets (P) and (T). The return hydraulic line (10) and the feed hydraulic line (7) have been connected to the inlets (A) and (B) of the solenoid valve. The feed and return lines have been connected to the double-acting hydraulic ram (9) of 333 mm travel; and 191 cm<sup>2</sup> effective area for push movement and 96 cm<sup>2</sup> effective area for pull movement. The solenoid valve (6) was

### Schematic Diagram Of The Hydraulic Circuit

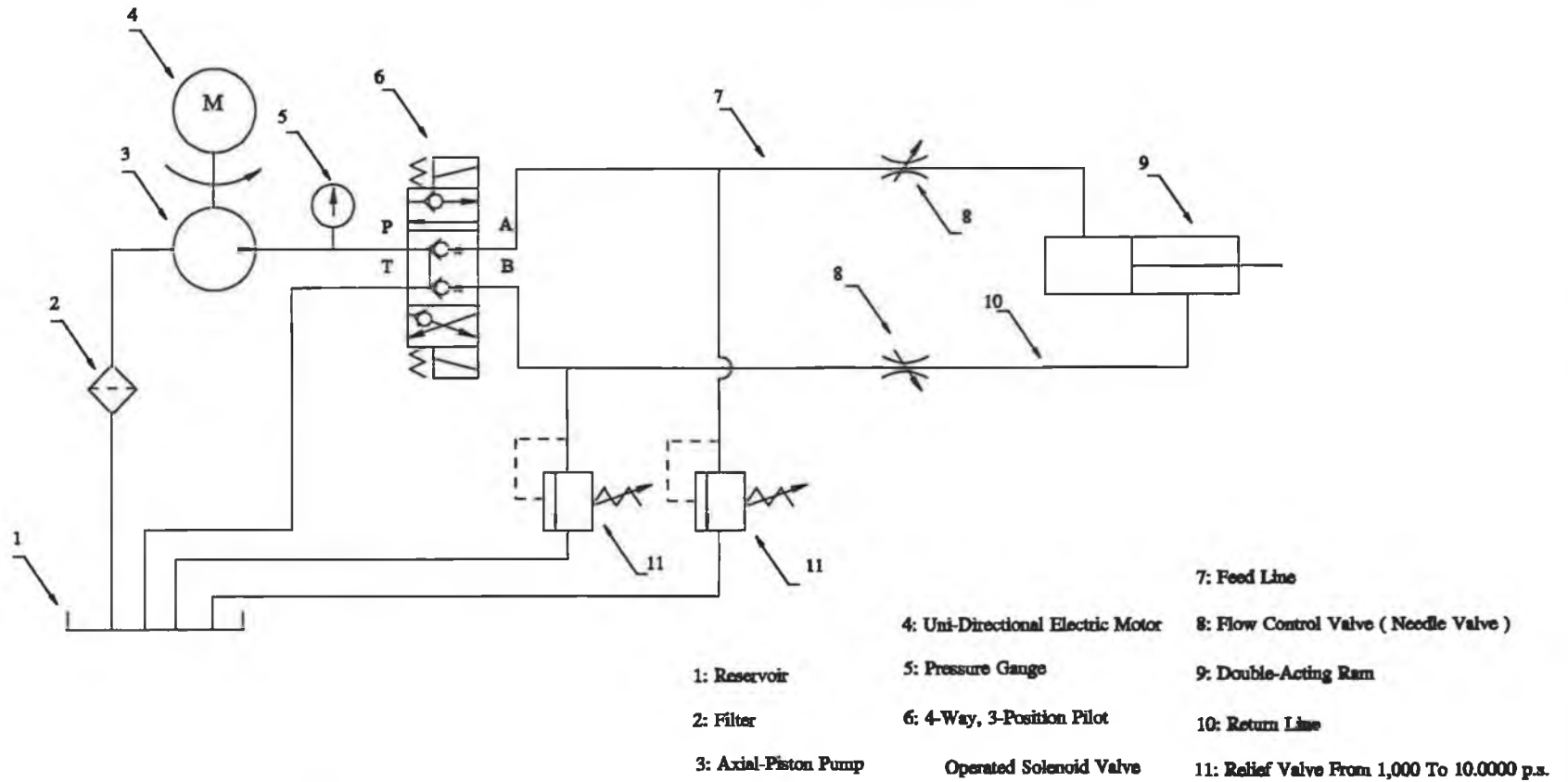


Fig ( 44 )

equipped with posi-check valve to hold the operational load when shifting from advance to hold position. Each of the hydraulic feed lines (7) and the return line (10) was equipped with a 10000 p.s.i. pressure relief valve (11) and 10000 p.s.i. needle valve. The relief valves (11) have been installed in the system to adjust the pressure in the feed and return line. Whereas the needle valves (8) have been used to obtain a variable speed for the forward and return motion of the hydraulic ram (9). The pressure gauge (5) has been used to measure the pressure of the hydraulic pump. Fig. (45) shows a photograph of the connection of the present hydraulic system.

#### **4.1.4 Designing the main stand**

The objective of using the main stand shown in Fig. (46) is to position the mobile L.V.D.T. to several positions so that different measuring points on the press structure can be measured. There are four arms (1) where the magnetic stand, which holds the mobile L.V.D.T's, is situated. Each arm has been linked to a collar (2) which can slide on a vertical pillar (5). The positions of these arms on the pillar (5) can be fixed using bolts (4) and nuts (3). The four channel beams (8); a circular plate (9) and the collar (7) have been welded together to compose the base of the main stand. The pin (6) joined the collar (7) by a thread. The pillar (5) was welded to pin (6). The bolts (10) and the nuts (11) were used to level the main stand on the ground. The full detailed design of the individual components of the main stand is Fig. (47) to (51).

Feed Line

Return Line

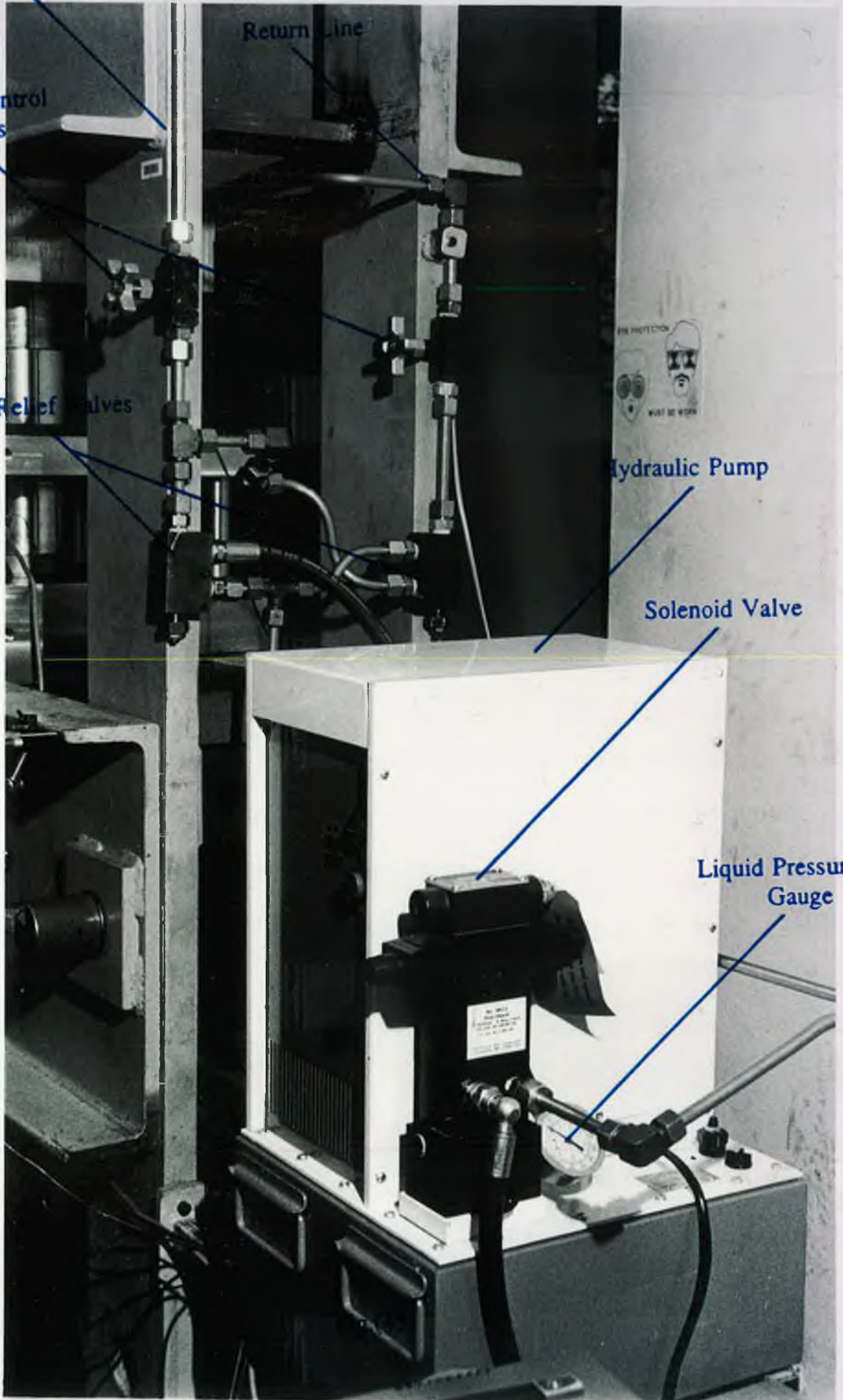
Flow Control  
Valves

Relief Valves

Hydraulic Pump

Solenoid Valve

Liquid Pressure  
Gauge





# The Main Stand

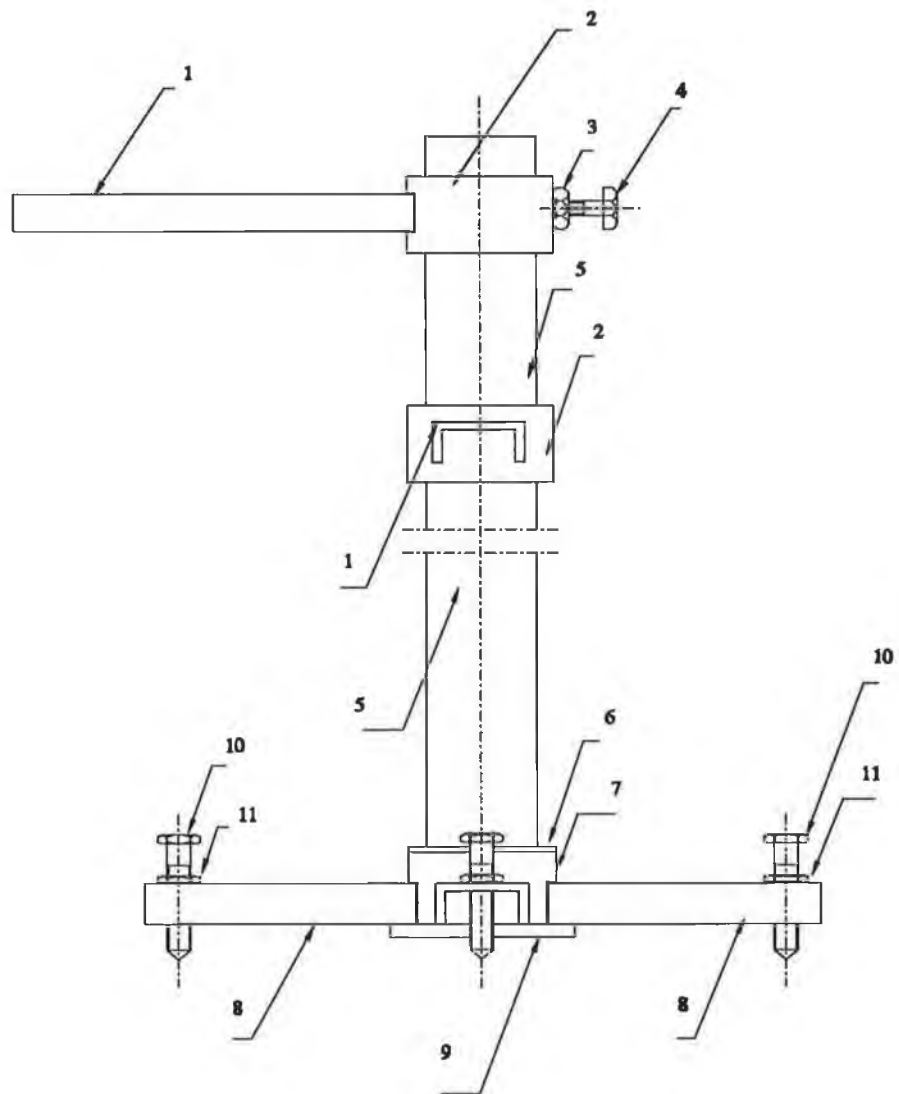
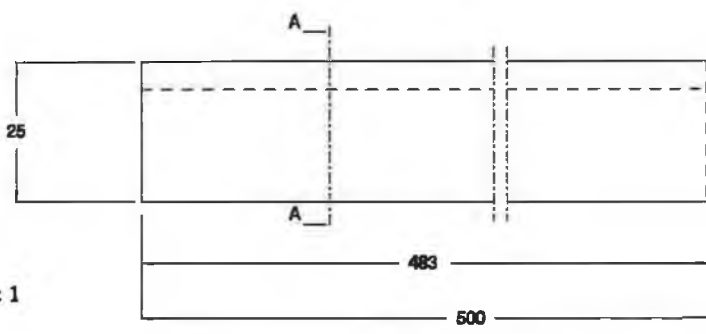
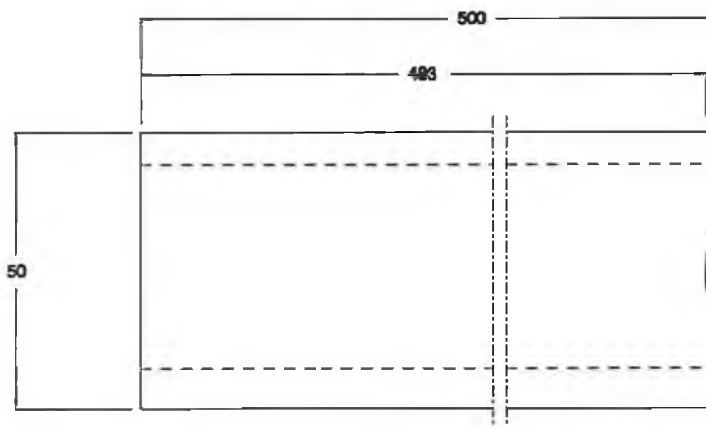


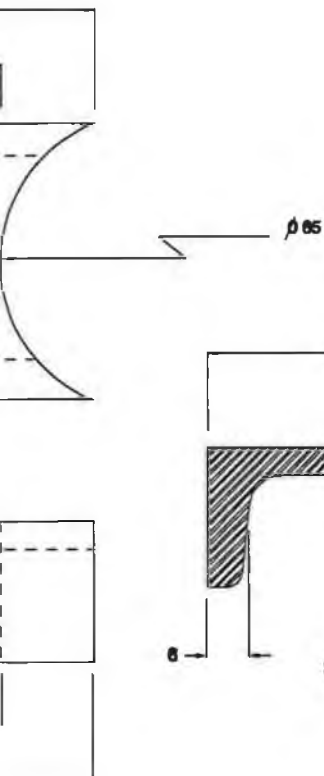
Fig ( 46 )

Assembly : 1

1.8



Part : 1



**Remarks :**

1 : All Tolerances Are To Be  
 $\pm 0.01$  mm Unless Otherwise  
Stated

2 : Break All Sharp Edges To  
1 $\times$ 45 Unless Otherwise  
Stated

**Assembly : 1**

**Material : Structural Steel**

**QTY : 1**

**Dimension : ( mm )**

**Fig ( 47 )**

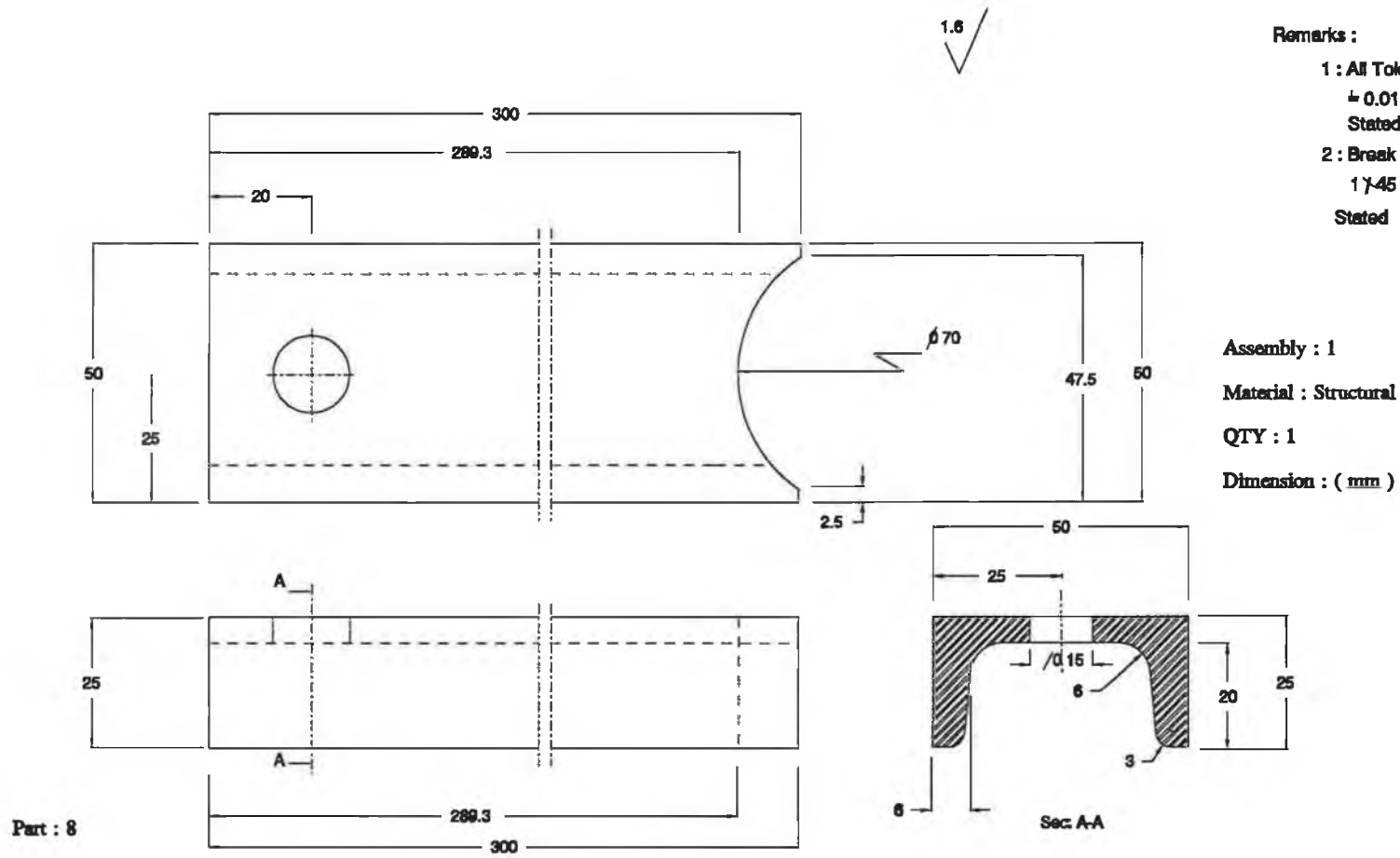
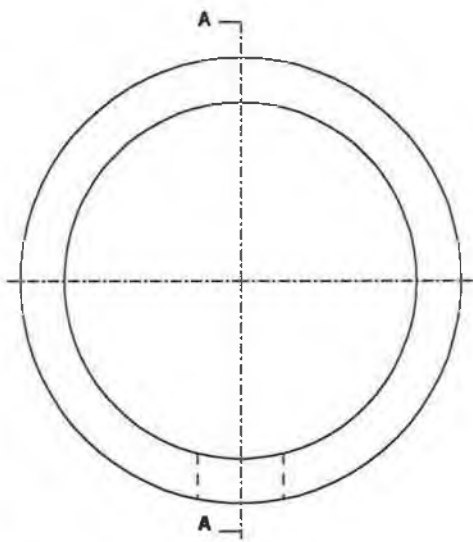
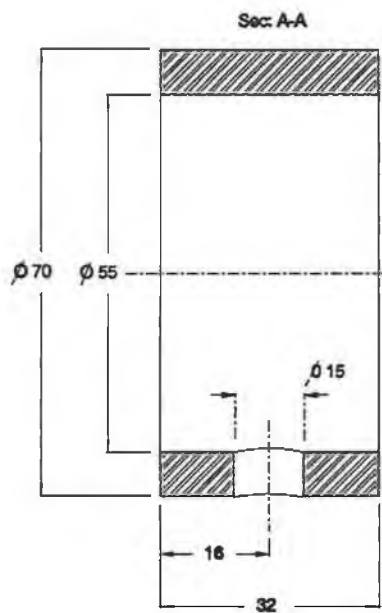


Fig ( 48 )



1.6  
✓

Remarks :

- 1 : All Tolerances Are To Be  $\pm 0.01$  mm Unless Otherwise Stated .
- 2 : Break All Sharp Edges To  $1/45$  Unless Otherwise Stated .

Part : 2

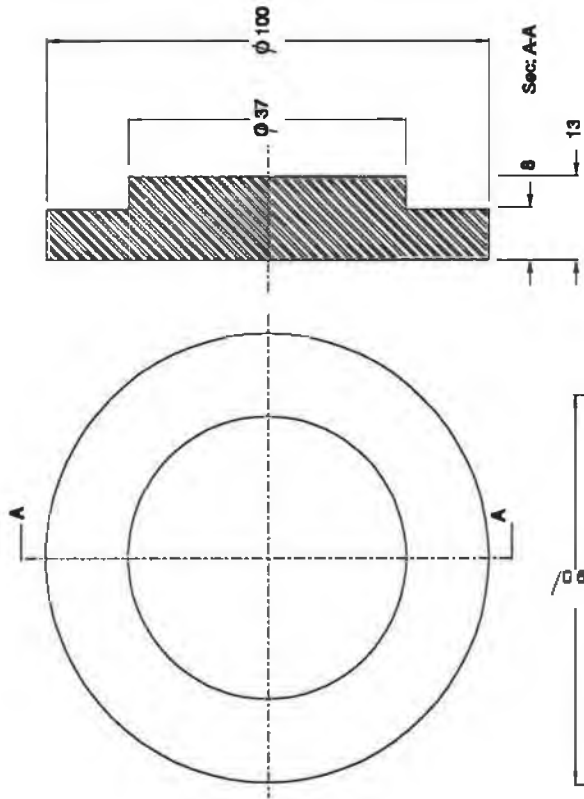
Assembly : 1

Material : Mild Steel

QTY : 1

Dimension : ( mm )

Fig ( 49 )



Part : 9

Fig ( 50 )

1.6



**Remarks :**

- 1 : All Tolerances Are To Be  $\pm 0.01$  mm Unless Otherwise Stated
- 2 : Break All Sharp Edges To  $1 \times 45$  Unless Otherwise Stated

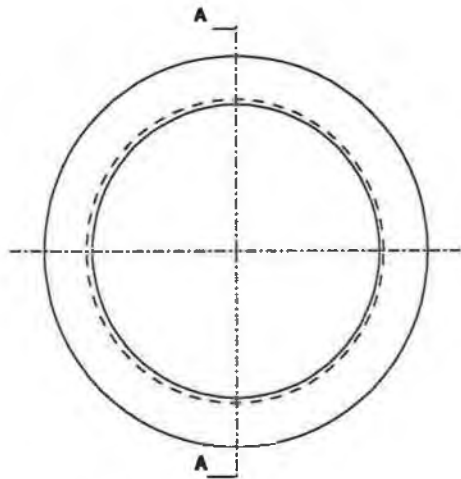
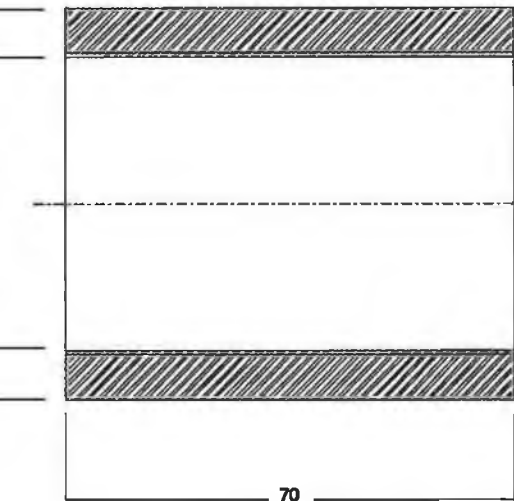
**Assembly : 1**

**Material : Mild Steel**

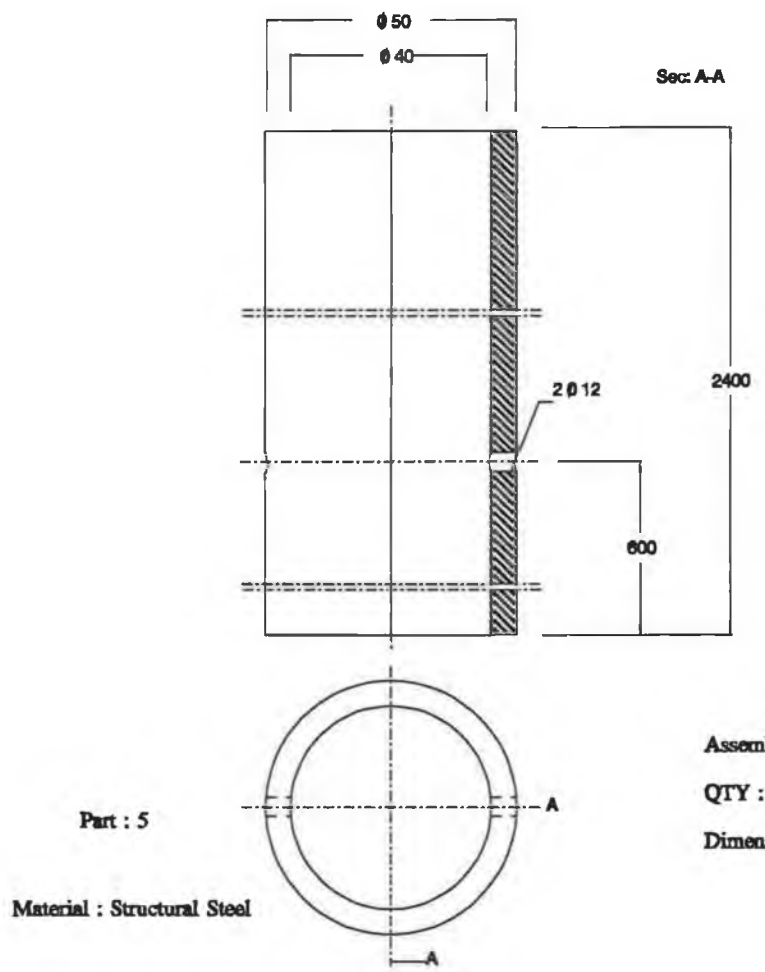
**QTY : 1 ( Each )**

**Dimension : ( mm )**

**Sec: A-A**

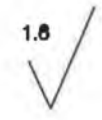


**Part : 7**

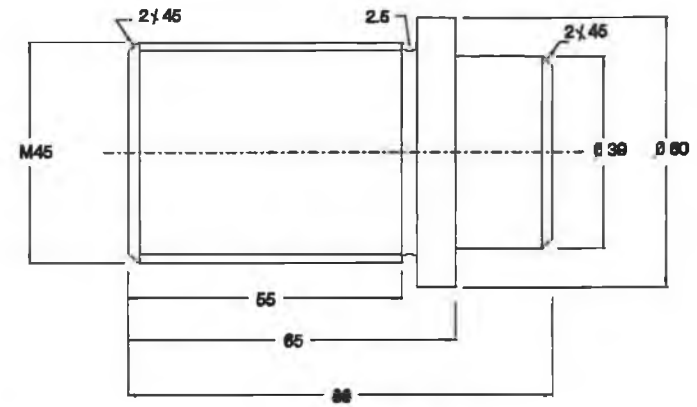


Part : 5  
Material : Structural Steel

Assembly : 1  
QTY : 1 ( Each )  
Dimension : ( mm )



Remarks :  
1 : All Tolerances Are To Be  
+ 0.01 mm Unless Otherwise  
Stated.  
2 : Break All Sharp Edges To  
1/45 Unless Otherwise  
Stated.



Part : 6  
Material : Mild Steel

Fig ( 51 )



#### **4.1.5 Designing the data acquisition system**

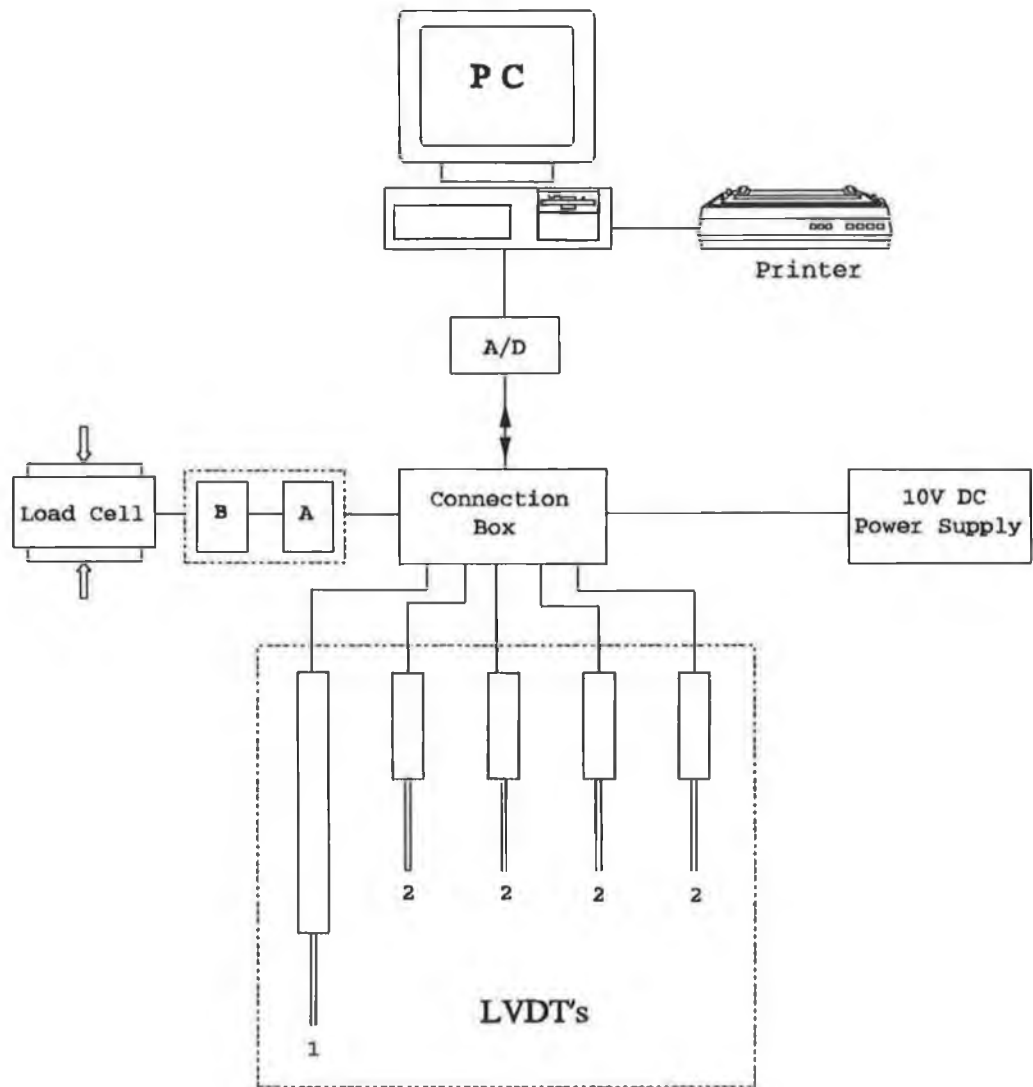
The manual performance of processing the experimental variables can be erroneous and time consuming. This may be due to the human management of collecting these variables and the stability of the experimental apparatus. Therefore, computerizing such process ensures speed and accuracy, and allows more sophisticated analysis and better management of the experimental variables.

The data acquisition system in the current investigation has been designed to establish a versatile measurement system so that processing of the experimental variables of interest can be performed by the computer. This system has been utilized to facilitate the measurement of the load deflection of the present hydraulic press at different measuring points on its structure. The system can also be used to obtain the total stiffness of the hydraulic press structure and to estimate the load deflection of a compressed workpiece.

#### **Hardware configuration**

The object of the present data acquisition is to collect the experimental data, process them into the desired fashion, and record the results in a form suitable for storage, presentation, or additional subsequent processing. The essential element in this system is the instrument transducer, which furnishes an electrical signal that is indicative of the physical variable being measured. The hardware configuration of the present data acquisition system is shown in Fig. (52). This consists of the following:

## Hardware Configuration



A : Flyde Amplifier  
B : Flyde Bridge Conditioner  
A/D : Analog-to-digital converter

Fig ( 52 )

- (i) The transducers (i.e. the load cell and the L.V.D.T.'s)
- (ii) The conditioning circuits
- (iii) The connection box
- (iv) The power supply
- (v) The A/D converter
- (vi) The personal-computer (PC) with a suitable unit for displaying the results (i.e. printer and V.D.U.).

In practice, the A/D converter receives the analog signals, which are sent by the transducer through the connection box, and converts them to digital printed form signals. This process starts in situations in which the transducers are physically remote from the location at which the data display is desired. The event of sending, receiving, converting, displaying and storing the electrical signals is fully monitored by a computing software exclusively developed for the present system. Besides this computing software other programs have been used for further refinement and representation of the desired stored results.

### **The Transducers**

These are the load cell and a set of L.V.D.T.'s. The load cell was used to measure the operational load of the hydraulic press. The electrical analog signal which is given by the load cell, after applying a load, was conditioned and converted automatically to the same physical meaning of the applied load. This was carried out on a computer using the load cell sensitivity which was obtained from the calibration process of the load cell.

The set of the L.V.D.T.'s, which have been used in the experimental work, contains 4 mobile L.V.D.T.'s (2) and one fixed L.V.D.T. (1) as shown in Fig. (52). The mobiles L.V.D.T.'s were positioned on the main stand to measure the maximum deflection of the press frame in the direction of the operational load, and to measure the out-of-plane deflection of different measuring points on the press frame. The fixed L.V.D.T. was used to measure the total maximum deflection of the whole press structure in the direction of the operational load. This fixed L.V.D.T. can also be used to measure the deformation of a compressed workpiece. The maximum range of the fixed L.V.D.T. was given as a 50 mm with a sensitivity of 60 mv/mm at 10 VDC excitation voltage. The mobile L.V.D.T.'s possess a range of 3 mm with a sensitivity of 280 mv/mm at 10 VDC excitation. The sensitivities of all the L.V.D.T.'s were used by the computer to convert the electrical signal to a form of displacement.

### **The conditioning circuits**

The electrical signals obtained from the load cell and the L.V.D.T.'s have been conditioned before being applied to the A/D converter. This was to allow these electrical signals to be read within the limit range and resolution of the A/D converter. Therefore, in Fig. (52), the unit which consists of a bridge conditioner (B) and a built-in amplifier (A) has been used to balance the strain gauge bridge and to obtain a variable output signal of the load cell. Fig. (53) shows two electrical circuits which have been designed to provide several choices of amplification of the output signal of the L.V.D.T.'s. The circuit shown in Fig. (53.a) used four operational amplifiers to vary the magnitude of the output signals of the mobile L.V.D.T.'s. One operational amplifier has been used in the circuit in Fig. (53.b) to obtain a variable amplification of the output signal of the

fixed L.V.D.T.

An electrical circuit board has been designed to connect the electrical components of the circuits shown in Fig. (53). Fig. (54) shows the position of these electrical components on that electrical circuit board (ECB) on which the 34 pin IDC has been used as an input connector to the ECB, whereas the 26 pin IDC has been used as an output connector of the ECB.

### **The connection box**

In order to connect the transducers and the conditioning circuits together with the A/D converter, and to protect the transmitting electrical signal from the environmental noise, an aluminium diecast box has been used. This box accommodates the electrical circuit board (ECB) and carries the input/output plugs. The input plugs have been connected to the input connector of the ECB. The output connector of the ECB has been connected to the output plug. This plug has been connected to the D type connector of the A/D converter to:

- (i) apply the signals of the transducers, after the amplification, to the A/D converter;
- (ii) supply an excitation voltage of 10 VDC from the power supply of the computer to the operational amplifiers on the ECB.

The L.V.D.T.'s have been connected to the 6-way common input plugs on the connection box. The load cell has been connected to one of the two BNC connectors

on the connection box. Transmission of the electrical signal from one location to another has been carried out by means of a coaxial cable outside the connection box. Therefore, any stray electromagnetic noise is attenuated by this outer shield before it can corrupt the signal present on the inner conductor. The connection between the transducers and the amplifiers is shown in Fig. (55). The connection between the amplifiers and the A/D converter is shown in Fig. (56). The connection box provides access to the variable resistors, which have been positioned on the ECB, so that a variable amplification of the electrical signal of the four built-in channels can be adjusted. The connection box also provides a channel for an alternative use of an instrumentation amplifier.

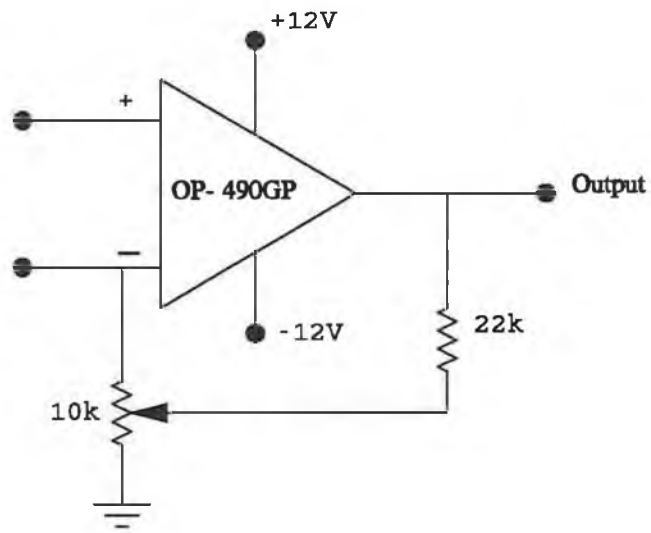
#### **The power supply**

This has been connected to a BNC connection on the connection box to provide a constant 10 V DC as an excitation voltage to the L.V.D.T.'s. Therefore, the electrical assembly of the connection box can be used to apply the desired excitation voltage to the electrical transducers.

#### **The A/D converter**

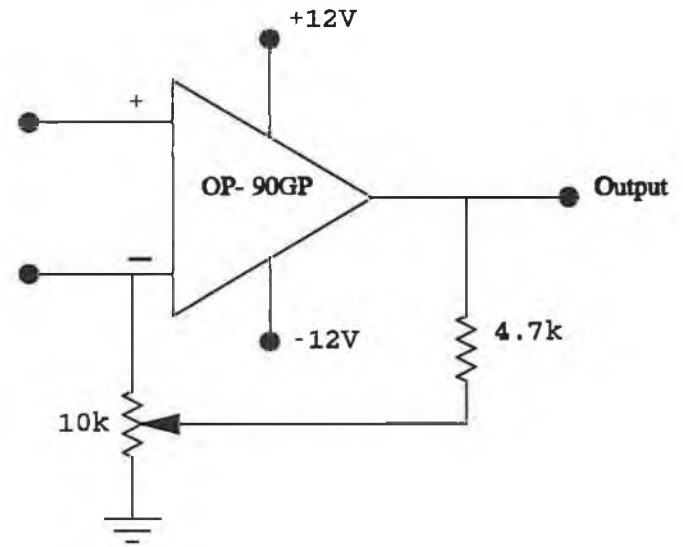
The A/D converter which has been used in the present data acquisition system permits the personal computer (PC) to interface with the electrical transducers. This converter converts analog voltages to binary words of 12-bit. The A/D converter is IBM-PC compatible and provides a fixed  $\pm 5$  VDC with a resolution of 0.00244 volts and an accuracy of 0.01% of reading  $\pm 1$ bit.

## Electrical Circuit Of The Amplifiers



LVDT DC3

(a)

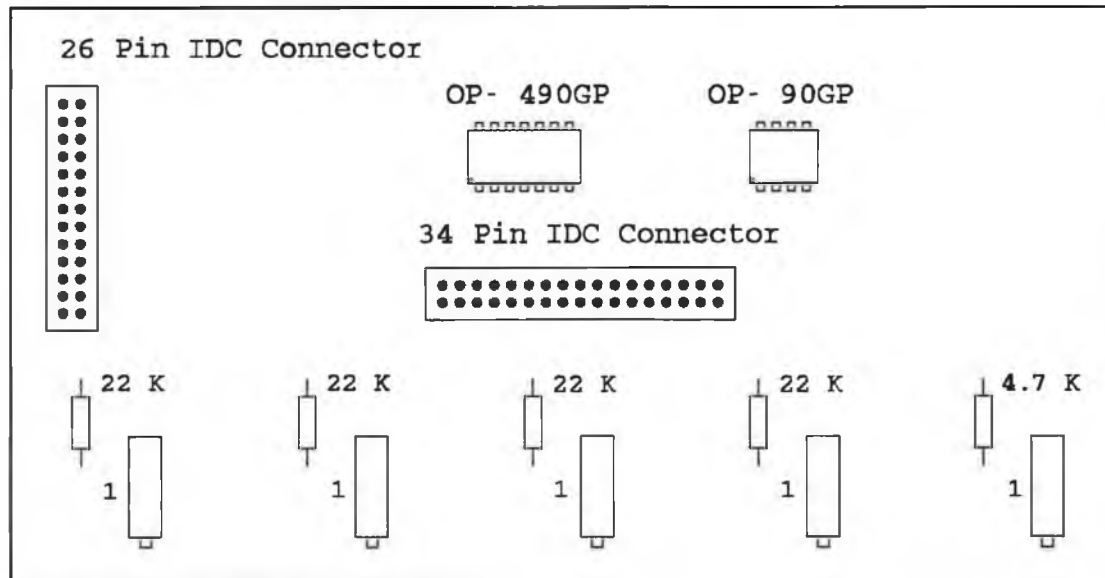


LVDT DC50

(b)

Fig ( 53 )

### POSITION OF THE ELECTRICAL COMPONENTS ON ECB



1 : 10K Variable Resistors

Fig ( 54 )



# TRANSDUCER TO AMPLIFIER CONNECTIONS

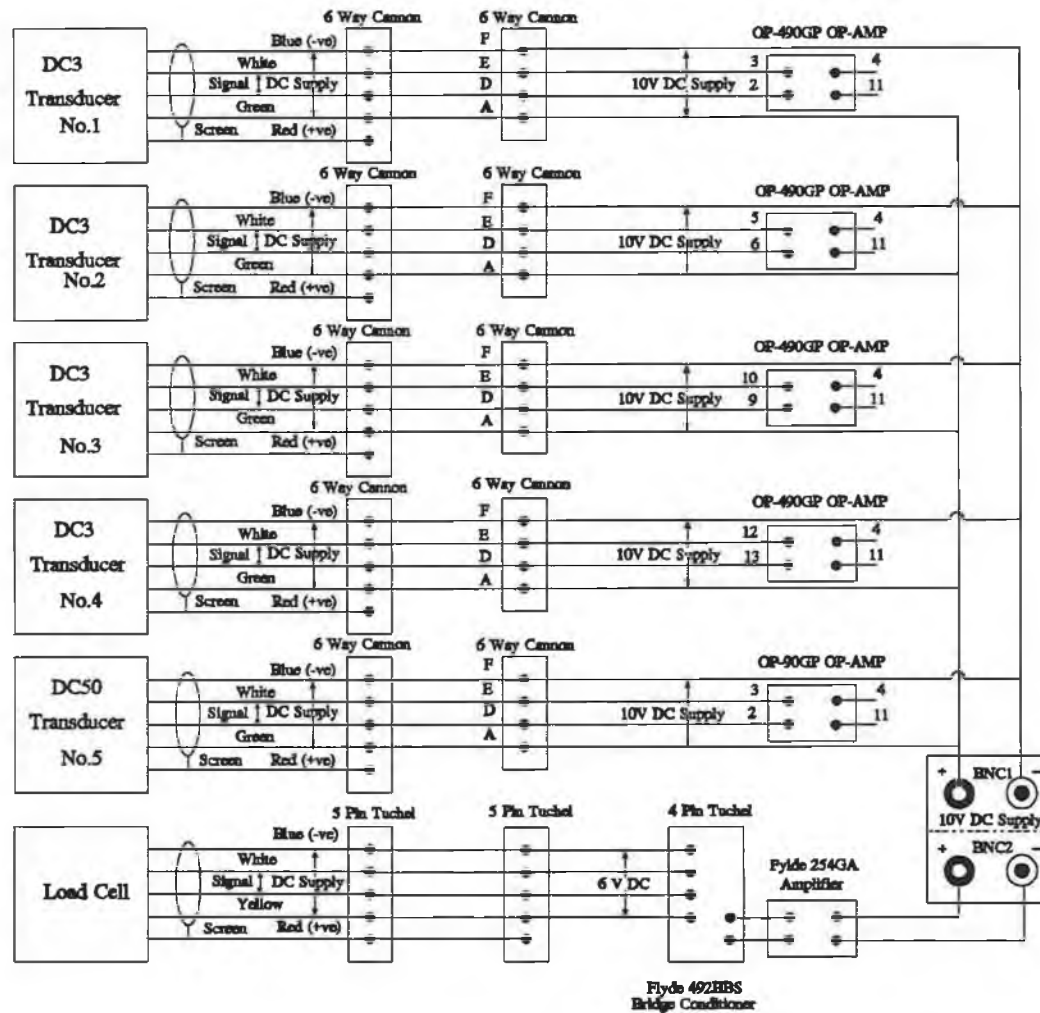
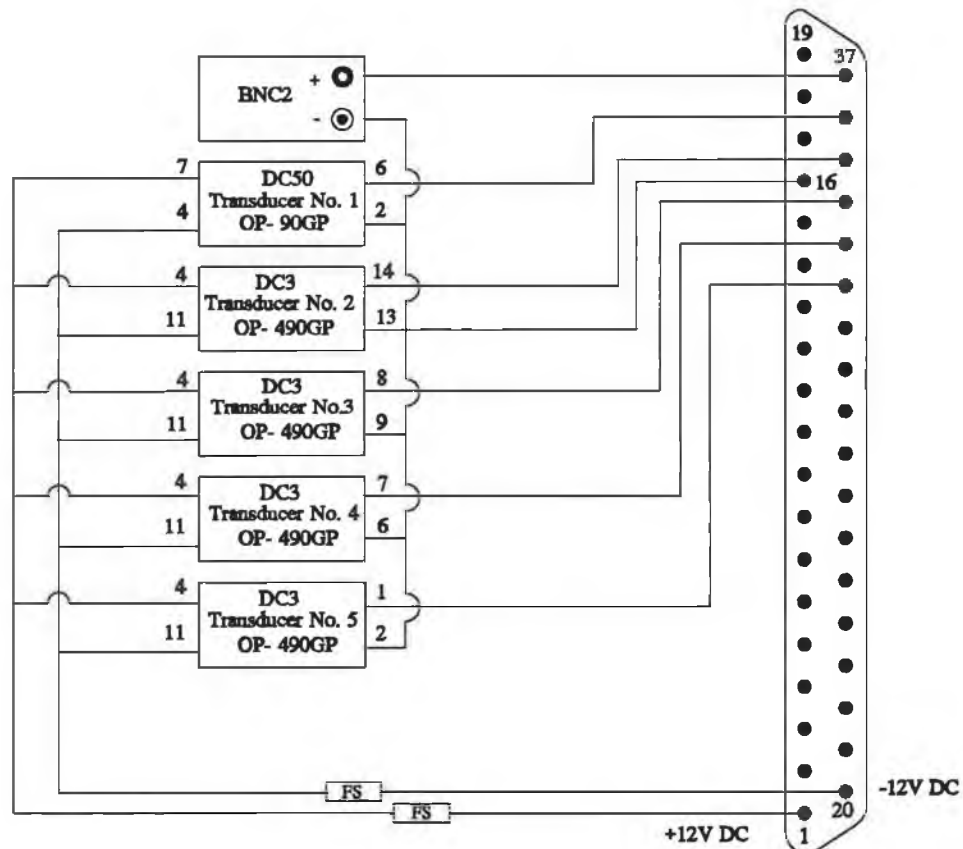


Fig ( 55 )

# AMPLIFIER TO THE A/D CONVERTER CONNECTIONS



FS : Are Fuses of 20 mA

Fig ( 56 )

37 pin "D" type male connector

### **The personal computer (PC)**

This computer is a general purpose IBM-PC compatible that allows plug-in of the printed-circuit of the A/D to expand its capability. This PC features a 1 Mbyte RAM with 40 Mbytes disk space with IBM compatible VDU. The process of converting the electrical signals of the transducers to the appropriate physical meaning has been carried out by this computer. This process has been performed after programming the A/D converter to collect, convert and store those electrical experimental signals.

### **Software Configuration**

The computing software which has been utilized to facilitate the process of collecting, storing and analyzing the experimental data are: a BASIC computer program; Plan Perfect Spreadsheet; and Havard Graphic computing program. The BASIC computer program has been developed in-house to monitor and store the desired form of the experimental data. The Plan Perfect Spreadsheet and the Havard Graphics computing software have been used to prepare and produce graphical presentation of the stored experimental results.

### **The BASIC computer program**

Generally this BASIC computer program has been developed for the PC to program the A/D converter and to facilitate measurements which involve digital-to-analog processing. The program has been used to monitor and store the measurement of the load deflection

of the present press structure. The program has been written in BASIC language and compiled with the I/O driver of the A/D converter using an IMB microsoftware compiler program. This is to translate the ASCII commands and instructions of the program to the computer code and store this in the memory of the computer. Therefore, the program can be executed from the prompt on the VDU. The I/O driver of the A/D converter is a software routine containing the binary code of the operating system of the A/D converter. This routine can be accessed from BASIC using a simple CAL statement. Various operating modes of CAL routine select the functions of the converter data formatting and error checking. The program is driven by a menu from which an option can be selected in order to collect a bulk of experimental data, process it and display it in a desired printed form. The clock of the computer is used by the program to synchronize the measuring process. The input data is read from an access file which contains information about the sensitivity; the gain factor and excitation voltage of the eight channels used by the A/D converter. The flow chart of the basic features of the present program are outlined in Fig. (57). A full detail on the program development and usage is listed in Appendix (D).

#### **Pattern of measuring the load deflection of a compressed workpiece**

The load deflection of a workpiece can be measured using the present hydraulic press after the design modification. This can be proceeded as follows:

- (i) position the workpiece at the centre of the top loading plate in the platen system.
- (ii) Run the BASIC computer program to initialize the test (the option of

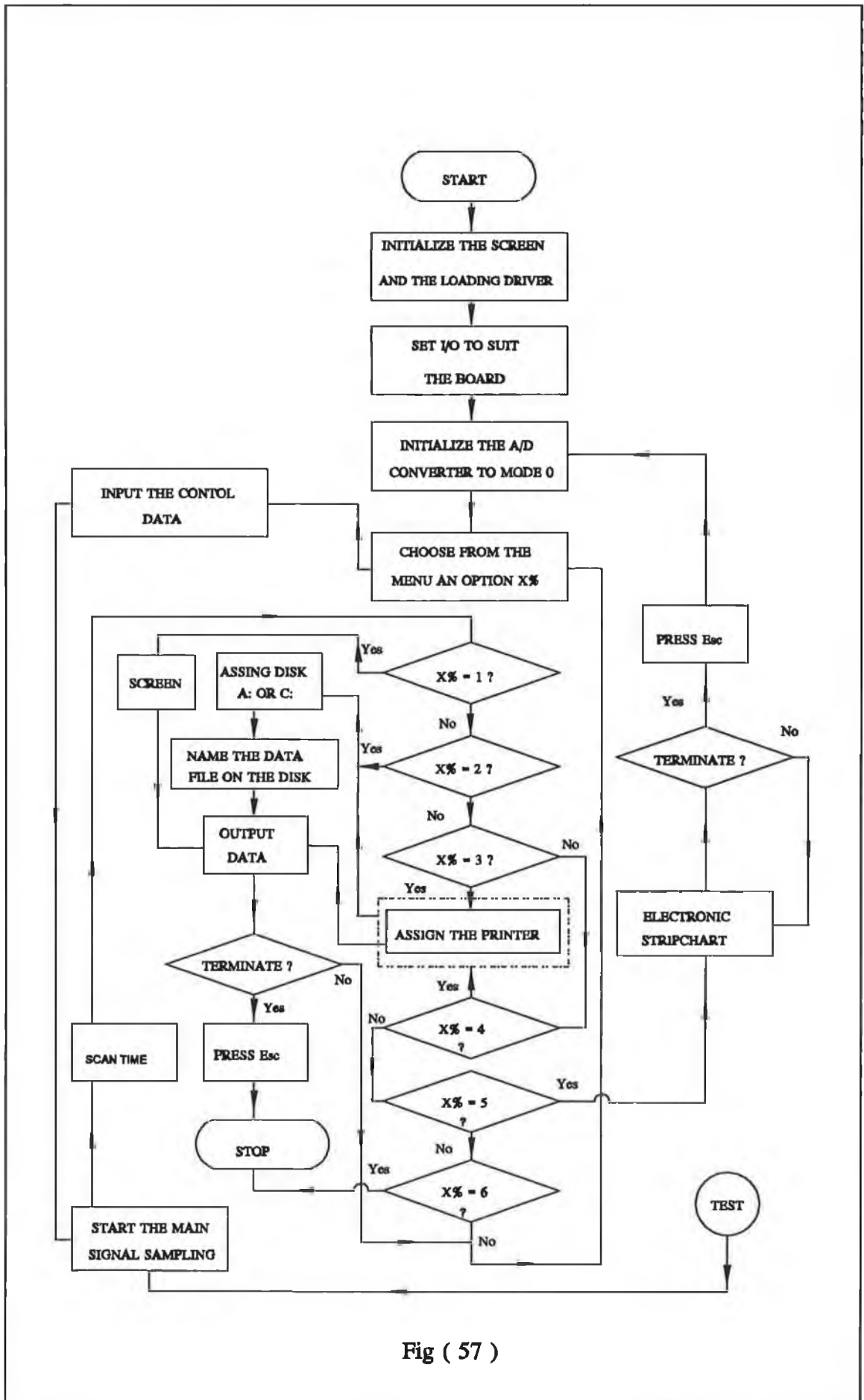


Fig ( 57 )

- displaying the electronic strip chart could be useful for the initial test).
- (iii) Initialize the position of the cap of the hydraulic ram and the fixed L.V.D.T. (i.e. move downward the plunger of the hydraulic ram until the cap of the ram touches the workpiece without causing a significant signal from the cell. Then position the fixed L.V.D.T. to give zero signal).
  - (iv) Abort the initial test by the computer and select an option from the main menu to start testing the workpiece.

Therefore, in this case the fixed L.V.D.T. measures the combination of the deformation of the whole structure and the deformation of the workpiece. In order to obtain the net measurement of the workpiece, in this process, and thus to eliminate the deformation of the whole press structure, the following is suggested:

- (a) Start steps (i) to (iv) without the workpiece (i.e. test the whole press structure).
- (b) After measuring the load deflection of the whole press structure, which exhibited a linear behaviour, the direct stiffness ( $St$ ) can be established.
- (c) The steps (i) to (iv) can be started again with the workpiece and the net deformation of the workpiece can be written as follows:

$$\delta_{net} = \delta_{tot} - \left(\frac{P}{St}\right) \quad 4.4$$

where:

- $\delta_{net}$  is the net deformation of the workpiece
- $\delta_{tot}$  is the total deformation of the whole press structure and the workpiece
- $P$  is the applied load
- $St$  is the direct stiffness of the whole press structure.

Equation (4.4) can be incorporated with the BASIC program listed in Appendix (D) to calculate the net deformation of the workpiece automatically.

## **CHAPTER 5**

### **RESULTS AND DISCUSSIONS**

#### **5.1 Introduction**

The hydraulic press structure has been analyzed theoretically and experimentally. The predicted results, obtained from the different theoretical approaches have been compared with those obtained experimentally. This comparative study is aimed to establish both the accuracy and cost of the analysis of the hydraulic press. The predicted theoretical and experimental results have also been compared with the internationally accepted design goal of the hydraulic press structure to evaluate the standardization of this structure. The load deflection characteristics and thus the stiffness of the press structure have been taken into account to determine the behaviour of the press structure. These have been obtained experimentally for ten test and the average values have been considered in this analysis. The results have been obtained for the following:

- (i) performance test
- (ii) the press structure before the modification
- (iii) the press structure after the modification
- (iv) new design of the press structure.



### 5.1.1 Performance Test:

The measurement system for the experimental setup has been checked out to evaluate the given nominal sensitivities. The displacements of the L.V.D.T.'s have been measured using the current measurement system and a displacement digital gauge of resolution of  $0.1 \times 10^{-3}$  mm. This has been carried out in several locations on each L.V.D.T. for ten times. The average values of these tests have been evaluated and as a result insignificant difference was found between the output of the measurement system and the output of the digital gauge. Although the nominal capacity of the press is 150-tonne, it has been found in the practice that the press is not able to give more than 140-tonne operational load.

The performance of the load cell has been examined using the present experimental setup and the equation (4.3) which was derived to obtain the sensitivity of the load cell. A liquid filled pressure gauge has been used to measure the operational load. The output voltage signal of the load cell has been measured by the present measurement system. This test has been performed ten times for several load levels. The average values of the applied load and the voltage output of the load cell have been obtained. Fig. (58) shows a linear relationship between the applied load and voltage output of the load cell when using:

- (i) Equation (4.3)
- (ii) The existing experimental setup.

## Load Cell Calibration Test

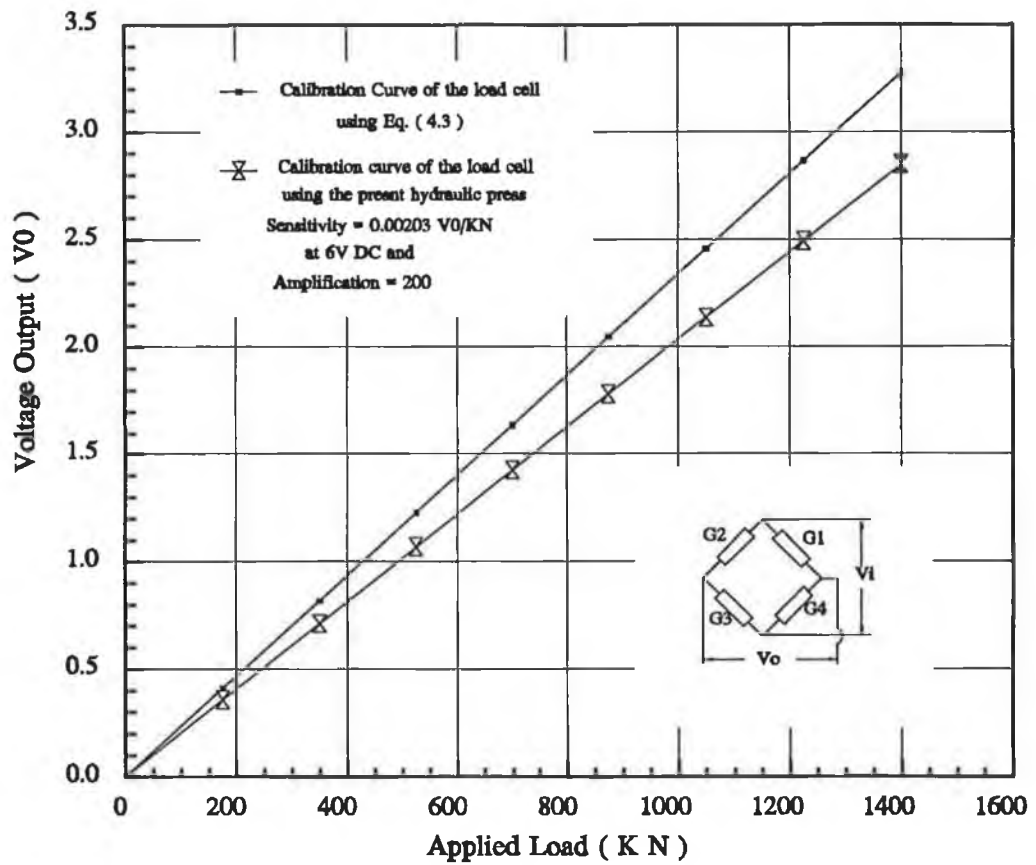


Fig ( 58 )

It can be seen that the calibration curve of the load cell using the experimental setup is lower than the calibration curve using Equation (4.3). The difference in the sensitivities of both curves has been found to be  $0.41 \times 10^{-3} \text{ Vo/KN}$ . This could be attributed to the misalignment of the mating subunits of the experimental setup. This might lead to an eccentric applied load which was absent when using equation (4.3). However, the difference has been used by the present measurement system of the experimental setup as a correction factor of the applied load.

### **5.1.2 Press Structure before Modification**

Although a 3-D thin shell FEA model of the complete hydraulic press structure, consisting of the assembly of the subunits, has been prepared with different mesh refinement, the finite element analytical results could not be obtained. This was due to the short-comings of the computing hardware used to perform the analysis of this model. During the analysis of this model an error message appears on the screen, after some hours, announcing the lack of memory and disk space of the personal computer (PC). Subsequently, the press structure was analyzed, using several alternative finite element approaches. This was carried out with the aim of making use of the existing hardware and software to establish the accurate analysis of the press structure at lower cost and less time. The results have been obtained for the following finite element analysis presentations:

- (i) Plane frame model
- (ii) Plane stress model
- (iii) 3-D thin shell model.

## **I . Plane frame model (PF)**

This model was considered to be the simplest finite element model of the press structure. It features the closest representation to the conventional analytical model. Therefore, the results of these two models have been compared with each other and then compared with the experimental results. The deformation mode of the plane frame model in Fig. (59.b) shows that the maximum deformation in Y direction can be found where the operational load is applied at nodes 6 and 8 in Fig. (59.a) in which node 8 has the largest deformation. The diagram of the axial forces in X direction is shown in Fig. (60.a). This suggests that the beams 1-2 and 10-11 in Fig. (59.a) are not subjected to any forces as shown in Fig. (60.a) (i.e.  $F_4 = 0$ ). It can be seen from the bending moment diagram shown in Fig. (60.b) that the bending moment  $b_4 = 0$ . This means that the beams 1-2 and 10-11 in Fig. (59.b) are also not subjected to any bending moment. Thus, it can be said that physically this part of the hydraulic press remains undeformed. Fig. (60.b) shows that the maximum bending moment  $b_1$  and  $b_3$  can be found where the maximum deformation was observed. The analysis of this model showed that the results obtained for the maximum and minimum number of beam elements; using the free bending moment at the nodes 2 and 11 in Fig. (59.a) or using the nonlinear joint elements at these nodes, were the same. In fact, these results have been compared with the results obtained from the conventional analytical model and no difference between the conventional analytical and the FEA results of this model has been found. The deflection of the nodes 6 and 8 in Fig. (59.a) have physically been measured using two mobile L.V.D.T.'s. The average of these measurements have been accumulated to give the total deflection of the press structure. The measured load deflection of the hydraulic

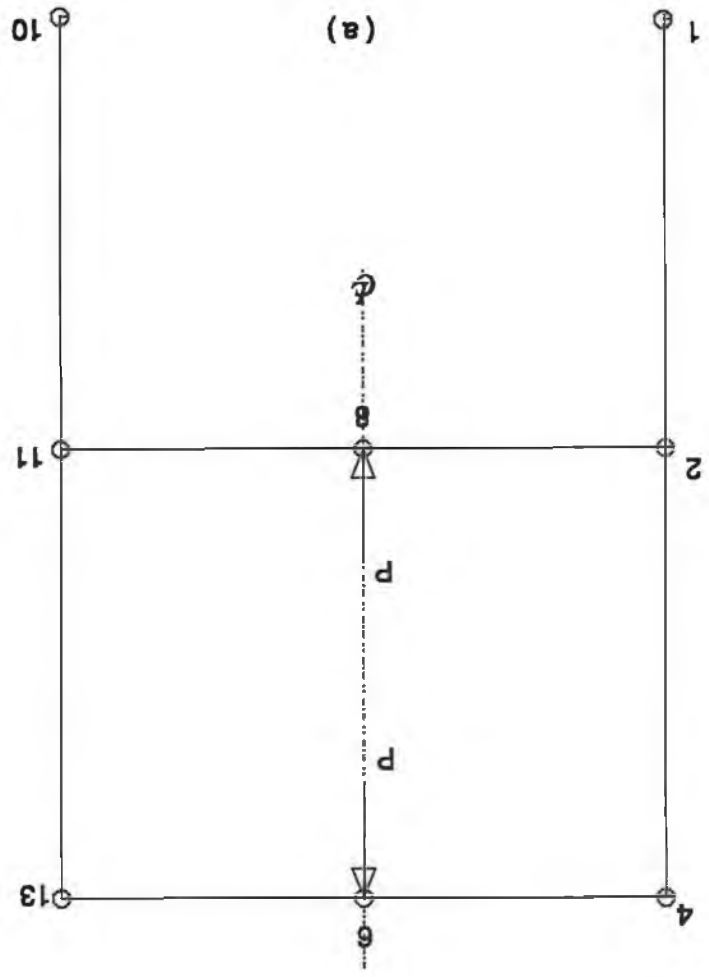
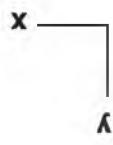
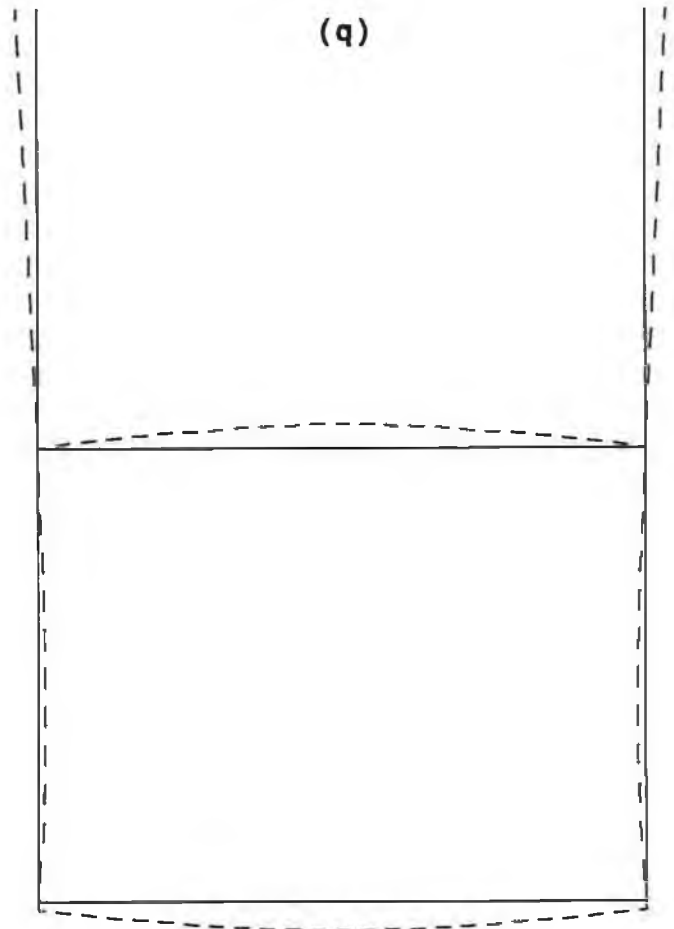
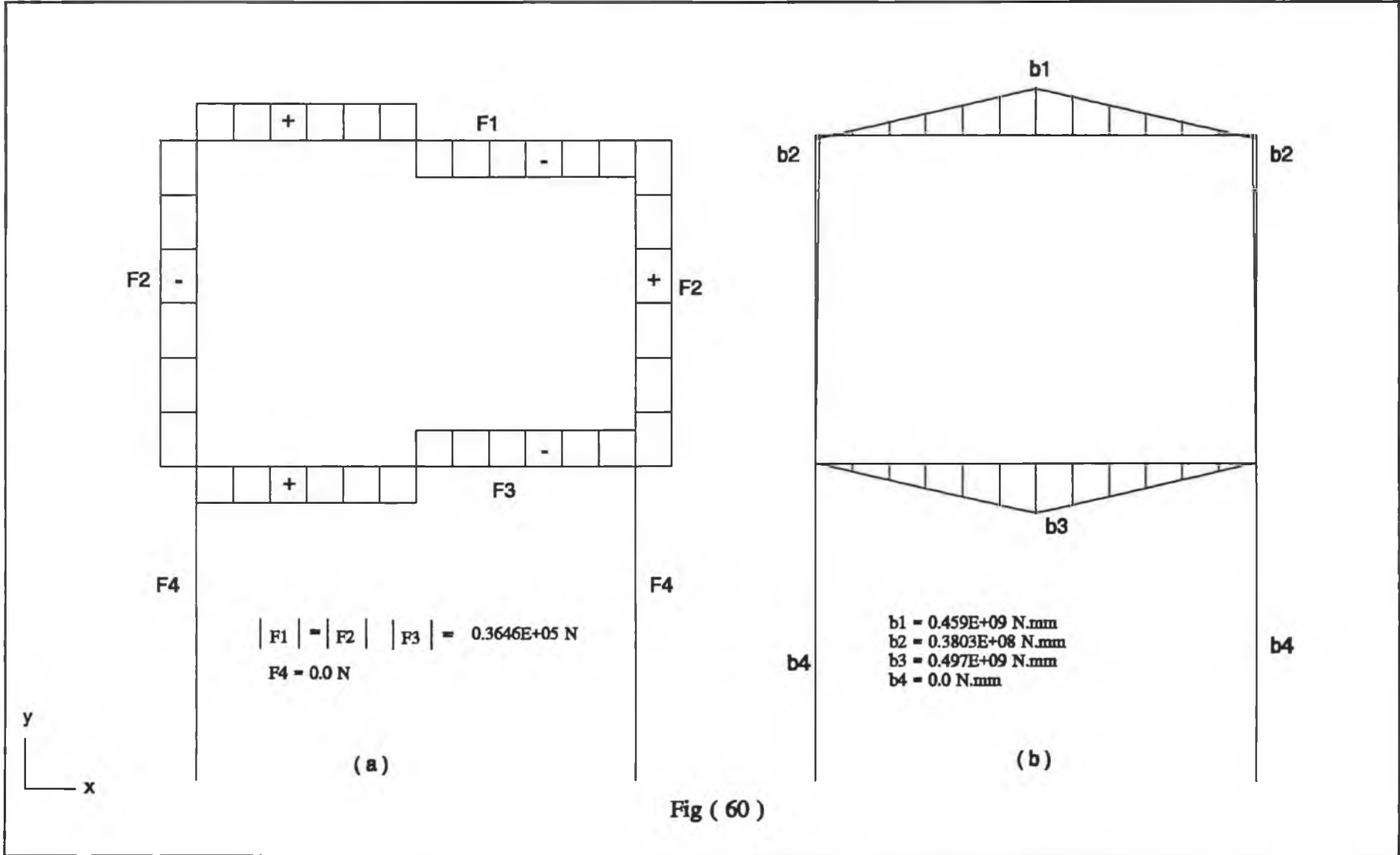


Fig (59)





## Load Vs. Deflection "Plane Frame FEA Model"

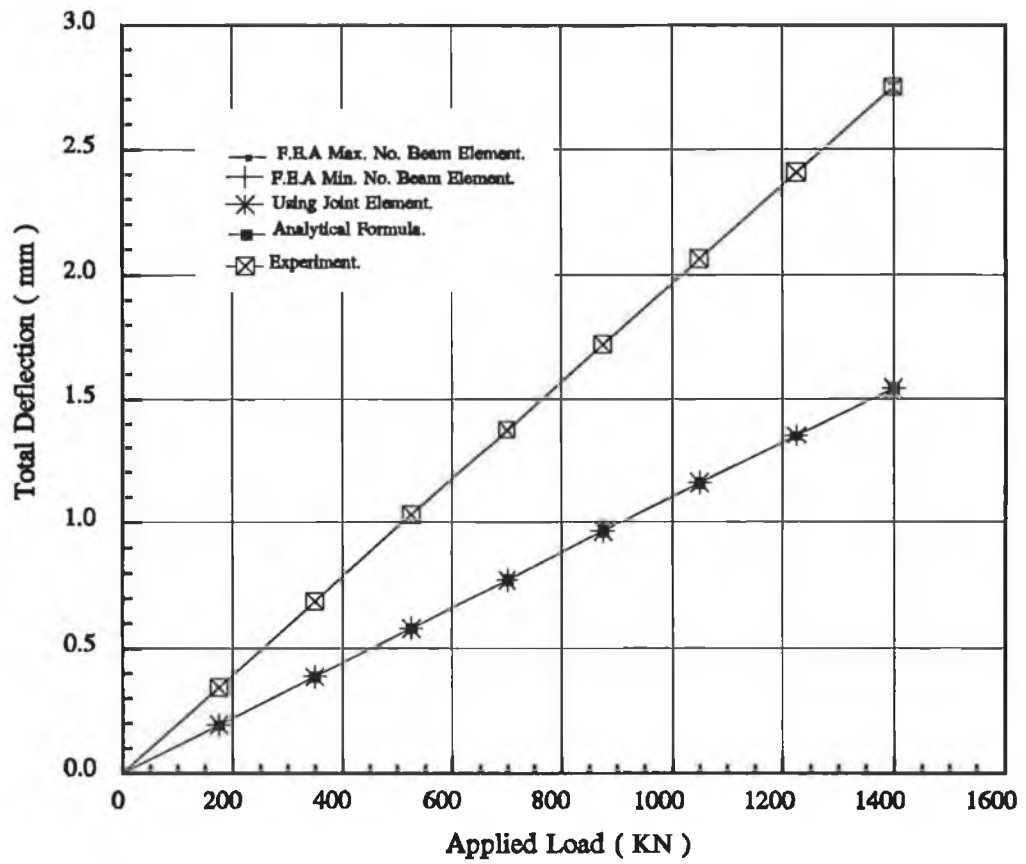


Fig ( 61 )

press structure has been compared with those theoretically predicted results. This comparison is illustrated in Fig. (61) which shows that the predicted results converge to the value of 43% lower than the experimental results at the maximum applied load. The maximum combined direct and bending stresses were predicted at the maximum applied load by the conventional model to be as follows: 190.65 N/mm<sup>2</sup> at bottom beam of the press bed; 117.3 N/mm<sup>2</sup> at the top corner; and 173.0 N/mm<sup>2</sup> at the top beam. The maximum combined stresses predicted by the conventional model at the maximum applied load shows lower than the permissible stress within 24%; 53% and 30% at the bottom beam; the corner and top beam of the model, respectively. However, these results were unobtainable using the plane frame model. The maximum deflection in Y direction has theoretically been predicted, at maximum applied load, by the conventional analytical model and the plane frame model to be (0.6934 mm) at node (8) which is shown in Fig. (59.a). The results shown in Fig(61) suggest the following:

- (i) Increasing the number of beam elements in the plane frame model (PF) did not increase the accuracy of the results.
- (ii) The results yielded the same degree of accuracy by using either the joint elements or the option of freeing the bending moment of the beam elements at the pin joints.
- (iii) The results obtained from the plane frame model when using:
  - (a) Maximum number of beam elements.
  - (b) Minimum number of beam elements.
  - (c) Joint elements at the pin joints.
  - (d) Free bending moment of the beam elements at the pin joints.

agreed a 100% with the results obtained from the conventional analytical model(C.A.M).



## **II . Plane stress model (PS)**

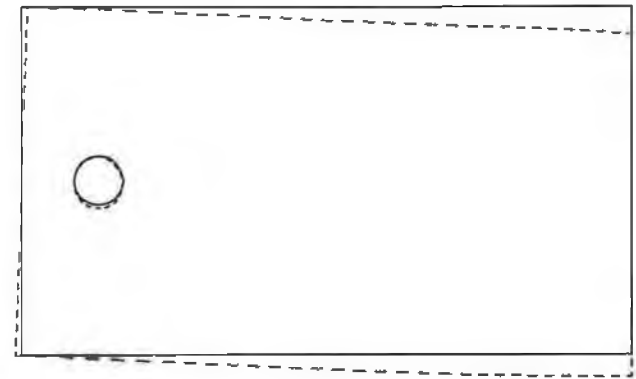
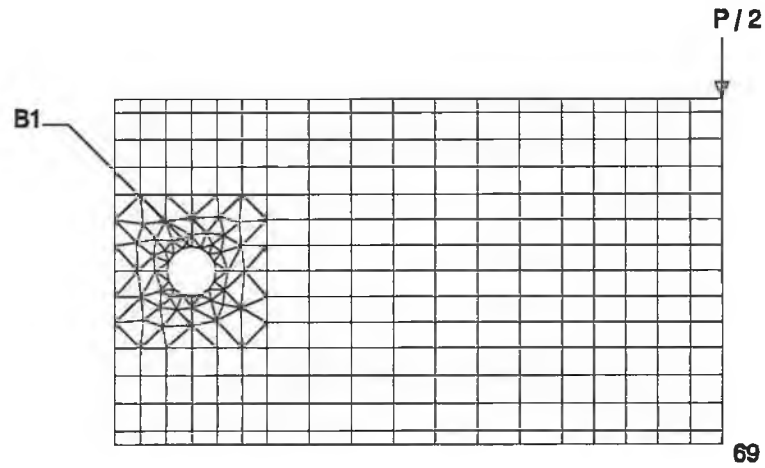
With regard to the symmetry of the press structure, half of this structure has been considered in this model. This half was broken into an L-shaped beam and half of the press bed. Before starting the discretization of this model half of the press bed was modelled and was subjected to the following analytical tests:

- (i) Test for the boundary condition
- (ii) Test for the mesh density.

### **Test for the boundary condition**

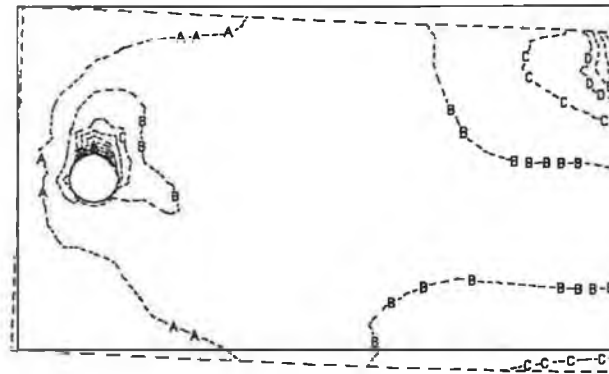
The aim of this test was to simplify the boundary conditions where the press bed joins the rest of the press structure. The following Figures are presented to illustrate the results obtained.

Fig. (62.a) shows the finite element model of half of the press bed modelled with simple boundary condition as it was stated in Chapter 3 for Fig.(11). The deformation mode of this model is shown in Fig. (62.b), whereas the equivalent stress contour values at the maximum applied load is shown in Fig. (62.c). The finite element model of half of the press bed using nonlinear boundary conditions at the housing of the pin is shown in Fig. (63.a). The mode of deformation and the equivalent stress contour values of this model at the maximum applied load are shown in Fig. (63.b) and Fig. (63.c) respectively. The



(a)

(b)



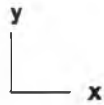
CONTOUR VALUE

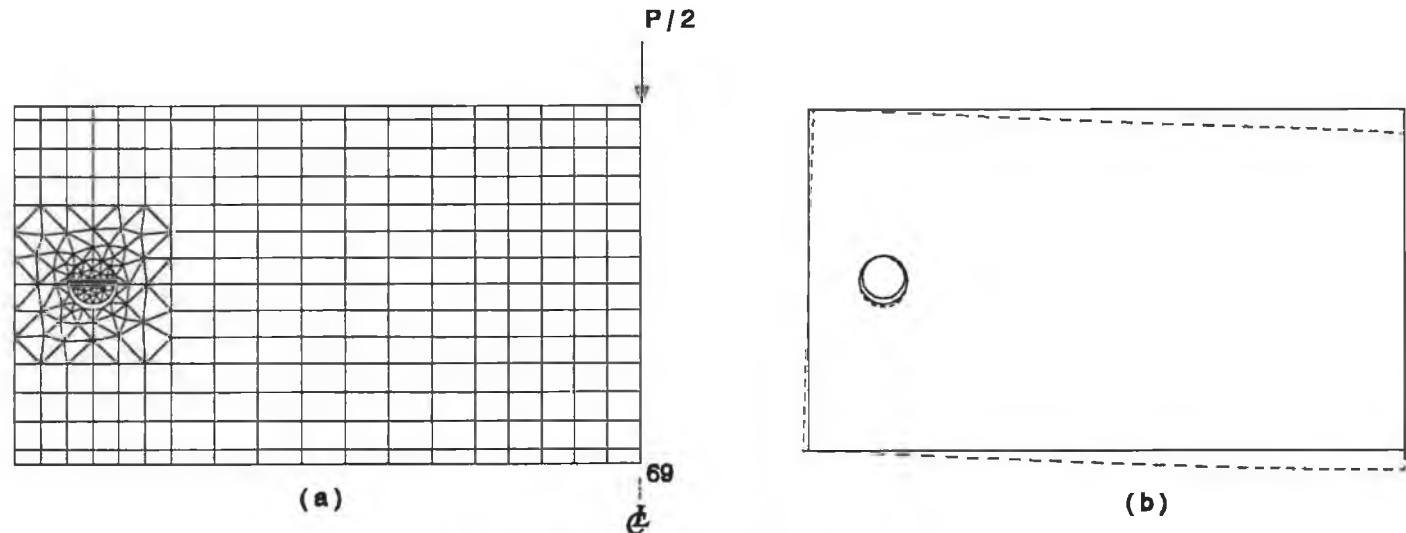
A	52.53
B	105.1
C	157.6
D	210.1
E	262.7
F	315.2
G	367.7
H	420.3
I	472.8
J	525.3
K	577.9
L	630.4
M	682.9
N	735.5
O	788.0

Contour value = Eq Stress (N/mm<sup>2</sup>)

(c)

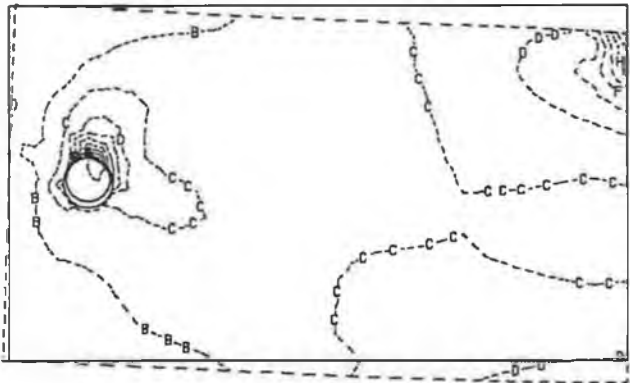
Fig ( 62 )





(a)

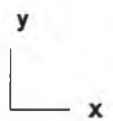
(b)



CONTOUR VALUE

A	0.0
B	48.92
C	97.84
D	146.8
E	195.7
F	244.6
G	293.5
H	342.4
I	391.4
J	440.3
K	489.2
L	538.1
M	587.1
N	636.0
O	684.9

Contour value = Eq Stress (N/mm<sup>2</sup>)



(c)

Fig ( 63 )

deflection according to the two models of half of the press bed has been measured and computed for several load levels at node (69) in Fig. (62) and Fig. (63). The computed results of the load deflection characteristics corresponding to the two models in Fig. (62) and Fig. (63), together with the experimental results, are shown in Fig. (64). The equivalent stresses at the bottom layer of the centre line of the two models in Fig. (62.c) and Fig. (63.c) have been compared at the maximum applied load. This comparison showed that the equivalent stress obtained from the model in Fig. (63.c) at contour (D) converges to within 7% lower than the contour (C) in Fig. (62.c). It is apparent that the model in Fig. (63) is stiffer than the model shown in Fig. (62). Also it can be seen that the load deflection characteristics in Fig. (64) of the model in Fig. (63) converges to a slightly lower value of deflection than the load deflection characteristics of the model with simple boundary conditions in Fig. (62). The reason for this is that the model in Fig. (63) is more constrained in the housing of the pin than the model in Fig. (62). Therefore, such constraint leads to a reduction in resulting deflection. In other words the constraint is equivalent to increasing the stiffness of the structure. Fig. (64) shows that the maximum deflection of the model in Fig. (62) (i.e. the maximum deflection of node 69 in Fig. (62.a)) at the maximum applied load converges to within 26% lower than the experimental results. The computing time for the analysis, excluding the time for data preparation, of the two models in Fig. (62) and Fig. (63) has been obtained. This showed that the computing time for the analysis of the model in Fig. (62) was 247.3 sec. whereas it was 2509.6 sec. to complete the analysis of the model in Fig. (63). Therefore, considering the convergence of the two models and the computing time for the analysis, it is more practical to use the simple boundary condition in the present analysis for the press structure.

## Load Vs. Deflection "Plane Stress FEA of The Press Bed"

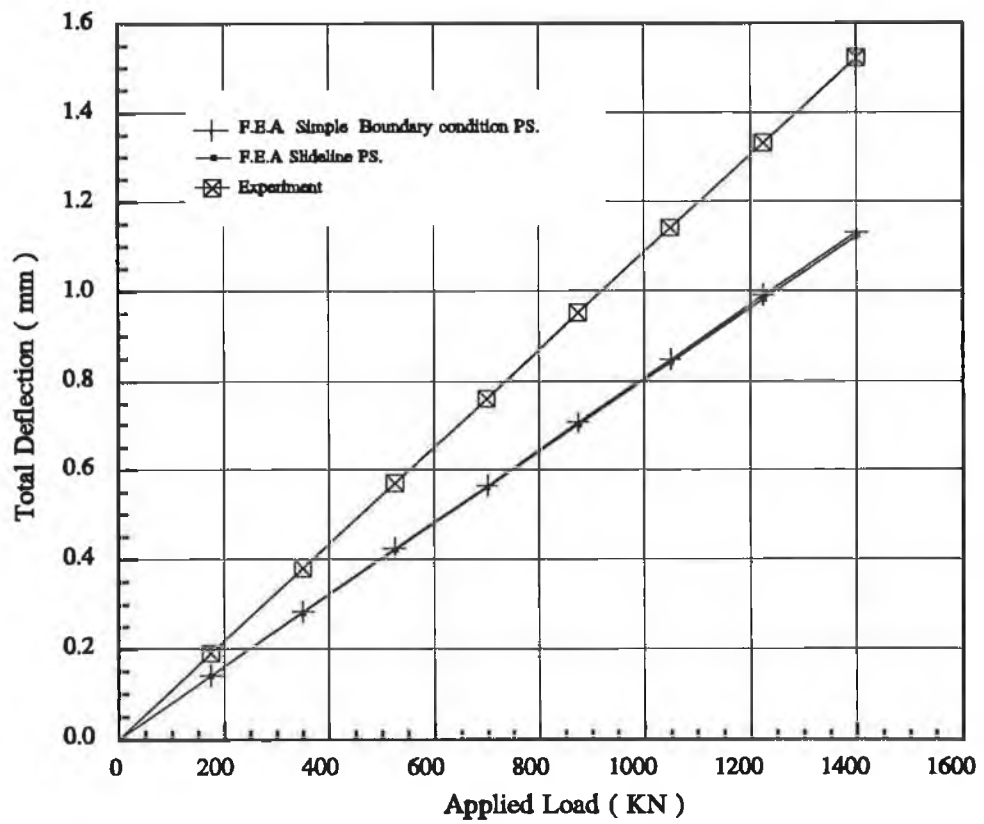


Fig ( 64 )

### Test for the mesh density

This test has been performed on half of the press bed with several mesh densities at half of the maximum operational load. These meshes were shown previously in Fig. (12), Chapter 3, where the objective of this test was explained. The results of this test has been summarised in Table (1). In this table the maximum deflection has been considered at the bottom layer of the centre line of the press bed. It was observed that exceeding the number of elements of mesh No. 4 in Table (1) does not produce a significant improvement but only increases the required computer core store.

TABLE (1)

No.of meshes	No.of elements	Load P/2 (KN)	Max. deflection (mm)	Convergence of max. deflection %	Max. time for solution (Sec.)	Convergence of the max. time for solution %
1	58	700	1.018	9.9	46	81.3
2	68	700	1.04	7.9	55.3	77.6
3	160	700	1.122	0.7	105.9	57.1
4	324	700	1.13	0	247.3	0

The results obtained from mesh No. 4 in Table (1) were taken as a base results in order to compare the results of the other meshes in this Table. The mesh with the optimum number of elements can be found to fulfil the requirement of accuracy of the results at minimum time for solution. The results in Table (1) were introduced in Fig. (65) which indicates that the optimum number of elements can be obtained from mesh No. 3. The maximum deflection of this mesh converges to within 0.7% lower than the maximum deflection of mesh No. 4. The maximum time for the solution of the mesh No. 3 converges to a value some 57.1% lower than the maximum time for solution of mesh

No. 4. The value of convergence of the maximum deflection of mesh No. 3 was used as a reference quantity to obtain the optimum number of elements of the meshes used in the present analysis of the press structure.

### **Results and discussion of the plane stress model**

The following are the results obtained from the analysis of the plane stress model and the discussion thereof.

Fig. (66.a) shows the plane stress FEA model of half of the press bed. Fig. (66.b) shows the deformation mode of this model. The equivalent stress contour values at the maximum applied load is shown in Fig. (66.c). The L-shaped beam FEA model is shown in Fig. (67.a). Fig. (67.b) and Fig. (67.c) illustrated respectively the deformation mode and the equivalent stress contour values at the maximum applied load of this L-shaped model. Table (2) shows the experimental and theoretical results of the maximum deflection in Y direction of the models shown in Fig. (66) and Fig. (67) at several load cases.

## Percentage of Max. Time & Deflection of The Press Bed Using Plane Stress FEA Model With Different Mesh Densities

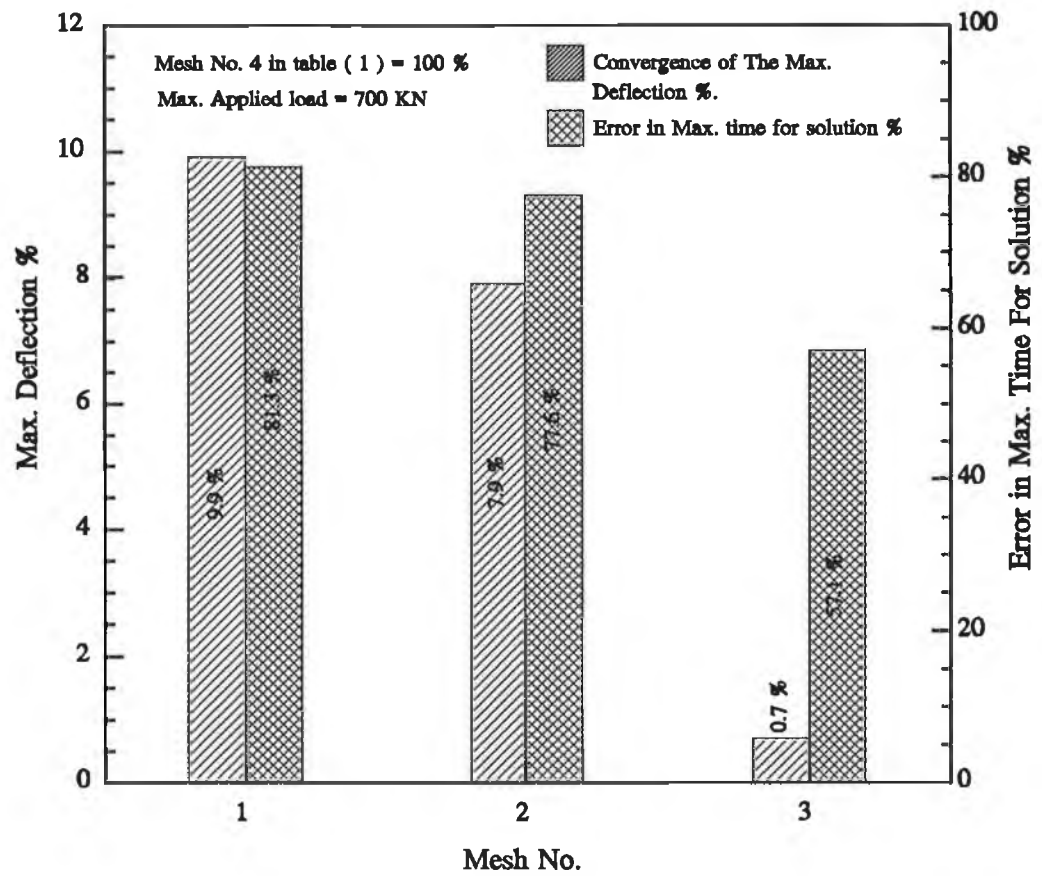


Fig ( 65 )



**TABLE (2)**

Applied Load (KN)	Max. deflection of half the press bed at node 39 (mm)		Max. deflection of L-shaped beam at node 594 (mm)	
	P.S	Experiment	P.S	Experiment
175	0.1413	0.1913	0.134	0.1535
350	0.2826	0.3817	0.268	0.3071
525	0.4239	0.5691	0.4021	0.4612
700	0.5652	0.7609	0.5361	0.6145
875	0.7065	0.9511	0.6701	0.7681
1050	0.8478	1.14101	0.8041	0.9209
1225	0.9891	1.3309	0.9382	1.0751
1400	1.13	1.5219	1.072	1.2289

Fig. (68) shows the experimental and theoretical load deflection characteristics of the whole press structure. At maximum load, Table (2) proves that the maximum FEA deflection of half of the press bed converges to a value some 26% lower than the maximum experimental results, whereas the maximum FEA deflection of the L-shaped beam converges to a value some 13% lower than the experimental results of this model. This contradiction in the accuracy between the two FEA models shown in Fig. (66) and Fig. (67) is perhaps, attributed to the fact that the physical behaviour of the press bed is not compatible with the plane stress analysis used.

It can be seen from Fig. (68) that the maximum total FEA deflection converges to a value some 20% lower than the total experimental deflection. The computed results in Fig. (66.c) show that the equivalent stress at the bottom layer of the centre line (i.e. contour D) converges to a value some 34% lower than the permissible stress. The equivalent stress at the top layer of the centre line in Fig. (67.c) (i.e. contour E)

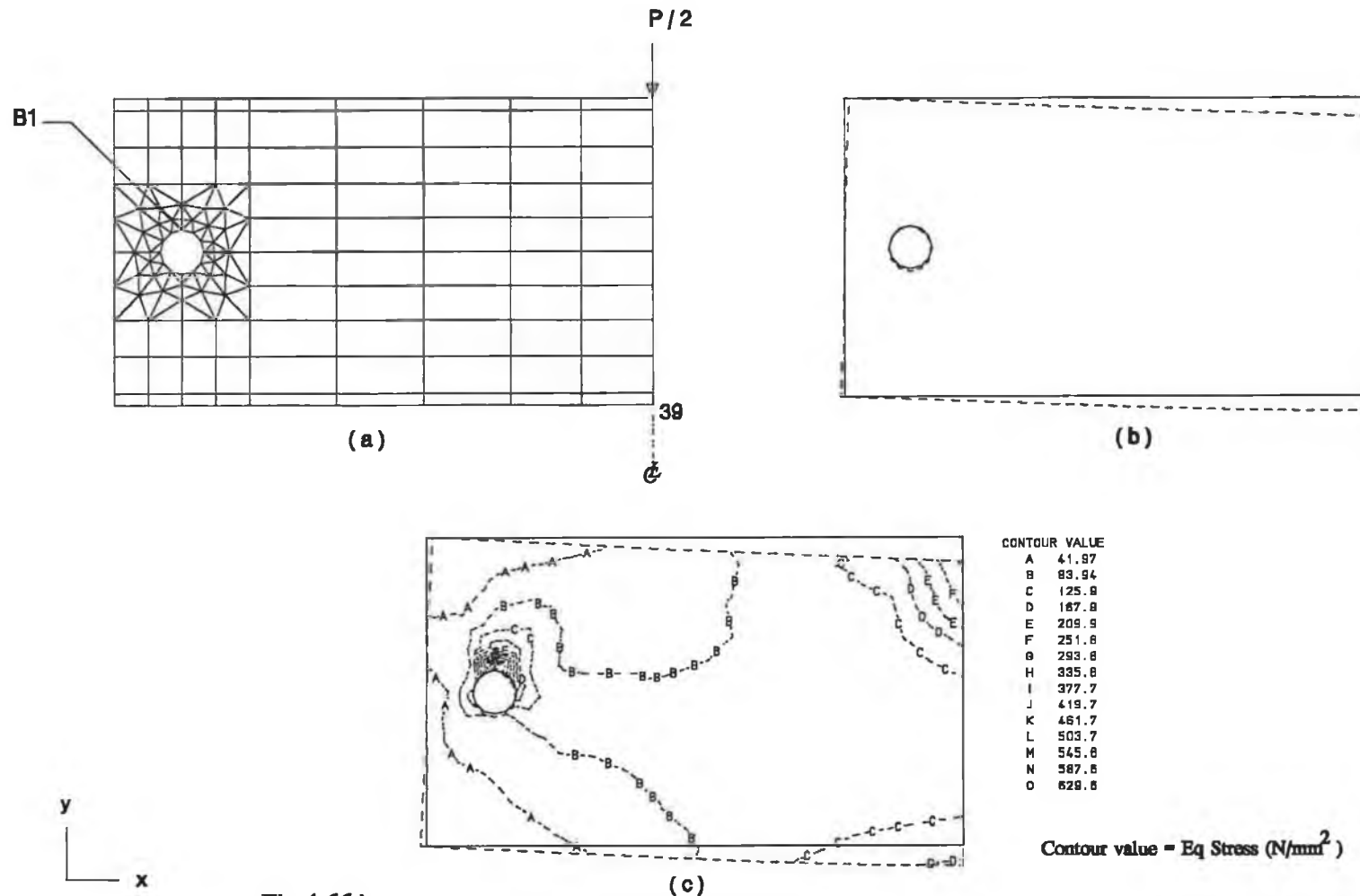
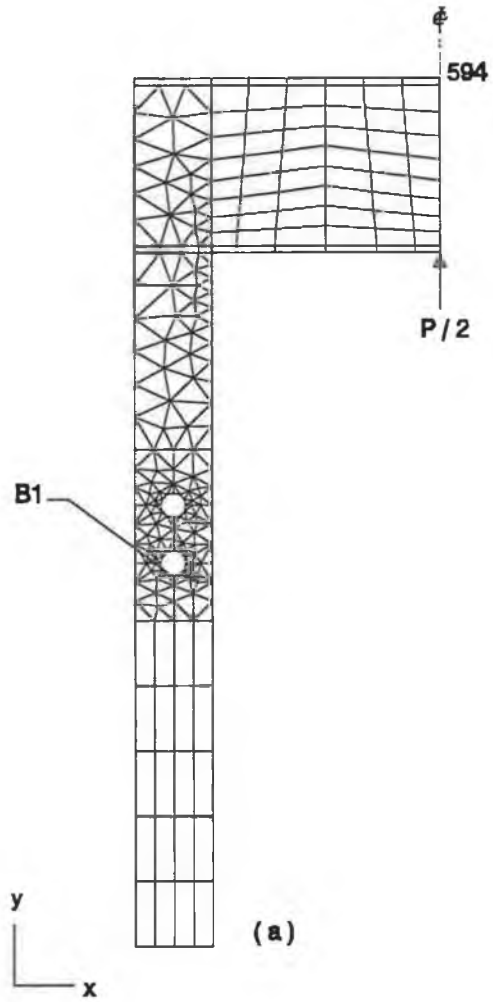
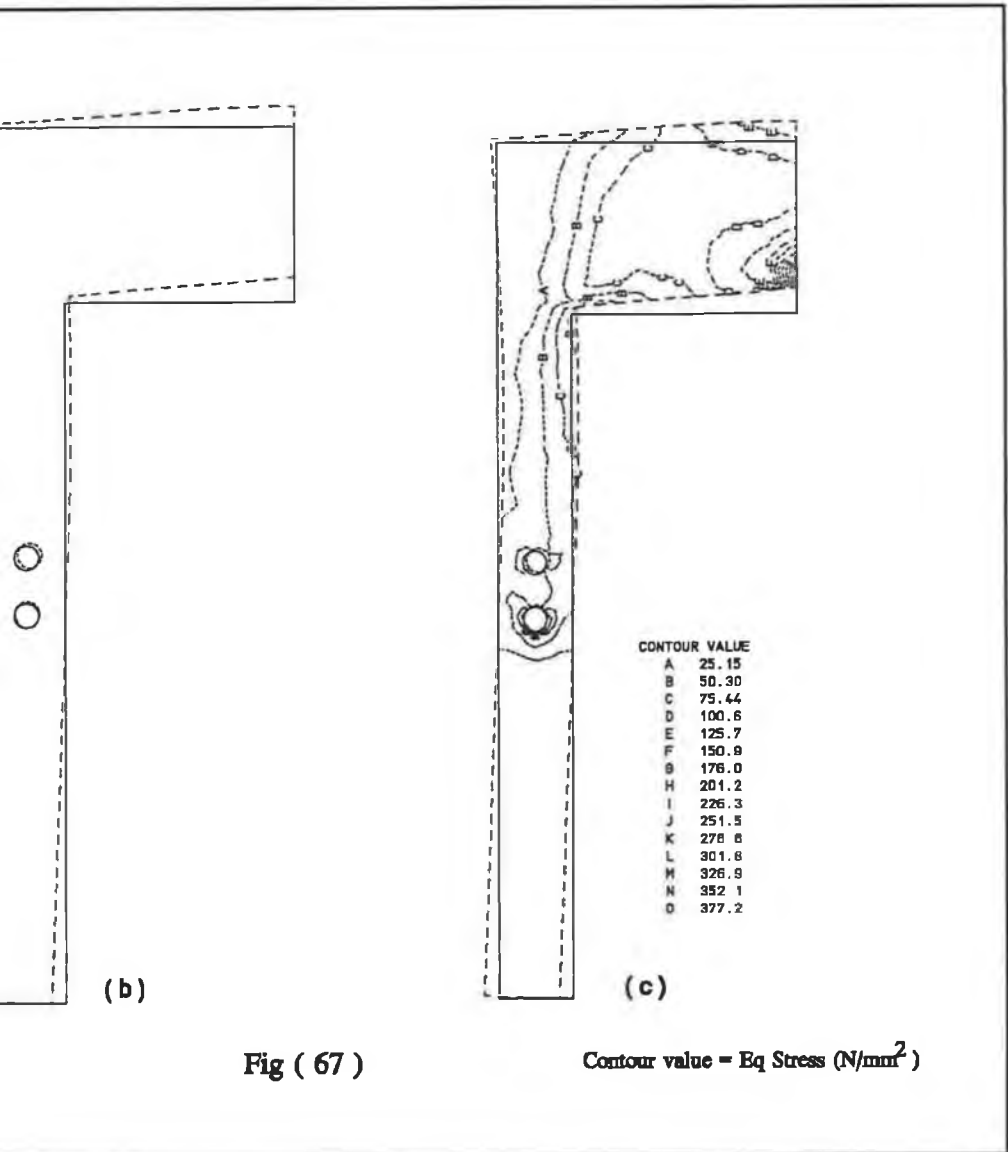


Fig ( 66 )





### Load Vs. Deflection "Plane Stress FEA Model of The Press Structure"

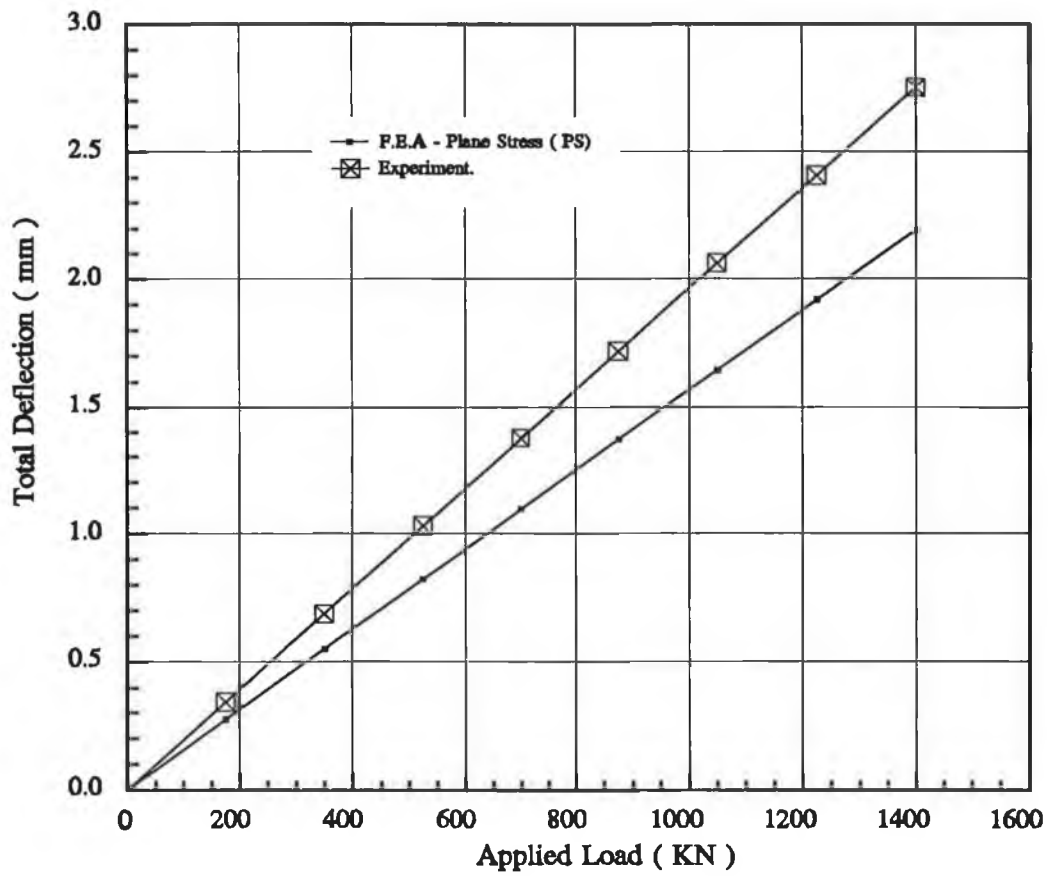


Fig ( 68 )

converges to within 50% lower than the permissible stress. The equivalent stress at the corner in Fig. (67.c) (i.e. contour D) converges to within 60% lower than the permissible stress.

### **III . 3-D thin shell model (3-D T.S)**

The detailed explanation of this model was stated earlier in Chapter 3. Fig. (69.a) shows the 3-D thin shell FEA model of quarter of the press bed. Fig. (69.b) and Fig. (69.c) show the mode deformation and the equivalent stress contour values at maximum applied load of this model, respectively. The 3-D thin shell FEA model of the L-shaped beam before and after deformation is shown in Fig. (70.a). The equivalent stress contour value of this model is shown in Fig. (70.b). Table (3) shows the theoretical and experimental results of the maximum deflection in Y direction of the model in Fig. (69) and Fig. (70) at several load cases. The accumulative experimental and theoretical load deflection characteristics of the whole press structure is shown in Fig. (71).

**TABLE (3)**

Applied Load (KN)	Max. deflection of the 3-D quarter of the press bed at node 282 (mm)		Max. deflection of the 3-D L-Shaped beam at node 116 (mm)	
	3-D.T.S. FEA	Experiment	3-D.T.S. FEA	Experiment
175	0.1622	0.1913	0.1309	0.1535
350	0.3245	0.3817	0.2617	0.3071
525	0.4867	0.5691	0.3926	0.4612
700	0.6489	0.7609	0.5235	0.6145
875	0.8111	0.9511	0.6544	0.7681
1050	0.9734	1.14101	0.7852	0.9209
1225	1.136	1.3309	0.9161	1.0751
1400	1.298	1.5219	1.047	1.2289

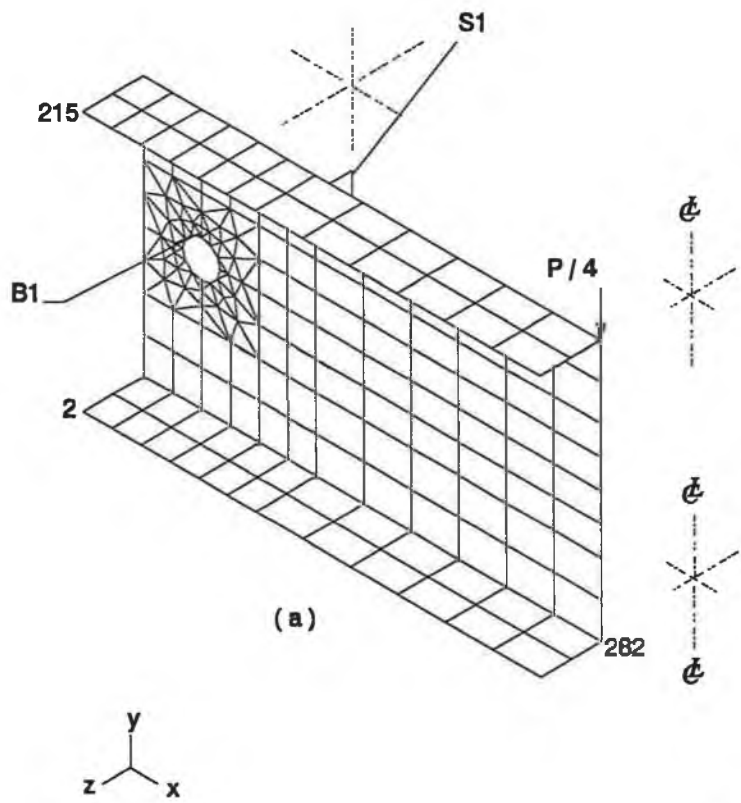
The computer results of the model shown in Fig. (70) showed that there was no appreciable deformation in Z direction compared to the permissible deformation in that direction. However, the computed results of the model shown in Fig. (69) showed that the deformation of the nodes 2; 215 and 282 in Z direction exceeded the limit of the permissible deformation in that direction. Table (4) shows the maximum experimental and theoretical deformation in Z direction of the model shown in Fig. (69) at the maximum applied load.

**TABLE (4)**

Node No.	Applied Load P (KN)	Max. deformation in Z direction (mm)	
		3-D.T.S. FEA	Experiment
2	1400	1.627	1.905
215	1400	-1.297	-1.524
282	1400	-1.42	-1.6671

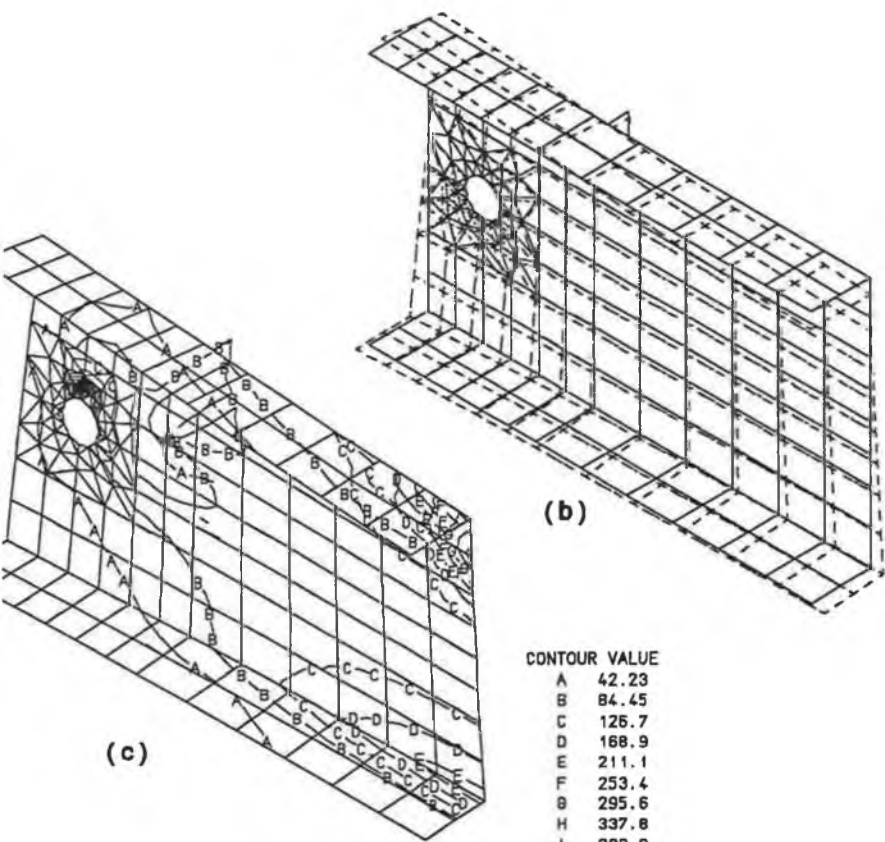
The results in Table (3) and Table (4) show that the FEA results coverage to a value some 15% of the experimental value. This meets satisfactorily with the convergent value of the L-Shaped beam in plane stress. Comparing the maximum deflection of the L-Shaped beam in Table (2) and Table (3) at the maximum applied load, the maximum deflection in Y-direction of the L-Shaped beam in 3-D T.S. model converges to within 3% lower than the maximum deflection in PS. Therefore, it can be said that the PS model of the L-Shaped beam gives a realistic representation of the 3-D T.S. model. The degree of freedom of the L-Shaped in PS is less than the degree of freedom in the 3D T.S. model, resulting in a 77% decrease in computing time. The accumulative experimental and theoretical results shown in Fig. (71) suggests that the total maximum FEA deflection of the press frame converges to within 15% lower than the experimental results. This suggests that the 3D T.S. model of quarter of the press bed and the L-Shaped beam describe the physical quantity of the maximum deflection of the press frame within the same degree of accuracy. The equivalent stress in Fig. (70.b) at the top layer (i.e. contour C) and at the corner (i.e. Contour B) are satisfactorily close to the equivalent stress of the L-Shaped beam in PS. However, the equivalent stress at the





(a)

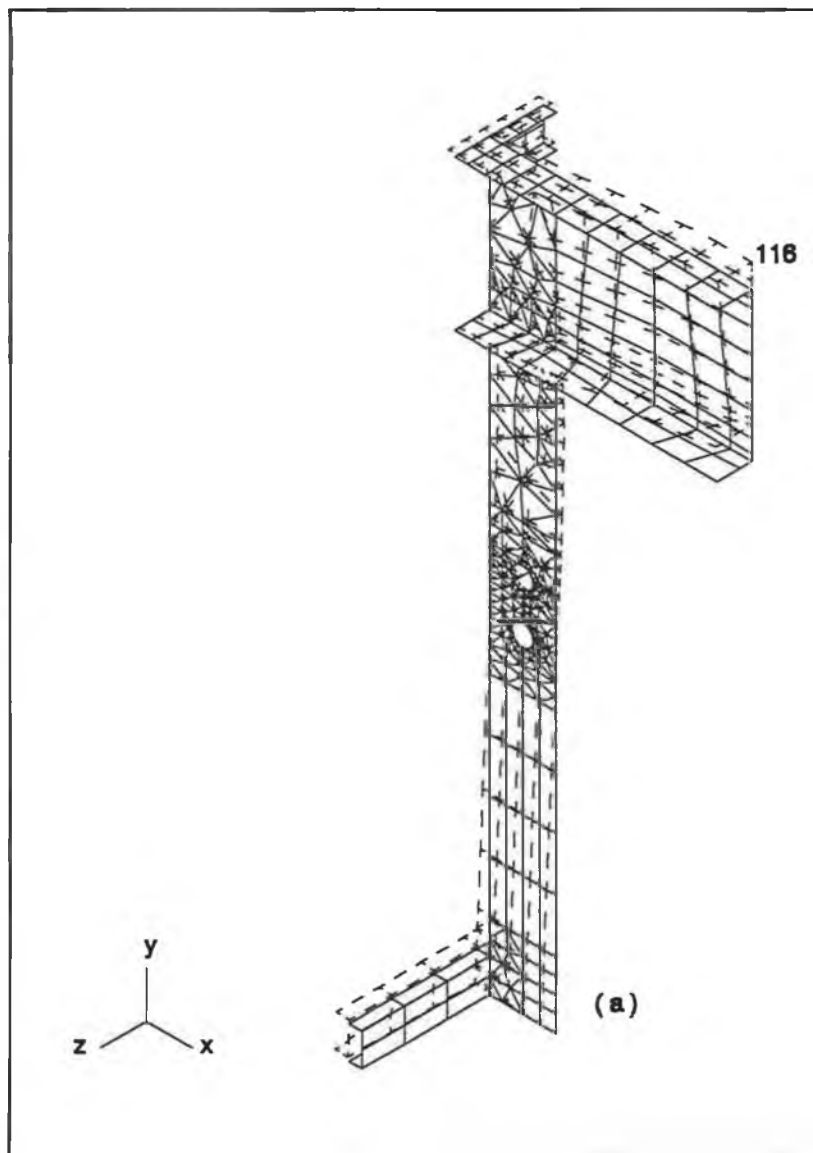
Fig ( 69 )

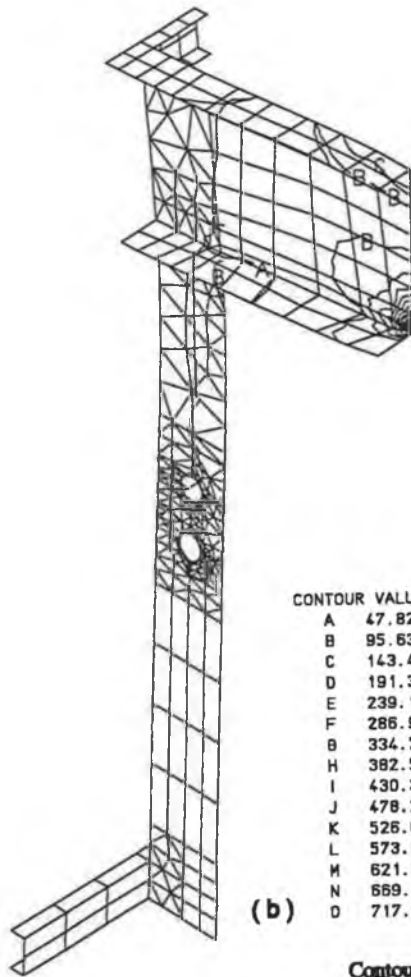


CONTOUR VALUE

A	42.23
B	84.45
C	126.7
D	168.9
E	211.1
F	253.4
G	295.6
H	337.8
I	380.0
J	422.3
K	464.5
L	506.7
M	548.9
N	591.2
O	633.4

Contour value = Eq Stress ( $N/mm^2$ )





CONTOUR VALUE

A	47.82
B	95.63
C	143.4
D	191.3
E	239.1
F	286.9
G	334.7
H	382.5
I	430.3
J	478.2
K	526.0
L	573.8
M	621.6
N	669.4
O	717.2

Contour value = Eq Stress ( $N/mm^2$ )

Fig ( 70 )

**Load Vs. Deflection**  
**"3-D Thin Shell FEA Model of The Press Structure"**  
**"Before Modification"**

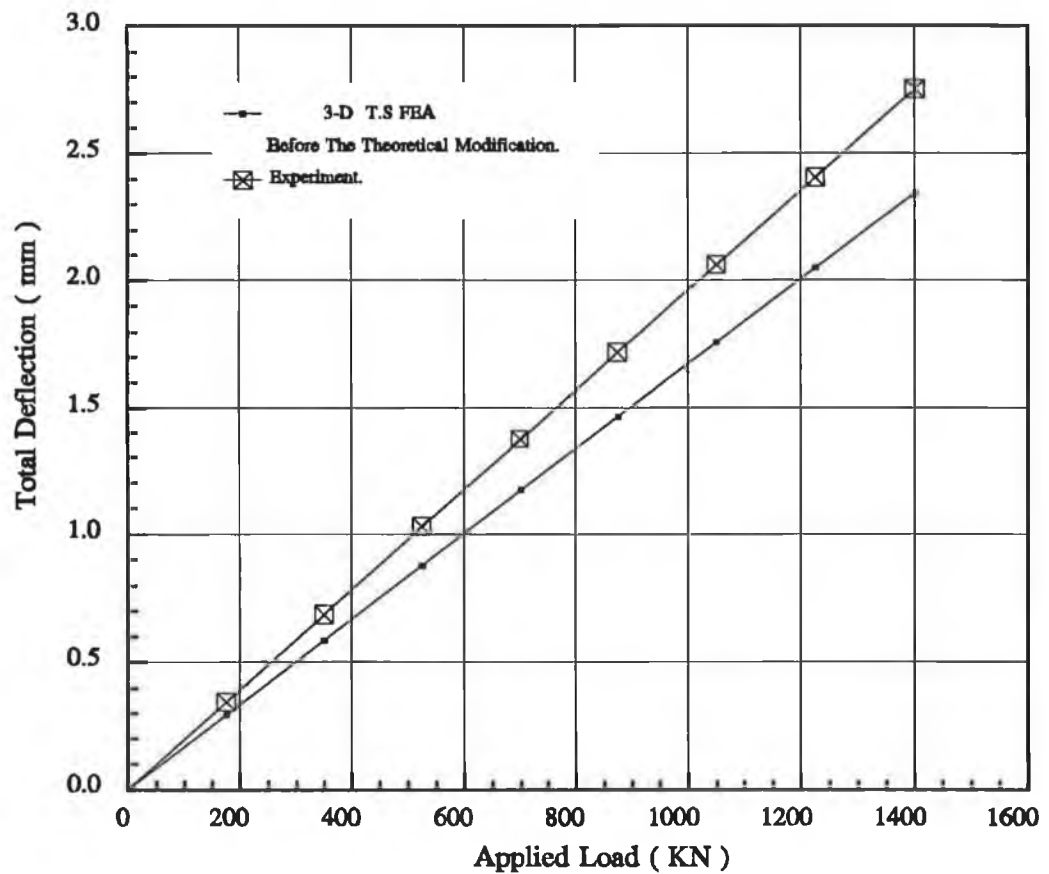


Fig ( 71 )

bottom layer of the centre line of Fig. (69.C) (i.e. contour E) indicates convergence to a value about 20% higher than that indicated in the PS model. This suggests the need to make the press bed stiffer by incorporating suitable stiffeners.

### **Summary of the comparison**

The theoretical and experimental results of the hydraulic press structure, as it stands, i.e before any modifications were made, were obtained and summarized in Table (5). The histogram in Fig. (72) indicates the percentage convergence of the computed FEA total stiffness of the press structure with respect to the experimental stiffness, together with the computing time spent for the solution, excluding the time for data preparation. It can be seen from Table (5) that both the conventional analytical model (C.A.M.) and the PF model predict the same direct stiffness of the press structure. The negative convergence of the total direct stiffness in Table (5) indicates that the computed stiffness is higher than the experimental direct stiffness. Although, the analysis of the P.F and C.A.M. model is not expensive in terms of the solution time, these models can be used accurately to determine the behaviour of the press structure. Fig. (72) shows that the computed direct stiffness, using the P.F. model, is higher than the experiment direct stiffness by about 78.3%.

**TABLE (5)**

<b>Model Name</b>	<b>Total time for solution (sec.)</b>	<b>Total No. of elements</b>	<b>Max. applied load P (KN)</b>	<b>Total max. deflection (mm)</b>	<b>Total direct stiffness (KN/mm)</b>	<b>Convergence of the total stiffness %</b>
C.A.M	3	-	1400	1.5428	907.44	-78.3
P.F	19.7	8	1400	1.5428	907.44	-78.3
P.S	297.9	483	1400	2.194	638.1	-25.3
3-D T.S	1275.9	684	1400	2.345	597.01	-17.3
Exp	-	-	1400	2.751	508.9	0

It is also difficult to estimate precisely by using these two models the amount of the stress concentration within the press structure. It can be seen from Fig. (72) that the P.S model is less expensive, in terms of the solution time, than the 3D T.S by about of 77%. However, the predicted direct stiffness by 3D T.S is closer than the direct stiffness predicted by P.S model to the experimental direct stiffness by about 15%. This difference is due to the out-of-plane deformation of the press bed which could not be predicted by the P.S model. Therefore, it can be said that the appropriate theoretical presentation of the press structure is the 3D T.S FEA model.

### **5.1.3 Press structure after modification**

These are the results obtained from the model stated in Chapter 3.

#### **Effect of stiffening the press bed**

The model which describes the 3-D Thin shell FEA after stiffening the press bed is shown in Fig. (73.a). In order to determine the optimum thickness of the stiffeners, this

model was computed using several thickness values. Table (6) shows the computed results of the effect of the thickness values of the stiffeners on the deflection of the press bed. Fig. (73.b) and Fig. (73.c) show the deformation mode and the equivalent stress contour values, respectively, with an optimum thickness of the stiffeners. Fig. (74), shows the total accumulative load deflection characteristics of the press structure after adding the stiffeners. The thickness values of the cases in Table (6) are shown in Table (I) in Fig. (73).

**TABLE (6)**

Case No.	Max. Applied Load P (KN)	Max. deflection (mm)		Total estimated weight (KN)	Relative total weight %
		in Y direction of node 282	in Z direction of node 2		
before stiffening	1400	1.298	1.627	3.18	100
1	1400	1.113	0.3125	3.329	104
2	1400	1.103	0.1853	3.478	109
3	1400	1.1	0.1357	3.627	114
4	1400	1.098	0.1276	3.776	119
5	1400	1.097	0.1195	3.925	123

It can be seen from Table (6) that each case increases the weight of the press structure by 0.149 KN. The increase in thickness of the stiffness after case No. 3 produces an insignificant reduction in the deflection of the nodes 282 and 2. Therefore, case No. 3 indicates the better use of the material. However, the weight of the press bed in this case increases by about 14% than that indicated in the case before stiffening. It can be observed that the maximum deflection in Y direction in case No. 3 is higher than the permissible deformation obtained from the design goal (0.5 mm/m) by 79%. However, the computed maximum deflection in case No. 3, in Z direction, is lower than the



## Percentage of The Max. Time & Total Stiffness of The FEA Models of The Press Structure

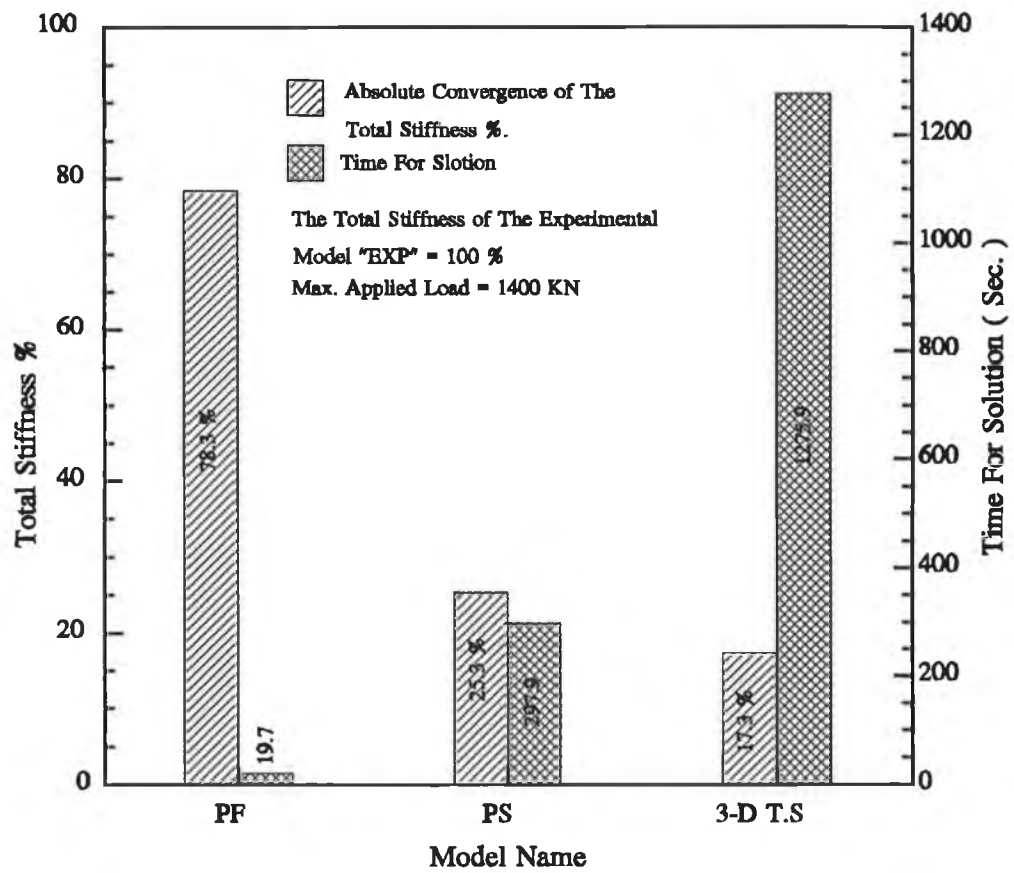
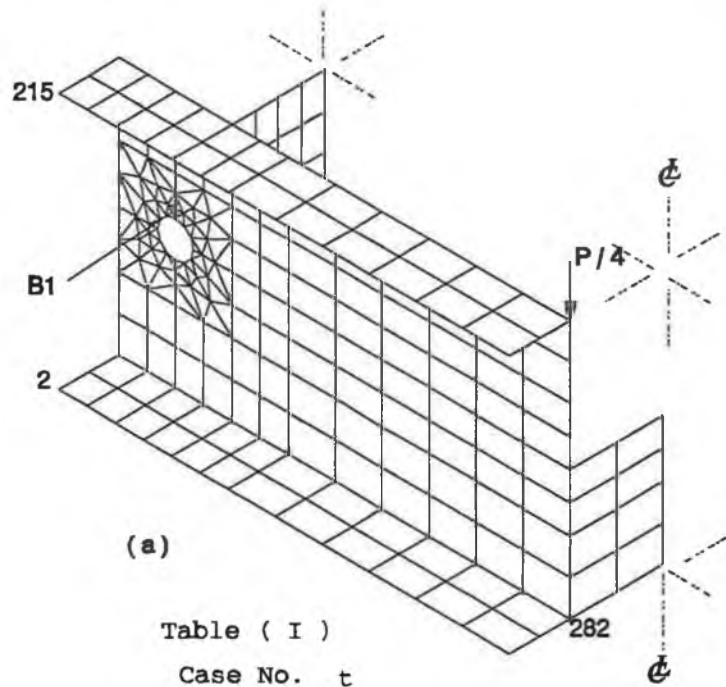


Fig ( 72 )



(a)

Table ( I )

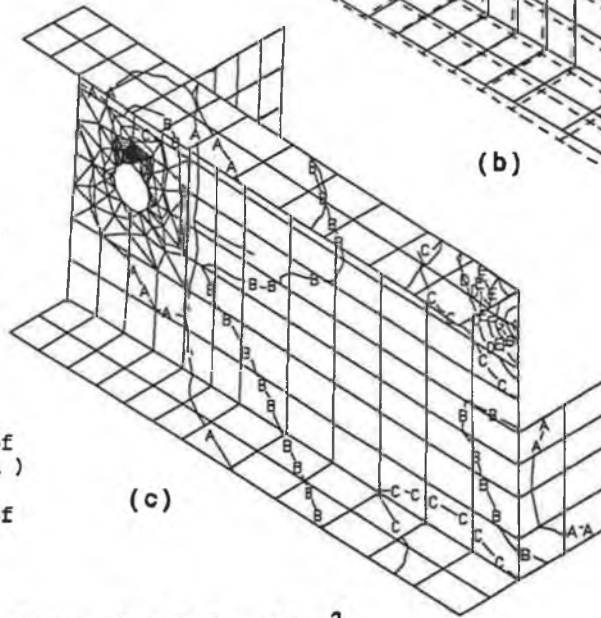
Case No.	t
1	5
2	10
3	15
4	20
5	25

t : is the thickness of the stiffeners ( mm )

t1: is the thickness of the bed ( mm ).

Table ( II )

Case No.	t1
1	28
2	38
3	48
4	58
5	68



(b)

(c)

CONTOUR VALUE

A	42.25
B	84.51
C	126.8
D	169.0
E	211.3
F	253.5
G	295.8
H	338.0
I	380.3
J	422.5
K	464.8
L	507.0
M	549.3
N	591.5
O	633.8

Contour value = Eq Stress (N/mm<sup>2</sup>)

Fig ( 73 )

**Load Vs. Deflection**  
**"3-D Thin Shell FEA Model of the Press Structure"**  
**"After Adding The Stiffeners To The Press Bed"**

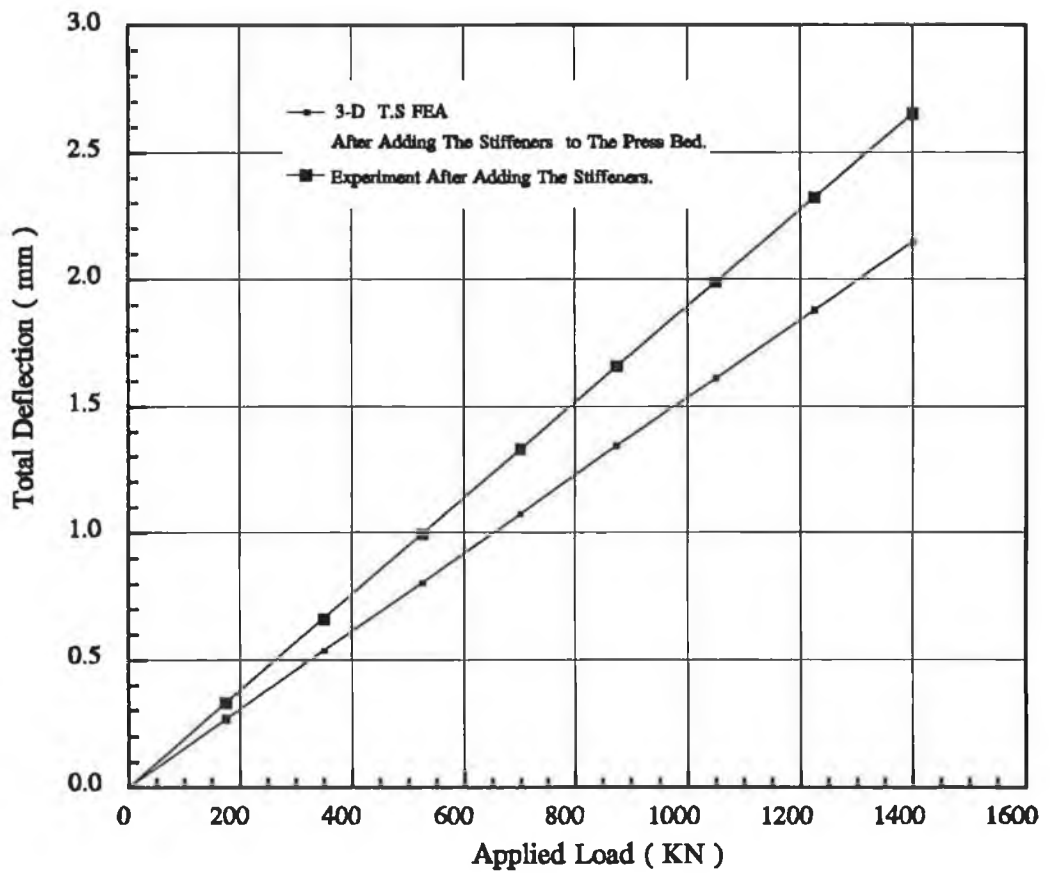


Fig ( 74 )

permissible deflection by about 24%. This indicates that the use of the stiffeners in case No. 3, given in Table (6), helps to increase the stiffness of the press bed in Z direction more than in the other directions. The equivalent stress contour values at the bottom layer of the centre line (contour C) in Fig. (73.c), converges to within 24% lower than that indicated in the PS model of the press bed. This suggests that the behaviour of the press bed can be described using the PS model. Fig. (74) shows that the computed maximum total accumulative deflection in Y direction of the press structure after adding the stiffeners converge to within 19% lower than the experimental results after stiffening the press bed. This value is higher than that indicated in the 3D T.S model by about 4%. This is probably due to the quality of welding of the stiffeners to the press bed. The 3D FEA model of the press bed assumes that the stiffeners are rigidly fixed with the press bed, whereas in fact there could be some flexibility at the joint regions. Comparing the 3D T.S. and P.S. FEA models after adding the stiffeners to the 3D T.S. model of the press bed, the total maximum deflection of the 3D T.S model turns out to be 2.147 mm. For comparison the 3D T.S analysis results (before and after adding the stiffeners) and the P.S analysis results are given in Table (7).

**TABLE (7)**

<b>Model name</b>	<b>Adding stiffeners ?</b>	<b>Max. Applied Load P (KN)</b>	<b>Max. total deflection in Y direction (mm)</b>
P.S	No	1400	2.194
3-D T.S	No	1400	2.345
3-D T.S	Yes	1400	2.147

It can be deduced from the results given in Table (7) that adding the stiffeners reduces the total maximum deformation of the whole press structure to within a value of 9% of

the value before adding the stiffeners. It can also be seen from Table (7) that the computed results of the total maximum deflection of the 3D T.S model, after adding the stiffeners converges to within 2% lower than the maximum total deflection obtained by the P.S model. This indicates that the press structure is more flexible in the P.S model than the 3D T.S model. The computed total maximum deflection in Y direction, after adding the stiffeners, is higher than that indicated by the permissible deformation of about 47%. Therefore, further modification on the press structure is needed.

**Effect of the thickness of the press bed after adding the stiffeners.**

The press bed has been theoretically analyzed with different wall thickness values. The objective was to determine the effect of the thickness on the deflection of the press bed. The computed FEA results, which are given in Table (8) with different cases of wall thickness, were obtained from the FEA model shown in Fig. (73.a). The thickness values of the cases in Table (8) are given in Table (II) in Fig. (73).

**TABLE (8)**

<b>Case No.</b>	<b>Max. Applied Load P (KN)</b>	<b>Max. deformation in Y direction (mm)</b>	<b>Total estimated weight</b>	<b>Relative total weight %</b>
original thickness	1400	1.1	3.627	100
1	1400	0.8005	4.796	132
2	1400	0.6354	5.965	164
3	1400	0.5289	7.134	197
4	1400	0.4539	8.303	229
5	1400	0.398	9.472	261

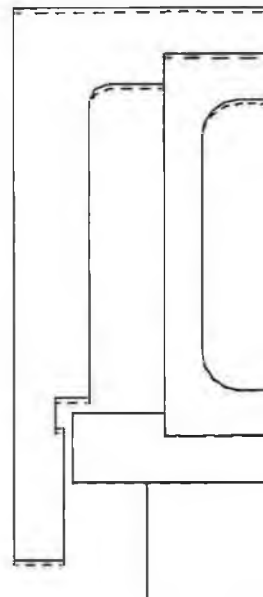
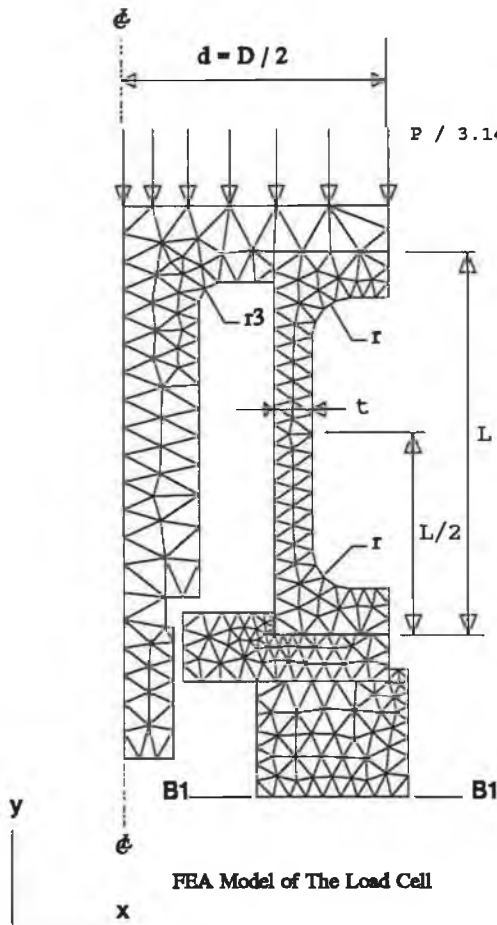
It can be seen from Table (8) that the deflection of the press bed approaches the deflection of the design goal when the wall thickness of the press bed increases. With regard to the design goal the maximum deflection of case No. 5 in Table (8) converges to within 42% higher than the permissible deflection. This indicates an increase in the material of the press structure by about 261% of the original press bed when the stiffeners were added. Therefore, increasing the wall thickness of the press structure would not be a practical solution to increase the stiffness of this structure.

### **Adding the platens and loading tools**

The objective of modelling the plates and loading tools was described earlier in Chapter 3. Fig. (75), Fig. (76) and Fig. (77) show the FEA results of the optimum design of the load cell, the cap of the ram and the lower loading plate model respectively. The total deformation of these components in Y direction has been accumulated with the total deformation of the press structure after adding the stiffeners, experimentally and mathematically, at several applied loads. The results of this are shown in Fig. (78). This suggests that the FEA computed results converge to within 20% lower than the experimental results. The computed maximum total deformation shown in Fig. (78) is higher than that indicated by the design goal by about 47%.

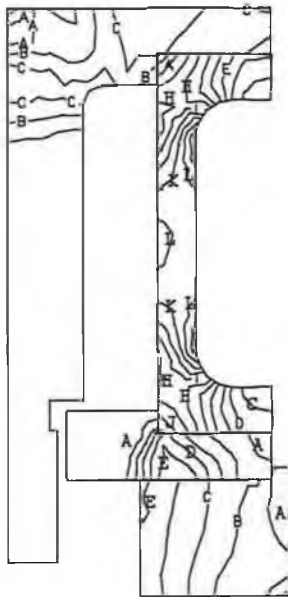
### **Summary of the comparison**

The press bed was analyzed with different factors to improve functional performance of the whole press structure under the operational load with regard to the design goal. The results obtained can be summarized as follows:



D : The outer diameter of the load cell

Contour value = Eq Stress ( $N/mm^2$ )



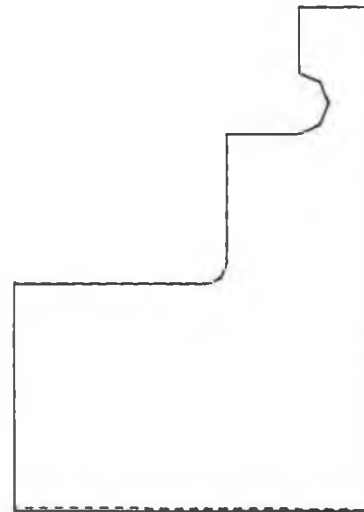
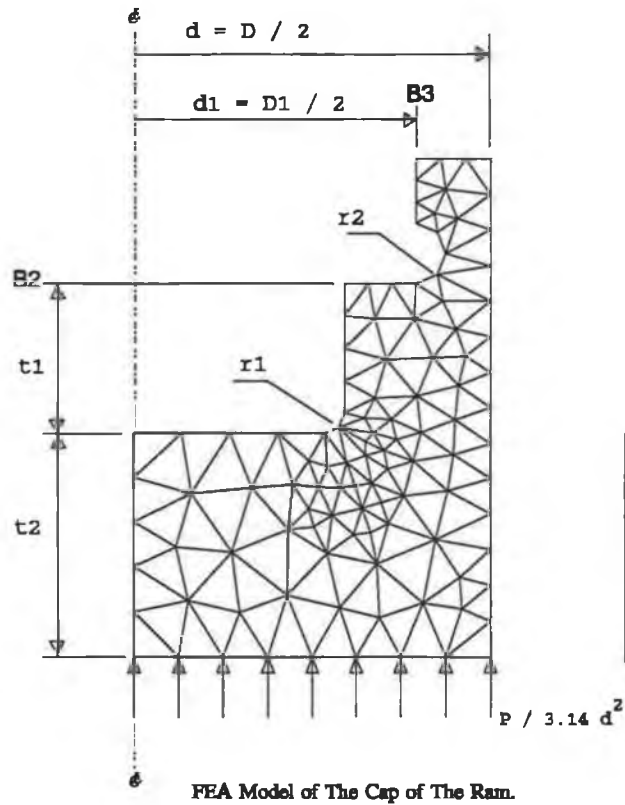
CONTOUR VALUE

A	38.82
B	77.64
C	116.5
D	155.3
E	194.1
F	232.9
G	271.7
H	310.6
I	349.4
J	388.2
K	427.0
L	465.8
M	504.7
N	543.5
O	582.3

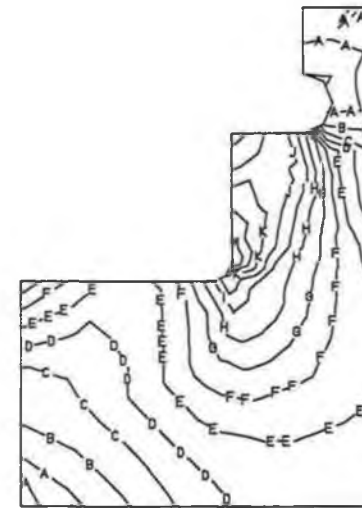
Eq. Stress Contoure At Max. App. Load

Fig ( 75 )

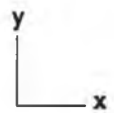




Contour value = Eq Stress (N/mm<sup>2</sup>)

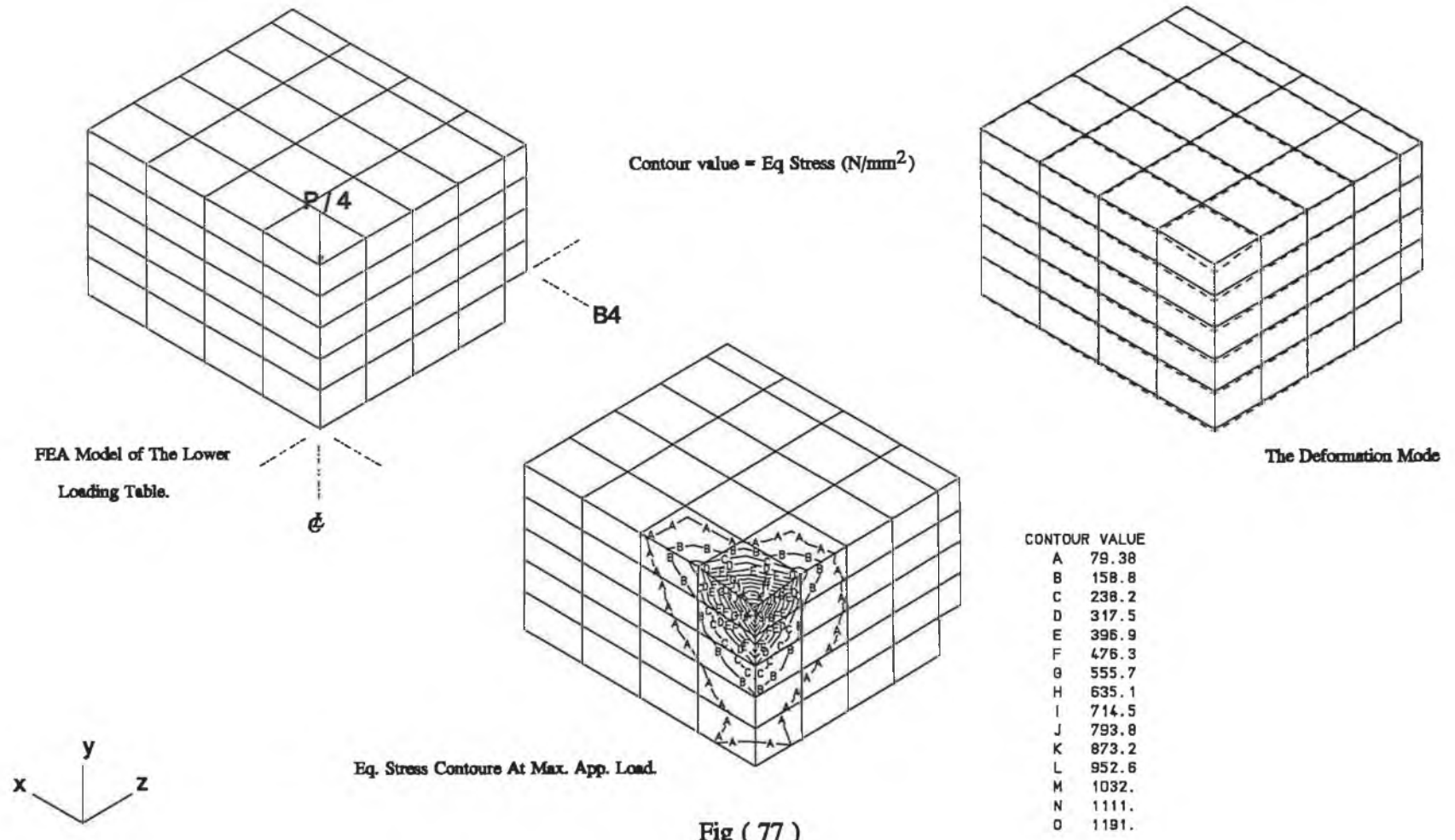


CONTOUR VALUE	
A	17.59
B	35.19
C	52.78
D	70.37
E	87.97
F	105.6
G	123.2
H	140.7
I	158.3
J	175.9
K	193.5
L	211.1
M	228.7
N	246.3
O	263.9



D : The outer diameter of the cap  
 D1 : The inner diameter of the cap " The outer diameter of the ram."

Fig ( 76 )



**Load Vs. Deflection**  
**"FEA Model of The Press Struture"**  
**"After The Total Modification"**

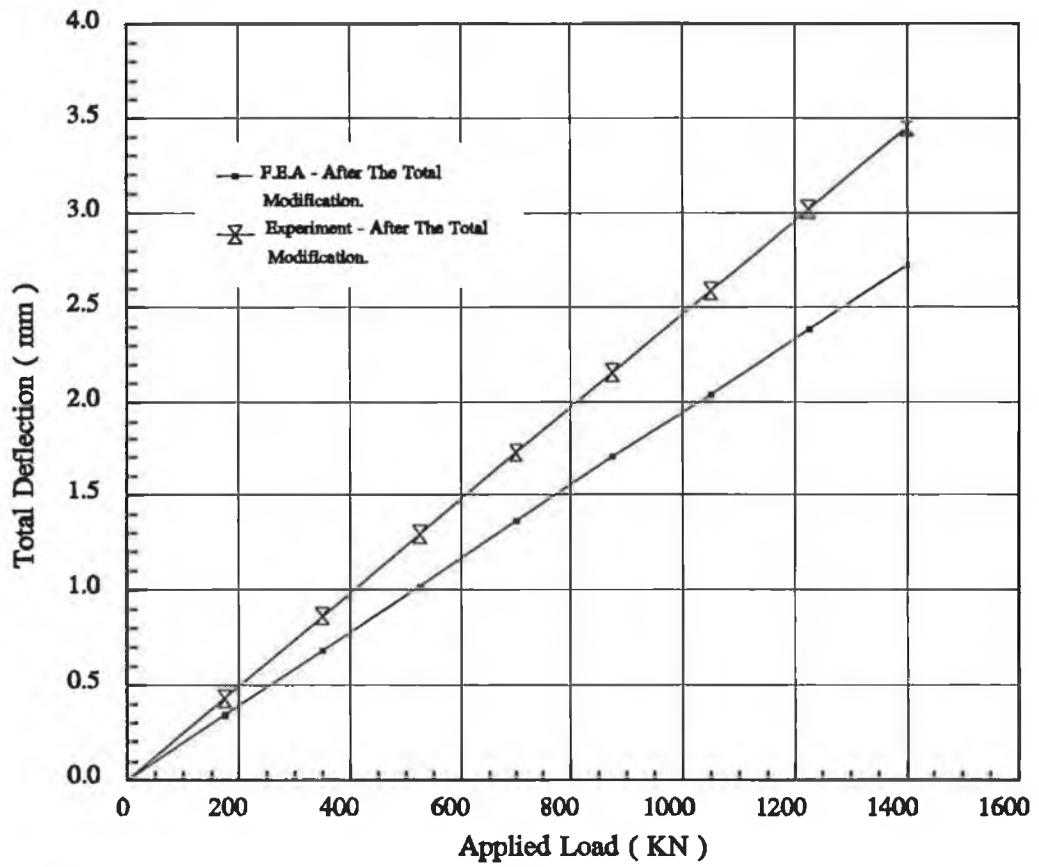


Fig ( 78 )

- (i) Adding the stiffeners to the press bed improved the stiffness of the press structure in Z direction more than the other directions.
- (ii) The convergence value between the experimental and theoretical deflection after adding the stiffeners was higher than indicated in the same model before adding the stiffeners by about 4%.
- (iii) Adding the stiffeners reduced the total maximum deformation of the whole press structure to within a value of 9% of the value before adding the stiffeners.
- (iv) The press structure is more flexible in the P.S model than the 3-D T.S model.
- (v) Increasing the wall thickness of the press bed indicated a sharp increase of the material of the press structure in order to increase its stiffness with regard to the design goal.
- (vi) After adding the stiffeners the computed stiffness of the press structure was higher than that indicated by the design goal by about 47%.
- (vii) The computed total maximum deformation of the whole press structure after including the analysis of the platen and loading tools, converged to within 20% lower than the experimental results. Generally speaking, it can be said that the discrepancy of the FEA models and the experimental model is perhaps due to:
  - (a) The approximations in describing the operation load and the boundary condition imposed on the theoretical model;

- (b) The negligence of the deformation of the hydraulic ram and the local deformation in the region of welding;
- (c) Avoiding the effects of the eccentricity on the total deformation of the press structure.

#### **5.1.4 New design of the press structure**

It was shown earlier that adding the stiffeners or increasing the wall thickness of the press bed, alone was not sufficient as the practical solution for stiffening the press structure with regard to the design goal. However, adding the stiffeners helped to optimize the out-of-plane deflection of the press structure. Therefore, the press structure was modelled theoretically as described in Chapter 3. The theoretical analysis was performed with the stiffeners described in Chapter 3 to optimize the design of the press structure at minimum analysis time. The factors considered are the width and the chamfering of the press structure. Fig. (79.a) shows the P.S FEA model of a completely new design of the press bed. Fig. (79.b) and Fig. (79.C) respectively, show the deformation mode and the equivalent stress contour values of the optimum design of this model at the maximum applied load. Fig. (80.a) shows the P.S FEA model of the L-Shaped beam of the new design of the press structure. Fig. (80.b) and Fig. (80.c) respectively, show the deformation mode and the equivalent stress contour value of the optimum design of the model in Fig. (80.a) at the maximum applied load. The total maximum deflection of the whole press structure has been obtained by accumulating the total computed deflection of the node 36 in Fig. (79.a) and the node 284 in Fig. (80.a).

### Effect of the width of the press structure

The press structure was analyzed with the different ratios of the width to the constant height of the press structure as shown in Table (2) in Fig. (80). The computed results are given in Table (9).

**TABLE (9)**

<b>Case No.</b>	<b>Max. applied load P (KN)</b>	<b>Max. deflection in Y direction (mm)</b>	<b>Total estimated weight (KN)</b>	<b>Relative total weight %</b>
1	1400	2.0685	12.7	100
2	1400	1.8679	12.395	102.4
3	1400	1.6829	12.09	104.8
4	1400	1.513	11.785	107.2
5	1400	1.3576	11.48	119.6
6	1400	1.216	11.175	112
7	1400	1.0952	10.87	114.4

The decreasing of the width of the press structure was considered without affecting the functional requirement of the press.

Case No. 1 in Table (9) denotes the original dimension of the press structure before reducing the width. Table (9) shows that the maximum deflection of the press structure approaches the permissible deflection by reducing its width. In other words, the stiffness of the press structure increases with the decrease of the width of this structure. With respect to the design goal, case No. 7 in Table (9) converges to a value some 4% lower than the permissible deflection. The use of case No. 7 in Table (9) enables the material of the press structure to be reduced by 14.5% and gives space to allocate the

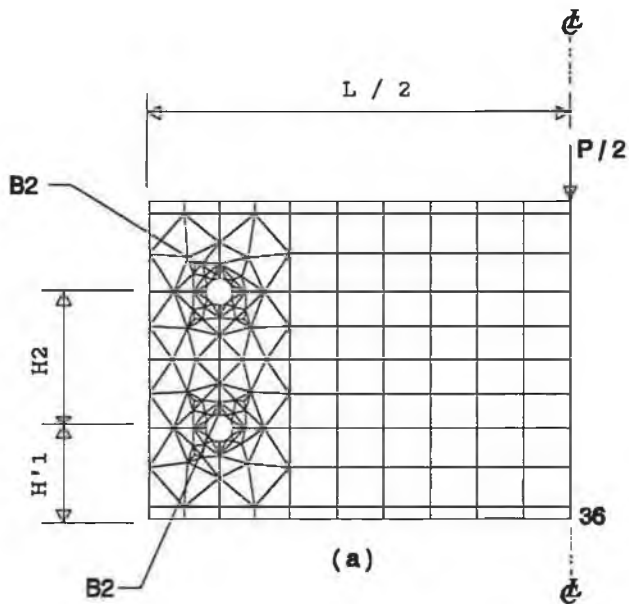


Table ( II )

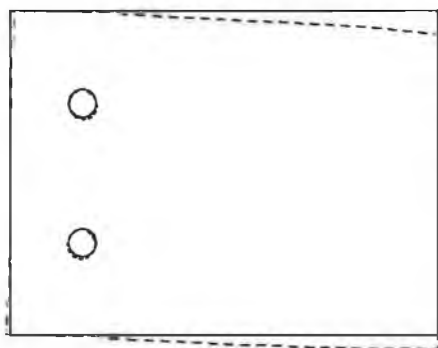
Case No.	L / H
1	0.7107
2	0.675
3	0.640
4	0.605
5	0.570
6	0.535
7	0.5

$H'1 = 130$  ( mm )

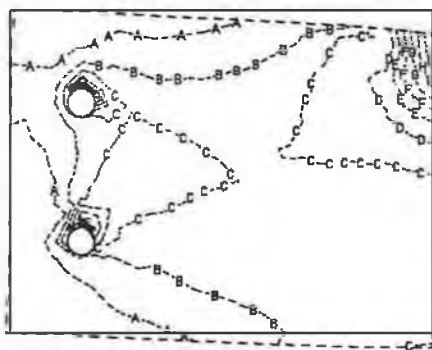
$H2 = 198$  ( mm )

Contour value = Eq Stress ( $N/mm^2$ )

Fig ( 79 )



(b)



(c)

CONTOUR VALUE

A	32.70
B	65.40
C	98.10
D	130.8
E	163.5
F	196.2
G	228.9
H	261.6
I	294.3
J	327.0
K	359.7
L	392.4
M	425.1
N	457.8
O	490.5

$L / H = 0.5$



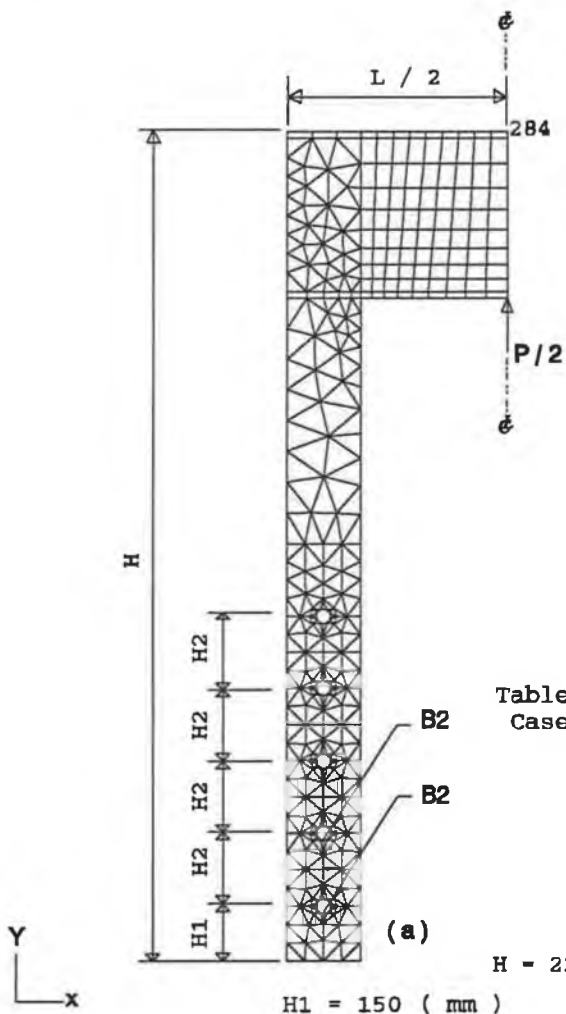
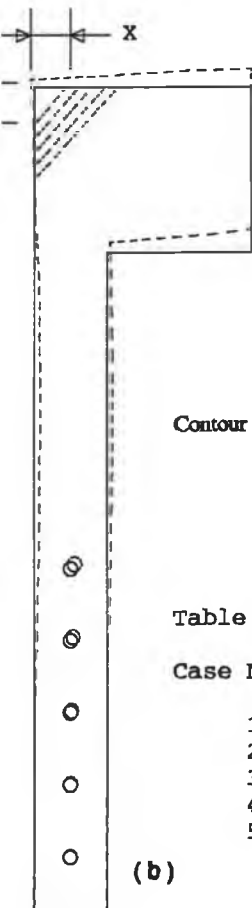


Table ( II )

Case No.	L/H
1	0.7107
2	0.675
3	0.640
4	0.605
5	0.570
6	0.535
7	0.5

$H = 2285$  ( mm )

$H1 = 150$  ( mm )



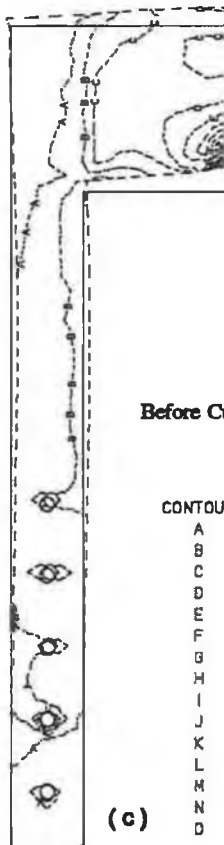
Contour value = Eq Stress ( $N/m^2$ )

Table ( III )

Case No.	X (mm)	Y (mm)
1	50	50
2	100	100
3	150	150
4	250	250
5	300	300

(b)

H2 = 198 ( mm )



Before Cutting The Edge

CONTOUR VALUE

A	26.12
B	52.24
C	78.36
D	104.5
E	130.6
F	156.7
G	182.8
H	209.0
I	235.1
J	261.2
K	287.3
L	313.4
M	339.6
N	365.7
D	391.8

(c)

L/H = 0.5

Fig ( 80 )

different accessories on the press.

### **Effect of the chamfering of the press structure**

It is well known from the theory of elasticity that the free edges of the structures under the plane stress conditions contribute little to the strength of the structure. Also these edges themselves are stress-free. It has been confirmed from the equivalent stress contour values of the press structure shown earlier that the free edge of the L-Shaped beam model is stress-free. Therefore, the free-edge in this model can be cut as shown in Fig. (80.b) with the details given in Table (III) in this Figure. The analytical results obtained from case No. 7 in Table (9) are given in Table (10).

The chamfering was arrived at without affecting the location of different accessories of the press. It can be seen from Table (10) that the change in the max. deflection in Y direction is insignificant. Therefore it is convenient to compare the direct stiffness values with respect to the weight of the press structure. The specific stiffness (direct stiffness/weight) values for the different cases in Table (10) vary from 117.5 to 129. In order to reduce the weight of the press structure and thus the cost, the edge on both sides of the press structure can be cut as detailed in Table (III) in Fig. (80.b) for case No. 3. In this case the reduction in weight is 2%.

**TABLE (10)**

<b>Case No.</b>	<b>Max. applied load P (KN)</b>	<b>Max. deflection in Y direction (mm)</b>	<b>Specific stiffness (mm<sup>-1</sup>)</b>	<b>Relative specific stiffness %</b>
No cutting	1400	1.0952	117.5	100
1	1400	1.0961	118	100.4
2	1400	1.096	119	101.2
3	1400	1.095	120	102
4	1400	1.0956	125.6	106.4
5	1400	1.095	129	109

**Summary of the comparison**

The new design analysis of the press structure was carried out theoretically using P.S FEA model. The following was concluded:

- (i) The use of the P.S FEA model in the analysis of the new design of the press structure reduced the analysis time to within 77% of that indicated in 3-D thin shell FEA model.
- (ii) Hinging the press bed by two pins from each side of the press structure reduced the deflection of the press structure by 6% of the original deflection. In other words, the stiffness was increased by 6% of that indicated in the original design of the press.
- (iii) Decreasing the width of the press structure without affecting the

functional requirement increased the stiffness of the structure.

- (iv) The free edges can be cut, keeping the functional requirement in view without impairing the strength and the stiffness of the press structure.
- (v) It can be seen from Fig. (79.c) and Fig. (80.c) that the strength of the press structure was improved compared with the original design of the press.

## 5.2 Computing costs

The computing cost was estimated from the computing time spent for the analysis. The computing time for the static analysis, excluding the cost for data preparation, can be divided into two categories:

- (i) The time for evaluating and storing the stiffness matrices of different elements.
- (ii) The time involved in assembling the individual element stiffness matrices in the final overall stiffness matrix and solving for the nodal deflection.

The total computing time depends upon a number of factors, the most important of which are:

- (a) The way of numbering the structural nodes in order to produce a minimum nodal band width.
- (b) The number of equations to be solved. This is equal to the product of the number of structural nodes and the number of degrees of freedom associated

with each node.

- (c) The number of different loading cases of interest.

As an indication of the cost of the type of analysis described for the current work earlier, considering the FEM results of the press structure, it has been found that the 3-D thin shell element (3-D T.S) analysis was the most expensive analysis of the press structure. However, the plane stress (P.S) and the plane frame (P.F) analyses were cheaper than the (3-D T.S) analysis by 77% and 99% respectively. This indicates that increasing the number of degrees of freedom of the structural nodes results in the increase of the computing time and thus the cost of the analysis. This view is commonly shared by the finite element analysts.

## CHAPTER 6

### CONCLUSION AND SUGGESTION

#### 6.1 Conclusion

In this work, the experimental and theoretical study has been carried out on the existing welded structure of a hydraulic press machine of a 150-tonne nominal operational load. The conventional analytical model together with several models for FEM analysis of the press structure were considered. The accuracy and the applicability of the existing PC based FE package, as a computer aided design tool, has been evaluated. It was proved that the finite element method is technically superior to the alternative technique of physical model analysis. The theoretically predicted results, those obtained experimentally together, have been compared with the design goal of the press structure. From the foregoing the following can be concluded:

1. The present experimental modification on the present hydraulic press enables it to be used in the process of metal working application.
2. The data acquisition system, which was developed in the current work, can be used for an automatic collection of the experimental data involved in digital-to-analogue signal processing in the laboratory.
3. Although the conventional analytical model agreed with the plane frame FEA model, this agreement deteriorates between these models and the experimental model by a about 43%.

4. The best accuracy obtained from the FEM analysis before the modification of the press bed was 15%. This was given by the 3-D thin shell FEM analysis of the press structure. However, this analysis was found to be the most expensive to perform for the press structure.
5. It was shown that the press structure was more flexible in the plane stress FEA model than the 3-D thin shell FEA model by about 2%.
6. A plane stress FEA model was used successfully to optimize the design of the press structure. This suggested that a new design of the press structure which converged to within 4% lower than that indicated by the design goal of the press structure. The analysis of this model was thorough at a minimum cost of material and analysis time.

To sum up, it can be said that the procedure described in this current work shows a significant trend towards using a PC based FE package at very low computing cost. The results obtained are quite important to the press and structural designers.

## **6.2 Suggestion for Further Work.**

In view of the current investigation the following should be considered for further investigation:

1. Investigate the stress distribution acting within the material of the press structure using the finite element and the strain gauge technique.



2. Modelling the welding joints of the press structure to study the effects of the welding on the strength and the accuracy of the analysis.
3. Investigate the effects of the clearance between the mating parts of the press structure on the accuracy of the analysis.
4. Investigate the effects of the eccentricity of the operational load on the accuracy of the analysis.
5. Investigate the possibility of controlling fully the present experimental model using a P.C. through an appropriate D/A and A/D signal converter.
6. Although the LUSAS FEA system has been used extensively to predict the behaviour of the present press structure, it would be worthwhile to reconsider the nonlinear boundary conditions algorithm used by this system in order to:
  - (i) reduce the efforts of data preparation and make this process more user friendly;
  - (ii) interfere with the users' algorithms specifying the boundary conditions of a region of interest of a model being analyzed.
7. I would suggest that more sophisticated piece of software should be used.

## REFERENCES

1. L.J. Sergerline, "Applied Finite Element Analysis", John Wiley and Sons, New York (1984).
2. R.V. Southwell, "Stress-Calculation in Framework by Method of 'Systematic Relaxation of Constraints' - I-II", Proc. Roy. Soc. 151, pp 59-95, (1935).
3. T.W. Chester, "A Beginners Guide to Finite Element Analysis", Proc. 6th Annual Conf. Design Eng. Birmingham, UK, pp 207-218, (1983).
4. M.J. Turner, R.W. Clough, H.C. Martin and L.J. Topp, "Stiffness and Deflection Analysis of Complex Structure", Journal of Aerospace Science, 25, pp 805-823, (1956).
5. J.H. Argyris, "Elasto-plastic Matrix Analysis of Three-Dimensional Continue", J. Royal Aero. Soc., 69, pp 633-636, (1965).
6. R.H. Gallagher, J. Padlog and P.P. Biulaard, "Stress Analysis of Heated Complex Shapes" J.Am.Rocket Soc.,32,pp 700-705,(1962).
7. O.C. Zienkiewicz, "Stress Analysis", Ed. O.C. Zienkiewicz and G.S. Holister, Pergamon Press, (1965), Chapter 8.
8. J.H. Argyris, S. Kelsy and H. Kamel, "Matrix Methods of Structural Analysis. A precis of Recent Developments", Pergamon Press (1963).
9. A. Mendelson and S.S. Manson, "Practical Solution of Plastic Deformation Problems in the Elastic-Plastic Range", NASA, T.R., R28, (1959).
10. O.C. Zienkiewicz, S. Valliappan and I.P. King, "Elasto-Plastic Solutions of Engineering Problems 'Initial Stress', Finite Element Approach" Int. J. Num. Meth. Engng., 1, pp 75-100, (1969).
11. Finite Element Systems - A Handbook - Ed. C.A. Brebbia, A Computational Mechanics Publications, (1985).
12. A.C. Stephen and S. Taylor, "Computer Analysis of Machine Tool Structures by The Finite Element Method", Proc. Conf. M.T.D.T., Birmingham, UK., pp 751-761, (1968).

13. C. Dimitriou, "On the Elastoplastic notched Plate in Plane Stress",  
S. Afr. Mech. Eng., 20, pp 146-156, (1970).
14. A. Cowley and S. Hinduja, "The Finite Element Method for Machine Tool  
Structural Analysis",  
Annals of the C.I.R.P., 19, pp 171-181, (1971).
15. O.C. Zienkiewicz and D.V. Phillips, "An Automatic Mesh Generation Scheme  
for Plane and Curved Surfaces by 'Isoparametric' Co-ordinates",  
Int. J. Num. Meth. Engng., 3, pp 519-528, (1971).
16. S. Hinduja and A. Cowley, "The Finite Element Method Applied to Deformation  
Analysis of Thin-Walled Columns",  
Proc. Conf. M.T.D.R., Manchester, U.K., pp 455-477, (1971).
17. H. Opitz and R. Noppen, "A finite Element Program System and its application  
for Machine Tool Structural Analysis",  
Proc. Conf. M.T.D.R., Birmingham, U.K., pp 55-60, (1972).
18. W.R. Buell and B.A. Bush, "Mesh Generation - A Survey",  
Journal of Engineering for Industry, Transactions of the American Society of  
Mechanical Eng., Series B, 95, pp 332-338, (1973).
19. S.W. Key, "A Finite Element Procedure for the large Deformation Dynamic  
Response of Axisymmetric Solids",  
ASME Publication, 71 - WA/PVP-7, (1974).
20. Johnny H. Biffle and Eric B. Becker, "Finite Element Stress Formulation for  
Dynamic Elastic-plastic Analysis",  
Comput. Meth. Appl. Mech. Eng., 6, pp 101-119, (1975).
21. M. Weck and L. Zangs, "Computing the Thermal Behaviour of Machine Tools  
Using the Finite Element Method",  
Proc. Conf. M.T.D.T., Manchester, U.K., pp 185-194, (1975).
22. U.P. Singh, P.C. Vernstra, J.A.H. Ramerkers and J.A.W. Hijink, "Numerical  
Analysis of Four Column Under-Drive Press, Equipped with 4-Guided Pillar Sub  
Press",  
Sheet Metal Industrial, 53, pp 242-247, (1976).
23. H. Blum, "The Elastic Behaviour of Mechanical Press Machines",  
Pro. Conf. M.T.d.R., Manchester, U.K., pp 155-162, (1978).
24. J. Radharkrishna Murthy, K. Jagadeesha and G. Chaima Reedy, "Thermal  
Deformation of a Surface Grinding Machine",  
Proc. Conf. A.I.M.T.D.R., Bombay, India, pp 134-138, (1978).
25. C.P. Reddy and S.S. Rao, "Design Parameter Variation and Machine Tool  
Structural Response",  
Pro. Conf. A.I.M.T.D.R., Bombay, India, pp 94-97, (1978).

26. T.J. Prabhu, N. Ganesan and G.V.N. Rayudu,, "Dynamic Analysis of Vertical Broaching Machine",  
Proc. Conf. A.I.M.T.D.R., Bombay, India, pp 77-81, (1978).
27. S. Haranath, N. Ganesan and B.V.A. Rao, "Dynamic and Static Analysis of Multicell Machine Tool Columns",  
Proc. Conf. A.I.M.T.D.R., Bombay, India, pp 62-64, (1978).
28. R.C. Bahl and P.C. Pandey, "Computer Aided Analysis and Design of Ribbed Beams",  
Proc. Conf. A.I.M.T.D.R., Bombay, India, pp 58-61, (1978).
29. Y.K. Gupta and S. Somasundaram, "Analysis of Stiffening Machine Tool Column by Finite Element Method",  
Proc. Conf. A.I.M.T.D.R., Bombay, India, pp 54-57, (1978).
30. J.N. Dube and N.K. Das Talukdar, "Dynamic Characteristics of Milling Machine Structure by Different Types of Ribbing of Cross-Arm",  
Proc. Conf. A.I.M.T.D.R., Bombay, India, pp 82-85, (1978).
31. Y.K. Gupta and S. Somasundaram, "Fastening of Machine Tool Column",  
Proc. Conf. A.I.M.T.D.R., Bombay, India, pp 37-41, (1978).
32. M. Okamoto and M. Nakazawa, "Finite Element Incremental Contact Analysis with Various Frictional Conditions",  
Int. J. Num. Meth. Engng., 14, pp 337-357, (1979).
33. J. Radhakrishna Murthy, G.C. Reddy and S.C. Singhvi, "Optimization of Functional Properties of Machine Tool Structures - A Finite Element Analysis",  
Proc. Conf. M.T.D.R., Birmingham, U.K., pp 435-442, (1979).
34. S.G. Madhava Rao, U.V. Ramana Murthy and G. Chalama Reddy, "Computer Aided Analysis of Two Designs of a Column for Horizontal Machine Centre",  
Proc. Conf. A.I.M.T.D.R., Durgapur, India, pp 496-505, (1982).
35. L.S. Gupta and P.V. Ramanamurti, "Stress Analysis of 400 Tonne Hydraulic Press Cross-Head",  
Proc. Conf. A.I.M.T.D.R., Durgapur, India, pp 579-585, (1982).
36. L. Vijayaraghavan, R. Krishnamurthy and J. Chandrasekaran, "Some Investigations on Broaching",  
Proc. Conf. A.I.M.T.D.R., Durgapur, India, pp 605-611, (1982).
37. S.P. Tayal, "Static and Dynamic Analysis of Tilted Two-Lobe Bearings Using FEA and their Application to Stability",  
Proc. Conf. A.I.M.T.d.R., Durgapur, India, pp 17-26, (1982).

38. J.W. Wissmann and C. Hauch, "Efficient Elastic-Plastic Finite Element Analysis with Higher Order Stress-Point Algorithms", *Computers & Structures*, 17, pp 89-95, (1983).
39. J. Radhakrishna Murthy and G. Chalama Reddy, "Floating Hinge in Machine Tool Structures - Finite Element Representation", *Computer Aided Design*, 15, pp 201-208, (1983).
40. G.Z. Voyiadjis, M. Asce and S. Navaee, "Finite Strain Contact problem of Cylinder Embedded in Body", *J. Eng. Mech.*, 110, pp 1597-1609, (1984).
41. Shu-Yu Wang, U. Sun and R.H. Gallagher, "Sensitivity Analysis in Shape Optimization of Continuum Structures", *Computers & Structures*, 20, pp 855-867, (1985).
42. J.R. Stafford, F. Tabaddor and J.A. Padovan, "Benchmarking Some Desk-Top Computers for Finite Element Analysis", *Proc. of The Pressure Vessels and Piping Conf., LA, USA*, pp 125-139, (1985).
43. M.S. Shephard and M.A. Yerry, "Automatic Finite Element Modelling for Use with Three-Dimensional Shape Optimization", *Proc. of Optimum Shape : Automated Structural Design Conf., MI, USA*, pp 113-137, (1985).
44. J.M. Kennedy, T. Belytschko and J.I. Lin, "Recent Developments in Explicit Finite Element Techniques and their Application to Reactor Structures", *Nucl. Eng. Des.*, 97, pp 1-24, (1986).
45. E.T. Moyer and H. Liebowitz, "Finite Element Methodology for Elastic-Plastic Fracture Problems in Three Dimensions", *Int. J. Num. Meth. Engng.*, 22, pp 289-306, (1986).
46. T. Chattopadhyay, "Computer Program for Solution of Extrusion Problems", *J. Inst. Eng., India*, 67, pp 23-31, (1986).
47. J.D. Dybbro and N.C. Holm, "On Minimization of Stress Concentration for Three-Dimensional Models", *Computers & Structures*, 24, pp 637-643, (1986).
48. S.P. Sinha and Murarka, "Computer-Aided Design of Hydraulic Press Structures", *Mathl. Comput. Modelling*, 10, pp 637-645, (1988).
49. S.V. Kumar, B. Pradhan and A.B. Chattopadhyay, "Stress Analysis and Geometrical Modification of Carbide Inserts for Improved Edge-Strength", *Proc. A.I.M.T.D.R. Conf. Jadavpur, India*, pp 29-33, (1988).

50. S.S. Patil, "A Study on the Development of Nomograms for Designing Machine Taps",  
Proc. A.I.M.T.D.R., Jadavpur, India, pp 1-6, (1988).
51. P.F. Chavez, M. Henderson and A. Tazdian, "Automatic 3-D Finite Element Modelling using Solid Model Data and AI Techniques",  
Pro. Computers In Eng. Conf., San Fran, USA, pp 631-636.
52. Dipendra K. Sinha, "A Model Curriculum for CAD",  
Proc. Frontiers In Edu. Conf., Snta Barbara, USA, pp 431-433, (1988).
53. J. Tang, J.T. Fong and D.E. Dietrich, "A Build-In Error Estimator for Optimizing Finite Element Modelling",  
Pro. Quality Use of the Computer : Computational Mechanics, Artificial, Intelligence, Robotics and Acoustic, Honolulu, Hi, USA, pp 73-88, (1989).
54. V. Kumar, S.J. Lee and M.D. German, "Finite Element Design Sensitivity Analysis and its Integration with Numerical Optimization Techniques for Structural Design",  
Computers & Structures, 32, pp 883-897, (1989).
55. D.E. Grierson and G.E. Cameron, "A Knowledge-Based Expert System for Computer Automated Structural Design",  
Proc. Application of Artificial Intelligence Techniques to Civil and Structural Eng. Conf, Waterloo, Canada, pp 93-77, (1989).
56. Gary J.E. Kramer and D.E. Grierson, "Computer Automated Design of Structures Under Dynamic Loads",  
Computers & Structures, 32, pp 313-325, (1989).
57. P.G. Galbraith and J.T. Bryant, "Effects of Grid Dimensions on Finite Element Models of an Articular Surface",  
J. Biomechanics, 22, pp 385-393, (1989).
58. P.M. Finnigan, A. Kela, and J.e. Davis, "Geometry as Basis for Finite Element Automation",  
Engineering with Computers, 5, pp 147-160, (1989).
59. Bruce W.R. Forde and Siegfried F. Stiemer, "Knowledge-Based Control for Finite Element Analysis",  
Engineering with Computers, 5, pp 195-204, (1989).
60. Timothy J. Baker, "Automatic Mesh Generation for Complex Three-Dimensional Regions Using Constrained Delauney Triangulation",  
Engineering with Computers, 5, pp 161-175, (1989).
61. M. Khosrowjerdi, "Utilization of a Commercial Finite Element Package for Correlation of Analytical and Experimental Analysis",  
Proc. ASME Int. Computers In Eng. Conf, CA, USA, pp 319-326, (1989).

62. U.P. Singh and P.P. Miller, "Finite Element Analysis of a Twin Head Horizontal Hydraulic Press",  
Proc. IMC-6, II, Dublin, IRL, pp 981-996, (1989).
63. M.R. Barone and R.J. Yang, "A Boundary Element Approach for Recovery of Shape Sensitivities in Three-Dimensional Elastic Solids",  
Comput. Method. Appl. Mech. Eng, 74, pp 69-82, (1989).
64. N. Kim and S. Kabayashi, "Three-Dimensional Simulation of Gap-controlled Plate Rolling by the Finite Element Method",  
Int. J. Mach. Tools Manufact, 30, pp 269-281, (1990).
65. Mohamad M. Saleh and M.S.J. Hashmi, "Finite Element Analysis of Thin Ring Structure Towards the CAD of Energy Absorbing Devices",  
Proc. Int. Conf. on CAD of Machinery, Beijing, China, pp 279-284, (1990).
66. P. Destuynder, "Computation of an Active Control in Fracture mechanics Using Finite Element",  
Eur. J. Mech. A/Solids, 9, pp 133-141, (1990).
67. Z. Young and Ian R. Grosse, "A Rule-Based Computational System for Automatic Finite Element Modelling",  
Proc. ASME. INTL, Boston, USA, pp 87-94, (1990).
68. R.J. Yang, "Design Modelling Considerations in Shape Optimization of Solids",  
Computers & Structures, 34, pp 727-734, (1990).
69. Paul Dvorak, "So Simple Even An Engineer Can Use It",  
Mach. Des, 63, pp 73-77, (1991).
70. M.E.M. El-Sayed and C.K. Hsuing, "Optimum Structural Design With Parallel Finite Element Analysis",  
Computers & Structures, 40, pp 1469-1474, (1991).
71. J. Mackerle and B. Fredriksson, "Handbook of Finite Element Software",  
Chartwell-Bratt Ltd. England, (1988).
72. O.C. Zienkiewicz, "The Finite Element Method",  
McGraw-Hill, London, (1977).
73. J.S. Przemieniecki, "The Theory of Matrix Structure Analysis",  
McGraw-Hill, New York, (1968).
74. Y.K. Cheung and M.F. Yeo, "A Practical Introduction to Finite Element Analysis",  
Pitman, London, (1979).
75. Finite Element Analysis ltd. (1990). The LUSAS Users Manual, London.
76. Finite Element Analysis Ltd. (1990). The MYSTRO Users Manual, London.

77. I. Onur, "Prediction of Chatter Behaviour of the Radial Drilling Machine", Ph.D. Thesis, University of Birmingham, (1964).
78. G. Oehler, "Hydraulic Presses", Translated by F. Minden, Edward Arnold Ltd. (1962).
79. Donald F. Eary, "Press Alignment", *The Tool and Manufacturing Eng*, 42, pp 109-112, (1962).
80. K. Adam, "A New Approach to Punch Press Design", *Sheet Met. Ind Rev*, 28, pp 924-928, (1978).
81. Ing. K. Adam, SMG, "Some Design Features of Hydraulic Presses Incorporating Transfer Equipment", *Sheet Met. Ind*, 56, pp 240-274, (1979).
82. U.P. Singh, P.C. Veenstra and J.A.H. Ramaekers, "Analysis of the Stress in the Corner Zone of a C-Frame Press", *Ann. CIRP*, 28, pp 171-175, (1979).
83. P.J. Wesolowski, "Investigation of the Model of Hydraulic Press by Means of Holographi", *Proc. SPIE Int. Soc. Opt. Eng*, 473, pp 73-76, (1984).
84. M.I. Budman and F.I. Kaganovskii, "Calculation of Hydraulic Press Columns", *Soviet Forging and Sheet Metal Stamping Tech*, 3, pp 45-5-, (1988).
85. F. Koenigsherger and J. Tlusty, "Machine Tool Structures", Pergmon Press, London, (1970).
86. S. Taylor, "Computer Aided Design of a Planing Machine Structure", *Proc. M.T.D.R. Conf, Birmingham, UK*, pp 739-748, (1968).
87. J. Hannah and M.J. Hillier, "Applied Mechanics", Longman Scientific and Technical, London, (1988), Chapter 14.
88. M.I. Korytko, "Damping-High-Pressure Low-Flow Energy Instantaneously", *Hydraul & Pneum*, 31, pp 55-57, (1978).
89. D.H. Anderson, "Servo System Controls Actuation of Hydraulic, High Speed, Can-Making Press", *Hydraul & Pneum*, 31, pp 79-31, (1978).
90. R.P. Pompei, "Designing A Hydraulic Press Circuit", *Hydraul & Pneum*, 32, pp 62-67, (1979).
91. A.J. Warner, "PC Directs Hydraulic Moulding Press Cycle", *Hydraul & Pneum*, 36, pp 39-43, (1983).



92. H. Lothammer and C. Sheppard, "Electronic Controller Sequences Assembly Press",  
Hydraul & Pneum, 37, pp 77-79, (1984).
93. R.W. Haviland, "Hydraulic Drives, Shop Air Power Blow Molder",  
Hydraul & Pneum, 42, pp 34-37, (1989).

## BIBLIOGRAPHY

1. C.T.F. Ross, "Finite Element Methods in Structural Mechanics"  
John Wiley & Sons, New York, (1985).
2. Edward R. Champion et al., "Finite Element Analysis with Personal Computer"  
Marcel Dekker, New York, 1988).
3. "What Every Engineer Should Know About Finite Element Analysis" - Ed. John  
R. Brawer  
Marcel Dekker, New York, (1988).
4. "Finite Element Analysis Ltd. (1990). The Theory Manual, London.
5. Tirupathi R. Chandrupatla et al., "Introduction to Finite Elements in Engineering"  
Prentice-Hall, New Jersey, (1991).
6. Arthur H. Burr, "Mechanical Analysis and Design"  
Elsevier, New York, (1981).
7. Shigley and Mischke, "Standard Handbook of Machine Design"  
MacGraw-Hill, New York, (1986).
8. "Design Engineering Handbook"  
Parker Hannifin Corp., Bulletin 0224-B1, USA (1979).
9. Morris Asimow, "Introduction to Design"  
Prentice-Hall, New Jersey, (1962).
10. Gordon L. Glegg, "The Design of the Design"  
Cambridge University Press, (1969).
11. Virgil M. Faires, "Design of Machine Elements"  
Macmillan, New York, (1965).
12. M.F. Spotts, "Mechanical Design Analysis"  
Prentice-Hall, New Jersey, (1964).
13. George E. Dieter, "Engineering Design - A Material and Processing Approach"  
McGraw-Hill, New York, (1991).
14. E. Atrek et al., "New Direction in Optimum Structural Design"  
John Wiley & Sons, New York, (1984).
15. Jasbir S. Arora, "Introduction to Optimum Design"  
McGraw-Hill, New York, (1989).

16. W.P. Lewis et al., "Fundamentals of Engineering Design"  
Prentice-Hall, New York, (1989).
17. Johnson, D., "Advanced Structural Mechanics"  
Collins, London, (1986).
18. E.J. Hearn, "Mechanics of Materials"  
Pergamon Press, New York, (1985).
19. C.T.F. Ross, "Applied Stress Analysis"  
John Wiley & Sons, New York, (1987).
20. P.P. Benham et al., "Mechanics of Solids and Structures"  
Pittman Publishing, New York, (1973).
21. J.A. Cain & R. Hulse, "Structural Mechanics"  
Macmillan, London, (1990).
22. F. Koenigsberger, "Design Principles of Metal-Cutting Machine Tools"  
Pergamon Press, New York, (1964).
23. M. Peter & G. Wilkening, "Report on the measurements carried out within the  
framework of the EC comparison between The PTB, Braunschweig and The  
LNE, Paris"  
ISSN0341-6720, (1983)
24. George Schlesinger, "Testing Machine Tools"  
The Machinery Publishing Co. Ltd., London, (1978).
25. J.P. Holman & W.J. Gayda, "Experimental Methods for Engineering"  
McGraw-Hill, New York, (1989).
26. Jimmie J. Cathey et al., "Basic Electrical Engineering"  
McGraw-Hill, New York, (1984).
27. Joseph J. Carr, "Data Acquisition and Control"  
TAB Book Inc., PA, U.S.A. (1988).
28. Harry N. Norton, "Handbook of Transducers"  
Prentice-Hall, New Jersey, (1989).
29. R.B. Ross, "Metallic Materials Specification Handbook"  
E.& F.N. Spon, New York, (1980).

## APPENDIX (A)

### 1.0 Program Variable Names

The following are some computer program variable names used in the program which calculates the design parameters of the frame of the hydraulic press by conventional analytical formula:

B <sub>1</sub> (3,30)	}	Stores of the bases; heights and the local centroids of the individual rectangles in the whole cross section.
H <sub>1</sub> (3,30)		
YL <sub>1</sub> (3,30)		
N <sub>1</sub> (30)	:	Number of the individual rectangles in the whole cross-section.
IB	:	Store of the total number of beams in half of frame of the hydraulic press.
IO	:	Print control variable, IO = 1 print data  <IO>  escape print data.
YO	:	Young's modulus.
ST	:	Yield stress.
FL	:	The first applied load.
DFL	:	The increment of the load.
PL1 (3)	:	The total length of each beam of the frame of the hydraulic press.
IC	:	Temporary store of the number of increments of applied load.

AR (30)	:	Store of the area of the cross-sections of the beams.
SEC (30)	:	The sum of the second moment of area of the individual rectangles about an axis passes through the base of the whole cross-section.
BMOM (30)	:	The sum of the first moment of area of the individual rectangles about an axis passes the base of the whole cross-section.
BLOC (30)	:	The sum of the local second moment of area of the individual rectangles about an axis passes through the local centroid.
YBAR (30)	:	The centroid of the whole cross-section from the axis passes through the base of the whole section.
BIXX (30)	:	The total second moment of area of the whole cross-section about an axis passes the base.
BINA (30)	:	The total second moment of area of the whole cross-sections about the centroids.
ARI (30)	:	Area of the individual rectangles.
SEC1 (30,30)	:	Local second moment of area of the individual rectangles.
SEGO <sub>1</sub> (40)	}	Stores of the maximum bending moment of the beams.
SEGO <sub>2</sub> (40)		
SEGO <sub>3</sub> (40)		
BMO <sub>1</sub> (40)	}	Stores of the maximum bending moment of the beams of press frame.
BMO <sub>2</sub> (40)		
the BMO <sub>3</sub> (40)		

DEOB (40) : The total vertical deflection of the frame.

## 2.0 Instructions for preparing the input data

The program runs by means of batch file which contains the input data. The batch files consists of:

CARD SET 1 : One Card (I3)

IO : Print control variable

CARD SET 2 : One card (I5) for each beam

N1 : Number of individual rectangles in the whole section.

CARD SET 3 : One card for each N1 in each cross-section (3 F10.4)

$B_1, H_1, YL_1$  : The base height and the local centroid of each individual rectangle in the whole cross-section.

CARD SET 4 : One card for each beam (F10.4)

PL1 : Total length of each beam

CARD SET 5 : One card (4F14.1)

FL, DFL, YO, ST : Are the first applied loads; the incremental applied load; Young' modulus and the yield stress, respectively.

### 3.0 Listing of the Program

```
C *****
C * CALCULATE THE DESIGN PARAMETERS OF THE
C * FRAME OF THE "H SHAPE" PRESS MACHINE
C *****
C CONTROL MAIN PROGRAM
COMMON/BLOCK01/ B1(3,30),H1(3,30),
1 YL1(3,30),N1(30),IB,IO,YO,
2 ST,FL,DFL,PL1(3),IC
COMMON/BLOCK02/AR(30),SEC(30),
1 BMOM(30),BLOC(30),YBAR(30),
2 BIXX(30),BINA(30),AR1(30,30),
3 SEC1(30,30)

C
C READ DATA INPUT
C
C CALL DATA
C
C INITIALIZE AND PRINT DATA INPUT
C
C CALL GDATA
C
C CALCULATE THE MOMENT OF AREA
C
C CALL INA
C
C CALCULATE THE STRESSES AND UNKNOWN
C PARAMETERS
C
C CALL CAL1
C STOP
C END
C *****
C *****
C SUBROUTINE DATA
COMMON/BLOCK01/ B1(3,30),H1(3,30),
1 YL1(3,30),N1(30),IB,IO,YO,
2 ST,FL,DFL,PL1(3),IC
COMMON/BLOCK02/AR(30),SEC(30),
1 BMOM(30),BLOC(30),YBAR(30),
2 BIXX(30),BINA(30),AR1(30,30),
3 SEC1(30,30)

C
C READ NUMBER OF BEAMS ON THE FRAME
C AND THE PRINT OPTION
C
C
C IB=3
C READ(5,'(2I3)') IO
```

```

IF(IB.LT.3) GOTO 90
IF(IB.GT.3) GOTO 90
IF(IO.LE.0) GO TO 70
C
C   READ THE MAXIMUM NUMBER OF THE DIVISIONS
C   ON EACH BEAM
C
C
C
C
C
C   READ THE NUMBER OF THE ELEMENT AREA OF THE
C   INDIVIDUAL CROSS-SECTIONS
C
C
DO 10 J=1,IB
READ(5,'(I5)') N1(J)
IF(N1(J).LE.0) GOTO 70
12  CONTINUE
10  CONTINUE
C
C
C   READ THE BASE,THE HIGHT AND THE CENTROID
C   OF THE ELEMENT AREA OF THE INDIVIDUAL
C   CROSS-SECTIONS
C
C
C
C
DO 40 K=1,IB
DO 50 I=1,N1(K)
READ(5,'(3F16.8)') B1(K,I),H1(K,I),
1   YL1(K,I)
IF(B1(K,I).LE.0.0) GOTO 70
IF(H1(K,I).LE.0.0) GOTO 70
IF(YL1(K,I).LE.0.0) GOTO 70
50  CONTINUE
45  CONTINUE
40  CONTINUE
C
C
C
C   READ THE TOTAL LENGTH OF THE FRAME
C
C
C
DO 55 I=1,IB
READ(5,'(F10.4)') PL1(I)
IF(PL1(I).LE.0.0) GOTO 70
55  CONTINUE
C
C
C
C   READ THE APPLIED LOAD AND THE
C   INCREMENTAL LOAD
C

```



```

      READ(5,'(4E14.4)') FL,DFL,YO,ST
      IF(FL.LT.0.0) GOTO 70
      IF(DFL.LE.0.0) GOTO 70
      RETURN
70    WRITE(6,80)
      WRITE(6,85)
      GOTO 98
80    FORMAT(1X,/, '****< Zero Input Data
1      >****',/)
85    FORMAT(2X,/, ' Error...!!
1      .. Check Zero Input Data...!!',//)
90    WRITE(6,95)
95    FORMAT(1X,/, ' THE NUMBER OF BEAMS
1      MUST BE "3" .....Error Data...!!',//)
98    STOP
      END
C *****
C *****
      SUBROUTINE GDATA
      COMMON/BLOCK01/ B1(3,30),H1(3,30),
1      YL1(3,30),N1(30),IB,IO,YO,
2      ST,FL,DFL,PL1(3),IC
      COMMON/BLOCK02/AR(30),SEC(30),
1      BMOM(30),BLOC(30),YBAR(30),
2      BIXX(30),BINA(30),AR1(30,30),
3      SEC1(30,30)
      INTEGER DEL1
C
C      INITIALIZATION
C
C
      DEL1=DFL
      IC=20000000/DEL1
      DO 285 K=1,3
      DO 290 I=1,N1(K)
      AR1(K,I)=0.0
      AR(K)=0.0
      SEC1(K,I)=0.0
      SEC(K)=0.0
      BMOM(K)=0.0
      BLOC(K)=0.0
      YBAR(K)=0.0
      BIXX(K)=0.0
      BINA(K)=0.0
290    CONTINUE
285    CONTINUE
280    CONTINUE
C
C      SKIP PRINT
C

```

```

IF(IO.GT.1)GOTO 260
C
C   PRINT INPUT DATA
C
C
WRITE(6,80) IB,IO
DO 10 J=1,IB
WRITE(6,100) J
WRITE(6,130) N1(J)
10 CONTINUE
WRITE(6,135)
DO 40 K=1,IB
WRITE(6,100) K
WRITE(6,140)
DO 50 I=1,N1(K)
WRITE(6,150) I,B1(K,I),
1      H1(K,I),YL1(K,I)
50 CONTINUE
40 CONTINUE
DO 45 J=1,IB
WRITE(6,160) J,PL1(J)
45 CONTINUE
WRITE(6,210)
WRITE(6,220)
WRITE(6,230) FL,DFL
WRITE(6,235)
WRITE(6,240)
WRITE(6,245) ST,YO
80 FORMAT(2X,/, ' NUMBER OF BEAMS=',I3,5X,
1      'PRINT OPTION:',I3)
100 FORMAT(/,1X, ' BEAM NUMBER:',I3)
130 FORMAT(1X, ' NUMBER OF THE ELEMENT AREA:',I3)
135 FORMAT(1X,/, ' ***** CROSS-SECTIONAL',
1      'SPECIFICATIONS *****',/)
140 FORMAT(1X' ELE N.      BASE      HIGHT
1      CENTROID')
150 FORMAT(3X,I3,6X,F12.3,5X,F12.3,8X,F12.3)
160 FORMAT(1X, ' LENGTH OF THE BEAM ',I3,':',F12.3,/)
200 FORMAT(2X,I3,18X,F12.3,11X,F12.3)
210 FORMAT(5X,/,
1      '***** APPLIED LOAD *****')
220 FORMAT(2X, '      LOAD
1      INCREMENT ')
230 FORMAT(4X,F12.3,19X,F12.3)
235 FORMAT(5X,/, ' ***** MATERIAL',
1      ' PROPERTIES *****')
240 FORMAT(2X,52H      YIELD STRESS
1      YOUNG'SMODULUS )
245 FORMAT(4X,F14.4,19X,F14.4,/)
260 CONTINUE

```

```

RETURN
END
C *****
C *****
SUBROUTINE INA
COMMON/BLOCK01/ B1(3,30),H1(3,30),
1 YL1(3,30),N1(30),IB,IO, YO,
2 ST,FL,DFL,PL1(3),IC
COMMON/BLOCK02/AR(30),SEC(30),
1 BMOM(30),BLOC(30),YBAR(30),
2 BIXX(30),BINA(30),AR1(30,30),
3 SEC1(30,30)
C
C
C CALCULATE THE AREA,AND THE LOCAL SECOND MOMENT
C OF AREA OF THE INDIVIDUAL ELEMENT AREA ABOUT
C LOCAL CENTROID AND THE TOTAL SECOND MOMENT OF
C AREA ABOUT X-X
C
C
DO 40 K=1,IB
DO 50 I=1,N1(K)
AR1(K,I)=B1(K,I)*H1(K,I)
SEC1(K,I)=((B1(K,I))*(H1(K,I)**3))/12.
AR(K)=AR(K)+AR1(K,I)
BMOM(K)=BMOM(K)+(AR1(K,I)*YL1(K,I))
SEC(K)=SEC(K)+((AR1(K,I))*(YL1(K,I)**2))
BLOC(K)=BLOC(K)+SEC1(K,I)
50 CONTINUE
40 CONTINUE
C
C
C CALCULATE THE THE CENTROID OF THE INDIVIDUAL
C CROSS-SECTIONS ON THE INDIVIDUAL BEAMS AND
C THE SECOND MOMENT OF AREA OF THESE CROSS-
C SECTIONS ABOUT X-X AND x-x
C
C
DO 52 K=1,IB
YBAR(K)=BMOM(K)/AR(K)
BIXX(K)=BLOC(K)+SEC(K)
BINA(K)=BIXX(K)-(AR(K)*(YBAR(K)**2))
52 CONTINUE
C
C PRINT THE SECTIONAL CENTROID FROM X-X,
C THE SECTIONAL AREA AND THE SECOND MOMENT
C OF AREA OF THE INDIVIDUAL CROSS-SECTIONS
C
WRITE(6,41)

```

```

WRITE(6,46)
DO 20 K=1,IB
WRITE(6,51)K,AR(K),YBAR(K),BINA(K)
30 CONTINUE
20 CONTINUE
WRITE(6,92)
41 FORMAT(1X,/, '          ***** < THE OUTPUT DATA
1      >*****',/)
46 FORMAT(1X, 'BEAM N.          SEC.AREA
1      SEC.CENT          2nd.M.A')
51 FORMAT(2X,I3,13X,E12.4,3X,E12.4,4X,E12.4)
92 FORMAT(/, '*****',/)
RETURN
END
C *****
C *****
SUBROUTINE CAL1
COMMON/BLOCK01/ B1(3,30),H1(3,30),
1      YL1(3,30),N1(30),IB,IO, YO,
2      ST,FL,DFL,PL1(3),IC
COMMON/BLOCK02/AR(30),SEC(30),
1      BMOM(30),BLOC(30), YBAR(30),
2      BIXX(30),BINA(30),AR1(30,30),
3      SEC1(30,30)
DIMENSION BMO1(40),BMO2(40),BMO3(40),SEGO1(40),
1      SEGO2(40),SEGO3(40),DEOB(40),STIF(40)
PL1(1)=PL1(1)*2.
PL1(3)=PL1(3)*2.
C
C      CALCULATE THE PRODUCTS OF THE BENDING
C      MOMENTS OF FRAME
C
DO 600 IG=1,IC
STIF(IG)=0.0
DEOB(IG)=0.0
OPE1=0.0
OPEN1=0.0
OPE2=0.0
OPEN2=0.0
OPE3=0.0
OPEN3=0.0
TMOH1=0.0
TMOH2=0.0
TMOH3=0.0
TMON1=0.0
TMON2=0.0
TMOS1=0.0
TMOS2=0.0
BMO1(IG)=0.0

```

BMO2(IG)=0.0  
 BMO3(IG)=0.0  
 DERO1=0.0  
 DERO2=0.0  
 DERO3=0.0  
 SEGO1(IG)=0.0  
 SEGO2(IG)=0.0  
 SEGO3(IG)=0.0  
 OPETN1=0.0  
 OPETN2=0.0  
 OPE1=OPE1+(PL1(1)\*PL1(2))/(6.\*BINA(2))  
 OPE2=OPE2+(PL1(1)\*\*2)/(8.\*BINA(1))  
 OPE3=OPE3+(PL1(1)\*\*2)/(2.\*(PL1(2)\*\*2)\*AR(1))  
 OPEN1=OPEN1+(PL1(1))/(2.\*BINA(1))  
 OPEN2=OPEN2+(PL1(2))/(3.\*BINA(2))  
 OPEN3=OPEN3+(PL1(1))/((PL1(2)\*\*2)\*AR(1))  
 OPETN1=OPETN1+(OPE1+OPE2+OPE3)  
 OPETN2=OPETN2+(OPEN1+OPEN2+OPEN3)

C  
C  
C  
C  
C  
C  
C

CALCULATE THE UNKNOWN BENDING MOMENT AND OTHERS  
BENDING MOMENTS FOR THE FRAME

BMO1(IG)=((OPETN1/OPETN2)\*(FL/2.))  
 BMO2(IG)=(FL\*(PL1(1))/4.)-BMO1(IG)  
 BMO3(IG)=-FL\*PL1(3)/4.  
 FO=((BMO1(IG)/PL1(2))-((FL\*PL1(1))/(4.\*PL1(2))))

C  
C  
C  
C  
C

CALCULATE THE STRESSES FOR THE OPENED FRAME

SEGO1(IG)=(FO/AR(1))+  
 1 ((BMO1(IG)\*YBAR(1))/BINA(1))  
 SEGO2(IG)=(FL/(2.\*AR(2)))+  
 2 ((BMO2(IG)\*YBAR(2))/BINA(2))  
 SEGO3(IG)=(FO/AR(3))+  
 3 ((BMO3(IG)\*YBAR(3))/BINA(3))

C  
C  
C  
C  
C

CALCULATE THE DEFLECTION OF THE FRAME

TMOH1=TMOH1+((1./(2.\*YO)))  
 TMOH2=TMOH2+((PL1(1)\*\*2)/(4.\*BINA(1)))  
 TMOH3=TMOH3+((FL\*PL1(1)/6.)-BMO2(IG))  
 TMON1=TMON1+(TMOH1\*TMOH2\*TMOH3)  
 TMOS1=TMOS1+(PL1(1)\*\*2/(2.\*AR(1)\*PL1(2)\*\*2))

```

TMOS2=TMOS2+(BMO1(IG)-(FL*PL1(1)/4.))
TMON2=TMON2+(TMOH1*TMOS1*TMOS2)
DERO1=DERO1+(TMON1+TMON2)
DERO2=DERO2+(((FL/2.)*(PL1(2)/(YO*AR(2))))))
DERO3=-((FL*(PL1(3)**3)/(48.*YO*BINA(3))))

```

C  
C  
C  
C  
C  
C  
C  
C  
C  
C  
C  
C  
C  
C

HORIZONTAL DEFLECTION AT THE BOTTOM

PRINT MAX DEFLECTION,BENDING MOMENT,AND  
STRESS OF INDIVIDUAL BEASMS ON THE  
FRAME

```

JO1=1
JO2=2
JO3=3
WRITE(6,72)
WRITE(6,82)JO1,BMO1(IG),DERO1,SEGO1(IG)
WRITE(6,82)JO2,BMO2(IG),DERO2,SEGO2(IG)
WRITE(6,82)JO3,BMO3(IG),DERO3,SEGO3(IG)
DEOB(IG)=ABS(DERO1)+ABS(DERO2)+ABS(DERO3)
STIF(IG)=FL/DEOB(IG)
WRITE(6,66)FL
WRITE(6,98)FO
WRITE(6,102)DEOB(IG)
WRITE(6,125)STIF(IG)
IF(IG.EQ.IC) GOTO 103
IF(ABS(SEGO1(IG)).GT.ST) GOTO 700
IF(ABS(SEGO2(IG)).GT.ST) GOTO 700
IF(ABS(SEGO3(IG)).GT.ST) GOTO 700
WRITE(6,62)
103 CONTINUE
FL=FL+DFL
600 CONTINUE
WRITE(6,128)
62 FORMAT(1X,/, ' .....',/)
66 FORMAT(2X,/, ' Applied Load = ',E12.4,/)
72 FORMAT(2X,'Beam N.      Max Bend.
1      Max Def.          Max Stress. ')
82 FORMAT(1X,I3,8X,E12.4,8X,E12.4,12X,E12.4)
98 FORMAT(1X,' The Lateral Force F = ',E12.4)
102 FORMAT(1X,' The Absolute Maximum Deflection =',E12.4)
125 FORMAT(3X,/, ' The Stiffness Of The Machine =',E16.8/,
1      '*****',/)

```

```
128  FORMAT(2X,/, ' Applied Load Reaches The ',/
1      ' Maximum designed Load "0.2E+08 N " ...!!!',///)
      RETURN
700  CONTINUE
      WRITE(6,705)
705  FORMAT(1X,/, ' Yielding Happend',/,
1      ' ...Applied Load Out OF The ',
2      'Range of Elasticity ....!!!',///)
      STOP
      END
```

\*\*\*\*\*

C \* **END OF THE PROGRAM.**

\*\*\*\*\*

## APPENDIX (B)

### NONLINEAR BOUNDARY CONDITIONS

Deformation dependent boundary condition models account for modifications to the external problem constraints resulting from structural deformation. Nonlinear boundary conditions are usually the result of contact of otherwise independent element assemblies. Nonlinear boundary conditions may be modelled, using LUSAS, in two ways:

- (i) Nonlinear joint models
- (ii) Slidelines.

This appendix describes the successful way of using the nonlinear boundary conditions, in LUSAS analyses, for two dimensional problems especially with a concentrating applied load. In fact, preparing the data for this way of modelling is not clearly described in the user manual. The two input datafiles are the modified datafile obtained from MYSTRO pre-processing session.

#### 1.0 Joint Elements

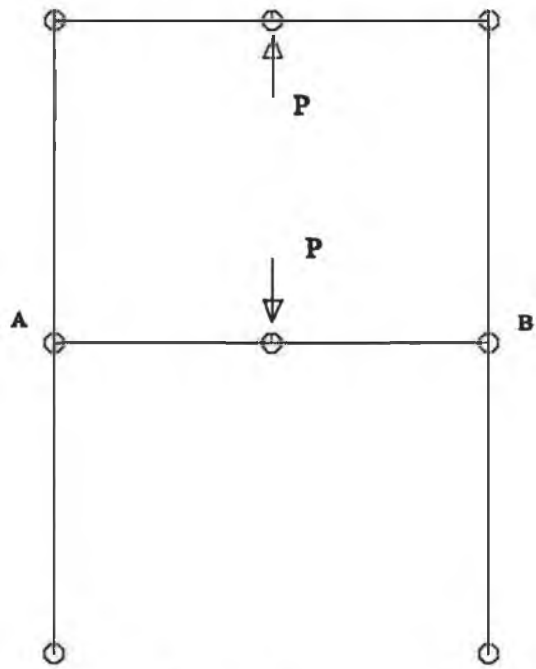
Joint elements may be introduced into the structure to represent:

- (i) Non-rigid connections
- (ii) Local material failure
- (iii) Simple contact
- (iv) Point masses.

Joint models may be used in static, dynamic and thermal problems. Joint elements have two active nodes and additional dummy nodes. Dummy nodes are used to define local direction and planes. If the definition joint-element topology is not correct an error message appears and the analysis will be aborted. Defining the element topology is the most crucial part of this model. In order to get this part of modelling correct the local



B-2



A and B are Pin Joints

Fig( B.1 )

4 \_\_\_\_\_ 6

6 \_\_\_\_\_ 14

4  
|  
2

14  
|  
12

8    8 \_\_\_\_\_ 9

9 \_\_\_\_\_ 17    .17

2  
|  
1

12  
|  
11

**Node Number**

coordinates of the joint element should be coincided with one of the local coordinates of the independent element assemblies. Generally, nonlinear control must be used in the input datafile for the nonlinear boundary condition models.

## 1.2 Input Datafile and Instructions

The following datafile is prepared for the beam element in 2D of the finite element model of the press machine, Fig (B.1), using the joint element (JPH<sub>3</sub>) at the pin joints at A and B.

```
PROBLEM TITLE Full model of the press ...
machine using beam and joint element
C
OPTION 2 48 117 118 146
C
C Define the topology of the Beam elements
C
BEAM ELEMENT TOPOLOGY
  1   1   2
  2   4   2
  3   4   6
  4   8   9
  5  11  12
  6  14  12
  7  14   6
  8  17   9
C
C Define the topology of the joint elements
C
JPH3 ELEMENT TOPOLOGY
  9   2 8 9
 10  12 17 9
C
C Define the nodal coordinates
C
NODE COORDINATES
  1  102.000000  0.000000000E+00
  2  102.000000  1000.00000
  4  102.000000  2043.00000
  6  812.000000  2043.00000
  8  102.000000  1000.00000
  9  812.000000  1000.00000
 11  1522.00000  0.000000000E+00
 12  1522.00000  1000.00000
 14  1522.00000  2043.00000
```

17 1522.00000 1000.00000

C

C Define the geometric properties of the beam  
C elements.

C

BEAM GEOMETRIC PROPERTIES

1	22970.0000	602400000. ...
	22970000.0	
2	15500.0000	53770000.0 ...
	15500000.0	

C

C Define the geometric properties of the joint  
C elements.

C

JPH3 GEOMETRIC PROPERTIES

3	0.0
---	-----

C

C Assign the geometric properties to the  
C relevant elements.

C

GEOMETRIC ASSIGNMENTS

1	2	1	2
3	4	1	1
5	6	1	2
7	8	1	1
9	10	1	3

C

C Define the material properties of the beam  
C elements.

C

MATERIAL PROPERTIES

1	200000.000	0.300000000 ...
	0.00000000E+00 ...	
	0.00000000E+00	0.00000000E+00

C

C Define the material properties of the joint  
C elements.

C

JOINT PROPERTIES

2	0.10E17	0.10E17	0.0
---	---------	---------	-----

C

C Assign the material properties to the  
C relevant element.

C

MATERIAL ASSIGNMENTS

1	8	1	1
9	10	1	2

C

C Apply the support conditions

C

SUPPORT NODES

1 0 0 F R F

6 0 0 R F F

9 0 0 R F F

11 0 0 F R F

C Apply the first load increment

C

LOAD CASE

CL

6 0 0 0.000000000E+00 175000.000

9 0 0 0.000000000E+00 -175000.000

C

C Apply the nonlinear control.

C

NONL CONT

ITERA 10 0 0

CONVER 0 0 D D

OUTP 0 1 1

C Apply the rest of the load increments.

LOAD CASE

CL

6 0 0 0.000000000E+00 350000.000

9 0 0 0.000000000E+00 -350000.000

LOAD CASE

CL

6 0 0 0.000000000E+00 525000.000

9 0 0 0.000000000E+00 -525000.000

LOAD CASE

CL

6 0 0 0.000000000E+00 700000.000

9 0 0 0.000000000E+00 -700000.000

LOAD CASE

CL

6 0 0 0.000000000E+00 875000.000

9 0 0 0.000000000E+00 -875000.000

LOAD CASE

CL

6 0 0 0.000000000E+00 1050000.00

9 0 0 0.000000000E+00 -1050000.00

LOAD CASE

CL

6 0 0 0.000000000E+00 1225000.00

9 0 0 0.000000000E+00 -1225000.00

LOAD CASE

CL

6 0 0 0.000000000E+00 1400000.00

9 0 0 0.000000000E+00 -1400000.00

C End of the datafile.

END

## **2.0 Slidelines**

Slidelines technique is the second way of modelling the nonlinear boundary condition problems using LUSAS. This technique may be used to model the contact behaviour between two or more structures in preference to joint elements if certain conditions are presented:

- (i) Finite relative surface deformations with arbitrary contact and separation.
- (ii) No exact prior knowledge of the contact process.
- (iii) A large number of nodes are defined within the probable contact region.
- (iv) Highly localised element density in the region of high stress gradient.

Slidelines may be used in dynamic, static and linear analysis. The most important parts of modelling the 2D continuum element with a concentrated applied load, are the assignment of the contact surfaces and the definition of the dummy restraint points. Nonlinear control should be used in this model, even in the linear analysis, and the first load increment should have a very small magnitude to allow contact to take and thus generate contact springs between the two bodies.

### **2.1 Slideline Applications**

Slidelines may be used to model the following problems:

- (i) Crash barrier evaluation
- (ii) Missile impact
- (iii) Vehicle rollover
- (iv) Crash helmet design
- (v) Interference fits.

### **2.2 Surface Assignments**

Each slideline consists of two surfaces, one is the "slave" and the other is the "master". After defining the two surfaces, the assignment of them to the region of interest in the finite element model is not random. It should be appreciated that many errors in this type of analyses are due to a fault in the assignment of the surfaces of the slideline,

especially when there are no rules given in the manuals on this matter. However, in order to do this assignment correctly, imagine one walking between the two surfaces parallel to their boundaries, the surface, which is on the left hand-side will be the "slave" surface and the other surface will be the "master" surface.

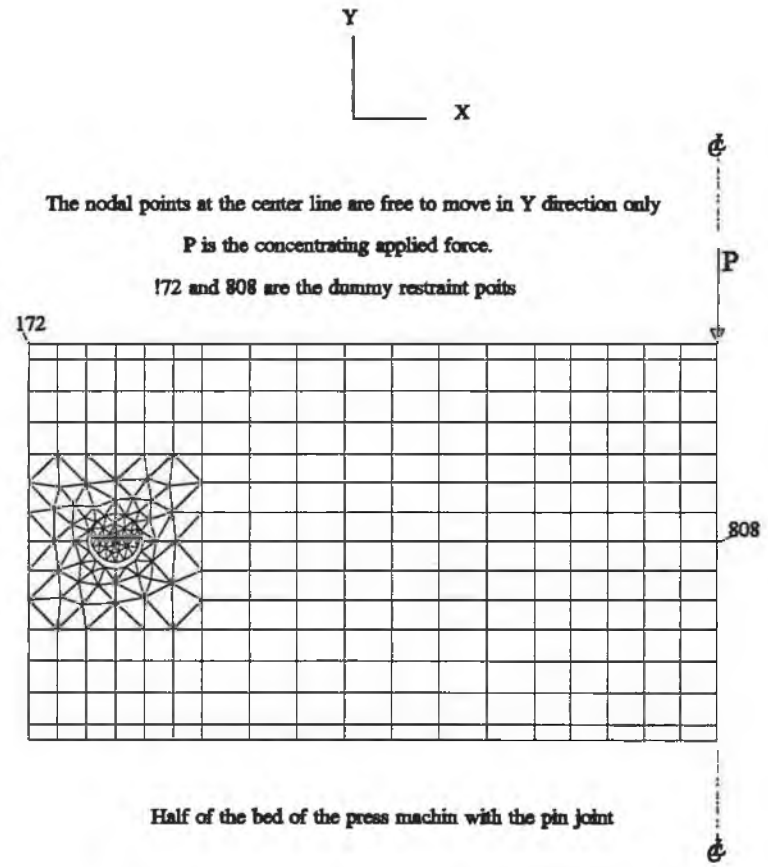
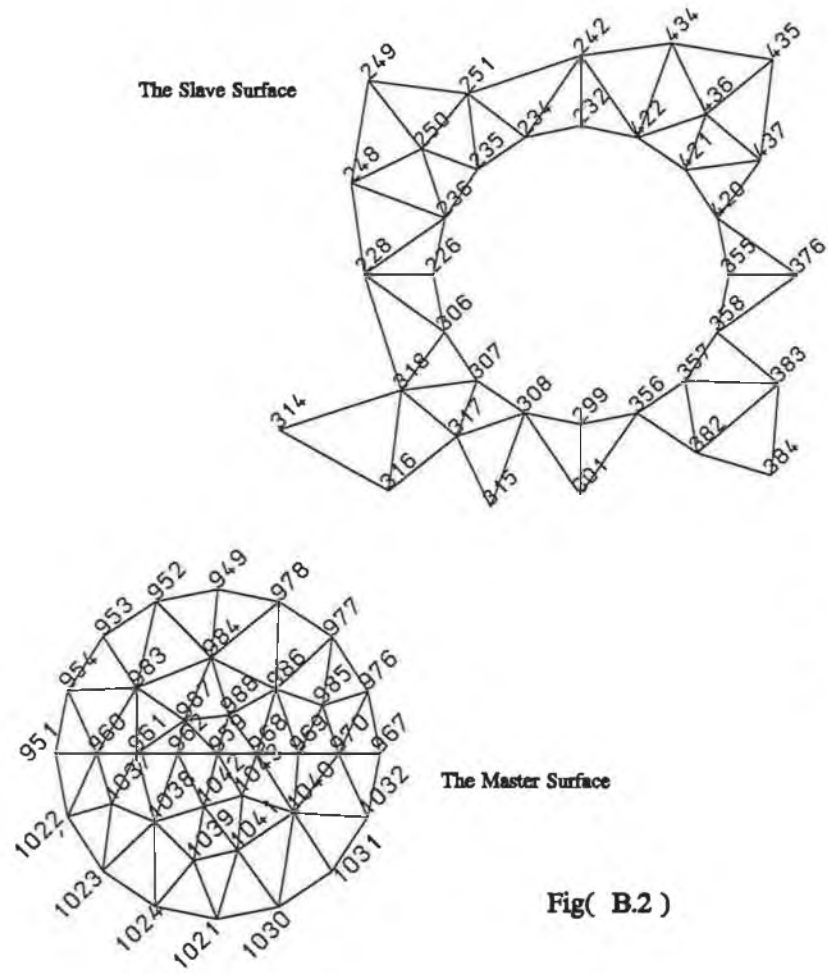
### **2.3 The Dummy Restraint**

For concentrating applied loads of 2D continuum problems, it is very important to define dummy restraint nodes to prevent one of the bodies from moving freely during the first load increment when the two bodies are still unconnected. Then these dummy restraint points will be freed up before the second load increment. Generally, experience plays a significant part in defining these dummies. However, it should be kept in mind that the whole structure must be supported so that no rigid body displacement or rotation is possible.

### **2.4 Modelling Considerations**

If the process does not converge the following should be taken into consideration:

- (i) Check carefully the assignment of the slideline surfaces.
- (ii) The interface stiffness scale factor should be increased slightly for slideline surfaces.
- (iii) The first load increment should be very small (i.e. total applied load X 10).
- (iv) The SOLUTION ORDER data section in the input datafile should be omitted.
- (v) PLOT FILE data section in the input datafile should be assigned when Option 51 is used.
- (vi) OPTIONS 62, 185 and 186 should be used.
- (vii) Dummy restraint nodes must be defined in the case of concentrated applied load.
- (viii) Sharp edges must be avoided in the slideline surfaces. Slidelines which have a sharp edge must be broken into two slidelines.



Fig( B.2 )



## 2.5 Input Datafile Presentation

The following is the input datafile for half of the press bed with the pin joint modelled together in plane stress, as shown in Fig. (B.2).

PROBLEM TITLE half of the bed of the ...  
press machine.

C

C

OPTION 2 48 62 117 118 146 185 186

C

C

QPM4 ELEMENT TOPOLOGY

9	2	1	5	13
10	13	5	6	12
11	12	6	4	10
19	10	4	20	28
20	28	20	21	27
21	27	21	19	25
37	19	35	50	25
38	35	36	51	50
39	36	37	52	51
40	37	38	53	52
41	38	39	54	53
42	39	40	55	54
43	40	34	48	55
55	34	70	81	48
56	70	71	82	81
57	71	72	83	82
58	72	73	84	83
59	73	69	79	84
72	94	95	98	109
73	109	98	99	110
74	110	99	100	111
75	111	100	101	112
76	112	101	97	107
92	94	128	143	95
93	128	127	142	143
94	127	126	141	142
95	126	125	140	141
96	125	124	139	140
97	124	123	138	139
98	123	122	136	138
106	122	159	165	136
107	159	158	166	165
108	158	157	163	166

116	157	174	180	163
117	174	173	181	180
118	173	172	178	181
128	178	188	204	181
129	181	204	205	180
130	180	205	199	163
131	188	189	206	204
132	204	206	207	205
133	205	207	200	199
134	189	187	194	206
135	206	194	195	207
136	207	195	193	200

TPM3 ELEMENT TOPOLOGY

150	227	222	220
151	236	228	226
152	242	234	232
153	195	241	193
154	194	187	221
155	246	222	227
156	246	221	222
157	247	242	241
158	247	241	195
159	247	195	194
160	248	246	227
161	248	227	228
162	248	228	236
163	249	246	248
164	250	248	236
165	250	236	235
166	250	249	248
167	251	234	242
168	251	242	247
169	251	235	234
170	251	247	249
171	251	250	235
172	251	249	250
173	252	194	221
174	252	221	246
175	252	247	194
176	252	249	247
177	252	246	249
191	288	227	220
192	294	289	287
193	300	295	293
194	308	301	299
195	306	226	228
196	313	295	300
197	313	294	295
198	314	288	289
199	314	228	227

200	314	227	288
201	315	313	300
202	315	300	301
203	315	301	308
204	316	313	315
205	317	315	308
206	317	308	307
207	317	316	315
208	318	306	228
209	318	228	314
210	318	307	306
211	318	314	316
212	318	317	307
213	318	316	317
214	319	289	294
215	319	294	313
216	319	314	289
217	319	316	314
218	319	313	316
232	301	356	299
233	364	300	293
234	370	365	363
235	375	371	369
236	376	355	358
237	380	301	300
238	380	300	364
239	380	364	365
240	381	380	365
241	381	365	370
242	381	370	371
243	381	371	375
244	382	356	301
245	382	301	380
246	382	357	356
247	383	376	358
248	383	381	375
249	383	375	376
250	383	358	357
251	383	357	382
252	384	383	382
253	384	382	380
254	384	380	381
255	384	381	383
266	241	414	193
267	422	242	232
268	376	420	355
269	427	375	369
270	428	413	415
271	432	414	241
272	432	415	414

273	433	376	375
274	433	375	427
275	433	427	428
276	434	432	241
277	434	241	242
278	434	242	422
279	435	432	434
280	436	434	422
281	436	422	421
282	436	435	434
283	437	420	376
284	437	376	433
285	437	421	420
286	437	433	435
287	437	436	421
288	437	435	436
289	438	428	415
290	438	415	432
291	438	433	428
292	438	435	433
293	438	432	435

**QPM4 ELEMENT TOPOLOGY**

300	293	295	483	479
301	479	483	484	478
302	478	484	12	10
303	295	294	485	483
304	483	485	486	484
305	484	486	13	12
306	294	287	473	485
307	485	473	474	486
308	486	474	2	13
312	363	365	504	500
313	500	504	505	499
314	499	505	27	25
315	365	364	506	504
316	504	506	507	505
317	505	507	28	27
318	364	293	479	506
319	506	479	478	507
320	507	478	10	28
334	95	143	544	540
335	540	544	545	539
336	539	545	531	525
337	143	142	546	544
338	544	546	547	545
339	545	547	530	531
340	142	141	548	546
341	546	548	549	547
342	547	549	529	530
343	141	140	550	548

344	548	550	551	549
345	549	551	528	529
346	140	139	552	550
347	550	552	553	551
348	551	553	527	528
349	139	138	554	552
350	552	554	555	553
351	553	555	526	527
352	138	136	521	554
353	554	521	520	555
354	555	520	413	526
365	525	531	607	603
366	603	607	608	602
367	602	608	594	588
368	531	530	609	607
369	607	609	610	608
370	608	610	593	594
371	530	529	611	609
372	609	611	612	610
373	610	612	592	593
374	529	528	613	611
375	611	613	614	612
376	612	614	591	592
377	528	527	615	613
378	613	615	616	614
379	614	616	590	591
380	527	526	617	615
381	615	617	618	616
382	616	618	589	590
383	526	413	428	617
384	617	428	427	618
385	618	427	369	589
396	588	594	670	666
397	666	670	671	665
398	665	671	657	651
399	594	593	672	670
400	670	672	673	671
401	671	673	656	657
402	593	592	674	672
403	672	674	675	673
404	673	675	655	656
405	592	591	676	674
406	674	676	677	675
407	675	677	654	655
408	591	590	678	676
409	676	678	679	677
410	677	679	653	654
411	590	589	680	678
412	678	680	681	679
413	679	681	652	653

414	589	369	371	680
415	680	371	370	681
416	681	370	363	652
420	651	657	719	715
421	715	719	720	714
422	714	720	55	48
423	657	656	721	719
424	719	721	722	720
425	720	722	54	55
426	656	655	723	721
427	721	723	724	722
428	722	724	53	54
429	655	654	725	723
430	723	725	726	724
431	724	726	52	53
432	654	653	727	725
433	725	727	728	726
434	726	728	51	52
435	653	652	729	727
436	727	729	730	728
437	728	730	50	51
438	652	363	500	729
439	729	500	499	730
440	730	499	25	50
449	97	101	778	774
450	774	778	779	773
451	773	779	767	763
452	101	100	780	778
453	778	780	781	779
454	779	781	766	767
455	100	99	782	780
456	780	782	783	781
457	781	783	765	766
458	99	98	784	782
459	782	784	785	783
460	783	785	764	765
461	98	95	540	784
462	784	540	539	785
463	785	539	525	764
472	763	767	823	819
473	819	823	824	818
474	818	824	812	808
475	767	766	825	823
476	823	825	826	824
477	824	826	811	812
478	766	765	827	825
479	825	827	828	826
480	826	828	810	811
481	765	764	829	827
482	827	829	830	828

483	828	830	809	810
484	764	525	603	829
485	829	603	602	830
486	830	602	588	809
495	808	812	868	864
496	864	868	869	863
497	863	869	857	853
498	812	811	870	868
499	868	870	871	869
500	869	871	856	857
501	811	810	872	870
502	870	872	873	871
503	871	873	855	856
504	810	809	874	872
505	872	874	875	873
506	873	875	854	855
507	809	588	666	874
508	874	666	665	875
509	875	665	651	854
513	853	857	903	899
514	899	903	904	898
515	898	904	84	79
516	857	856	905	903
517	903	905	906	904
518	904	906	83	84
519	856	855	907	905
520	905	907	908	906
521	906	908	82	83
522	855	854	909	907
523	907	909	910	908
524	908	910	81	82
525	854	651	715	909
526	909	715	714	910
527	910	714	48	81
528	136	165	933	521
529	521	933	934	520
530	520	934	415	413
531	165	166	935	933
532	933	935	936	934
533	934	936	414	415
534	166	163	199	935
535	935	199	200	936
536	936	200	193	414

TPM3 ELEMENT TOPOLOGY

553	960	954	951
554	976	970	967
555	983	953	954
556	983	954	960
557	983	960	961
558	983	952	953

559	984	978	949
560	984	949	952
561	984	952	983
562	985	969	970
563	985	970	976
564	985	976	977
565	986	968	969
566	986	969	985
567	986	985	977
568	986	977	978
569	986	978	984
570	987	983	961
571	987	961	962
572	987	984	983
573	987	962	959
574	988	986	984
575	988	959	968
576	988	968	986
577	988	987	959
578	988	984	987
587	1022	960	951
588	970	1032	967
589	1037	961	960
590	1037	960	1022
591	1037	1022	1023
592	1038	962	961
593	1038	961	1037
594	1038	1037	1023
595	1038	1023	1024
596	1039	1038	1024
597	1039	1024	1021
598	1040	1031	1032
599	1040	1032	970
600	1040	970	969
601	1040	969	968
602	1040	1030	1031
603	1041	1039	1021
604	1041	1021	1030
605	1041	1030	1040
606	1042	959	962
607	1042	962	1038
608	1042	1038	1039
609	1042	1039	1041
610	1043	1041	1040
611	1043	1040	968
612	1043	1042	1041
613	1043	968	959
614	1043	959	1042

NODE COORDINATES

1	0.000000000E+00	0.000000000E+00
---	-----------------	-----------------



2	0.000000000E+00	18.0000000
4	102.000000	0.000000000E+00
5	34.0000000	0.000000000E+00
6	68.0000000	0.000000000E+00
10	102.000000	18.0000000
12	68.0000000	18.0000000
13	34.0000000	18.0000000
19	204.000000	0.000000000E+00
20	136.000000	0.000000000E+00
21	170.000000	0.000000000E+00
25	204.000000	18.0000000
27	170.000000	18.0000000
28	136.000000	18.0000000
34	597.000000	0.000000000E+00
35	260.142857	0.000000000E+00
36	316.285714	0.000000000E+00
37	372.428571	0.000000000E+00
38	428.571429	0.000000000E+00
39	484.714286	0.000000000E+00
40	540.857143	0.000000000E+00
48	597.000000	18.0000000
50	260.142857	18.0000000
51	316.285714	18.0000000
52	372.428571	18.0000000
53	428.571429	18.0000000
54	484.714286	18.0000000
55	540.857143	18.0000000
69	812.000000	0.000000000E+00
70	640.000000	0.000000000E+00
71	683.000000	0.000000000E+00
72	726.000000	0.000000000E+00
73	769.000000	0.000000000E+00
79	812.000000	18.0000000
81	640.000000	18.0000000
82	683.000000	18.0000000
83	726.000000	18.0000000
84	769.000000	18.0000000
94	597.000000	458.000000
95	597.000000	440.000000
97	812.000000	440.000000
98	640.000000	440.000000
99	683.000000	440.000000
100	726.000000	440.000000
101	769.000000	440.000000
107	812.000000	458.000000
109	640.000000	458.000000
110	683.000000	458.000000
111	726.000000	458.000000
112	769.000000	458.000000
122	204.000000	458.000000

123	260.142857	458.000000
124	316.285714	458.000000
125	372.428571	458.000000
126	428.571429	458.000000
127	484.714286	458.000000
128	540.857143	458.000000
136	204.000000	440.000000
138	260.142857	440.000000
139	316.285714	440.000000
140	372.428571	440.000000
141	428.571429	440.000000
142	484.714286	440.000000
143	540.857143	440.000000
157	102.000000	458.000000
158	136.000000	458.000000
159	170.000000	458.000000
163	102.000000	440.000000
165	170.000000	440.000000
166	136.000000	440.000000
172	0.000000000E+00	458.000000
173	34.0000000	458.000000
174	68.0000000	458.000000
178	0.000000000E+00	440.000000
180	68.0000000	440.000000
181	34.0000000	440.000000
187	0.000000000E+00	331.000000
188	0.000000000E+00	403.666667
189	0.000000000E+00	367.333333
193	102.000000	331.000000
194	34.0000000	331.000000
195	68.0000000	331.000000
199	102.000000	403.666667
200	102.000000	367.333333
204	34.0000000	403.666667
205	68.0000000	403.666667
206	34.0000000	367.333333
207	68.0000000	367.333333
220	0.000000000E+00	229.000000
221	0.000000000E+00	297.000000
222	0.000000000E+00	263.000000
226	69.0000000	229.000000
227	30.6666667	229.000000
228	53.6666667	229.000000
232	102.000000	262.000000
234	89.3714467	259.488025
235	78.6654762	252.334524
236	71.5119754	241.628553
241	102.000000	300.333333
242	102.000000	277.333333
246	28.9103243	267.072639

247	67.7516819	296.129338
248	50.9866589	249.194707
249	54.6201486	271.776954
250	66.4565532	256.777423
251	76.4775511	268.973266
252	37.0564310	292.595786
287	0.000000000E+00	127.000000
288	0.000000000E+00	195.000000
289	0.000000000E+00	161.000000
293	102.000000	127.000000
294	34.0000000	127.000000
295	68.0000000	127.000000
299	102.000000	196.000000
300	102.000000	157.666667
301	102.000000	180.666667
306	71.5119754	216.371447
307	78.6654762	205.665476
308	89.3714467	198.511975
313	63.9273610	155.910324
314	34.8706619	194.751682
315	81.8052930	177.986659
316	59.2230458	181.620149
317	74.2225773	193.456553
318	62.0267339	203.477551
319	38.4042137	164.056431
355	135.000000	229.000000
356	114.628553	198.511975
357	125.334524	205.665476
358	132.488025	216.371447
363	204.000000	127.000000
364	136.000000	127.000000
365	170.000000	127.000000
369	204.000000	229.000000
370	204.000000	161.000000
371	204.000000	195.000000
375	173.333333	229.000000
376	150.333333	229.000000
380	135.847947	163.960061
381	168.260285	180.837260
382	128.075289	189.784157
383	146.057003	205.074562
384	144.560131	184.914010
413	204.000000	331.000000
414	136.000000	331.000000
415	170.000000	331.000000
420	132.488025	241.628553
421	125.334524	252.334524
422	114.628553	259.488025
427	204.000000	263.000000
428	204.000000	297.000000

432	140.072639	302.089676
433	169.129338	263.248318
434	122.194707	280.013341
435	144.776954	276.379851
436	129.777423	264.543447
437	141.973266	254.522449
438	165.595786	293.943569
473	0.000000000E+00	90.6666667
474	0.000000000E+00	54.3333333
478	102.000000	54.3333333
479	102.000000	90.6666667
483	68.0000000	90.6666667
484	68.0000000	54.3333333
485	34.0000000	90.6666667
486	34.0000000	54.3333333
499	204.000000	54.3333333
500	204.000000	90.6666667
504	170.000000	90.6666667
505	170.000000	54.3333333
506	136.000000	90.6666667
507	136.000000	54.3333333
520	204.000000	367.333333
521	204.000000	403.666667
525	597.000000	331.000000
526	260.142857	331.000000
527	316.285714	331.000000
528	372.428571	331.000000
529	428.571429	331.000000
530	484.714286	331.000000
531	540.857143	331.000000
539	597.000000	367.333333
540	597.000000	403.666667
544	540.857143	403.666667
545	540.857143	367.333333
546	484.714286	403.666667
547	484.714286	367.333333
548	428.571429	403.666667
549	428.571429	367.333333
550	372.428571	403.666667
551	372.428571	367.333333
552	316.285714	403.666667
553	316.285714	367.333333
554	260.142857	403.666667
555	260.142857	367.333333
588	597.000000	229.000000
589	260.142857	229.000000
590	316.285714	229.000000
591	372.428571	229.000000
592	428.571429	229.000000
593	484.714286	229.000000

594	540.857143	229.000000
602	597.000000	263.000000
603	597.000000	297.000000
607	540.857143	297.000000
608	540.857143	263.000000
609	484.714286	297.000000
610	484.714286	263.000000
611	428.571429	297.000000
612	428.571429	263.000000
613	372.428571	297.000000
614	372.428571	263.000000
615	316.285714	297.000000
616	316.285714	263.000000
617	260.142857	297.000000
618	260.142857	263.000000
651	597.000000	127.000000
652	260.142857	127.000000
653	316.285714	127.000000
654	372.428571	127.000000
655	428.571429	127.000000
656	484.714286	127.000000
657	540.857143	127.000000
665	597.000000	161.000000
666	597.000000	195.000000
670	540.857143	195.000000
671	540.857143	161.000000
672	484.714286	195.000000
673	484.714286	161.000000
674	428.571429	195.000000
675	428.571429	161.000000
676	372.428571	195.000000
677	372.428571	161.000000
678	316.285714	195.000000
679	316.285714	161.000000
680	260.142857	195.000000
681	260.142857	161.000000
714	597.000000	54.3333333
715	597.000000	90.6666667
719	540.857143	90.6666667
720	540.857143	54.3333333
721	484.714286	90.6666667
722	484.714286	54.3333333
723	428.571429	90.6666667
724	428.571429	54.3333333
725	372.428571	90.6666667
726	372.428571	54.3333333
727	316.285714	90.6666667
728	316.285714	54.3333333
729	260.142857	90.6666667
730	260.142857	54.3333333

763	812.000000	331.000000
764	640.000000	331.000000
765	683.000000	331.000000
766	726.000000	331.000000
767	769.000000	331.000000
773	812.000000	367.333333
774	812.000000	403.666667
778	769.000000	403.666667
779	769.000000	367.333333
780	726.000000	403.666667
781	726.000000	367.333333
782	683.000000	403.666667
783	683.000000	367.333333
784	640.000000	403.666667
785	640.000000	367.333333
808	812.000000	229.000000
809	640.000000	229.000000
810	683.000000	229.000000
811	726.000000	229.000000
812	769.000000	229.000000
818	812.000000	263.000000
819	812.000000	297.000000
823	769.000000	297.000000
824	769.000000	263.000000
825	726.000000	297.000000
826	726.000000	263.000000
827	683.000000	297.000000
828	683.000000	263.000000
829	640.000000	297.000000
830	640.000000	263.000000
853	812.000000	127.000000
854	640.000000	127.000000
855	683.000000	127.000000
856	726.000000	127.000000
857	769.000000	127.000000
863	812.000000	161.000000
864	812.000000	195.000000
868	769.000000	195.000000
869	769.000000	161.000000
870	726.000000	195.000000
871	726.000000	161.000000
872	683.000000	195.000000
873	683.000000	161.000000
874	640.000000	195.000000
875	640.000000	161.000000
898	812.000000	54.333333
899	812.000000	90.666667
903	769.000000	90.666667
904	769.000000	54.333333
905	726.000000	90.666667

906	726.000000	54.3333333
907	683.000000	90.6666667
908	683.000000	54.3333333
909	640.000000	90.6666667
910	640.000000	54.3333333
933	170.000000	403.666667
934	170.000000	367.333333
935	136.000000	403.666667
936	136.000000	367.333333
949	102.000000	262.000000
951	73.0000000	233.000000
952	90.9021805	259.792506
953	81.4939033	253.506097
954	75.2074936	244.097820
959	102.000000	233.000000
960	80.2500000	233.000000
961	87.5000000	233.000000
962	94.7500000	233.000000
967	131.000000	233.000000
968	109.250000	233.000000
969	116.500000	233.000000
970	123.750000	233.000000
976	128.792506	244.097820
977	122.506097	253.506097
978	113.097820	259.792506
983	87.4813095	244.605354
984	100.887048	249.905117
985	120.800875	241.598814
986	112.455159	244.378397
987	96.1271050	238.892786
988	104.143862	239.835260
1021	102.000000	204.000000
1022	75.2074936	221.902180
1023	81.4939033	212.493903
1024	90.9021805	206.207494
1030	113.097820	206.207494
1031	122.506097	212.493903
1032	128.792506	221.902180
1037	83.0329070	224.286626
1038	90.7211409	221.018462
1039	97.7969576	214.247745
1040	115.768864	222.686034
1041	105.786837	216.125484
1042	99.5883559	223.855578
1043	106.478811	225.733419

QPM4 GEOMETRIC PROPERTIES

1	216.000000	216.000000 ...
	216.000000	216.000000
2	36.0000000	36.0000000 ...
	36.0000000	36.0000000

TPM3 GEOMETRIC PROPERTIES

3 36.0000000 36.0000000 ...  
36.0000000

GEOMETRIC ASSIGNMENTS

9	11	1	1
19	21	1	1
37	43	1	1
55	59	1	1
72	76	1	1
92	98	1	1
106	108	1	1
116	118	1	1
128	136	1	2
150	177	1	3
191	218	1	3
232	255	1	3
266	293	1	3
300	308	1	2
312	320	1	2
334	354	1	2
365	385	1	2
396	416	1	2
420	440	1	2
449	463	1	2
472	486	1	2
495	509	1	2
513	536	1	2
553	578	1	3
587	614	1	3

MATERIAL PROPERTIES

1 200000.000 0.300000 ...  
0.000000E+00 0.0000E+00 ...  
0.000E+00

MATERIAL ASSIGNMENTS

9	11	1	1
19	21	1	1
37	43	1	1
55	59	1	1
72	76	1	1
92	98	1	1
106	108	1	1
116	118	1	1
128	136	1	1
150	177	1	1
191	218	1	1
232	255	1	1
266	293	1	1
300	308	1	1
312	320	1	1
334	354	1	1



365 385 1 1  
396 416 1 1  
420 440 1 1  
449 463 1 1  
472 486 1 1  
495 509 1 1  
513 536 1 1  
553 578 1 1  
587 614 1 1

C

C

C Define the slideline properties.

C

C

SLIDEL PROPERTIES 1

1 10 10 0.15 D

C

C

C Define the slideline "Surface 1"

C

C

SLIDEL DEFINI 1

949 978

978 977

977 976

976 967

967 1032

1032 1031

1031 1030

1030 1021

1021 1024

1024 1023

1023 1022

1022 951

951 954

954 953

953 952

952 949

C

C

C Define the slideline "Surface 2"

C

C

SLIDEL DEFINI 2

232 422

422 421

421 420

420 355

355 358

358 357

357 356  
356 299  
299 308  
308 307  
307 306  
306 226  
226 236  
236 235  
235 234  
234 232

C

C

C Assign two pairs of the defined  
C surfaces of one slideline to the  
C relevant area in the model as a  
C slave and a master surface.

C

SLIDEL ASSIG

1 1 2 1 2

SUPPORT NODES

69 0 0 R F

79 0 0 R F

97 0 0 R F

107 0 0 R F

C

C

C These are the dummy restraint to  
C prevent the half of the bed from  
C moving freely during the first  
C increment when the half of the bed  
C and the pin joint are still  
C unconnected.

C

C

172 0 0 R R

808 0 0 R R

C

763 0 0 R F

773 0 0 R F

774 0 0 R F

818 0 0 R F

819 0 0 R F

853 0 0 R F

863 0 0 R F

864 0 0 R F

898 0 0 R F

899 0 0 R F

959 0 0 R R

962 0 0 R R

968 0 0 R R

987 0 0 R R  
988 0 0 R R  
1042 0 0 R R  
1043 0 0 R R

C  
C

C This is a small proportional of the  
C total load to allow contact to take  
C place in the first increment and  
C thus generate contact springs between  
C the half of the bed and the pin joint.

C  
C

LOAD CASE

CL

107 0 0 0.000E+00 -0.80000

C Apply the nonlinear control

NONL CONT

ITERATION 10 0 0

CONVERG 0 0 D D

OUTP 0 1 1

C  
C

C Free up the dummy restraint since the  
C contact spring will now have been  
C defined and there will, therefore, be  
C a restraint on the top block.

C  
C

SUPP NODE

172 0 0 F F

808 0 0 R F

C

C Apply the rest of the load increments.

C

LOAD CASE

CL

107 0 0 0.000E+00 -87500.0000

LOAD CASE

CL

107 0 0 0.000E+00 -175000.000

LOAD CASE

CL

107 0 0 0.000E+00 -262500.000

LOAD CASE

CL

107 0 0 0.000E+00 -350000.000

LOAD CASE

CL

107 0 0 0.000E+00 -437500.000

```
LOAD CASE
CL
  107 0 0  0.000E+00  -525000.000
LOAD CASE
CL
  107 0 0  0.000E+00  -612500.000
LOAD CASE
CL
  107 0 0  0.000E+00  -700000.000
END
```

## APPENDIX (C)

### CALIBRATION PROCEDURE OF THE LOAD CELL

#### 1.0 Conventional Colours of the Wires:

The colours of the wires of the full bridge strain gauge circuits represent the following:

- |       |                |   |        |
|-------|----------------|---|--------|
| (i)   | RED            | = | $+V_i$ |
| (ii)  | BLUE           | = | $-V_i$ |
| (iii) | YELLOW & WHITE | = | $V_o$  |

#### 2.0 Calibration Instrumentation

The instrumentations used in the calibration procedure of the load cell were as follows:

- |       |                                        |
|-------|----------------------------------------|
| (i)   | X-Y chart plotter "LINSEIS LY 17100"   |
|       | The graph factor = 50 mv/cm            |
| (ii)  | Amplifier "LYLDE, FE.254.GA"           |
|       | The amplification = 200                |
| (iii) | Bridge conditioner "FYLDE, FE-492-BBS" |
|       | Excitation voltage = 6 VDC             |
| (iv)  | Instron testing machine of a 250 KN.   |

#### 3.0 The Calibration Procedure:

The load cell was loaded up to 250 KN, it was observed that the maximum limit of the nonlinearity was up to 100 KN. Therefore, the pre-loading was considered to be 100 KN and an increment load of 25 KN was used to increase the applied load from a 100 KN up to 250 KN. Five tests of calibration were carried out and the results are shown in Table (C.1)

TABLE (C.1)

Applied Load (KN)	Incremental Load (KN)	L = Length of the graph (cm)				
		Test No. 1	Test No. 2	Test No. 3	Test No. 4	Test No. 5
25	25	1.25	1.20	1.16	1.12	1.13
50	25	1.20	1.18	1.18	1.17	1.18
75	25	1.15	1.21	1.18	1.18	1.21
100	25	1.17	1.17	1.17	1.16	1.16
125	25	1.18	1.17	1.17	1.18	1.17
150	25	1.12	1.12	1.16	1.15	1.16
Average		1.17833	1.175	1.17	1.16	1.16833

Therefore, the overall average of the length of the graph is  $L_{ave} = 1.17033$  cm. In the following the subscript "in" refers to the input voltage of the amplifier whereas "out" refers to the output voltage of the amplifier. Thus the following can be written:

$$\begin{aligned}
 V_{out} &= L_{ave} \times \text{Graph factor} & (C.1) \\
 &= 1.17033 \times 50 \\
 &\approx 58.517 \text{ mv}
 \end{aligned}$$

$$\begin{aligned}
 V_{in} &= V_{out}/\text{amplification} & (C.2) \\
 &= 292.58 \mu\text{V}
 \end{aligned}$$

Usually the sensitivity is given as follows:

$$\text{sensitivity} = V_{in} / P / V_i \quad (C.3)$$

where P is the incrementally applied load (25 KN) and  $V_i$  is the excitation voltage (6VDC). Thus

$$\begin{aligned}
 \text{sensitivity} &= 292.58/25/6 \\
 &= 1.95 \mu\text{V}/\text{KN}/V_i & (C.4)
 \end{aligned}$$

## APPENDIX (D)

### 1.0 The File Suite of the Program

In order to run the program successfully the following files should be available in the directory where the program is executed:

- (i) DASH8.BIN : This is the I/O routine driver which contains the commands and the instructions of the operating system of the A/D converter in binary code.
- (ii) DASH8.ADR : This file contains one ASCII number which can be changed to set the address of the A/D converter to be high speed (12-bit) or low speed (8-bit).
- (iii) CAL.TEP : This is an access file which contains the ASCII input data. This data can be changed to suit the specifications of the apparatus test. This file contains three data lines, each line has eight variables which present eight channels. The first line contains the sensitivities of the apparatus test. The second line contains the gain factors. The third line contains the input data for the excitation voltage.
- (iv) BASRUN.EXE : This is the I/O routine driver which contains the binary commands and instructions of the IBM microsoftware compiler which was used to compile the program and link it with the DASH8.BIN.

### 2.0 Program Variable Names:

The following are some of the variable names of the computer program. The other variable names have been explained in the listing of the program:

A, G and V : are the stores of the sensitivities; the gain factors and the

excitation voltages of the apparatus test, respectively.

BASADR % : store of the address number of the A/D converter

DI% (8) }  
NY (8) } stores of the converted signals of the  
NY1 (8) } channels

SI : store of scanning time of processing the signals.

### 3.0 Listing of the Program

```
0120 '*****
0130 '*****BASIC PROGRAM *****
0190 '*****
0210 'This program shows how to set up
0220 'an A/D converter to convert 8 analog signals
0230 'to 8 digital signals with respect to
0240 'the function of each one of them
0250 'the digital signals can be shown either
0260 'on the screen , printer , floppy disk
0270 'or all of them.The electronic strip chart
0280 'can be shown as well for each signal .
0290 'The time limit of measurement is 0.001.
0300 'This means that each 0.001 Sec. one measurement
0310 'can be obtained.
0350 '
0360 'Structure of the program -----
0370 '
0380 'LINE 710 - 1015... INITIALIZATION :
0390 ' driver declare variables etc.
0400 'line 1020 - 1160 ... choose the options from menu
0405 ' -----
0408 '*****
0410 ' <1> display data on the screen
0420 ' <2> display data on a floppy disk
0430 ' <3> display data on the printer
0440 ' <4> display data on 1,2 & 3
0450 ' <5> display electronic strip chart
0460 'line 1170 - 1530.... logging the control data
0470 'line 1540 - 1708 ... start the main logging signal
0480 ' from the channels 1 - 8
0490 'line 1709 - 1735 ... the calibration of the
0500 ' the measurements.
0510 'line 1735 - 1767 ... control print
```



```

0520 'line 1767 - 2040 ... options for printing .
0530 'line 2190 - 2280 ... wait in delay loop = scan
0540 '           interval then loop back to
0550 '           start of logging loop .
0560 '*****
0565 COLOR 15,1,4:CLS:LOCATE 25,27:PRINT "Press any key
to continue"
0570 LOCATE 9,27:PRINT "This programme is written by :'"
0575 LOCATE 11,27:PRINT"Mohamad M.Saleh"
0580 LOCATE 12,27:PRINT"School of Mechanical Manufacturing
Engineering"
0585 LOCATE 13,27:PRINT"Dublin City University"
0590 LOCATE 14,27:PRINT"Ireland."
0600 A8$=INKEY$:IF A8$="" THEN GOTO 600
0700 'C***** INITIALIZE *****
0710 DIM DI%(8)
0720 DIM NY(8)
0725 DIM NY1(8)
0730 COLOR 15,1,4:CLS:PRINT SPC(79)
0785 NCHAN%=8
0790 'SET I/O ADDRASS TO SUIT YOUR BOARD-----
0810 '
0900 OPEN "DASH8.ADR" FOR INPUT AS #1
0910 INPUT #1,BASADR%
0920 CLOSE #1
0930 'DO MODE 0 INITIALIZATION OF A/D CONVERTER -----
0940 DASH8 = 0
0950 FLAG% = 0
0960 MD% = 0
0970 CALL DASH8 (MD% ,BASADR%, FLAG%)
0980 IF FLAG%<> 0 THEN PRINT "INSTALLATION ERROR ":END
0990 LOCATE 12,1 :PRINT SPC(79)
0992 OPEN "CAL.TEP" FOR INPUT AS #4
0994 INPUT #4,A1,A2,A3,A4,A5,A6,A7,A8
0996 INPUT #4,G1,G2,G3,G4,G5,G6,G7,G8
0998 INPUT #4,V1,V2,V3,V4,V5,V6,V7,V8
1004 CLOSE #4
1014 'DISPLAY MENU WITH SETUP OPTIONS-----
1015 COLOR 15,1,2:CLS:PRINT SPC(79)
1020 LOCATE 3,23 :PRINT "***** M A I N   M E M U ***** "
1030 LOCATE 7,5 :PRINT "<1>- DISPLAY DATA ON THE SCREEN .."
1040 LOCATE 8,5 :PRINT "<2>- DISPLAY DATA ON A FLOPY DISK .."
1050 LOCATE 9,5 :PRINT "<3>- DISPLAY DATA ON THE PRINTER .."
1060 LOCATE 10,5 :PRINT "<4>- DISPLAY DATA ON 1,2 & 3 .."
1065 LOCATE 11,5 :PRINT "<5>- DISPLAY THE ELECTRONIC SIGNAL
WITH THE TIME .."
1067 COLOR 15,3,2
1070 LOCATE 13,2:COLOR 15,0,0:PRINT"CHOOSE OPTION (1-5)
< press <6> to Exit >:";:COLOR 7,0,0
1075 COLOR 15,1,3

```

```

1080 A1$ = INKEY$:IF A1$="" THEN GOTO 1080
1090 PRINT A1$
1100 X%= VAL(A1$)
1110 IF X%>=1 AND X%<=6 GOTO 1130
1120 LOCATE 14,2:PRINT"IT IS NOT A VALID RESPONSE. REENTER "
:LOCATE 13,1:PRINT SPC(79):GOTO 1070
1130 LOCATE 14,1 :PRINT SPC(79)
1140 IF X%=6 THEN:COLOR 15,1,4:CLS:END
1150 IF X%=5 THEN:COLOR 15,1,4:CLS:GOTO 2310
1170 '
1180 LOCATE 15,1:INPUT "SCAN TIME 'sec'";SI
1190 PRINT SPC(79)
1200 IF SI <=0 THEN LOCATE 16,1:PRINT"THE TIME SHOULD BE
MORE THAN 0 .RE-ENTER.":LOCATE 15,1:PRINT SPC(79):GOTO 1180
1205 LOCATE 16,1 :PRINT SPC(79)
1220 '*****
1250 '*****
1450 CLS
1460 ON X% GOTO 1465,2040,2040,1465
1465 '
1466 COLOR 15,1,7:CLS
1470 LOCATE 25,1:PRINT"Hello Mohamad --> This is your
digital measurements "
1480 LOCATE 1,1:PRINT "START THE MEASUREMENTS "
1490 LOCATE 3,1:PRINT "   ch1     ch2     ch3
   ch4     ch5     ch6     ch7     ch8 "
1495 PRINT" ( KN )   (mm)   (mm)   (mm)
   (mm)   (mm)   (mm)   (mm) "
1500 PRINT" -----
----- "
1510 LOCATE 20,1:COLOR 0,7,0:PRINT"-PRESS <ESC>
TO TERMINATE LOGGING -";:COLOR 7,0,0
1515 IF X%=4 THEN GOTO 2040
1520 '
1530 'START OF THE MAIN LOGGING LOOP -----
1550 '
1560 COLOR 0,7,0:LOCATE 24,1:PRINT"SCANNING";
:COLOR 7,0,0
1570 MD%=2:CH%=0
1580 CALL DASH8(MD%,CH%,FLAG%)
1590 MD%=4
1600 '
1610 FOR I=0 TO 7
1620 CALL DASH8(MD%,DI%(I),FLAG%)
1630 NY(I)=DI%(I)
1640 NEXT I
1650 'LOCK TIME -----
1660 TI$=TIMES$:DAT$=DATE$
1670 '
1680 'CONVERT TO DIGITAL -----

```

```

1690 FOR I=0 TO 7
1700 DI%(I)=(DI%(I)*5/2047)*1000
1705 NY(I)=(NY(I)*5/2047)*1000.00
1707 NEXT I
1708 'CALIBRATE THE MEASUREMENTS -----
1709 FOR I=0 TO 7
1710 NY1(I)=NY(I)/1000
1711 NEXT I
1713 '
1715 NY1(0)=(NY1(0)/(A1*1E-06*V1*G1))
1718 NY1(1)=-((NY1(1)/G2)/A2)
1719 NY1(2)=-((NY1(2)/G3)/A3)
1720 NY1(3)=-((NY1(3)/G4)/A4)
1721 NY1(4)=-((NY1(4)/G5)/A5)
1722 NY1(5)=-((NY1(5)/G6)/A6)
1724 NY1(6)=-((NY1(6)/G7)/A7)
1726 NY1(7)=-((NY1(7)/G8)/A8)
1750 '*****
1765 IF X%=1 GOTO 2180
1767 IF X%=2 GOTO 2120
1769 IF X%=3 GOTO 2158
1770 IF X%=4 GOTO 2120
2040 IF X%=4 THEN:LOCATE 12,8:COLOR 15,1,0:PRINT"
NAME OF DATA FILE (e.g.A:MYFILE.DAT)";:
INPUT FILE$:COLOR 15,1,0:LOCATE 12,8:
PRINT SPC(79):LOCATE 12,28:
PRINT" << PRINTING >>":GOTO 2110
2041 CLS
2042 IF X%=3 THEN:COLOR 15,1,0:CLS:
LOCATE 12,28:PRINT " << PRINTING >>":
LOCATE 25,1:
PRINT"Hello Mhamad -->
your measurements on the printer now":
LOCATE 20,1:COLOR 0,7,0:PRINT"-
PRESS <ESC> TO EXIT ";:COLOR 7,0,0:GOTO 2111
2050 LOCATE 12,8:
PRINT"NAME OF DATA FILE
(e.g. A: or C:MYFILE.DAT)";
2060 INPUT FILE$
2065 CLS
2070 '
2080 LOCATE 20,1:COLOR 0,7,0:
PRINT "-PRESS <ESC> TO TERMINATE LOGGING -";:
COLOR 7,0,0
2090 LOCATE 12,20:
PRINT" << DISPLAY DATA ON A: DRIVE >>"
2100 LOCATE 25,1:
PRINT"Hello Mohamad
---> your measurements on A: now "
2110 OPEN FILE$ FOR OUTPUT AS #2

```

```

2111 OPEN "LPT1:" FOR OUTPUT AS #3
2116 GOTO 1530
2120 GOSUB 9190
2125 '
2158 IF X%=2 THEN GOTO 2189
2160 PRINT #3,"-----
-----"
2169 PRINT #3,USING"\      \" ;DAT$;
2170 PRINT #3,USING"\      \" ;TI$
2171 PRINT #3,USING"####.###";NY1(0);
2172 PRINT #3,USING"####.###";NY1(1);
2173 PRINT #3,USING"####.###";NY1(2);
2174 PRINT #3,USING"####.###";NY1(3);
2175 PRINT #3,USING"####.###";NY1(4);
2176 PRINT #3,USING"####.###";NY1(5);
2177 PRINT #3,USING"####.###";NY1(6);
2178 PRINT #3,USING"####.###";NY1(7)
2179 IF X%=3 THEN GOTO 2189
2180 LOCATE 7,1:COLOR 15,1,0
2182 '
2184 '
2185 FOR I=0 TO 7
2186 PRINT USING"####.###";NY1(I);
2187 NEXT I
2188 '
2189 LOCATE 24,1:PRINT SPC(20)
2190 DEF SEG=&H40
2200 TNOW=PEEK (&H6C)+256*PEEK(&H6D)
2210 TNOW=TNOW*65536!/1193180!
2220 A2$=INKEY$:IF A2$="" GOTO 2240
2230 IF ASC(A2$)=27 GOTO 2290
2240 LOCATE 25,55:
PRINT USING"\      \" ;DAT$;TI$;
2250 IF TNOW<=(TSL-.06) THEN TSL=TNOW
2260 IF TNOW-TSL<(SI-1/18.2)
GOTO 2200 ELSE TSL=TNOW
2270 LOCATE 24,1:PRINT SPC(20)
2280 GOTO 1530
2290 LOCATE 24,1:COLOR 0,7,0:
PRINT"TERMINATED";:COLOR 7,0,0
2300 LOCATE 22,1:CLOSE #2:CLOSE #3:
COLOR 15,1,6:CLS:GOSUB 9400:CLS:GOTO 710
2310 DIM D%(7)
2313 DIM DIO%(7)
2315 COLOR 1,2,4:CLS
3027 VL=1
3030 'SET PROPER OUTPUT SCALE-----
3040 IF VL=0 THEN RESTORE 5070
3050 DIM CH%(16)
3055 DIM YL%(16)

```

```

3060 FOR I%=0 TO 16:YL%(I%)=-32768!:NEXT I%
3070 LOCATE 25,1:PRINT"";:LOCATE 1,1
3080 PRINT " Number of Channels is : "
;NCHAN%;" Channels"
3090 PRINT
4000 INPUT "Which channel do you want plotted
<e.g. 0-3-7 use hyphen>? : ",X$
4005 'ADD A LEADING DASH -----
4010 X$="-"+X$
4020 L%=LEN(X$)
4030 FOR I%=1 TO L%
4035 'GET RID OF SPACES-----
4040 IF MID$(X$,I%,1)=" "
THEN MID$(X$,I%,1)="-"
4050 NEXT I%
4055 'SPACES WRECK VAL($) FUNCTION ----
4057 'ZERO CH%(*) ARRAY -----
4060 FOR I%=0 TO NCHAN%-1:CH%(I%)=0:NEXT I%
4070 CR% =ASC(LEFT$(X$,1))
4080 IF ((CR%>=48 AND CR%<=55) AND (VAL(X$)
<=NCHAN%-1 AND VAL(X$)>=0)) THEN CH%(VAL(X$))
=1:L%=LEN(X$):X$=RIGHT$(X$,L%-(1+INT(VAL(X$)/10)))
4090 IF VAL(X$)>NCHAN%-1 THEN PRINT"One
more entries are incompatible with
the configuration. Please re-enter "
:PRINT "Valid channel numbers range
from 0 to ";NCHAN%-1:PRINT:GOTO 3080
5000 IF I%<NCHAN%-1 THEN N%=ASC(MID$(X$,I+1,1))
5010 L% = LEN(X$):IF L%>=1 THEN X$ =
RIGHT$(X$,L%-1):GOTO 4070
5020 IF U%>=48 AND U%<=55 AND N%>=48 AND
N%<=55 THEN CH%(10*(U%-48)+N%-48)=1:I=I+1
5030 '
5040 SCREEN 2:CLS
5050 LOCATE 25,1:PRINT"Press +
to speed up, - to slow down, <Esc> to exit"
5060 X%=32:U%=1:C%=1:
LOCATE 23,50:PRINT"Grid in 1 second intervals";
5070 DATA +.5,+.4,+.3,+.2,+.1, 0 ,-.1,-.2,-.3,-.4,-.5
5080 DATA +FS,+.9,+.8,+.7,+.6,+.5,+.4,+.3,+.2,+.1," 0 "
5090 FOR I%=1 TO 11:
READ A3$:LOCATE I%*2-1,1:PRINT A3$;:NEXT I%
6000 'MOVE CURSOR LINE 1 STEP RIGHT-----
6010 IF X%>=640 THEN LINE (X%,0) -
(X%,168),0:X%=30:LINE (X%-1,0)-(X%-1,168),0
6015 'PLOT CURSOR LINE -----
6020 LINE (X%+1,0) - (X%+1,168),0
6025 'REMOVE PREVIOUS CURSOR LINE -----
6030 LINE (X%,0) - (X%,168),0
6040 '

```

```

6050 'GET DATA AND PLOT IT -----
6060 '
6070 MD%=1:D%(0)=0:D%(1)=NCHAN%-1
6080 CALL DASH8 (MD%,D%(0),FLAG%)
6090 MD%=4
6095 'DO A/D CONVERSIONS -----
7000 FOR Z%=0 TO NCHAN%-1
7010 CALL DASH8 (MD%,D%(0),FLAG%)
7020 IF VL=0 THEN DIO%(Z%)=(D%(0)*5/2047)
ELSE DIO%(Z%)=D%(0)
7030 NEXT Z%
7040 FOR Z%=0 TO NCHAN%-1
7050 IF CH%(Z%)=0 THEN GOTO 8010
7055 'PLOTTING START 30 UNITS TO RIGHT -----
7060 IF X%<30 THEN X%=30
7070 Y%=DIO%(Z%)
7075 'SKIP PLOTTING FIRST POINT -----
7080 IF YL%(Z%)=-32768! THEN GOTO 8000
7090 LINE (X%-1,84-YL%(Z%)*80!/2047!)
-(X%,84 - Y%*80!/2047!)
7095 'INCREMENT TO NEXT POINT -----
8000 YL%(Z%)=Y%
8010 NEXT Z%
8020 GOSUB 9105:IF Q+C%>T THEN GOTO 8050
8025 'PLOT TIME DOTES -----
8030 FOR I%=1 TO 11:PSET (X%,I%*16-12):NEXT I%
8040 Q=T
8050 X%=X%+1
8060 FOR I%=1 TO U%
8070 A$=INKEY$:IF A$="" GOTO 9080
8080 I%=U%
8090 IF ASC(A$)=27 THEN LOCATE 1,1:SCREEN 0:CLS:GOTO 710
9000 IF A$="+" THEN U%=(U%/2):IF U%=1 THEN GOSUB 9135
9010 IF A$="-" AND U%<=16000 THEN
U%=(U%*2):IF U% >16000 THEN GOSUB 9135
9020 IF A$="-" AND U%>16000 THEN GOSUB 9135
9030 IF U%<=200 THEN C%=1:LOCATE 23,1:
PRINT SPC(79):LOCATE 23,50:
PRINT "Grid in 1 second intervals";
9040 IF U%>2000 THEN C%=60:
LOCATE 23,1:PRINT SPC(79):
LOCATE 23,50:
PRINT"Grid in 1 minute intervals";:GOTO 9060
9050 IF U%>200 THEN C%=10:LOCATE 23,1:
PRINT SPC(79):LOCATE 23,50:
PRINT"Grid in 10 second intervals";
9060 IF A$="" THEN 9070 ELSE GOTO 9080
9070 IF INKEY$="" GOTO 9070
9080 NEXT I%
9090 GOTO 6000

```

```

9105 T$=TIMES$
9110 T=3600!*VAL(LEFT$(T$,2))+
60*VAL(MID$(T$,4,2))+VAL(RIGHT$(T$,2))
9120 RETURN
9135 IF U%=1 THEN LOCATE 23,1:PRINT"MAX SPEED";
9140 IF U%>10000 THEN LOCATE 23,1:PRINT"MIN SPEED";
9150 SOUND 500,3:SOUND 400,3
9160 LOCATE 23,1:PRINT" ";
9170 RETURN
9190 '*****
9240 PRINT #2,USING" ####.### ";NY1(0);
9250 PRINT #2,",";
9260 PRINT #2,USING" ####.### ";NY1(1);
9270 PRINT #2,",";
9280 PRINT #2,USING" ####.### ";NY1(2);
9290 PRINT #2,",";
9300 PRINT #2,USING" ####.### ";NY1(3);
9310 PRINT #2,",";
9320 PRINT #2,USING" ####.### ";NY1(5);
9330 PRINT #2,",";
9340 PRINT #2,USING" ####.### ";NY1(6);
9350 PRINT #2,",";
9360 PRINT #2,USING" ####.### ";NY1(6);
9370 PRINT #2,",";
9380 PRINT #2,USING" ####.### ";NY1(7)
9390 RETURN
9620 '**** END OF PROGRAM ****

```